LINKING THE MULTIPLE FUNCTIONS OF XPF-ERCC1 ENDONUCLEASE IN DNA REPAIR TO HEALTH OUTCOMES: CANCER AND AGING

by

Advaitha Madireddy

B. Tech, SRM University, India, 2008

Submitted to the Graduate Faculty of

Graduate School of Public Health in partial fulfillment

of the requirements for the degree of

Doctor of Philosophy

University of Pittsburgh

2012

UNIVERSITY OF PITTSBURGH

Graduate School of Public Health

This dissertation was presented

by

Advaitha Madireddy

It was defended on

June 25th, 2012

and approved by

Candace M. Kammerer, PhD, Assistant Professor, Human Genetics, Graduate School of Public Health, University of Pittsburgh

Susanne M. Gollin, PhD, Professor, Human Genetics, Graduate School of Public Health, University of Pittsburgh

Patricia L. Opresko, PhD, Assistant Professor, Environmental and Occupational Health, Graduate School of Public Health, University of Pittsburgh

Dissertation Advisor: Laura J. Niedernhofer, MD, PhD, Associate Professor, Microbiology and Molecular Genetics, School of Medicine, University of Pitttsburgh

LINKING THE MULTIPLE FUNCTIONS OF XPF-ERCC1 ENDONUCLEASE IN DNA REPAIR TO HEALTH OUTCOMES: CANCER AND AGING

Advaitha Madireddy, PhD

University of Pittsburgh, 2012

XPF-ERCC1 is a structure specific endonuclease in which the XPF subunit is involved in nucleolytic activity and the ERCC1 subunit is involved in DNA binding. They are essential for multiple genome maintenance mechanisms which include the repair of bulky DNA monoadducts via nucleotide excision repair (NER) and also the repair of DNA interstrand crosslinks. In humans, the deficiency of XPF-ERCC1 results in two major syndromes: Xeroderma pigmentosum (XP), characterized by predisposition to skin cancer and XFE, characterized by symptoms of premature aging. The mechanism behind XP has been attributed to the inability to carry out NER. However, the mechanism behind the contribution of XPF-ERCC1 deficiency to aging has not yet been established.

The most successful chemotherapeutic agents are crosslinking agents that cause both monoadducts and interstrand crosslinks in DNA. Unfortunately, ~50% of tumors are resistant to these drugs. Numerous studies implicate XPF-ERCC1 as a major culprit in tumor resistance because of its pivotal role in repairing DNA damage but to date, there is no conclusive evidence of this.

This dissertation aims to advance our understanding of the mechanistic contribution of XPF-ERCC1 to two major issues of public health relevance, cancer and aging. The first chapter examines the importance of DNA binding residues of XPF-ERCC1 located in the c-terminus of both proteins. The results revealed that mutations in DNA binding residues located in the HhH

domain of ERCC1 and the nuclease domain of XPF have a deleterious effect on nuclease and NER activity. Analysis of the n-terminus of XPF revealed that mutations in the n-terminus confer selective crosslink sensitivity to cells thereby identifying target regions of the *XPF* gene that could be exploited to generate an ICL repair pathway specific defect. To probe the functionality of XPF-ERCC1 as biomarkers of chemoresistance, we developed a novel monoclonal antibody, 1E4, which could be used to establish a positive correlation between XPF-ERCC1 protein levels and patient sensitivity to crosslinking regimes. To examine whether DNA repair capacity of an individual can predict lifespan, and to determine a way to diagnose disorders such as XP, we developed a novel semi-automated assay to measure the NER capacity of suspension cells.

TABLE OF CONTENTS

LIST OF TABLES

LIST OF FIGURES

PREFACE

Numerous people from different walks of my life have been instrumental in helping me make this contribution to the world of science. I would like to dedicate my thesis to my brother, Abhinand Madireddy. His selfless career choice of becoming a sailor to take over the financial burden of our family gave me the wonderful opportunity to pursue my dream of becoming a scientist. This achievement would not have been possible without his undying love and support. I would like to thank my wonderful parents for all the sacrifices, and the hardships that they had to face in order to help me reach this point in my life. I owe everything that I am and everything that I will ever be to them. I will forever owe a debt of gratitude to my best friends, SK and Anushri, who have always been there for me. Their support and motivation has given me the strength to sail through some of the most stressful moments in my life. A special thank you to Priya Mittal. She has been an enormous source of support, especially over the last 6 months.

My mentor Dr. Laura Niedernhofer has been a great source of inspiration to me. She has been a constant source of encouragement and has taken the effort every single day to push me to become a better scientist. She has been instrumental in instilling in me perseverance, confidence and purpose in my career.

Every single member of my lab, both past and present, has helped me a great deal over the last 4 years. I would especially like to thank Nikhil Bhagwat for his patience in teaching me

most of what I know today. The most important factor that contributes to a person's success is the work environment. I would like to thank all my friends from lab for providing a work environment filled with scientific enthusiasm and motivation.

1.0 INTRODUCTION

This chapter was adapted from a review on XPF-ERCC1 that is pending publication.

Bhagwat, N.R.[1], Su, Y.[2]., Madireddy, A.[1], Scharer, O.D.[3], and L.J. Niedernhofer[4]

[1]Department of Human Genetics, University of Pittsburgh Graduate School of Public Health, 130 DeSoto Street, Pittsburgh, PA, 15261, USA

[2]Department of Chemistry, [3]Department of Pharmacological Sciences, Stony Brook University, Stony Brook, NY 11794-3400, 3current address: Herbert Irving Comprehensive Cancer Center, Columbia University, New York, NY 10032,

[4]Department of Microbiology and Molecular Genetics, University of Pittsburgh School of Medicine, Pittsburgh, Pennsylvania.

XPF-ERCC1 is a structure-specific endonuclease initially discovered for its role in nucleotide excision repair (NER), a DNA repair pathway that removes helix distorting lesions formed by UV light and environmental mutagens from the nuclear genome (Sijbers et al., 1996a). Consistent with this finding, people with mutations in the XPF gene suffer from Xeroderma pigmentosum (XP), a prototypical inherited DNA repair disorder characterized by extreme

sensitivity to UV light and a more than 1000-fold increased incidence of skin cancer. Subsequently, XPF-ERCC1 and its homologs in yeast, *Drosophila* and plants have been found to function in a p lethora of DNA damage repair and DNA damage tolerance mechanisms. Consequently, mice deficient in XPF-ERCC1 and two more recently identified human patients not only suffer from cancer predisposition, but also show developmental abnormalities and symptoms of accelerated aging (Jaspers et al., 2007; Niedernhofer et al., 2006). Here we review our understanding of the biochemical, structural, cell biological and genetic basis of the various functions of XPF-ERCC1 and aim to connect their functions to the aging and cancer related phenotypes caused by XPF-ERCC1 deficiency.

1.1 XPF FAMILY MEMBERS

XPF-ERCC1 is a member of the XPF family of endonucleases. This family is characterized by the presence of at least two out of three structural motifs: a DEXH-helicase, an $ERKX_3D$-nuclease and a C-terminal helix-hairpin-helix motif. The XPF family has no known homologs in bacteria (Aravind et al., 1999). It likely arose in archaea, in which there is just one family member, Hef (Figure 1-1) (Komori et al., 2002). The N-terminal region of the XPF-family shows similarities to the archaeal superfamily 2 (SF2) RNA helicases, and the C-terminal region has a conserved $(V/I)ERKX_3D$ nuclease (Sgouros et al., 1999). Euryarchaeal Hef orthologs retain the DExH helicase motif (Komori et al., 2002), though crenarchaea, e.g., *Aeropyrum pernix* and *Sulfolobus solfataricus*, do not (Figure 1-1) (Nishino et al., 2003). In eukaryotes, the XPF family has diversified, giving rise to multiple orthologs that specialize in different DNA repair

pathways. Eukaryotic XPF homologs show conservation of the N-terminus but have lost their ability to hydrolyze ATP by mutation in the DEXH motifs and are therefore helicase-inactive (Sgouros et al., 1999).

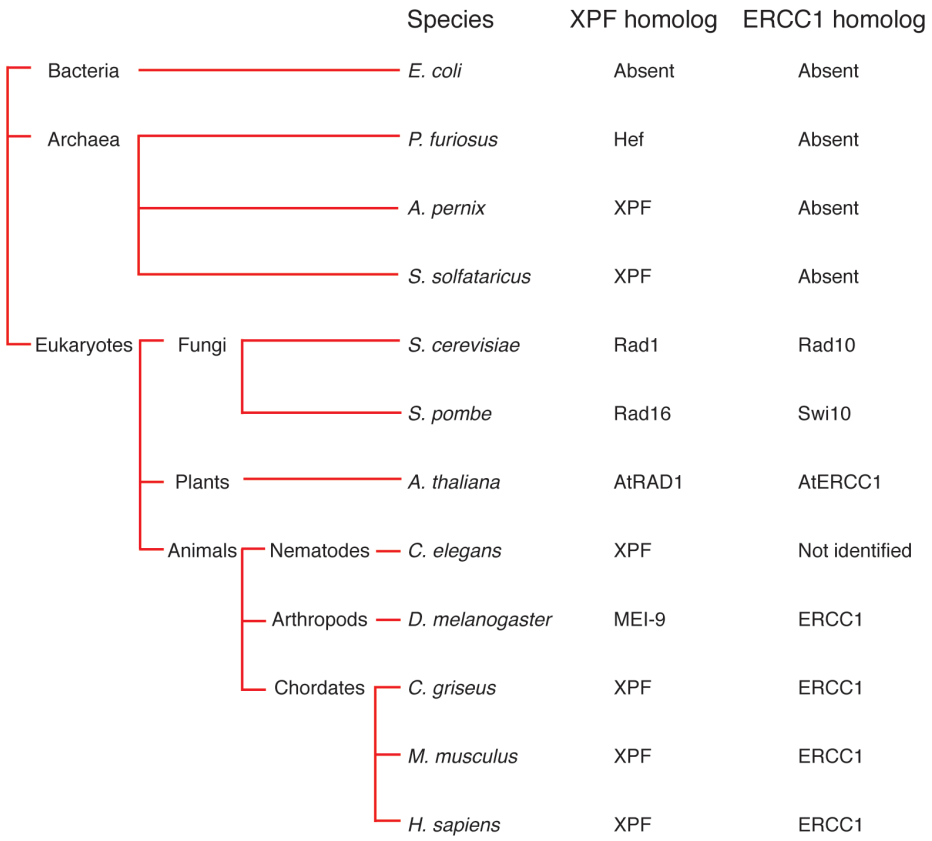

Figure 1-1 Homologs of XPF and ERCC1

Homologs of ERCC1 and XPF in different model organisms are shown with their relative position on the evolutionary tree.

In eukaryotes, XPF heterodimerizes with ERCC1, with XPF retaining the nuclease motif (Enzlin and Scharer, 2002) whereas in archaea, Hef/XPF forms homodimers. The XPF family is highly conserved and all eukaryotes studied to date have homologs of XPF-ERCC1 (Figure 1-1). The eukaryotic XPF has three major domains: a DEXH helicase-like domain, an ERKX$_3$D

nuclease domain and a helix-hairpin-helix like domain (Figure 1-2) (Aravind et al., 1999; Sgouros et al., 1999). ERCC1, the smaller of the two partners, does not have the DEXH domain and has lost its ERKX$_3$D motif through gene divergence (Gaillard and Wood, 2001). It has only two domains: the central domain, which is nuclease-dead, but is involved in protein-protein interactions (Tsodikov et al., 2007) and a C-terminal HhH2 domain (Figure 1-2), which interacts with the corresponding domain of XPF (de Laat et al., 1998d). The heterodimeric interaction of ERCC1 and XPF stabilizes these proteins *in vivo* (Niedernhofer et al., 2006). Consequently, XP-F cells have a reduced expression of ERCC1 (Biggerstaff et al., 1993; Yagi et al., 1997), which is restored by the expression of exogenous wild-type XPF (Yagi et al., 1998), and *Ercc1* mutant cells have a reduced level of XPF, which is restored by exogenous expression of ERCC1 (Houtsmuller et al., 1999).

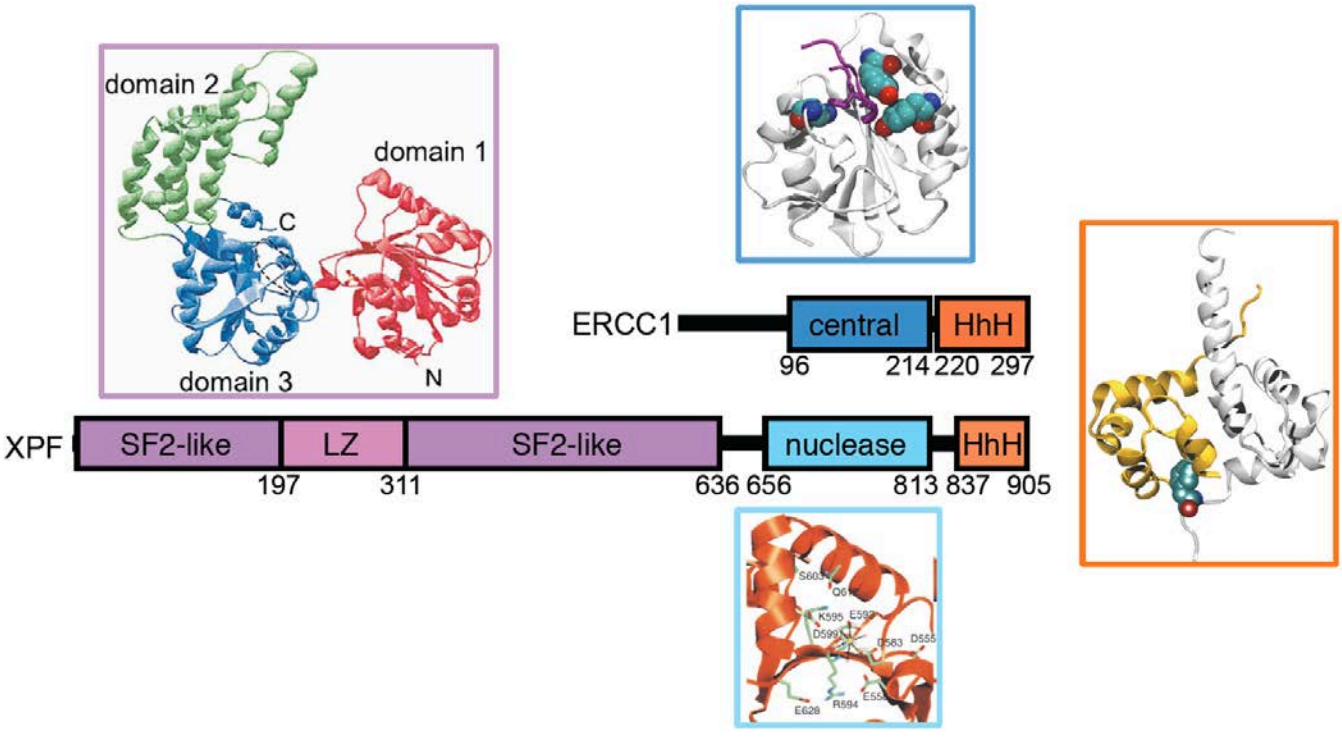

Figure 1-2 Structural domains in XPF and ERCC1

Schematic representation of XPF and ERCC1 showing the extents in amino acid numbers of the helicase-like (black box), the nuclease (red box) and the HhH2-like (dark green box) domains of XPF and the central (orange box) and HhH2 (light green box) domains of ERCC1.

All XPF family members in eukaryotes function as heterodimers (Bailly et al., 1992; Bardwell et al., 1992; Boddy et al., 2001; Ciccia et al., 2007; Sijbers et al., 1996a). In vertebrates there are three types of proteins in the XPF family: those that have nuclease activity (XPF and MUS81), one with translocase activity (FANCM), and those that do not have either of these activities, but are binding partners of proteins with these activities (ERCC1, EME1 and 2, and FAAP24). Together, they form three endonucleases and one translocase (Figure 1-3).

All XPF family members in eukaryotes function as heterodimers (Bailly et al., 1992; Bardwell et al., 1992; Boddy et al., 2001; Ciccia et al., 2007; Sijbers et al., 1996a). In vertebrates there are three types of proteins in the XPF family: those that have nuclease activity (XPF and MUS81), one with translocase activity (FANCM), and those that do not have either of these activities, but are binding partners of proteins with these activities (ERCC1, EME1 and 2, and FAAP24). Together, they form three endonucleases and one translocase (Figure 1-3).

The most recently discovered members of the XPF family are FANCM and FAAP24 (Ciccia et al., 2007; Meetei et al., 2005). These proteins heterodimerize to form a translocase that has an affinity for splayed arm substrates (Ciccia et al., 2007). It lacks helicase or nuclease activity and may be involved in loading of the Fanconi anemia (FA) core complex onto the chromatin during ICL repair (Kim et al., 2008a).

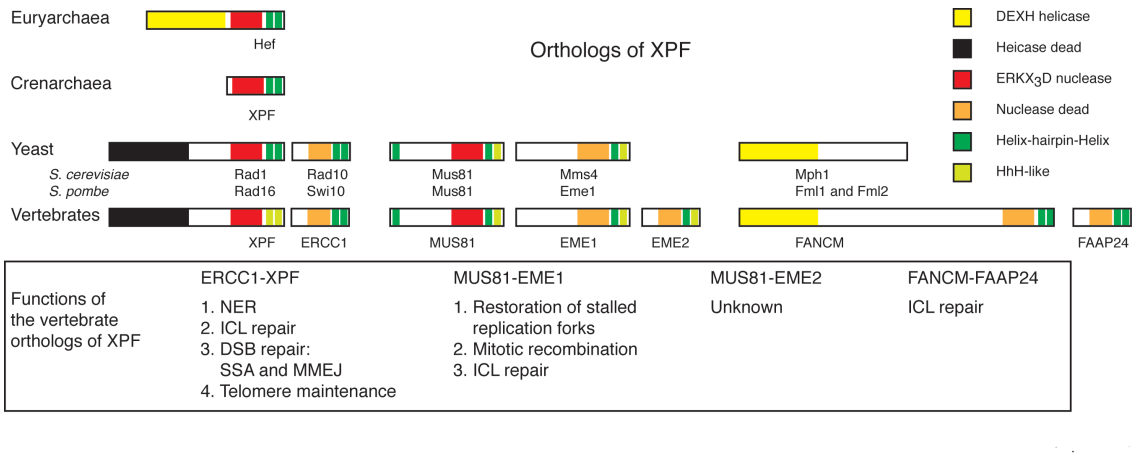

Figure 1-3 Orthologs of XPF

Members of the XPF family in archaea, yeast and vertebrates are shown. Archaea have only one member of the family (Hef/XPF). Yeast *S. cerevisiae* and *S. pombe* have 4 members, the homologs of ERCC1 (Rad10/Swi10) and XPF (Rad1/Rad16) and homologs of MUS81 (Mus81) and EME1 (Mms4/Eme1). Vertebrates possess three additional members, EME2, which dimerizes with MUS81 to form the EME2-MUS81 endonuclease, and FANCM and FAAP24, which participate in the Fanconi anemia DNA repair pathway. Heterodimers formed by these proteins and their functions in vertebrates are listed in the box.

1.2 BIOLOGICAL FUNCTIONS OF XPF-ERCC1 AND ITS HOMOLOGS

1.2.1 Nucleotide Excision Repair

NER is a DNA repair pathway that repairs a wide variety of helix-distorting lesions formed by ultra violet (UV) light, environmental mutagens and cancer chemotherapeutic agents. It is a complex pathway involving over 30 proteins that perform a highly coordinated excision of the damage as a single-stranded oligonucleotide and restoration of the original DNA sequence using the non-damaged strand as a template (de Laat et al., 1999; Gillet and Scharer, 2006).

A role of XPF-ERCC1 in NER was first identified for its homologs in *S. cerevisiae*. *rad1* and *rad10* mutants were found to be hypersensitive to UV irradiation and defective in the incision step of NER (Reynolds et al., 1981; Wilcox and Prakash, 1981). Rad10-Rad1 showed that it was only functional as an endonuclease when it was a heterodimer (Davies et al., 1995). It showed specificity for substrates with singlestrand/doublestrand (ss/ds) DNA junctions with 3' single-stranded overhangs, releasing the 3' overhangs (Bardwell et al., 1994; Davies et al., 1995). Similarly, in higher eukaryotes, the roles for ERCC1 and XPF in NER was discovered by the ability of these proteins to restore UV resistance to NER-deficient Chinese Hamster Ovary (CHO) cell lines (Brookman et al., 1996; van Duin et al., 1986). Subsequently, XPF-ERCC1 was shown to possess structural specificity similar to Rad10-Rad1 in incising ss/dsDNA junctions, consistent with performing the incision 5' to a lesion in NER (de Laat et al., 1998a; Sijbers et al., 1996a).

NER consists of two pathways, global genome NER (GG-NER) and transcription-coupled NER (TC-NER) that feed into a common nucleotide excision repair pathway (Hanawalt and Spivak, 2008) (Figure 1-4). As the name suggests, GG-NER deals with DNA d amage throughout the genome, whereas TC-NER allows the cell to preferentially repair the transcribed strand of genes. TC-NER is initiated by a stalled RNA polymerase II at a DNA lesion (Leadon and Lawrence, 1991; Venema et al., 1992) and also requires the CSA, CSB and XAB2 proteins (Henning et al., 1995; Nakatsu et al., 2000; Troelstra et al., 1992). GG-NER by contrast is initiated by XPC-RAD23B, which detects the helical distortion induced by lesions in DNA (Araki et al., 2001; Min and Pavletich, 2007; Sugasawa et al., 1998; Volker et al., 2001), and in some cases with the help of the UV-DDB protein complex (Scrima et al., 2008). Following damage recognition the two pathways are believed to operate by the sequential recruitment and

assembly of the same downstream proteins (Fousteri et al., 2006; Houtsmuller et al., 1999; Volker et al., 2001)Figure 1-4. The ten-subunit transcription factor and NER factor TFIIH is recruited to the site of damage, the DNA opens up and the presence of the lesion is then verified by one of the two helicase subunits of TFIIH, XPD (Schaeffer et al., 1993) (Schaeffer et al., 1994) (Sugasawa et al., 2009). Engagement of TFIIH with the lesion provides a landing platform for the next set of NER factors, XPA, RPA and XPG (Riedl et al., 2003; Tapias et al., 2004; Wakasugi and Sancar, 1998). RPA has a preferred binding site of 30 nucleotides of ssDNA, binds the non-damaged strand of DNA to help position the two endonucleases XPF-ERCC1 and XPG and to protect the gap during repair synthesis (de Laat et al., 1998a; Riedl et al., 2003) XPG is a latent endonuclease with a role in assembling the NER preincision complex as well as making the inision 3' to the lesion (Mu et al., 1997; Wakasugi et al., 1997). XPA interacts with TFIIH, RPA and DNA in the pre-incision complex and then recruits XPF-ERCC1 through its interaction with ERCC1 (Li et al., 1994; Li et al., 1995; Park and Sancar, 1994; Saijo et al., 1996). In addition to a core folded region, XPA has unstructured regions. One of these, encompassing a GGGF motif undergoes a disorder to order transition upon binding to the central domain of ERCC1 and is necessary and sufficient for the interaction with XPA and recruitment of XPF-ERCC1 to damaged sites in DNA (Orelli et al., 2010a; Tsodikov et al., 2007). Previously thought to be a simple matter of cutting and pasting, dual incision and repair DNA synthesis is now known to be a complex and tightly coordinated process starting with 5' incision by XPF-ERCC1, followed by initiation of repair DNA synthesis, 3'incision by XPG and completion of repair synthesis and ligation (Staresincic et al., 2009a). Repair synthesis involves at least three polymerases (Pol δ, Pol ε and Pol κ) and accessory factors and the nick may be sealed by either DNA ligase III/XRCC1 (Moser et al., 2007; Shivji et al., 1995).

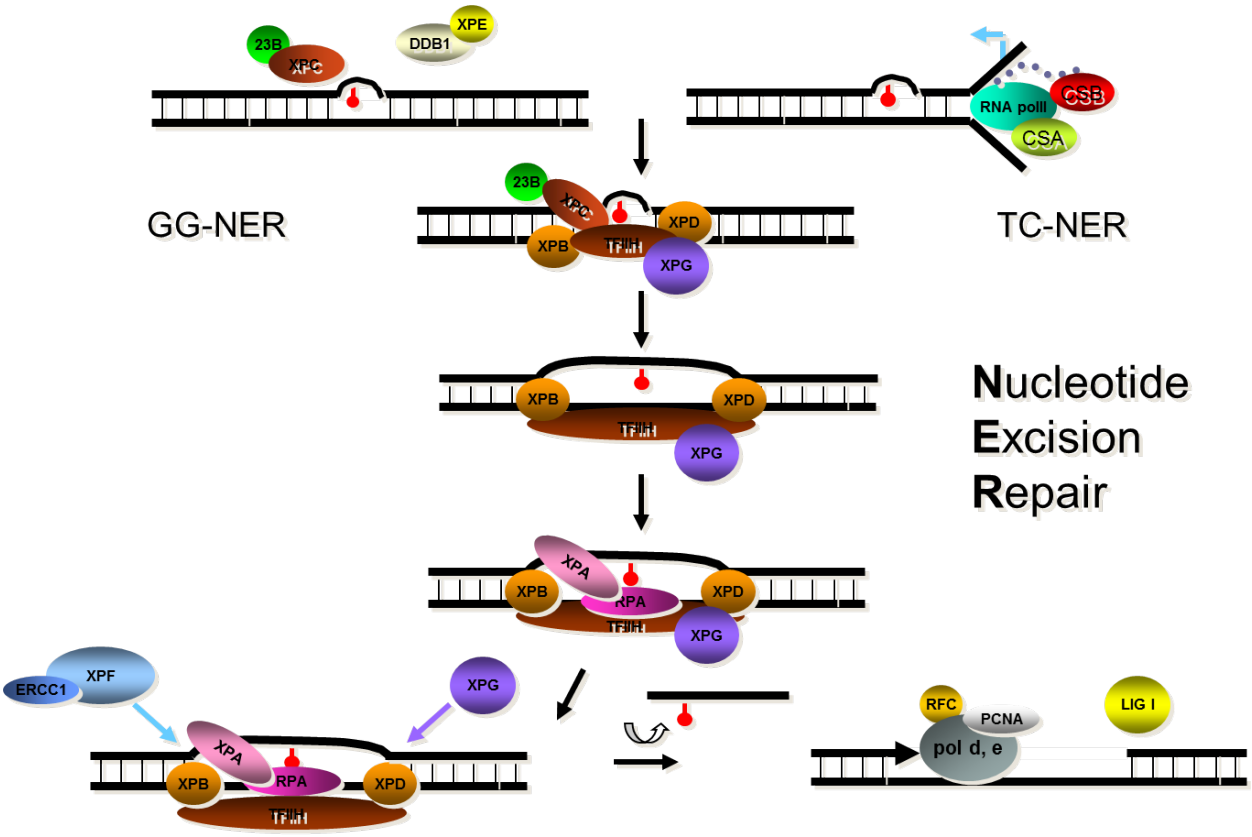

Figure 1-4 Schematic of the NER pathway

1.2.2 Interstrand Crosslink Repair

ICLs are formed when a bifunctional alkylating agent covalently binds a base on each strand of duplex DNA, thereby preventing strand separation necessary for replication or transcription (McHugh et al., 2001). In S-phase cells ICLs are converted into DSBs making crosslinks extremely cytotoxic. The basic model of ICL repair has been developed based on research in prokaryotic and eukaryotic model systems (Dronkert and Kanaar, 2001). In *E.coli*, ICL repair consists of the removal of the crosslink from the DNA by a process controlled by uvrB and subsequent recombination repair by the recA gene product (Kohn et al., 1965; Lawley and

Brookes, 1965, 1968). The ICL repair mechanism in *S. cerevisiae* is well studied and appears to be different from its mammalian counterpart. In this case, unlike XPF-ERCC1 in mammals, Rad10-Rad1 seems to be involved in ICL repair as a part of the NER machinery. In yeast, ICL REPAIR is performed by a combination of NER proteins, homologous recombination (HR) repair proteins (Jachymczyk et al., 1981), PSO2/SNM1 (Henriques and Moustacchi, 1980; Henriques et al., 1989; Ruhland et al., 1981), base excision repair (BER) proteins (McHugh et al., 1999), mismatch repair (MMR) proteins (Durant et al., 1999) and translesion synthesis (TLS) proteins (Sarkar et al., 2006). The ICL repair mechanism in mammals remains poorly defined (for detailed review, see (Sengerova et al., 2011). Proteins from multiple DNA damage repair and tolerance pathways appear to be involved in ICL repair. Data from genetic analysis and crosslink hypersensitivity of mutant cells and organisms shows the involvement of XPF-ERCC1 (Collins, 1993), HR proteins such as XRCC2 and XRCC3 (De Silva et al., 2000; Liu et al., 1998), MSH2-MSH3 (MutSβ) heterodimer (Zhang et al., 2002), RPA, PCNA (Li et al., 2000; Zhang et al., 2003), PSO4 complex (PSO4/PRP19, CDC5L, PLRG1, SPF27) (Zhang et al., 2005), WRN (Zhang et al., 2005), BRCA2 (Yu et al., 2000), EME1-MUS81 (Abraham et al., 2003; McPherson et al., 2004), SNM1a and SNM1b (Bae et al., 2008; Dronkert et al., 2000; Hazrati et al., 2008; Ishiai et al., 2004; Wang et al., 2011) and the Fanconi anemia (FA) proteins (Auerbach and Wolman, 1976; Crossan and Patel, 2012; Crossan et al., 2011b; Fujiwara and Tatsumi, 1977; Sasaki and Tonomura, 1973; Thompson and Hinz, 2009).

When the replication machinery encounters a crosslink, because the two strands of DNA cannot be separated, it cannot move past the damage, and the replication fork is therefore blocked. This activates ataxia telangiectasia and Rad3 related (ATR) protein (Stiff et al., 2006), which along with its downstream target CHK1 phosphorylates multiple proteins, which include

the FA proteins FANCA, FANCG, FANCE, FANCD2, FANCI and FANCM (Andreassen et al., 2004; Collins et al., 2009; Matsuoka et al., 2007; Meetei et al., 2005; Pichierri and Rosselli, 2004; Qiao et al., 2004; Smogorzewska et al., 2007; Wang et al., 2007; Yamashita et al., 1998), and Histone H2A.x (H2AX) (Ward and Chen, 2001) and Nijmegen breakage syndrome 1(NBS1) (Pichierri and Rosselli, 2004). These phosphorylations activate the FA DNA repair pathway leading to monoubiquitination of FANCD2 and FANCI – the ID complex – that act as a signal for cell cycle checkpoints and DNA repair (Meetei et al., 2003; Smogorzewska et al., 2007). This step is not dependent on XPF-ERCC1, and FANCD2 monoubiquitination appears to be normal although persistent in XPF-ERCC1 deficient cells (Bhagwat et al., 2009b) (Figure 1-5). The repair of a crosslink involves its removal from both strands of DNA one at a time and therefore poses a considerable challenge to cells. A number of endonucleases have been implicated in the incision step of ICL repair, such as XPF-ERCC1 (De Silva et al., 2000; Kuraoka et al., 2000; Niedernhofer et al., 2004) EME1-MUS81 (Hanada et al., 2007; Hanada et al., 2006), SLX1-SLX4 (Andersen et al., 2009; Fekairi et al., 2009; Joyce et al., 2009; Munoz et al., 2009b; Parmar et al., 2009; Stoepker et al., 2011a; Svendsen et al., 2009) and FAN1 (O'Donnell and Durocher, 2010; Smogorzewska et al., 2010). Initial incision is probably made by the XPF-ERCC1 ortholog EME1-MUS81, producing a DSB (Hanada et al., 2007; Hanada et al., 2006). ICL-induced DSBs can occur even in the absence of XPF-ERCC1 (Niedernhofer et al., 2004). However, XPF-ERCC1 is required for the resolution of these breaks as it makes the incision on the other side of the crosslink, thereby releasing it from one strand, a process known as “unhooking” (De Silva et al., 2000; Kuraoka et al., 2000; Niedernhofer et al., 2004). This function of XPF-ERCC1 is necessary for the efficient binding of FANCD2 to the chromatin (Bhagwat et al., 2009b; McCabe et al., 2008). Once the ICL is unhooked, the hSNM1a

exonuclease then removes the crosslinked oligonucleotides giving rise to a gapped intermediate which forms a good substrate for (Wang et al., 2011) a translesion polymerase, such as polζ to fill the gap in an error prone fashion (Raschle et al., 2008). The FA proteins then coordinate the repair of the replication fork through recruitment of the homologous recombination repair (HRR) (Thompson and Hinz, 2009).

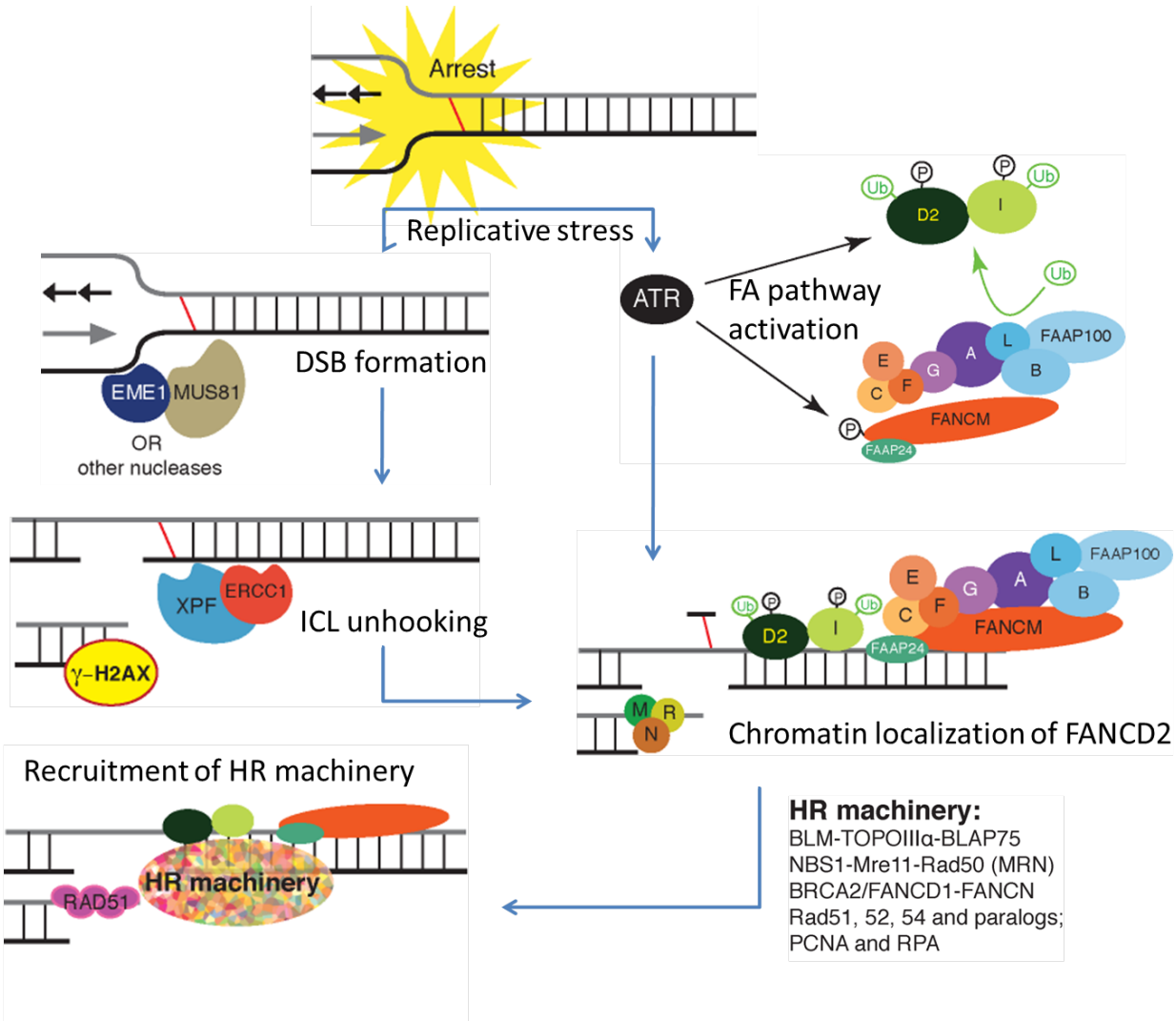

Figure 1-5 Schematic of the ICL DNA repair pathway

1.2.3 Double Strand Break Repair

DNA DSBs are extremely cytotoxic and can lead to cell cycle arrest, and cell death if left unrepaired (Khanna and Jackson, 2001). Homologous recombination and non-homologous end joining are the two major DSB repair pathways. In addition, a number of often overlapping error-prone pathways take over when repair by classical pathways is not possible. These alternate pathways, including single strand annealing (SSA) and microhomology-mediated end joining (MMEJ), depend on sequence homology to a variable degree. A large portion of our knowledge about these alternative DSB repair pathways comes from yeast systems (for detailed review, see (Paques and Haber, 1999).

Rad10-Rad1, the Saccharomyces cerevisiae homolog of XPF-ERCC1 functions in single strand annealing (SSA) and micro homology mediated end joining (MMEJ), which repair DSBs in regions of DNA containing sequence-repeats. SSA (Figure1-4) is a Rad52 dependent process (Mortensen et al., 1996) that uses regions of intrachromosomal sequence repeats with 29bp or more homology (Sugawara et al., 2000). After exonuclease-processing of the DSB ends, 3' overhangs are formed on both sides (Sugawara and Haber, 1992; Sun et al., 1991). Rad10-Rad1 can prune the ends to remove nonhomologous sequences and allow repair to occur (Fishman-Lobell and Haber, 1992; Ivanov and Haber, 1995). SSA is dependent on Msh2 and Msh3 for regions of homology <1kb (Sugawara et al., 1997). Msh2 interacts with Rad10 (Bertrand et al., 1998) and probably recruits Rad10-Rad1 to the DSB for end processing (Paques and Haber, 1997).

A role for mammalian XPF-ERCC1 in SSA-mediated DSB repair was suggested by the deficiency of *Ercc1* mutant CHO cells in processing heteroduplex intermediates of the recombination between repeat sequences (Sargent et al., 2000; Sargent et al., 1997). XPF-ERCC1 is required to remove 3' single stranded tails that are formed in these intermediates and failure to remove these, leads to deletions at the sites of recombination. XPF-ERCC1 interacts with RAD52 and this interaction enhances the ability of the nuclease in incising 3' single stranded flaps (Motycka et al., 2004). It was later discovered that XPF-ERCC1 has a role in SSA and in gene conversions similar to yeast (Al-Minawi et al., 2008). Irrespective of the sequence homology status, XPF-ERCC1 is required for integration of exogenous DNA into the genome, for example, the targeted gene replacement in mouse ES cells (Niedernhofer et al., 2001).

MMEJ is an alternative end joining pathway that depends on sequence homologies as small as 1-5 nucleotides (Roth and Wilson, 1986). Studies in yeast show that it is independent of Rad52 and Ku86 (Yu and Gabriel, 2003), but requires Mre11-Rad50-Xrs2 (the MRX complex) (Haber, 2006; Ma et al., 2003), Msh2, Pms1 (Decottignies, 2007), Nej1, error prone DNA polymerases including Pol4, Rad30, Rev3, and Pol32, the flap endonuclease Sae2, and Tel1 (Lee and Lee, 2007). Similar to SSA, the role of Rad10-Rad1 in this pathway is probably the removal of non-homologous 3' single stranded overhangs.

In mammals, the existence of the MMEJ pathway is evident from persistent end joining repair in non-homologous end joining (NHEJ) deficient cells (Feldmann et al., 2000; Guirouilh-Barbat et al., 2004; Kabotyanski et al., 1998). *Ercc1*$^{-/-}$ mouse embryonic fibroblasts (MEFs) are hypersensitive to γ-irradiation, but *Ercc1*$^{-/-}$ mouse embryonic stem (ES) cells are not (Ahmad et al., 2008). This pattern of cell type-specific hypersensitivity is reminiscent of that seen in the NHEJ-deficient DNA-PK$_{CS}$ null cells (Gao et al., 1998) suggesting that this is not a defect in

HRR. *Ercc1*$^{-/-}$*Ku86*$^{-/-}$ mice are not viable and the double knockout MEFs are more sensitive to radiation than either of the single mutants. However, a linearized plasmid DNA with microhomologies on both ends shows large deletions after repair in *Ercc1* mutant CHO cells (Ahmad et al., 2008). These data suggest that XPF-ERCC1 functions in MMEJ.

In *S. pombe*, individual cells undergo spontaneous mating-type switch during growth. This involves formation of a defined DSB at a switching signal locus followed by recombination-mediated repair. Strains *rad16* (*swi9, RAD10* homolog) and *swi10* (*RAD1* homolog) have a defect in mating-type switching recombination (Carr et al., 1994; Schmidt et al., 1989). Additionally, they are sensitive to ionizing radiation (IR) (Schmidt et al., 1989). In *A. thaliana*, deficiency of AtERCC1 leads to IR sensitivity, indicating a role for AtERCC1 in DSB repair (Hefner et al., 2003). In *Drosophila*, mutation of *mei-9* (*XPF* homolog) also leads to IR sensitivity (Baker et al., 1978). Thus, XPF-ERCC1 and its homologs function in multiple subtypes of DSB repair.

1.2.4 Meiotic Recombination

Meiosis is accompanied by crossover events between homologous chromosomes, allowing for segregation of polymorphisms. This crossover is brought about by meiotic recombination, a mechanism akin to the HRR mechanism, but between homologous chromosomes with divergent sequences, instead of sister chromatids that are identical at the sequence level. *Drosophila mei-9* mutants are defective in meiotic crossover. They display a marked decrease in crossovers and an increase in chromosome non-disjunction (Carpenter and Baker, 1982; Yildiz et al., 2004). There is also an increase in postmeiotic segregation, indicating a failure to repair heteroduplex DNA formed during noncrossover recombination events (Yildiz et al., 2004). These findings suggest

that MEI-9 is required for the resolution of Holliday junctions (HJ) formed during meiosis. MEI-9 interacts with MUS312, and disruption of the MUS312-MEI-9 interaction produces a phenotype similar to the loss of either MUS312 or MEI-9 (Yildiz et al., 2002). Recent evidence suggests that HDM, a single-stranded-DNA binding protein, forms a complex with MUS312, MEI-9 and ERCC1 that resolves the HJs (Joyce et al., 2009). Interestingly, the human ortholog of MUS312, SLX4/FANCP binds multiple different endonucleases including XPF-ERCC1 (Fekairi et al., 2009; Svendsen et al., 2009).

Mice have elevated *Xpf* and *Ercc1* mRNA levels in the meiotic and early postmeiotic cells involved in spermatogenesis (Shannon et al., 1999). Both male and female *Ercc1*-mutant mice are infertile. XPF-ERCC1 is important at all stages of development and maturation of both male and female gametes, but there is no evidence that it is required for meiotic crossovers (Hsia et al., 2003).

1.2.5 Telomere Maintenance

Telomeres have 3' single stranded overhangs with G-rich repeat sequences. This is an ideal substrate for cleavage by XPF-ERCC1. XPF-ERCC1 was found to be associated with the telomeric TRF2 complex, and prevents recombination of telomeric DNA with interstitial telomere-like repeats. The absence of XPF-ERCC1 produces telomeric DNA-containing double minute (TDM) chromosomes. On the other hand, in the absence of TRF2, XPF-ERCC1 cleaves the 3' overhangs allowing telomeres to be subjected to NHEJ. This leads to telomere fusions and dicentric chromosomes (Zhu et al., 2003). In essence, XPF-ERCC1 and TRF2 seem to be acting antagonistically, preventing each other from damaging the telomere. Strangely, TRF2-dependent loss of telomeres, caused by TRF2 overexpression is dependent on XPF-ERCC1 (Munoz et al.,

2005). What is even more perplexing is that this action requires the physical presence of XPF-ERCC1, but not its nuclease activity (Wu et al., 2007). Also, overexpression of wild-type but not nuclease-dead XPF reduces the telomere binding of TRF2. Apparently, XPF-ERCC1 acts on the telomere through two distinct mechanisms, a nuclease-dependent mechanism that affects TRF2 binding, and a nuclease-independent mechanism that limits telomere length (Wu et al., 2008). XPF-ERCC1 interacts with TRF1 in a very similar way and contributes to telomere shortening and end-fusions in the absence of TRF1 (Munoz et al., 2009b). A similar mechanism exists in *A. thaliana*, where XPF-ERCC1 prevents recombination of telomeres with interstitial telomeric repeats (Vannier et al., 2009).

1.2.6 Repair of Topoisomerase 1 Lesions

Progression of replication forks along DNA creates superhelical strain on the unreplicated duplex. Topoisomerase I (Top1) releases this supercoiling by transiently cutting one strand of the duplex and forming a protein-DNA complex with that strand, allowing it to unwind in an ATP dependent mechanism (Champoux, 2001). When a replication fork collides with a Top1-DNA intermediate, it is blocked, leading to a DSB (Hsiang et al., 1989). Top1 poisons such as camptothecin cause the Top1 protein to remain attached to the 3' end of the unreplicated DNA rendering it inaccessible to repair. Tdp1 removes the Top1 molecule and creates a 3' phosphate (Pouliot et al., 1999). In *S. cerevisiae* this substrate is further processed by the activities of Tpp1, Apn1 and Apn2 to convert it from a repair-blocking lesion to a 3' hydroxyl group amenable to repair (Vance and Wilson, 2001). Although the yeast *RAD1* and *RAD10* mutants are not sensitive to Top1 poisons such as camptothecin, Rad10-Rad1 was found to function in a backup pathway for repair of Top1 lesions (Liu et al., 2002; Vance and Wilson, 2002). In the absence of Tdp1,

Rad10-Rad1 likely incises a 3' single stranded flap, removing an oligonucleotide containing the Top1-DNA intermediate and allowing for a Rad52-dependent homologous recombination to repair the fork (Vance and Wilson, 2002).

1.2.7 Repair of Abasic Sites

Apurinic/apyrimidinic (AP) sites are produced as a result of depurination or depyrimidination of DNA due to spontaneous hydrolysis of the bond between the base and the DNA backbone. In a mammalian cell, over a span of 24 hours, approximately 10,000 purines (Lindahl, 1979) and about 500 pyrimidines (Lindahl and Karlstrom, 1973) are lost by this process. AP sites are also produced by DNA glycosylases as intermediates of base excision repair (BER) (Duncan et al., 1976; Lindahl, 1976). In *S. cerevisiae* removal of misincorporated uracil by uracil DNA glycosylase appears to be the major endogenous contributor towards AP sites (Guillet and Boiteux, 2003). *S. cerevisiae* mutants defective in both yeast AP endonucleases are viable, but triple mutants *apn1 apn2 rad1* and *apn1 apn2 rad10* are not viable, suggesting that Rad10-Rad1 functions in a backup pathway of AP site repair (Guillet and Boiteux, 2002). Although NER plays a role in removal of AP sites (Swanson et al., 1999; Torres-Ramos et al., 2000) this mechanism seems to be independent of NER, as evident from the viability of *apn1 apn2 rad14* strains (Guillet and Boiteux, 2002). In this case, the genetic evidence suggests that similar to the Top1 lesion repair, Rad10-Rad1 works by removing the 3' flap resulting from the spontaneous hydrolysis of the abasic site (Boiteux and Guillet, 2004). Similarly, in mammals, the abasic sites produced by activation-induced cytidine deaminase (AID) during class-switch recombination in B-cells are repaired by XPF-ERCC1 (Schrader et al., 2004).

1.3 PHYSIOLOGOCAL FUNCTIONS OF XPF-ERCC1

1.3.1 Human diseases associated with defects in XPF-ERCC1

The severity and manifestation of XPF-ERCC1 deficiency in humans varies significantly. Interpretation of the phenotype is complicated by the involvement of XPF-ERCC1 in multiple genome maintenance mechanisms.

1.3.1.1 Xeroderma pigmentosum

Xeroderma pigmentosum (XP) was the first hereditary condition to be associated with a defect in the repair of UV-induced DNA damage (J.E. Cleaver, Nature 1968). XP is an autosomal recessive syndrome characterized by sun sensitivity with a 2000-fold increase in skin cancers over sun-exposed areas, which include basal cell carcinoma, squamous cell carcinoma, malignant melanoma, keratoacanthoma, fibrosarcoma, and angioma (Kraemer et al., 1987). There is also evidence for increased incidence of sarcomas. Patients with mutations affecting both global and transcription-coupled NER present with progressive neurodegeneration, probably due to accumulation of damage in transcribed genes (Brooks, 2008). The severity and age of presentation varies widely amongst patients, depending on the mutation and the protein affected. Using somatic cell hybridization, the eight complementation groups of XP from XP-A through G and the variant form, XP-V were identified (de Weerd-Kastelein et al., 1974; Keijzer et al., 1979; Kraemer et al., 1975; Lehmann et al., 1975). XP-F was first reported in Japan and usually presents with a mild phenotype with late onset of disease (Matsumura et al., 1998), although in some cases a late onset neurodegenerative phenotype is seen. Mutant XPF protein may fail to localize to the nucleus, leading to mislocalization of both ERCC1 and XPF to the cytoplasm

(Ahmad et al., 2010). This produces a phenotype disproportionate to the ability of these mutants to reconstitute NER *in vitro*. There is no known *ERCC1* mutation that presents as XP.

1.3.1.2 XFE progeroid syndrome

Most patients with *XPF* mutations have a mild XP phenotype. However, a patient with XPF R153P mutation presented with a progeroid phenotype in addition to sun sensitivity (Niedernhofer et al., 2006). Arginine-153 lies in the helicase-like domain of XPF and is highly conserved. To date this remains the only published case of the XFE (XPF-ERCC1) progeroid syndrome. Remarkably, despite photosensitivity and abnormal skin pigmentation, there was no evidence of skin cancer. There was evidence of growth retardation, including short stature, microcephaly and developmental delay. Further investigations showed an array of aging-related degenerative changes. Although the patient had a normal birth-weight, he was cachexic at presentation. His skin was dry and atrophic, and lacked subcutaneous fat. He had bird-like facies with prominent bones and an aged appearance. Neurodegeneration was evident from cerebral atrophy, tremors and ataxia with loss of coordination, impaired hearing and vision loss with optic atrophy. Scoliosis, muscle wasting and hypotonia suggested musculoskeletal degeneration. In addition, there was hypertension, renal and hepatic insufficiency, and anemia, which distinguished this case from the DeSanctis-Cacchione and Cockayne syndromes. The patient died at the age of 16 years from multi-organ failure following pneumonia. These symptoms are remarkably similar to the presentation of the *Ercc1*$^{-/-}$ (Niedernhofer et al., 2006) and the *Xpf* $^{-/-}$ (Tian et al., 2004) mouse models which also show an accelerated aging phenotype.

Fibroblasts obtained from a skin biopsy of the patient showed markedly decreased UV induced unscheduled DNA synthesis (UV-UDS) (~5% of wild-type). They were more sensitive to UV than XP-F patient fibroblasts, though less so than XP-A fibroblasts. They were exquisitely

hypersensitive to the crosslinking agent MMC, indicating that a deficiency in ICL repair may have a significant contribution to this phenotype. XPF has been shown to play an important role in mitosis by its suggested interaction with kinesin, KIF11 (Tan et al., 2012). Consequently, the abnormality in mitosis caused by the severe deficiency of XPF in the XFE patient might be responsible for the accelerated aging phenotype observed.

1.3.1.3 Cranio-occulo-facio-skeletal syndrome (COFS)

The only known patient with an *ERCC1* mutation was born with low birth-weight, microcephaly with premature closure of the fontanels, bilateral microphthalmia, blepharophimosis, high nasal bridge, short filtrum, micrognathia, low-set and posteriorly-rotated ears, arthrogryposis with rocker-bottom feet, flexion contractures of the hands, and bilateral congenital hip dislocation. Magnetic resonance imaging showed a simplified gyral pattern and cerebellar hypoplasia. This patient was diagnosed with COFS. Classic COFS is defined by microcephaly, hypotonia, microphthalmia, cataracts, blepharophimosis, large ear pinnae, prominent root of the nose, micrognathia, widely set nipples, camptodactyly, flexure contractures at the elbows and knees, generalized osteoporosis, dysplastic acetabula, coxa valga, rocker-bottom feet and failure to thrive (Pena and Shokeir, 1974). Previously, COFS has been diagnosed in patients with mutations of either *CSB* (Meira et al., 2000) or *XPD* (Graham et al., 2001).

1.3.2 Mouse models of XPF-ERCC1 deficiency

1.3.2.1 *Ercc1*$^{-/-}$ mouse

Two groups independently made *Ercc1*$^{-/-}$ mice (McWhir et al., 1993a; Weeda et al., 1997a). In the first case, *Ercc1* was targeted with a *neo* insert between exons 4 and 6 using an HPRT

minigene based system (Selfridge et al., 1992). In the second case, two mouse models were made, one with a *neo* insert in exon 7 (*Ercc1*-knockout mouse) and the other with a stop codon at position 292 of ERCC1, producing a truncated version of the transcript (*Ercc1*^{*292} or *Ercc1*$^{7\Delta}$ allele, discussed further under *Ercc1* hypomorphs). The *Ercc1*-knockout mice are born at sub-Mendelian ratios due to an early embryonic lethality. All mutant mice are runted at birth and display shortened lifespan of about 3 - 4 weeks. The mutant mice show abnormalities of liver, with large polyploid nuclei. Mice die of hepatic failure and show increased p53 in liver, kidneys and brain (McWhir et al., 1993a). The primary MEFs isolated from these mice grow slower than their wild-type counterparts (Niedernhofer et al., 2006; Weeda et al., 1997a). These MEFs and mouse livers have elevated p21 levels, suggesting that they are undergoing senescent changes (Nunez et al., 2000; Weeda et al., 1997a). Also, as noted before, the *Ercc1*$^{-/-}$ mice have delayed cerebellar development (Jaspers et al., 2007). This phenotype is dramatically different from that of *Xpa*$^{-/-}$ mice, which are phenotypically nearly indistinguishable from the wild-type littermates (de Vries et al., 1995). *Ercc1*$^{-/-}$ mice have reduced hematopoietic reserve and demonstrate a multilineage cytopenia with reduction in stress induced erythropoiesis and fatty replacement of the bone marrow (Prasher et al., 2005). This resembles Fanconi anemia, a disease characterized by hypersensitivity to ICL repair (Parmar et al., 2009). This suggests that at least a part of the phenotype of *Ercc1*$^{-/-}$ mice is due to a deficiency in ICL repair. Additionally, these mice show neurodegenerative changes including dystonia and ataxia, musculoskeletal degeneration evident from sarcopenia and kyphosis and renal failure. Combined with the cellular senescence these findings suggest accelerated aging and led to the identification of anew human progeria caused by the reduced expression of XPF-ERCC1 (Niedernhofer et al., 2006).

1.3.2.2 *Xpf* $^{m/m}$ mouse

Mutant XPF mice were generated by mimicking the XPF mutation in patient XP23OS (Tian et al., 2004). Mouse *Xpf* was mutated with a *neo* insert between exons 7 and 8 and a stop codon at position 445 (Tian et al., 2004). This mutation eliminated Xpf activity without affecting normal mouse development. In keeping with the obligate heterodimeric nature of ERCC1 and XPF, the mouse is a phenocopy of the *Ercc1*$^{-/-}$ mouse. The mice are runted, with enlarged and polyploid hepatocytes and die within 3 weeks of birth. Further analysis was not done.

1.3.2.3 *Ercc1* hypomorphs

The *Ercc1*$^{\Delta/\Delta}$ mice were generated by inserting a stop codon at position 292 of *Ercc1* (Weeda et al., 1997a). This resulted in a truncated transcript and presumably a protein that is seven amino acids short at the C-terminus. The C-terminus of ERCC1 is indispensible for its function (Sijbers et al., 1996b) and so the truncation should significantly affect the function of XPF-ERCC1. In fact, the transcript from the Δ allele is reduced to about 15% of the wild-type allele (Weeda et al., 1997a). The *Ercc1*$^{\Delta/\Delta}$ mice live for about 6 months from birth, a lifespan intermediate between the *Ercc1*$^{-/-}$ and wild-type mice. Aside from liver changes reminiscent of the knockout mice, they also display ferritin deposition in the spleens, thin skin lacking subcutaneous fat and renal tubular dilatation with abnormal nuclei and proteinuria indicative of renal insufficiency. Unlike the *Ercc1*$^{-/-}$ mice, TUNEL assay shows no evidence of increased apoptosis in tissues. The mice are infertile, but histologically both ovaries and testes appear normal. The hepatocellular functions observed in the *Ercc1*$^{-/\Delta}$ mice mimic the phenotype observed in old wild-type mice (Gregg SQ., 2012). *Ercc1*$^{-/\Delta}$ mice with LacZ transgene were analyzed by recovery of LacZ containing plasmid and isolating clones lacking LacZ expression. LacZ mutants were further analyzed to determine the type of mutations leading to inactivation of the gene. This LacZ

mutation analysis shows a rapid accumulation of mutations in the livers of these animals. Mutations included point mutations similar to the NER deficient *Xpa*$^{-/-}$ mice and deletions and translocations, probably stemming from the loss of ICL repair and DSB repair related functions of XPF-ERCC1 (Dolle et al., 2006).

1.3.2.4 *Ercc1* conditional mutants

In order to correct the hepatic failure of *Ercc1*$^{-/-}$ mice, transgenic *Ercc1* was expressed with a liver specific transthyretin promoter (Selfridge et al., 2001). This prevented the polyploidy of hepatocytes and liver failure, and increased lifespan up to 61 – 88 days, but the mice died of renal failure with a similar polyploid phenotype in the proximal tubule cells. These mice also had elevated plasma lactate levels, pointing towards possible mitochondrial consequences of ERCC1 deficiency. Neurodegeneration was evident from lack of coordination, ataxia and loss of visual acuity, but no histological changes in the brain were detected (Lawrence et al., 2008).

Ercc1$^{-/-}$ mice have an extremely short lifespan, making it difficult to study the UV sensitivity of their skin. To overcome this problem, mice were made with a floxed *Ercc1* allele under bovine *K5* promoter. These mice showed 20-fold increase in sensitivity to the short-term erythematous changes in epidermis with UV-B irradiation. They also displayed a rapid onset of tumors, mainly squamous cell carcinomas, which grew faster than those in wild-type animals (Doig et al., 2006).

1.3.3 Altered expression of XPF-ERCC1 in cancers

XPF-ERCC1 functions in major genome maintenance pathways including NER (Sijbers et al., 1996a), ICL repair (De Silva et al., 2000), DSB repair (Murray et al., 1996; Murray and

Rosenberg, 1996) and telomere maintenance (Wu et al., 2008; Zhu et al., 2003). Various chemotherapeutic agents and radiotherapy kill cancer cells by damaging their DNA. Cisplatin, a common chemotherapeutic drug, induces cytotoxicity through DNA lesions that are cleared by the NER and ICL repair pathways. Being the only proteins to be essential to both pathways has made ERCC1 and XPF attractive biomarkers. If XPF-ERCC1 expression is variable in cancers, it may have a bearing on the growth characteristics of tumors, their response to various therapies and overall patient survival. This promise has led to extensive attempts at devising strategies to evaluate the effect of both ERCC1 and XPF, but mainly ERCC1, on tumor biology. These include studies of short nucleotide polymorphisms (SNP), mRNA levels, and Immunohistochemistry for protein levels.

1.3.3.1 SNPs

SNPs may affect protein expression or function based on their nature and location. A non-conservative base substitution may change amino acid sequence, thereby directly affecting protein function. A conservative substitution may alter rate of mRNA translation by altering the choice of tRNA or effect on protein folding due to slow translation. Polymorphisms near promoters or introns can affect protein expression through transcription. There is however no direct evidence that, polymorphisms of *ERCC1* or *XPF* can affect protein levels. A survey of polymorphisms in NER genes found that *ERCC1* contains at least seven SNPs and *XPF* has six. *ERCC1* contains no SNPs with amino acid substitutions, while *XPF* has one that leads to P379S substitution (Shen et al., 1998). A commonly studied silent polymorphism of ERCC1, codon 118(C/T) changes a commonly used codon AAC to AAT, one that is infrequently used. This can potentially reduce the translation of the mRNA leading to reduced protein levels (Yu et al., 1997). Once again, there is no evidence of a difference in protein or mRNA levels caused by this

SNP. Despite this, *ERCC1* SNPs have shown correlation with outcomes of many different types of tumors. Of these, non-small cell lung carcinoma (NSCLC) has been the most extensively studied. Numerous studies have found correlation between risk, survival and treatment response in NSCLC with either or both of codon 118 and C8092A polymorphisms of *ERCC1* (Isla et al., 2004; Kalikaki et al., 2009; Park et al., 2006; Su et al., 2007; Takenaka et al., 2009; Zienolddiny et al., 2006). On the other hand, a large meta-analysis of multiple studies failed to find any correlation (Kiyohara and Yoshimasu, 2007). Several other cancers, including esophageal cancer (Doecke et al., 2008; Pan et al., 2009), ovarian cancer (Steffensen et al., 2008), squamous cell carcinoma of head and neck (Quintela-Fandino et al., 2006), basal cell carcinoma (Yin et al., 2003) and bladder cancer (Garcia-Closas et al., 2006) have shown correlation of outcome or chemotherapy resistance to *ERCC1* genotypes. However, studies involving pancreatic adenocarcinoma (McWilliams et al., 2008), carcinoma of prostate (Hooker et al., 2008), colorectal carcinoma (Hansen et al., 2008; Monzo et al., 2007), glioma (Chen et al., 2007), renal cell carcinoma (Hirata et al., 2006) and cervical carcinoma (Chung et al., 2006) did not find any link to *ERCC1* SNPs.

1.3.3.2 mRNA

Interest in *ERCC1* mRNA levels stemmed from the thought that these may be representative of the functional ERCC1 in cells. There is no evidence to suggest that ERCC1 is regulated at the level of transcription. In fact, mRNA levels of *ERCC1* and *XPF* have absolutely no correlation to their respective protein levels (Deloia et al., 2012). All the same, multiple studies have suggested a correlation between the level of *ERCC1* mRNA in tumors or tumor cell lines from gastric, ovarian, colorectal, esophageal and non-small cell lung cancer and resistance to cisplatin (Altaha et al., 2004; Dabholkar et al., 1992; Dabholkar et al., 1994; Joshi et al., 2005; Langer et al., 2005;

Lord et al., 2002; Metzger et al., 1998; Reed et al., 2000; Rosell et al., 2002; Shirota et al., 2001; Warnecke-Eberz et al., 2004). However, the mechanism behind the predictive correlation remains undefined and may not be dependent on the DNA repair functions of the proteins. Similar to SNPs, mRNA levels of *ERCC1* are the most extensively studied in Non-small cell lung cancer (NSCLC). Based on findings that patients with low *ERCC1* expression in tumors respond better to cisplatin-based therapy (Lord et al., 2002), a clinical trial was carried out. Patients who received tailored chemotherapy based on the *ERCC1* expression performed better than those who received a standard control therapy with docetaxel and cisplatin (Cobo et al., 2007). Patients with low *ERCC1* levels performed somewhat better than those with high *ERCC1* levels and this is further certified by a recent study that identified that down regulation of XPF-ERCC1 by RNAi in cell lines from NSCLC, breast and ovarian cancer patients led to a significantly increased cisplatin cytotoxicity (Arora et al., 2010).

1.3.3.3 Protein levels in tumors

Measurement of XPF-ERCC1 levels by IHC of paraffin-embedded tumor samples is an attractive biomarker to study the effect of the protein levels on tumor response to various chemotherapeutic agents and patient survival. This is due to the relative ease of availability of samples, relative stability of proteins over RNA and advantage of processing large sets of samples economically over a short period of time. ERCC1 protein levels have been implicated in conferring resistance to a wide range of cancer types. Amongst the various tumors that have been under investigation, melanomas (Li and Melton, 2012), NSCLC (Niedernhofer et al., 2007), esophageal cancer (Kim et al., 2008b), ovarian cancer (Steffensen et al., 2008), testicular cancer (Welsh et al., 2004), breast cancer (Chen et al., 2012), and HNSCC (Jun et al., 2008) have shown a significant correlation between chemotherapy resistance and ERCC1. These studies demonstrate the utility

of ERCC1 as a predictive marker in a wide variety of tumors. NSCLC remains the most studied tumor type (Hwang et al., 2008; Lee et al., 2008; Olaussen et al., 2006a; Zheng et al., 2007). However, there are mixed results as to whether ERCC1 levels are predictive of resistance depending on the type of therapy administered. High ERCC1 expression correlated with poor response to cisplatin chemotherapy and poor survival outcome (Olaussen et al., 2006a). On the other hand, high ERCC1 was associated with better survival following surgery (Lee et al., 2008; Zheng et al., 2007). Unfortunately, the antibody (8F1) used in almost all studies is not specific for ERCC1 (Niedernhofer et al., 2007). It recognizes human ERCC1, but also a second unknown nuclear antigen, and is unable to discriminate between cells expressing XPF-ERCC1 and cells that do not (Niedernhofer et al., 2007). We rigorously tested antibodies against ERCC1 and XPF and found ones that are best suited for clinical measurement of XPF-ERCC1 (Bhagwat et al., 2009c). Our results show that ERCC1 and XPF levels in lung tumors vary considerably between patients, but are closely correlated to each other and either of these proteins can be used as a surrogate biomarker. The use of XPF as a biomarker to predict patient outcome has been largely unexplored with the exception of a report that suggests that low expression of XPF is a significant risk factor for HNSCC as measured by the reverse-protein microarray assay (Wei et al., 2005). This evidence is supported by reports that suggest a significant correlation between lower XPF protein expression and longer progression-free survival of HNSCC treated with DNA damaging agents and evidence of significantly higher XPF protein levels that were found in metastases of HNSCC as compared to primary cancer tissue (Koberle et al., 2010; Vaezi et al., 2011). These studies highlight the influence of ERCC1 and XPF protein levels on cancer outcome, but more analysis is essential to clarify the utility of ERCC1 and XPF as cancer biomarkers.

1.4 SIGNIFICANCE

In summary, XPF-ERCC1 is a structure specific endonuclease that is important for multiple genome maintenance mechanisms which include nucleotide excision repair, interstrand crosslink repair, and double strand break repair. The proteins are evolutionarily conserved in eukaryotes highlighting the biological importance of the proteins and they function as heterodimers that are unstable is the absence of one another. In humans, deficiency of XPF-ERCC1 leads to the development of the cancer prone syndrome Xeroderma pigmentosum and also the progeroid syndrome, XFE, are characterized by accelerated aging. It has been well established that XP that results from a deficiency in XPF is due to its inability to efficiently participate in NER. However, the specific repair pathway of XPF-ERCC1 and the kind of lesions that lead to the accelerated aging phenotype observed in both mice and humans deficient in XPF-ERCC1 remain unknown.

XPF-ERCC1 is involved in the repair of bulky monoadducts and intrastrand crosslinks by the nucleotide excision repair pathway and are also involved in the repair of interstrand crosslinks through the ICL repair pathway. These lesions collectively constitute the damage induced by chemotherapeutic drugs and the involvement of XPF-ERCC1 in repair of all of these lesions via multiple DNA repair mechanism has implicated them being used as biomarkers of chemoresistance. Even though the DNA repair functions of XPF-ERCC1 have been associated with chemoresistance, the exact mechanism remains unclear. In addition, since chemotherapeutic agents such as platinum drugs exert their cytotoxicity primarily through the formation of interstrand crosslinks, identifying ways to weaken the crosslink repair capacity of the cancer cells will help overcome chemoresistance.

Having reviewed the major functions of XPF-ERCC1 in DNA repair and their biological importance in preventing a wide range of disorders in the first chapter, we continue the journey and take another step forward in an attempt to provide more scientific insight into the mechanisms underlying the contribution of XPF-ERCC1 to cancer and aging.

Chapter 2 aims to collectively probe the importance of four DNA binding domains of XPF-ERCC1 located in the c-terminus of both proteins in NER and ICL repair. Analysis of cells harboring mutations in the DNA binding domains of XPF-ERCC1, the nuclease domain of XPF and the central domain of ERCC1, by testing their ability to incise model substrates and also comparing their sensitivities to different forms of DNA insult will help categorize the domains of both XPF and ERCC1 by their importance in DNA repair functions.

Chapter 3 of the dissertation document aims to test the hypothesis that the roles of XPF-ERCC1 in repair can be uncoupled by the disruption of specific protein:protein interactions that recruit XPF-ERCC1 to different DNA repair pathways. The c-terminus of XPF-ERCC1, the central domain of ERCC1, and the nuclease domain of XPF are well characterized. However, not much is known about the n-terminus of *XPF* and conserved residues in this region of *XPF* have been implicated in being important to interstrand crosslink repair. To explore the n-terminus and determine regions of the *XPF* gene that might be selectively essential for ICL repair but not NER, mutations in different conserved residues of the n-terminus of XPF will be targeted. The *XPF* mutants include an n-terminal deletion, a hemagglutin (HA) tag in the n-terminus, the G314E mutant that is known to disrupt the interaction between XPF and SLX4 in Drosophila, and the WLF-A mutant that harbors mutations in 3 conserved residues that lie in the n-terminus of *XPF*. The impact of each of these mutations on the protein function is estimated by observing the sensitivities of each mutant cell line to different forms of DNA insult such as UV, Mitomycin

C (MMC) and ionizing radiation (IR). In the future, this mutation that renders cells selectively sensitive to crosslink agents would in invaluable in understanding the link between XPF-ERCC1, cancer and aging. With respect to chemoresistance, this region of the *XPF* gene can be utilized to generate small molecule inhibitors that can sensitize patients who are resistant to chemotherapy. In addition, studying the phenotype of a mouse model harboring this mutant form of the XPF protein, that is deficient in ICL repair while still being able to carry out NER, will help understand whether the accelerated aging that is observed in both mice and humans deficient in XPF-ERCC1 is due to the accumulation of ICLs in the organism.

Chapter 4 of the dissertation aims to develop and characterize novel monoclonal antibodies against purified XPF-ERCC1 in complex that can be used to establish a conclusive association between the proteins levels and chemosensitivity by immunohistochemical analysis. Efforts towards breaching chemoresistance have been confined to utilizing the SNP data, mRNA levels and protein levels of XPF-ERCC1 as biomarkers. In the last few decades, there have been over 1000 published papers looking at the association between XPF-ERCC1 and the sensitivity of patients to chemotherapeutic regimes. However, the data does not conclusively establish an association between XPF-ERCC1 protein or mRNA levels and chemoresistance. The major cause for this is the lack of mechanistic understanding and also the deficit of proper scientific tools for analysis. The identification of good antibodies with good specificity and sensitivity will take us a step closer in predicting a patient response to a chemotherapeutic regime. The second and extended implication of the study is in identifying an antibody that will have antigen specificity to both XPF and ERCC1 thereby having the inherent potential to bind and destabilize the proteins. An antibody of this nature could potentially be used for adjuvant antibody therapy.

Finally, in Chapter 5, we aim to develop a method to measure the NER capacity of suspension cells. Measurement of repair has been mainly focused on determining the activity of one or more proteins in a repair pathway. While this approach shows promise, the activity of one or more proteins cannot be trusted to represent the overall repair capacity of a cell considering each pathway involves the coordinated activity of more than 30 proteins. Hence, the development of assays that can measure overall repair representative of all the proteins in a pathway will overcome this shortcoming. An assay that can measure the NER capacity of suspension cells such as blood cells will help tremendously in predicting an individual's predisposition to disorders such as XP very easily thereby helping patients and their families incorporate protective measures as early as possible. Measuring the repair capacity of lymphocytes from cancer patients using the method developed will help prospectively predict the extent of side effects that may be expected when a patient is exposed to a chemotherapeutic regime. In addition, the assay thus developed can be used to determine whether DNA repair capacity is heritable and also to determine whether DNA repair capacity if predictive of extended lifespan. A mechanistic understanding of aging is expected to help pave the way toward delaying the degenerative changes associated with age thereby improving quality of life and alleviating the age related financial burden on health care.

2.0 MULTIPLE DNA BINDING DOMAINS MEDIATE THE FUNCTION OF XPF-ERCC1 IN NUCLEOTIDE EXCISION REPAIR

This chapter was published in the Journal of Biological Chemistry. My contribution to this chapter is included as figure 7.

[2]Su, Y., [3]Orelli, B., [1]Madireddy, A., [5]Niedernhofer, L.J., and [3]Scharer, O.D. (2012). Multiple DNA binding domains mediate the function of XPF-ERCC1 in nucleotide excision repair. J Biol Chem. [PMID: 22547097]

[1]Department of Human Genetics, University of Pittsburgh Graduate School of Public Health, 130 DeSoto Street, Pittsburgh, PA, 15261, USA

[2]Department of Chemistry, [3]Department of Pharmacological Sciences, Stony Brook University, Stony Brook, NY 11794-3400, [4]current address: Herbert Irving Comprehensive Cancer Center, Columbia University, New York, NY 10032,

[5]Department of Microbiology and Molecular Genetics, University of Pittsburgh School of Medicine, Pittsburgh, Pennsylvania.

2.1 INTRODUCTION

Structure-specific endonucleases are widespread enzymes that incise DNA as components of most DNA repair and recombination pathways. The activity of these enzymes needs to be tightly regulated since they might otherwise inadvertently fragment DNA (Fagbemi et al., 2011). One of the most important pathways depending on the action of endonucleases is nucleotide excision repair (NER), which addresses lesions induced by UV light, environmental mutagens and certain cancer chemotherapeutic agents. In NER, an oligonucleotide of 24-32 nucleotides in length containing the damage is removed and the original DNA sequence restored using the non-damaged strand as a template (Gillet and Schärer, 2006). NER can be initiated in two ways: Transcription coupled NER (TC-NER) is triggered when RNA polymerase II is stalled by a bulky DNA lesion during transcription (Hanawalt and Spivak, 2008); Global genome NER (GG-NER) occurs anywhere in the genome and is initiated by the damage sensor XPC-RAD23B, in some cases with the help of the UV-DDB-ubiquitin ligase complex (Min and Pavletich, 2007; Sugasawa et al., 1998; Sugasawa et al., 2005). Subsequently, TFIIH verifies the presence of the lesion and opens up the DNA helix, allowing the formation of a pre-incision complex containing the endonuclease XPG, the single stranded DNA binding protein RPA and the architectural protein XPA (Riedl et al., 2003; Tapias et al., 2004; Wakasugi and Sancar, 1998). Finally, the second endonuclease, XPF-ERCC1 is recruited to the pre-incision complex (Tsodikov et al., 2007; Volker et al., 2001) and incises the DNA 5' to the lesion, triggering initiation of repair

synthesis, incision 3' to the lesion by XPG, completion of repair synthesis and ligation (Moser et al., 2007; Ogi et al., 2010; Staresincic et al., 2009b).

The two structure-specific endonucleases involved in NER, XPG and XPF-ERCC1, are multifunctional proteins, with diverse roles in NER and other pathways. XPG is a latent endonuclease, fulfilling first a structural and subsequently a catalytic role in NER. It has additional roles in transcription in conjunction with TFIIH (Fagbemi et al., 2011). The roles of XPG outside of NER are manifest in the severe phenotypes of many XP-G patients (Lehmann, 2003; Raschle et al., 2008). By contrast, most of the known XP-F patients present with a mild XP phenotype and have significant residual NER activity due to the presence of low levels of active XPF protein (Ahmad et al., 2010). However, a subset of patients and mice with deficiencies in XPF or ERCC1 are much more severely affected and suffer symptoms not caused by NER deficiency alone including developmental abnormalities, premature aging and early death, (Jaspers et al., 2007; McWhir et al., 1993b; Niedernhofer et al., 2006; Tian et al., 2004; Weeda et al., 1997b). It is believed that these additional symptoms are due to the roles of XPF-ERCC1 in interstrand crosslink (ICL) repair, homologous recombination and possibly telomere maintenance (Ahmad et al., 2008; Bhagwat et al., 2009a; Gregg et al., 2011; Niedernhofer et al., 2004; Zhu et al., 2003).

XPF-ERCC1 forms an obligate heterodimer and contains a number of distinct domains that contribute to various aspects of its function (Figure 2-1). Both proteins contain helix-hairpin-helix (HhH) domains at their C-termini that are required for heterodimer formation (de Laat et al., 1998d; Tsodikov et al., 2005). The active site with the conserved nuclease motif is located adjacent to the HhH domain in XPF (Enzlin and Schärer, 2002). The central domain of ERCC1 is structurally homologous to the XPF nuclease domain (Nishino et al., 2003; Tsodikov et al.,

2005), however, instead of the active site rich in acidic residues, it contains a groove lined with basic and aromatic residues that interact with the XPA protein, connecting XPF-ERCC1 to the NER machinery (Li et al., 1995; Orelli et al., 2010b; Tripsianes et al., 2007; Tsodikov et al., 2007). XPF, the larger of the two proteins, contains an N-terminal SF2-helicase like domain (HLD), which has lost the ability to bind ATP and to unwind duplex DNA (Sgouros et al., 1999). This domain has been implicated in DNA binding and protein-protein interactions, possibly mediating an interaction with SLX4 in ICL repair and other pathways (Andersen et al., 2009; Fekairi et al., 2009; Munoz et al., 2009a; Svendsen et al., 2009).

Interestingly, these five domains have been implicated in DNA binding, but evidence to date has been based on analysis of individual domains or on studies of archaeal XPF proteins (Newman et al., 2005; Nishino et al., 2005a; Nishino et al., 2005b; Tripsianes et al., 2005; Tripsianes et al., 2007; Tsodikov et al., 2005; Tsodikov et al., 2007). We investigated the role of four C-terminal DNA binding domains by mutational analysis in the context of full-length XPF-ERCC1. Our studies show that mutations in any single domain are insufficient to abolish NER *in vitro* and *in vivo*. Instead, we report that mutations in multiple domains are necessary to disrupt NER and that there is a hierarchy of importance of the individual domains. Our studies are consistent with the notion that multiple weak interactions among proteins and DNA substrates drive progress through the NER reaction (Gillet and Schärer, 2006; Stauffer and Chazin, 2004).

2.2 RESULTS

2.2.1 Generation of XPF-ERCC1 with mutations in four DNA binding domains

We used information from structural and functional studies to design XPF-ERCC1 proteins with mutations in four DNA binding domains in the C-terminal halves of the two proteins. Previous studies have shown that a protein containing only the two HhH, XPF nuclease and ERCC1 central domains can still cleave ss/dsDNA junctions, albeit with much reduced efficiency (Tsodikov et al., 2005). HhH domains have been shown to contribute to DNA binding in XPF-ERCC1 (Tripsianes et al., 2005; Tsodikov et al., 2005) and other proteins (Doherty et al., 1996). Based on structural studies, we chose two basic residues in each HhH domain, K247 and K281 in ERCC1, and K850 and R853 in XPF, which have been suggested to play a role in DNA binding (Figure 2-1) (Tripsianes et al., 2005; Tsodikov et al., 2005). NMR studies revealed that the HhH domain in ERCC1 appears to be more important for DNA binding (Tripsianes et al., 2005). We expected the nuclease active site in XPF to interact with DNA directly and chose to include R678 , as we ~~ha~~ve previously shown that mutating this residue to alanine resulted in a protein with only marginal activity on m odel substrate, while being active in NER in the presence of the other NER proteins. We suggest that this residue contributes to positioning of the active site on the substrate rather than the catalytic mechanism (Enzlin and Schärer, 2002; Staresincic et al., 2009b). Although the central domain of ERCC1 can bind DNA (Tripsianes et al., 2007; Tsodikov et al., 2005), its main function is likely to interact with XPA. We included the N110A mutant, which has a weakened interaction with XPA (Figure 2-1**B**) (Tripsianes et al., 2007; Tsodikov et al., 2007), to determine to what extent defects in the interaction with XPA synergize with defects in DNA binding. We mutated all of these residues to alanine and

combined the different mutations to study how these four domains contribute to the DNA binding and NER activity of XPF-ERCC1.

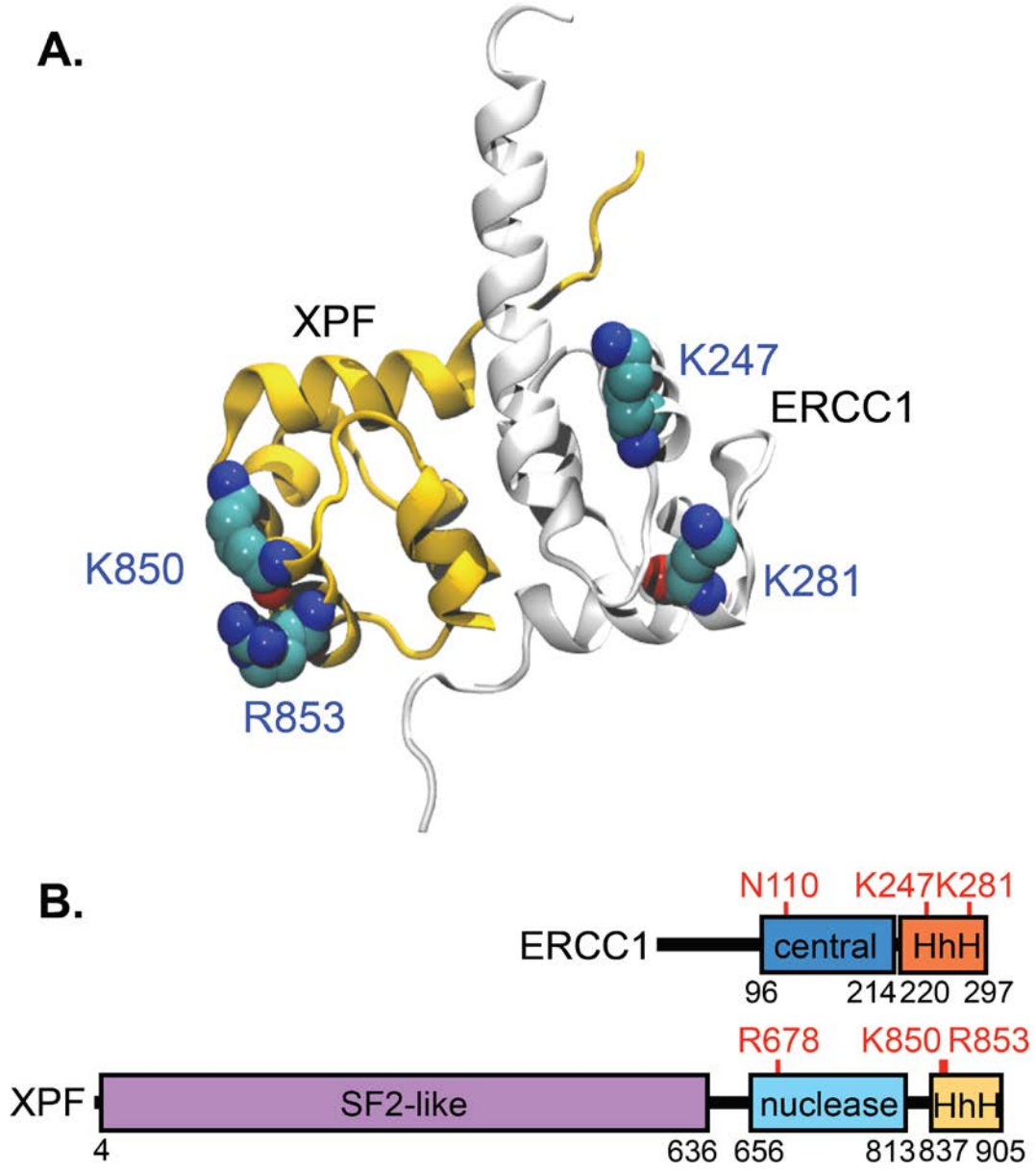

Figure 2-1 Structure of the XPF-ERCC1 HhH domains and scheme of the DNA binding domains in XPF-ERCC1

A. The HhH domains of ERCC1 (gray) and XPF (yellow) contribute to dimerization. The residues shown in atom color are believed to contribute to DNA binding and were mutated in our study. The figure is adapted from (Tsodikov et al., 2005). **B.** Five domains of XPF-ERCC1 that may contribute to DNA binding are shown. Residues in the central and HhH domains of ERCC1 and in the nuclease and HhH domains of XPF mutated to alanine in our study are highlighted in red.

2.2.2 Mutations in the HhH domain of ERCC1 and the nuclease domain of XPF lead to the loss of incision activity on stem loop substrates

Heterodimeric XPF-ERCC1 containing mutations in the HhH, nuclease and central domains were expressed in insect cells and purified using our established protocol (Enzlin and Schärer, 2002). All the proteins, including those containing mutations in two domains formed heterodimers similar to the wild-type protein. Only fractions eluting at 60-70ml, representing heterodimeric XPF-ERCC1 were collected during the gel filtration chromatography step (Figure 2-9**A**). We have previously shown that these fractions contain the active protein (30). Furthermore, the CD spectrum of selected mutants were identical to that of wild-type XPF-ERCC1 suggesting that they were properly folded (Figure 2-8B). The endonuclease activity of XPF-ERCC1 in wild-type and mutant form was tested on a 3' fluorescently labeled stem-loop model substrate, in which the protein cut at the ss and dsDNA junction in the presence of Mg^{2+} (de Laat et al., 1998b). XPF-ERCC1 in wild-type form and with mutations in the HhH domain of XPF or the central domain of ERCC1, cleaved the stem-loop substrate with similar efficiencies as the wild-type protein in a concentration-dependent manner (Figure 2-2). By contrast, no such incision products were observed for proteins containing mutations in the HhH domain of ERCC1 (Figure 2-2) , $ERCC1^{K247A/K281A}$, lanes 4-5) or in the nuclease domain of XPF (Figure 2-2), XPF^{R678A}, lanes 4-5). From these results we conclude that the HhH domain of ERCC1 and the

nuclease domain of XPF are more important than the ERCC1 central and XPF HhH domains in mediating nuclease activity.

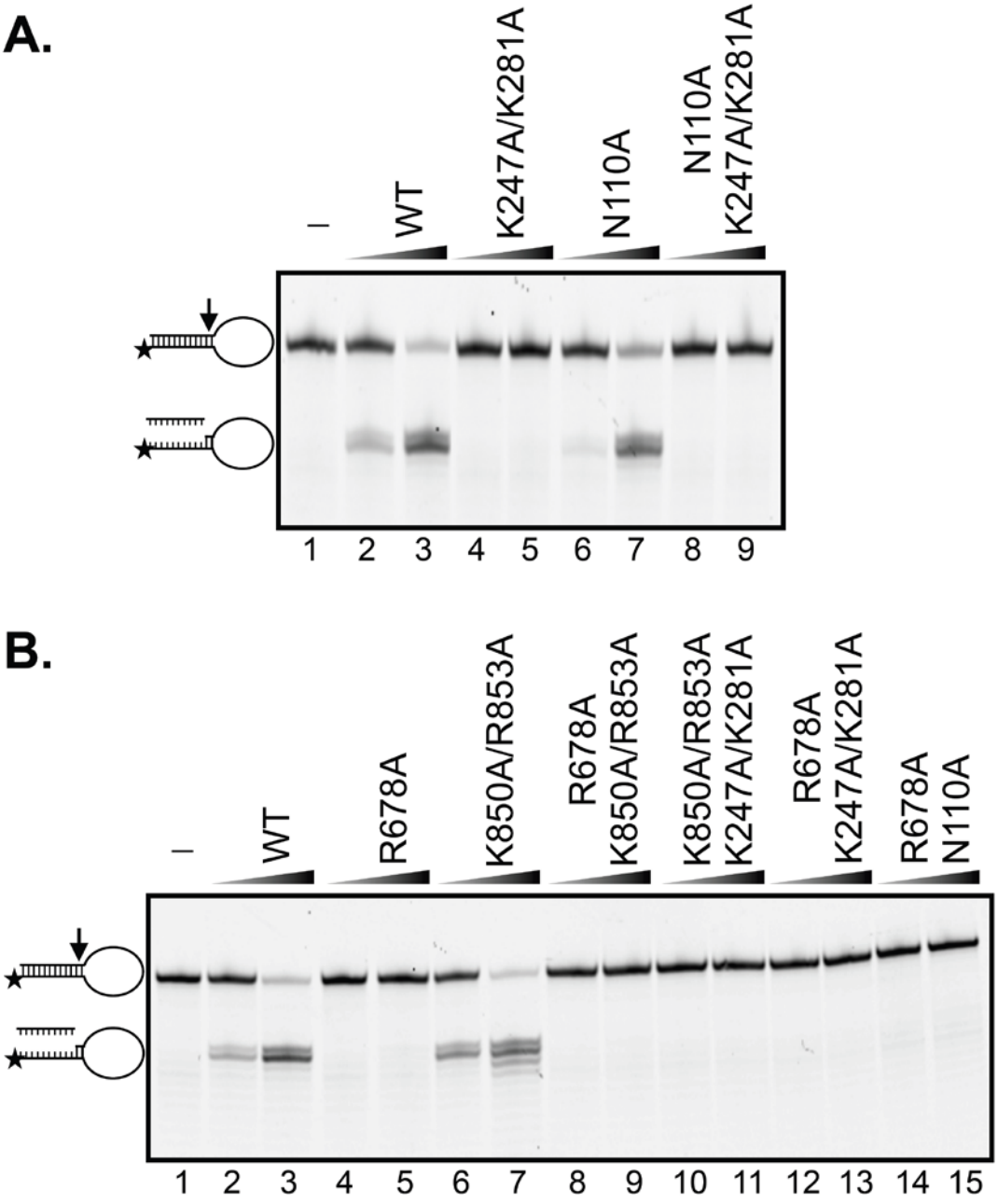

Figure 2-2 Mutations in the HhH domain of ERCC1 and the nuclease domain of XPF impact nuclease activity on a stem-loop substrate.

XPF-ERCC1 in wild-type form or with mutations in ERCC1 (**A.**), XPF or both (**B.**) were incubated with 3'-Cy5 labeled stem-loop DNA substrate (6.7 nM) at 37 °C for 30 min, and products were visualized on 12% denaturing polyacrylamide gels. Concentrations of XPF-ERCC1: lanes 1: no protein; Lanes 2, 4, 6, 8 and 10, 12 and 14: 3.3 nM; Lanes 3, 5, 7, 9 and 11: 26.7 nM. The position of the substrate and product are indicated on the left side of the gel.

2.2.3 The HhH domain of ERCC1 is a key contributor for DNA binding affinity

We wanted to gain insight into whether the reduced nuclease activity caused by mutations in the ERCC1 HhH and XPF nuclease domains correlated with reduced DNA binding activity. We used fluorescence anisotropy to measure the binding affinity of XPF-ERCC1 to model DNA substrates. We titrated 3' labeled splayed arm, stem loop or duplex DNA substrates with wild-type XPF-ERCC1 and measured the increase in anisotropy as a function of the protein concentration. Surprisingly, XPF-ERCC1 bound dsDNA with similar affinity as the splayed arm or stem-loop substrates (data not shown), although XPF-ERCC1 did not incise dsDNA (de Laat et al., 1998b). However, addition of a tenfold excess of non-labeled dsDNA abolished the binding of XPF-ERCC1 to dsDNA, but not to the splayed arm and stem loop substrates, confirming that XPF-ERCC1 specifically bound ss/dsDNA junctions.

To determine the effect of mutations in the four domains on DNA binding quantitatively, 3'-FAM-labeled spayed arm substrates were incubated with increasing amounts of protein in the presence of a tenfold excess of non-labeled dsDNA competitor. The anisotropy binding curves for the WT, XPF^{R678A}, $ERCC1^{N110A}$ and $XPF^{K850A/K853A}$ proteins displayed a similar shape, while the anisotropy signal of $ERCC1^{K247A/K281A}$ was about 40% lower, suggesting that the architecture of this protein-DNA complex was different from that of the wild-type protein (Figure 2-3). Quantification of the data revealed that the $ERCC1^{K247A/K281A}$ also displayed the lowest binding affinity for the splayed arm substrate (Kd = 219 ± 9 nM), about two fold lower than the WT,

XPF^{R678A} and ERCC1^{N110A} proteins. The affinity of XPF$^{K850A/K853A}$ was about 1.6 fold lower than that of the wild-type protein. The results suggest that the HhH domains of both ERCC1 and XPF contribute to substrate binding by XPF-ERCC1, with a more prominent contribution from the ERCC1 HhH domain. Our data also show that mutations in a single domain alone are not sufficient to completely abolish DNA binding by XPF-ERCC1.

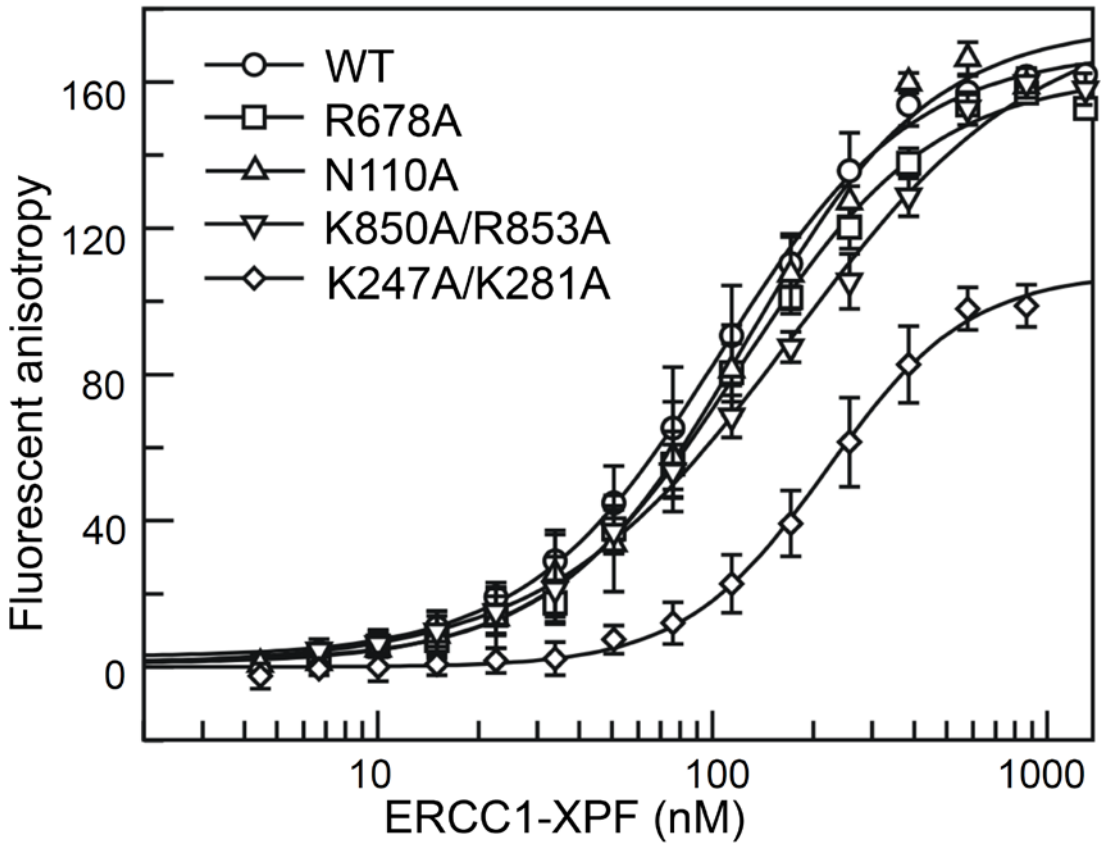

Figure 2-3 Mutations in the HhH domain of ERCC1 lead to reduced DNA binding affinity.

Fluorescein-labeled splayed arm DNA substrate (10nM) in the presence of 100 nM non-labeled competitor double strand DNA was titrated with wild-type and mutant XPF-ERCC1. DNA affinities were measured by fluorescence anisotropy. Error bars represent the standard deviation from a minimum of 4 experiments.

2.2.4 Mutations in multiple DNA binding domains synergistically affect NER activity in vitro

We then investigated the effect of these mutations on the overall NER reaction in the context of cell-free extracts. Plasmids containing site-specific bulky DNA substrates, either 1,3-intrastrand cisplatin crosslinks (cis-Pt) or acetylaminofluorene adducts of dG (dG-AAF), were incubated with XPF-deficient cell-free extract and wild-type or mutant XPF-ERCC1 to observe the ability of the protein to excise DNA in the context of other NER proteins (Dunand-Sauthier et al., 2005; Gillet et al., 2005; Shivji et al., 1999). XP-F extracts are devoid of ERCC1 and XPF and did not display any NER activity, but addition of wild-type XPF-ERCC1 restored NER activity as shown previously (Figure 2-4**A/B**, lanes 1-3) (Orelli et al., 2010b; Staresincic et al., 2009b). Mutations in the HhH domain of ERCC1 ($ERCC1^{K247A/K281A}$) led to a mild reduction in NER activity, at least on the cisplatin substrates, while the analogous mutation in XPF ($XPF^{K850A/R853A}$) had no effect (Figure2-4**A/B**, lanes 4-5, and 12-13). Therefore, a defect in the intrinsic DNA binding activity can be overcome at least partially in the context of the full NER complex. XPF^{R678A} was similarly active in NER, although with a slightly shifted incision pattern (Figure2-4, compare lanes 10-11 to lanes 2-3). This suggests that R678 contributes to the proper positioning of active site residues to carry out the incision. As observed previously, $ERCC1^{N110A}$ displayed reduced NER activity, due to a weakened interaction with XPA (Figure 4A/B, lanes 6-7 (Orelli et al., 2010b).

Since mutations in the individual domains led to only partial inhibition of NER activity, we tested if a combination of multiple mutations would lead to a more severe defect. We found that, in all cases, a combination of mutations in multiple domains led to reduced NER activity compared to the respective mutations in any single domain. Combining the $ERCC1^{K247A/K281A}$

mutation with ERCC1^{N110A} (Figure 2-4A, lanes 8-9), XPF$^{K850A/R853A}$ (Figure2-4A, lanes 16-17) or XPF^{R678A} (Figure2-4A, lanes 18-19) led to a loss of detectable NER activity on the cis-Pt substrate, while some activity was preserved for the dG-AAF substrate for the combination of ERCC1$^{K247A/K281A}$ with ERCC1^{N110A} (Figure 2-4B, lanes 8-9) and XPF$^{K850A/R853A}$ (Figure 2-4B, lanes 16-17). Similarly, a combination of XPF^{R678A} with XPF$^{K850A/R853A}$ (Figure 2-4**A/B**, lanes 14-15) or ERCC1^{N110A} (Figure 2-4**A/B**, lanes 20-21) led to decreased NER activity with both the cis-Pt and dG-AAF substrates. These studies show that combined mutations in multiple DNA binding domains of XPF-ERCC1 synergistically affected NER activity and that many domains simultaneously contributed to the DNA binding and cleavage activity of XPF-ERCC1. Interestingly, the reactions of cis-Pt substrates were generally more severely affected than those of the dG-AAF substrates. This could be due to differences in the structure of the substrates in the NER complex and/or because dG-AAF were more efficiently processed by NER under our reaction conditions.

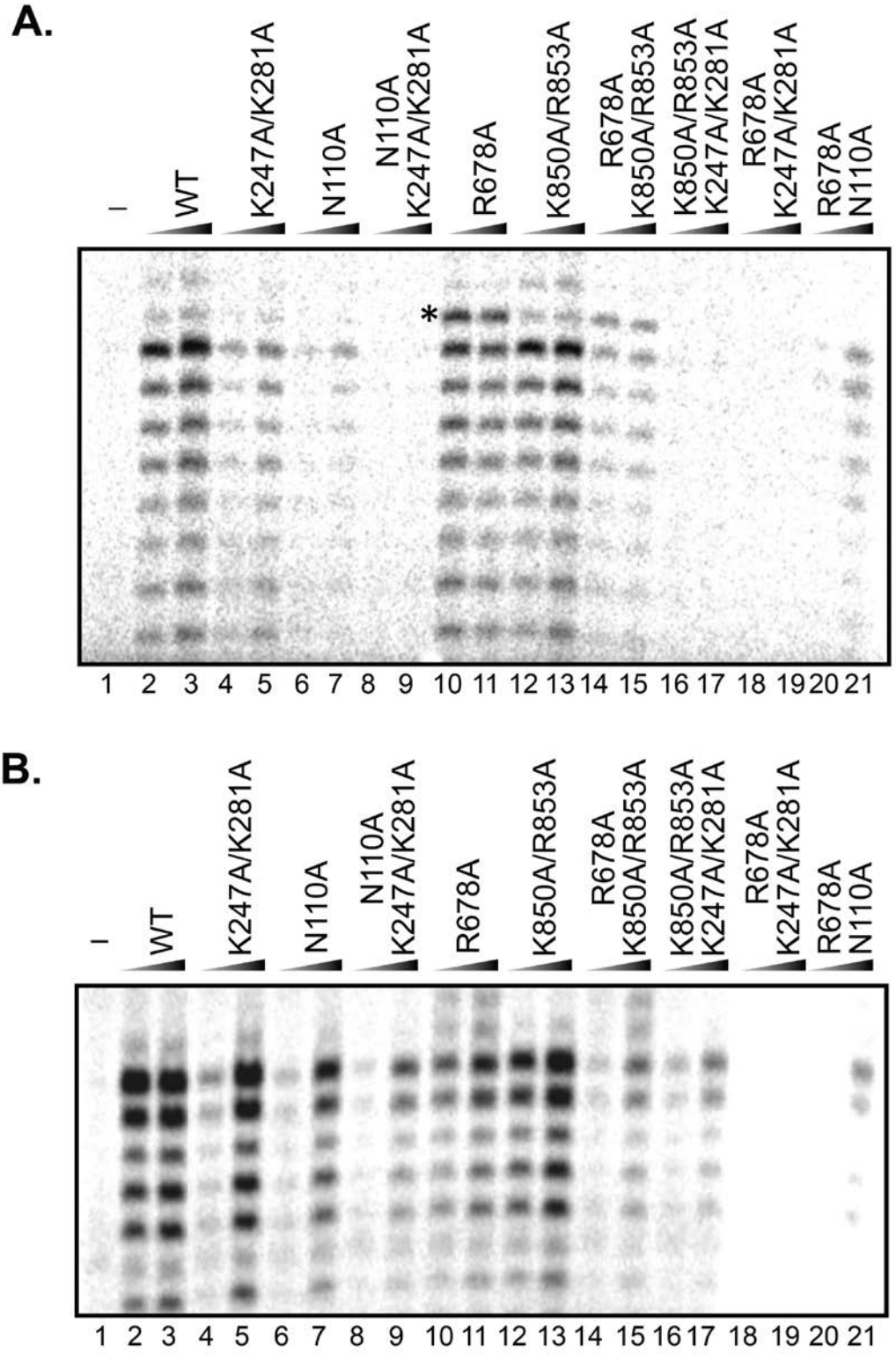
A.
–
WT
K247A/K281A
N110A
N110A K247A/K281A
R678A
K850A/R853A
R678A K850A/R853A
K850A/R853A K247A/K281A
R678A K247A/K281A
R678A N110A
*
1 2 3 4 5 6 7 8 9 10 11 12 13 14 15 16 17 18 19 20 21
B.
–
WT
K247A/K281A
N110A
N110A K247A/K281A
R678A
K850A/R853A
R678A K850A/R853A
K850A/R853A K247A/K281A
R678A K247A/K281A
R678A N110A
1 2 3 4 5 6 7 8 9 10 11 12 13 14 15 16 17 18 19 20 21

Figure 2-4 Mutations in multiple domains are needed to affect NER *in vitro*.

Plasmids containing site-specific cis-Pt (**A.**) or dG-AAF (**B.**) lesions were incubated with XPF-deficient cell extracts and recombinant purified XPF-ERCC1 in wild-type or mutant form. The excised 25-32mer oligonucleotide was annealed to a complementary strand with a 4G overhang followed by a fill-in reaction with ^{32}P-dCTP. Products were analyzed on 14% denaturing polyacrylamide gels and visualized by phosphorimaging. XPF-ERCC1 concentrations: lane 1: no protein; even lanes: 5 nM; odd lanes except lane 1: 40 nM. An asterisk denotes the unique band observed with XPF^{R678A}.

2.2.5 XPF-ERCC1 with impaired DNA binding ability associates with NER complexes in cells

We wished to define how the DNA binding mutations of XPF-ERCC1 affected NER activity *in vivo*, by studying the recruitment of the protein to sites of UV damage and the repair kinetics of 6-4 photoproducts ((6-4)PPs). ERCC1-deficient UV20 and XPF-deficient XP2YO cells were transduced with lentiviral vectors expressing wild-type or mutant ERCC1 and XPF proteins, respectively (Orelli et al., 2010b; Staresincic et al., 2009b). Western blot analysis of the transduced cells revealed that wild-type (ERCC1^{WT}, XPF^{WT}) and mutant proteins (ERCC1$^{K247A/R281A}$, ERCC1$^{N110A/K247A/K281A}$, XPF^{R678A}, XPF$^{K850A/R853A}$ and XPF$^{R678A/K850A/R853A}$) were expressed at or above endogenous level (Figure 2-9). As it has been shown that only about 30% of the cellular XPF-ERCC1 is engaged in NER following UV irradiation (53), we believe that slight differences in expression levels do not influence the outcome of the experiments described here. Cells were irradiated with UV light (254 nm) through a filter with 5 μm pores to generate sites of local UV damage in the cell nuclei. After incubation for 30 min following UV irradiation, cells were fixed and stained with antibodies to detect (6-4)PPs and XPF-ERCC1. As previously shown (Orelli et al., 2010b), around 90% of wild-type protein co-localized with (6-4)PPs (Figure 2-5). Interestingly, similar amounts of co-localization were observed for the

proteins with mutations affecting DNA binding (ERCC1$^{K247A/R281A}$, XPF^{R678A}, XPF$^{K850A/R853A}$ and XPF$^{R678A/K850A/R853A}$), indicating that the DNA binding activity of XPF-ERCC1 was not required for the stable association of XPF-ERCC1 with NER complexes. The only variant that showed decreased co-localization with (6-4)PPs was ERCC1$^{N110A/K247A/K281A}$ (Figure 2-5), but this was expected, as we have shown previously that the N110A mutation affected binding to XPA (Orelli et al., 2010b).

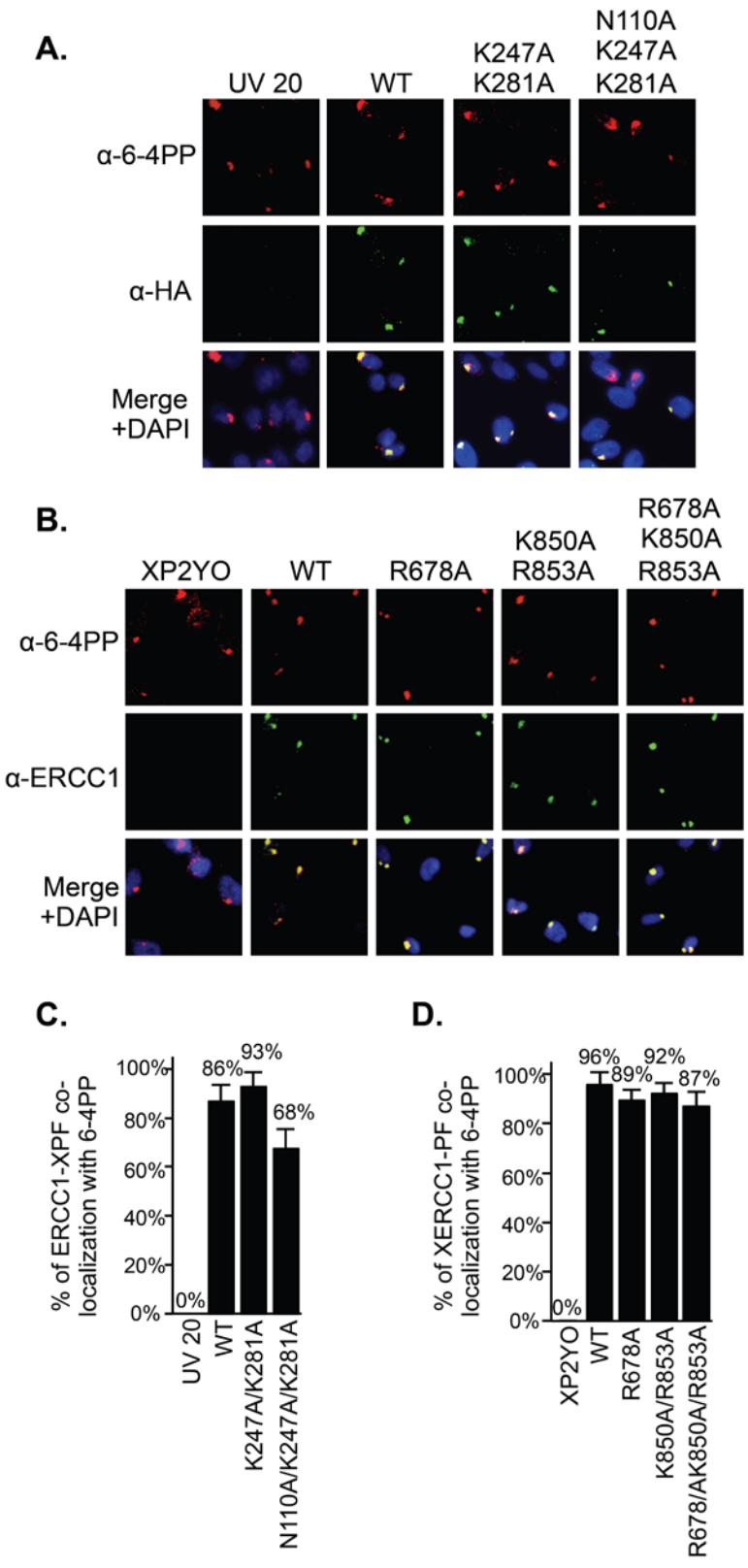
A.
UV 20
WT
K247A
K281A
N110A
K247A
K281A
α-6-4PP
α-HA
Merge
+DAPI
B.
XP2YO
WT
R678A
K850A
R853A
R678A
K850A
R853A
α-6-4PP
α-ERCC1
Merge
+DAPI
C.
% of ERCC1-XPF co-localization with 6-4PP
100%
80%
60%
40%
20%
0%
0%
86%
93%
68%
UV 20
WT
K247A/K281A
N110A/K247A/K281A
D.
% of XERCC1-PF co-localization with 6-4PP
100%
80%
60%
40%
20%
0%
0%
96%
89%
92%
87%
XP2YO
WT
R678A
K850A/R853A
R678/AK850A/R853A

Figure 2-5 Mutations in DNA binding domains of XPF-ERCC1 do not affect the recruitment to sites of UV damage.

ERCC1-deficient UV20 cells were transduced with wild-type or mutant ERCC1, and XPF-deficient XP2YO with wild-type or mutant XPF. Cells were irradiated with UV light (254nm, 120 J/m^2 for UV20 cells; 150 J/m^2 for XP2YO cells) through a polycarbonate filter with 5 μm pores and incubated at 37°C for 30 min. Cells were fixed and stained with antibodies against (6-4)PPs (red), XPF-ERCC1 (green, using an anti-HA antibody in UV20 cells (**A.**), and an anti-ERCC1 antibody in XP2YO cells (**B.**)). Nuclear DNA was visualized by DAPI staining. **C.** Graphical representation of the percentage of co-localization of XPF-ERCC1 with (6-4)PPs in UV20 cells. **D.** Graphical representation of the percentage of co-localization of XPF-ERCC1 with (6-4)PPs in XP2YO cells. The quantification is based on at least three independent experiments and error bars represent the standard deviation.

2.2.6 The repair of (6-4)PPs is delayed by DNA binding mutations

We next measured how the mutations in ERCC1 and XPF affected the rate of repair of UV lesions. Cells were incubated for various times after local UV irradiation and fixed. The percentage of cells containing (6-4)PPs was determined. 30 minutes after UV irradiation, about 40% of all UV 20 cells contained sites of (6-4)PPs. At 24 h 17% of the non-transduced UV20 cells contained 6-4PPs, establishing the rate of removal rate in the absence of NER (Figure 2-6A,C). In ERCC1^{WT}-expressing cells, the damage was almost all gone at 2h and detectable at only marginal levels at later time points. The rate of repair was significantly reduced in ERCC1$^{K247A/R281A}$-expressing cells with 24% and 18% of the cells containing (6-4)PPs at 2 h and 4 h, respectively. Repair appeared to be mostly completed however at later time points (8 h, 24 h), indicating that this mutation in the HhH domain of ERCC1 slowed down, but did not abrogate NER. Adding the XPA-interacting mutation N110A to K247A/K281A led to further delay in repair, although repair was still completed at the 24 h time point (Figure 2-6A,C).

In the XP-F deficient XP2YO cells, significant level (~ 16%) of (6-4)PPs also persisted at 24 h, and the observed damage levels at 30min was slightly higher than in the UV20 cells.

Transduction of XPF^{WT} restored the complete removal of (6-4)PPs and the repair rate in $XPF^{K850A/R853A}$-expressing cells was only marginally slower than in wild-type cells. However, the damage removal was impaired in XPF^{R678A}-expressing cells, and a combination of the R678A and K850A/R853A mutations led to a further reduction in the repair rate (Figure 2-6B,D). The cellular studies are thus consistent with the *in vitro* results showing that DNA binding mutations in the nuclease domain of XPF and the HhH domain of ERCC1 synergistically affected NER.

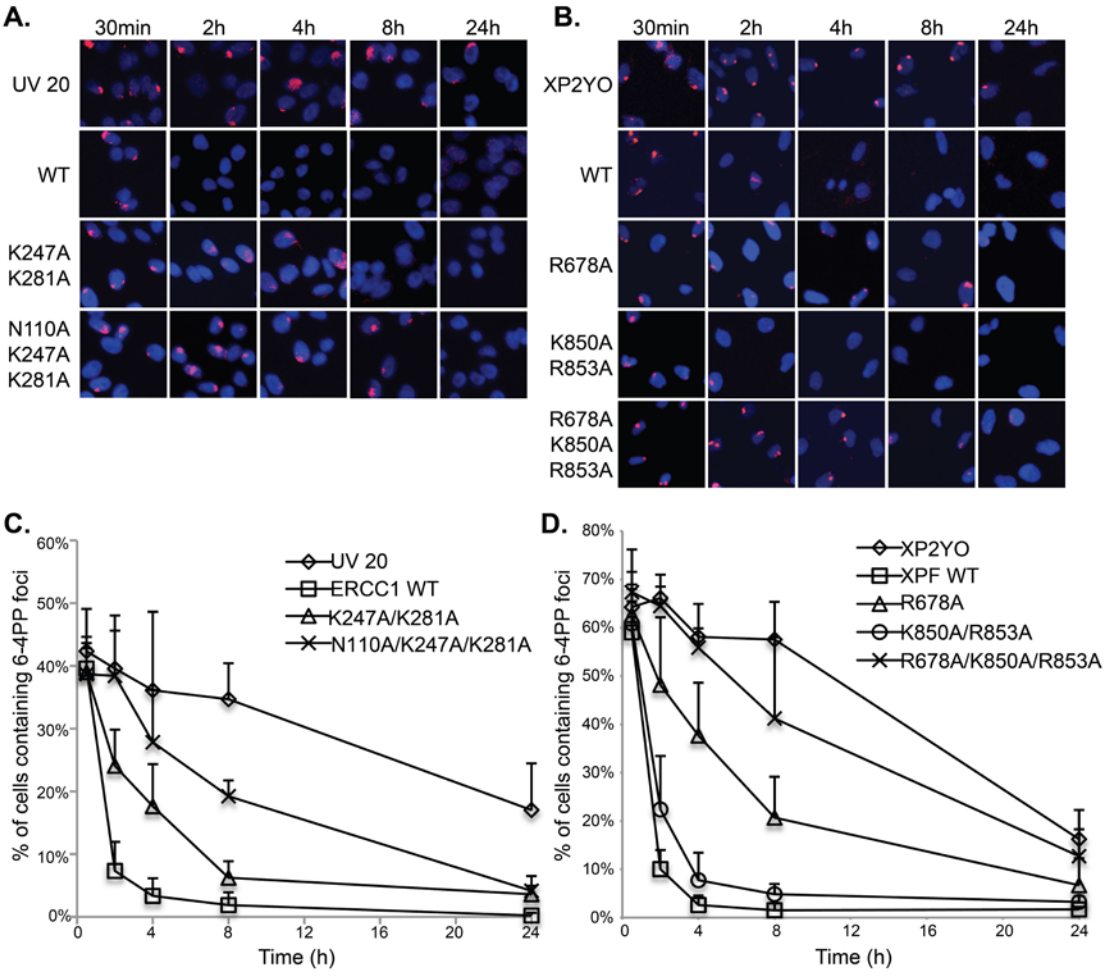

Figure 2-6 Mutations in DNA binding domains of XPF-ERCC1 affect repair kinetics of (6-4)PPs *in vivo*.

ERCC1-deficient UV20 cells were transduced with wild-type or mutant ERCC1 (**A.**), XPF-deficient XP2YO cells with wild-type or mutant XPF (**B.**). Cells are irradiated with UV light

(254nm, 120 J/m^2 for UV20; 150 J/m^2 for XP2YO) through a polycarbonate filter with 5 μm pores, incubated at 37°C for 30 min, 2 h, 4 h, 8 h, 24 h, fixed and stained with antibody against (6-4)PPs (red) and with DAPI (blue). **C.** Graphical representation of the percentage of cells containing (6-4)PPs in (transduced) UV20 cells. **D.** Graphical representation of the percentage of cells containing (6-4)PPs in (transduced) XP2YO. Quantification is based on at least three independent experiments and the standard deviation is indicated by error bars.

2.2.7 Mutations in multiple DNA binding domains render cells hypersensitive to UV and Mitomycin C

Having shown that mutations in DNA binding domains in XPF-ERCC1 synergistically affected NER *in vitro* and *in vivo*, we wanted to test whether these mutations also render cells hypersensitive to UV irradiation as well as Mitomycin C (MMC), an agent that causes DNA interstrand crosslinks (ICLs). Cells were first treated with different doses of UV light (254 nm) and the sensitivity was assessed using clonogenic survival assays. Consistent with the results from the NER studies above, mutations in single domains (XPF^{R678A}, XPF$^{K850A/R853A}$ and ERCC1$^{K247A/K281A}$) led to mild UV sensitivity, while mutations in two domains (XPF$^{R678A/K850A/R853A}$ or ERCC1$^{N110A/K247A/K281A}$) led to a more pronounced effect. The hypersensitivity to MMC was even more prominent: Cells expressing XPF-ERCC1 with mutations in single domains (XPF^{R678A}, XPF$^{K850A/R853A}$ and ERCC1$^{K247A/K281A}$) were already associated with dramatic sensitivity, especially XPF^{R678A}. Cells expressing XPF$^{R678A/K850A/R853A}$ or ERCC1$^{N110A/K247A/K281A}$ were as sensitive as non-transfected cells to MMC (Figure 2-7). These results demonstrate that proper DNA binding is even more important in the context of ICL repair.

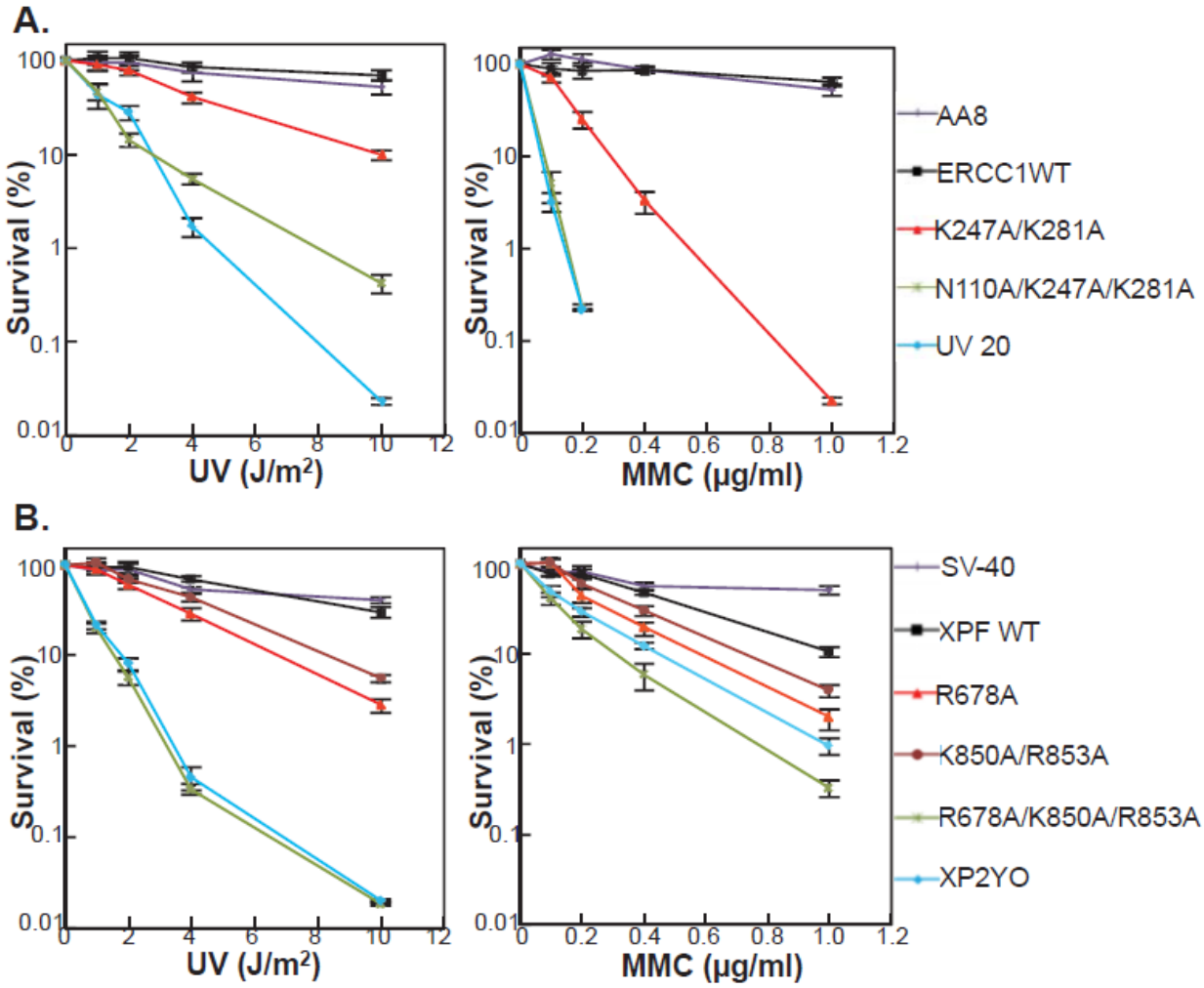

Figure 2-7 Mutations in DNA binding residues render cells more sensitive to MMC than to UV.

Cells were challenged with UV (254nm) to determine the impact of the mutations on NER or with MMC to determine the impact on ICL repair. Top row: WT (AA8), ERCC1-deficient (UV20) and complemented Chinese hamster ovary cell lines. Bottom row: WT (SV-40, SV40-transformed human fibroblasts), XPF-deficient (XP2YO) and complemented cell lines. The data were plotted as the percentage of colonies that were formed on the treated plates relative to the untreated plates ± S.E (error bars) for a minimum of 2 independent experiments each done in triplicate.

2.3 DISCUSSION

2.3.1 Multiple DNA- and protein-binding domains of XPF-ERCC1 control its function in NER

In our study, we investigated the role of four C-terminal DNA binding domains in XPF-ERCC1 (Figure 2-1) and show that there is a hierarchy of importance of these domains in mediating the interaction with its DNA substrates. Mutations of DNA binding residues located in the HhH domain of ERCC1 and the nuclease domain of XPF have a more deleterious effect on nuclease and NER activity than mutations in the HhH domain of XPF or the central domain of ERCC1. Importantly, mutations in multiple DNA binding domains are required to significantly suppress NER activity in cultured cells and cell-free extracts, whereas mutations in the ERCC1 HhH or XPF nuclease domain alone are enough to deplete nuclease activity of the purified heterodimer on model substrates. These findings are consistent with current models of NER positing that this process is driven by the dynamic assembly and disassembly of the factors involved (Houtsmuller et al., 1999; Riedl et al., 2003). Accordingly, multiple protein-protein and protein-DNA interactions drive NER and enable the ordered hand-off of the substrates in damage recognition, damage verification, pre-incision complex assembly, dual incision, repair synthesis and ligation (Gillet and Schärer, 2006; Stauffer and Chazin, 2004). Our studies allow us to propose how multiple interactions between XPF-ERCC1, XPA and DNA control incision 5' to the damage during NER. XPF-ERCC1 is recruited to NER complexes by interaction of the central domain of ERCC1 with XPA, in the context of a pre-incision complex consisting of XPA, RPA, TFIIH and XPG (Orelli et al., 2010b; Tsodikov et al., 2007). Our cellular studies suggest that DNA binding of XPF-ERCC1 is not required to localize the endonuclease to NER complexes (Figure 2-5).

DNA binding domains therefore anchor the protein at the junction following recruitment, allowing the nuclease domain of XPF to be positioned at the incision site and to cleave the DNA, triggering dual incision and repair synthesis (Staresincic et al., 2009b). It is likely that interactions with other NER proteins, for example RPA and TFIIH (Coin et al., 2004; de Laat et al., 1998c), contribute to the fine-tuning of the incision and coordination with other steps in the NER pathway.

2.3.2 The HhH domains of ERCC1 and XPF have distinct roles in NER

In accordance with NMR studies of individual domains of XPF-ERCC1 (Tripsianes et al., 2005), our results show that mutations in the HhH domain of ERCC1 affect DNA binding, nuclease and NER activity more severely than analogous mutations in the HhH domain of XPF. XPF and ERCC1 are believed to have evolved from a common ancestor (Gaillard and Wood, 2001), which has been studied in the form of archaeal XPF homologs (Rouillon and White, 2011). During divergent evolution, XPF retained the nuclease active site and ERCC1 conserved a typical double HhH domain. ERCC1 now harbors an XPA-interacting domain instead of a nuclease domain, and the HhH in XPF has lost some typical features. In accordance with this observation and with structural studies, our work demonstrates that the HhH domain of ERCC1 is more important for substrate binding and NER activity than the analogous domain in XPF (Tripsianes et al., 2005). We know less about how the HhH of XPF contributes to the interaction with DNA. Based on studies of the homologous domain in the Hef helicase, the HLD is expected to contribute to the interaction with ss/dsDNA junctions. Consistent with this observation, human XPF-ERCC1 lacking the HLD has been shown to cut model substrates only with marginal efficiency (Tsodikov et al., 2005).

2.3.3 How does XPF-ERCC1 bind substrates in different pathways?

XPF-ERCC1 has been known for a long time to have roles outside of NER in the repair of interstrand crosslinks and in homologous recombination (Ahmad et al., 2008; Bardwell et al., 1994; Hoy et al., 1985; Niedernhofer et al., 2004). Deficiencies in these processes have been implicated to cause the severe phenotypes of select ERCC1- or XPF-mutant patients and mice that cannot be explained by NER deficiency (Jaspers et al., 2007; McWhir et al., 1993b; Niedernhofer et al., 2006; Tian et al., 2004; Weeda et al., 1997b). Recent evidence suggests that an interaction between XPF and the Fanconi anemia protein SLX4/FANCP, rather than with XPA, is crucial for ICL repair (Andersen et al., 2009; Crossan et al., 2011a; Fekairi et al., 2009; Kim et al., 2011; Munoz et al., 2009a; Stoepker et al., 2011b; Svendsen et al., 2009).

With respect to our present study, it will be of great interest to determine whether DNA binding by XPF-ERCC1 in ICL repair is similar as in NER or whether it follows a distinct pattern. We have shown that even within the NER pathway the repair efficiency of cis-Pt and dG-AAF adducts is affected to different extents by mutations in DNA binding domains of XPF-ERCC1 (Figure 2-4 compare, lanes 8-9, 16-17), perhaps reflecting a different conformation of the substrates in the NER complex. These differences may be even bigger between substrates for NER and ICL repair, as reflected by the sensitivities to UV light and MMC: cells expressing XPF^{R678A} or $ERCC1^{K247A/K281A}$ are more sensitive to MMC than to UV (Figure 2-7).

High resolution structures of other structure-specific endonucleases such as FEN1 or EXO1 in complex with DNA substrates have shown that these proteins firmly bind the double-stranded portion of the DNA and induce a kink of about 90° in the non-cleaved DNA strand at the junction (Orans et al., 2011; Tsutakawa et al., 2011). The cleaved strand undergoes local unpairing of the dsDNA at the incision site, and the ssDNA overhang of the cleaved strand may

be bound at different sites of the protein. Based on the structures of archaeal homologs of XPF (Newman et al., 2005; Nishino et al., 2005a) a similar arrangement can be envisioned for XPF-ERCC1. Interestingly, the residue equivalent to R678 in XPF in the *Aeropyrum pernix* XPF homolog (R26) is located at a site that possibly binds the ssDNA overhang. Mutation of R678 of XPF affects ICL repair more severely than NER, showing that this residue is more crucial for the positioning of the endonuclease in the context of ICL repair.

We therefore believe that further studies of the five DNA binding domains in XPF-ERCC1 will provide valuable insight into how this protein operates in multiple DNA repair pathways. Furthermore, introduction of specific mutations in those domains may lead to pathway-specific defects, enabling new approaches to study the importance of XPF-ERCC1 in maintaining genome stability.

2.4 EXPERIMENTAL PROCEDURES

2.4.1 Protein expression and purification

Site directed mutagenesis of pFastBac-XPF and pFastBac-ERCC1-His (Enzlin and Schärer, 2002) was performed using the QuikChange site-directed mutagenesis kit (Stratagene) to generate the following mutations: XPF^{R678A}, $XPF^{K850A/R853A}$, $XPF^{R678A/K850A/K853A}$, $ERCC1^{K247A/K281A}$, $ERCC1^{N110A}$, and $ERCC1^{N110A/K247A/K281A}$. Bacmid DNA was generated in DH10Bac cells and transfected into the Sf9 insect cells to obtain baculoviruses according to a standard protocol (Bac-to-Bac, Invitrogen). The following combination of ERCC1 and XPF proteins were co-expressed in Sf9 cells for 60 to 65 hours with an MOI of 5: XPF-ERCC1, XPF-

ERCC1^{R678A}, XPF-ERCC1$^{K850A/R853A}$, XPF-ERCC1$^{R678A/K850A/R853A}$,ERCC1$^{K247A/K281A}$-XPF, ERCC1^{N110A}-XPF, ERCC1$^{N110A/K247A/K281A}$-XPF, ERCC1$^{K247A/K281A}$-XPF^{R678A}, ERCC1^{N110A}–XPF^{R678A}, and ERCC1$^{K247A/K281A}$-XPF$^{K850A/K853A}$. Cells were lysed and proteins purified over a 1 ml Nickel (His Trap) column (Amersham Biosciences), a HiLoad 16/60 Superdex 200 column (Amersham Biosciences) and a 1 ml Hitrap Heparin column (Amersham Biosciences) as described in (Enzlin and Schärer, 2002). The proteins eluted at 650 mM NaCl from the Heparin column and were in some cases concentrated on an Amicon Ultra-4 Centrifugal Filter (Millipore). Proteins were frozen in aliquots in liquid N_2 and stored at -80°C.

2.4.2 Endonuclease Assays

10 pmol of a stem-loop oligonucleotide (GCCAGCGCTCGG(T)$_{22}$CCGAGCGCTGGC) labeled with fluorescent dye Cy5 at the 3' end (IDT) were annealed in 200 µl solution (10 mM Tris pH 8.0, 50 mM NaCl, 1 mM $MgCl_2$) by heating at 90°C for 10 min and allowing to cool to RT for 2 h. 100 fmol of the substrate were incubated in 25 mM Tris pH 8.0, 2 mM $MgCl_2$, 10% glycerol, 0.5 mM β-mercaptoethanol, 0.1 mg/ml BSA, 40 mM NaCl with various amounts of protein in a volume of 15 µl. The reactions were incubated at 37°C for 30 min and quenched by adding 10 µl of 80% formamide/10 mM EDTA. After heating at 95°C for 5 min and cooling on ice, 3µl of each sample were analyzed on a 12% denaturing polyacrylamide gel. Bands were visualized by fluorescence imaging on a Typhoon 9400 imaging system (Amersham Biosciences).

2.4.3 In vitro NER Assay

Extracts derived from XPF-deficient XP2YO cells and plasmids containing dG-acetylaminofluorene (dG-AAF) or 1,3-intrastrand cisplatin (cis-Pt) lesions were prepared as described previously (Biggerstaff and Wood, 1999; Gillet et al., 2005; Shivji et al., 1999). For each reaction, 2 µl of repair buffer (200 mM Hepes-KOH (pH 7.8), 25 mM $MgCl_2$, 2.5 mM DTT, 10 mM ATP, 110 mM phosphocreatine (di-Tris salt, Sigma), and 1.8 mg/ml BSA), 0.2 µl of creatine phosphokinase (2.5 mg/ml, sigma), 3 µl of XPF-deficient cell extract (about 10 mg/ml), NaCl (to a final concentration of 70 mM), and different amounts of purified XPF-ERCC1 in a total volume of 9 µl were pre-warmed at 30°C for 10 min. 1 µl plasmid containing dG-AAF or cis-Pt (50 ng/µl) was added to each reaction and the samples were incubated at 30°C for 45 min. After adding 0.5 µl of 1 µM of an oligonucleotide complementary to the excision product with a 4G overhang for either dG-AAF (5' GGGGCATGTGGCGCCGGTAATAGCTACGTAGCTCp-3') or cis-Pt (5'GGGGGAAGAGTGCACAGAAGAAGACCTGGTCGACCp-3'), the mixtures were denatured by heating at 95°C for 5 min. After cooling to RT for 15 min, 1 µl sequenase mixture (0.13 units of sequenase (USB), and 2.0 µCi [α-^{32}P] dCTP for each reaction) was added and incubated at 37°C for 3 min, followed by addition of 1.2 µl dNTP mixture (50 µM dCTP, 100 µM dTTP, 100 µM dATP and 100 µM dGTP). The reactions were incubated at 37°C for 12 min and stopped by addition of 8 µl of 80% formamide/10 mM EDTA. After heating to 95°C for 5 min, samples were placed on ice and analyzed on a 14% denaturing polyacrylamide gel. Gels were exposed to a phosphor screen and visualized by PhosphorImager (Typhoon 9400, Amersham Biosciences).

2.4.4 DNA binding measurements by fluorescent anisotropy

For the anisotropy experiments, the protein storage buffer was exchanged to 25 mM KH_2PO_4 (7.6), 5 mM β-mercaptoethanol, 10% glycerol, 150 mM NaCl. Increasing concentrations of protein were incubated with the splayed arm substrate (10 nM) which was made by annealing the following oligonucleotides: 5'-CTTTCGAACATCCAGGAGAGCACGGCC TTTTTTTTTTTTTTTTTTT with an FAM label at the 3' end and 5'-TTTTTTTTTTTTTTTTTTTTGGCCGTGCTCTCCTGGATGTTCGAAAG. 100nM of competitor double stranded DNA (5'-TCAAAGTCACGACCTAGACACTGCGAGCTCGAATTCACTGGAGTGACCTC and 5'-GAGGTCACTCCAGTGAATTCGAGCTCGCAGTGTCTAGGTCGTGACTTTGA) were used in each reaction. Each reaction was incubated in 20 µl of buffer (25mM Hepes-KOH (pH 8.0), 15% glycerol, 0.1mg/ml BSA, 2 mM $CaCl_2$, 0.5 mM β-mercaptoethanol, and 40 mM NaCl) at 30°C for 5 min. The experiments were conducted at least 4 times and measured on Infinite M1000 plate reader (Tecan). The data were fitted using the grafit4 program to the equation f=y+a*x^b/(c^b+x^b), where x is the protein concentration, f is the fluorescent anisotropy and c is the Kd value.

2.4.5 Generation of mutant cell lines using lentiviral transduction

Human XP-F mutant fibroblasts XP2YO, Chinese hamster ovary cells UV20 (with a mutation in ERCC1), and 293T cells were cultured in Dulbecco's modified Eagle's medium high glucose 1 x (GIBCO), 10% fetal bovine serum, 100 units/ml penicillin, and 0.1 mg/ml streptomycin at 37°C in a 5% CO_2 humid incubator. Wild-type or mutant XPF cDNA with an hemaglutinin (HA) tag

at C-terminal was inserted into the pWPXL vector, which was co-transfected with the packaging plasmid psPAX2 and the envelop plasmid pMD2G into 293T cells to generate lentiviral particles. The particles were transduced into XP2YO cells to produce cell lines stably expressing wild-type or mutant XPF proteins according to established procedures (http://www.lentiweb.com) (Salmon et al., 2000; Salmon and Trono, 2006). The same procedure was applied to generate cell lines expressing wild-type or mutant ERCC1 in UV20 cells.

2.4.6 Local UV-irradiation and immunofluorescence

About 50,000 cells were plated on a coverslip in 6-well plates, grown for 2-3 days and irradiated through a polycarbonate membrane with 5 μm pores (Millipore) with UV light (254 nm) with a dose of 150 J/m^2 (XP2YO cells) or 120 J/m^2 (UV20 cells). Cells were incubated at 37°C, 5% CO_2 for 30 min to 24 hr. They were washed first with PBS and then with PBS plus 0.05% triton X-100 and fixed with 3% paraformaldehyde plus 0.1% triton X-100 (XP2YO cells) or washed first with PBS and then with PBS plus 0.1% triton X-100, and fixed by 3% paraformaldehyde plus 0.2% triton X-100 (UV20 cells). After fixation, cells were washed with PBS containing 0.2% triton X-100. To stain for (6-4)PPs, cells were treated with 0.07 M NaOH in PBS for 5 min, followed by washing with PBS plus 0.2% triton X-100. After blocking with PBS plus 5 mg/ml BSA and 1.5 m g/ml glycine, cells were stained with mouse monoclonal anti-(6-4)PP antibody (Cosmo Bio) 1:400, rabbit polyclonal anti-ERCC1 antibody (FL-297, Santa Cruz) 1:100, or rabbit polyclonal anti-HA antibody (ChIP grade, Abcam) 1:2000 for 1.5 h and washed with PBS containing 0.2% triton X-100. Cells were then incubated with secondary antibodies: Cy3-conjugated affinipure goat anti-mouse IgG(H+L) (Jackson ImmunoResearch) 1:1000 and Alexa Fluor 488-labeled $F(ab')_2$ fragment of goat anti-rabbit IgG (H+L) (Invitrogen) 1:800 for 1

h, followed by washing with PBS with 0.2% triton X-100. Samples were washed with PBS, embedded in Vectashield Mounting Medium with 1.5 µg/ml of DAPI (Vector Laboratories) and analyzed using a confocal microscope (Zeiss LSM 510). About 100 cells were counted in at least three independent experiments for quantification.

2.4.7 Clonogenic Survival Assay

Exponentially growing cells were plated in 6 cm dishes in triplicate at a density of 1-20 x 10^3-cells/plate for human cells or 250-5,000 cells/plate for Chinese hamster ovary cells, depending on the dose of genotoxin used and the predicted phenotype of the cells. For the hamster cells, wild-type cells were plated as follows: 3 plates at 250 cells/plate (untreated) 3 plates at 250 cells/plate (dose 1), 3 plates at 250 cells/plate (dose 2), 3 plates at 500 cells/plate (dose 3), and 3 plates at 500 cells/plate (dose 4). For hamster cells, knock-out cells were plated as follows: 3 plates at 250 cells/plate (untreated), 3 plates at 250 cells/plate (dose 1), 3 plates at 500 cells/plate (dose 2), 3 plates at 1000 cells/plate (dose 3), and 3 plates at 5,000 cells/plate (dose 4). The next day, the cells were transiently exposed to genotoxins. For UV treatment, the media was aspirated from the plates; the cells were washed with PBS; irradiated with UV (254 nm, Spectroline X-15) and the cells were replenished with fresh medium. For Mitomycin C (MMC) treatment, the cells were treated with medium containing MMC (Fisher) at 37°C for 1 hr. The plates were then washed twice with PBS and replenished with fresh medium. Seven to ten days after exposure to genotoxins, when colonies are visible to the naked eye, the cells were fixed and stained with 50% methanol, 7% acetic acid and 0.1% Coomassie brilliant blue. The colonies (defined as containing >10 cells) were counted using an Olympus SZ61 stereomicroscope with a 10X eyepiece. The

data was plotted as the number of colonies on treated plates divided by the number of colonies on untreated plates ± S.E. for a minimum of 2 independent experiments, both done in triplicate.

2.4.8 CD Experiment

Protein (XPF-ERCC1WT, XPF-ERCC1R678A, ERCC1k247A/K281A-XPFR850/K853A) was diluted to 680 nM (dilution buffer containing 25 mM K-phosphate (pH=7.6), 10% glycerol, 5 mM beta-mercaptoethanol, and 650 mM NaCl), and the CD spectrum measured on an Applied Photophysics Chirascan CD spectrometer. The scan was a 1-nm/s interval over 0.1 cm path length at 4°C with a wavelength range of 200 nm to 260 nm. The background signal for the buffer was subtracted and two experiments were conducted twice.

2.4.9 Western Blot

Cells were lysed in NETT buffer (50 mM Tris pH8.0, 150mM NaCl, 1mM EDTA, 0.5% NP40, and protease inhibitor (Roche). 30 µg of protein (60 µg for HeLa cell extracts) were separated on a 10% sodium dodecyl sulphate (SDS) gel and transferred to a Hybond-LFP membrane (low fluorescent Polyvinylidene fluoride (PVDF) membrane, Amersham Biosciences) at 350 mA for 2 h. After blocking with a 5% bovine serum albumin (BSA) solution, the membranes were incubated with primary antibodies: rabbit polyclonal anti-ERCC1 (FL-297, Santa Cruz) 1:200 (for UV20 cells), mouse monoclonal anti-XPF (3F2/3, Santa Cruz) 1:200 (for XP2YO cells), and mouse anti-tubulin (Sigma) 1:1000 for 1.5 h, washed by PBS plus 0.1%tween 20. Membranes were incubated with secondary antibodies: Cy3-conjugated affinipure goat anti-mouse IgG(H+L) (Jackson ImmunoResearch) 1:1000 and Alexa Fluor 488 F(ab')2 fragment of goat anti-rabbit IgG

(H+L) (Invitrogen) 1:1000 for 1 h, a nd washed with PBS plus 0.1% tween 20. A t last, membranes were washed with PBS, dried at room temperature and visualized by fluorescence on a Typhoon imaging system (Amersham Biosciences).

2.5 SUPPLEMENTAL DATA

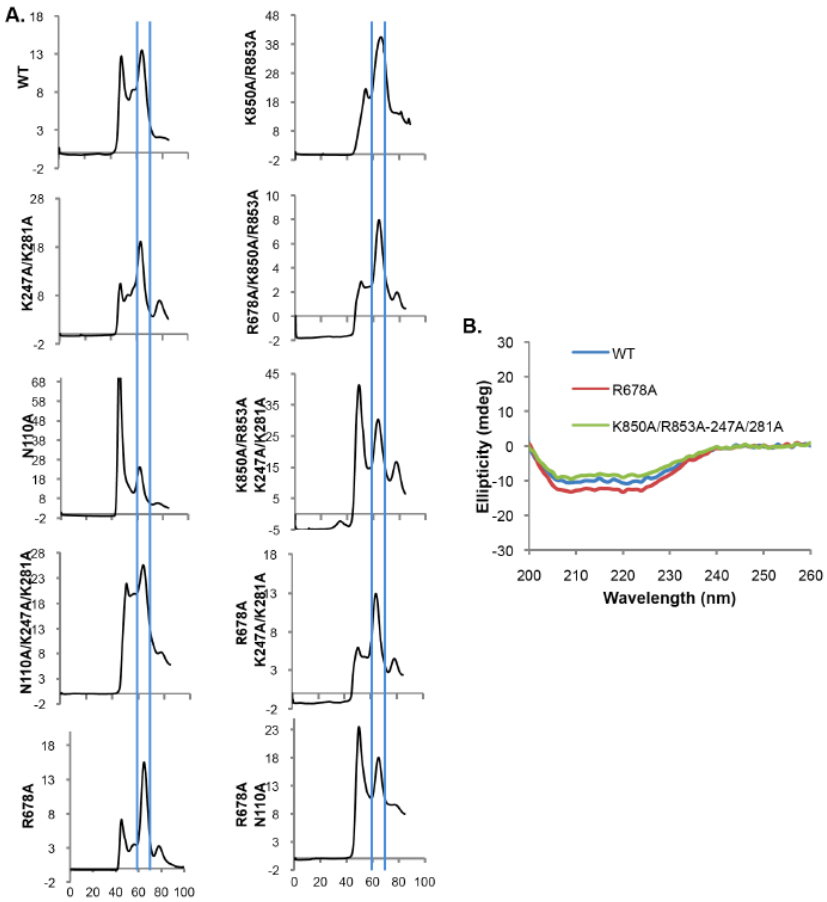

Figure 2-8 XPF-ERCC1 proteins with mutations in the HhH, nuclease and central domains are properly folded.

Wild type and mutant XPF-ERCC1 are purified through Nickel column, HiLoad 16/60 Superdex 200 column and Hitrap Heparin column. On the HiLoad 16/60 Superdex 200 c olumn, heterodimeric, active wild type and mutant XPF-ERCC1 were eluted at 60-70 ml and fractions in that range were collected around the peaks and used for further purification (A.). Wild type,

XPFR678A, and ERCC1K247A/K281A-XPFK850A/R853A proteins were test on t he CD spectrum. They had the similar peaks (B.).

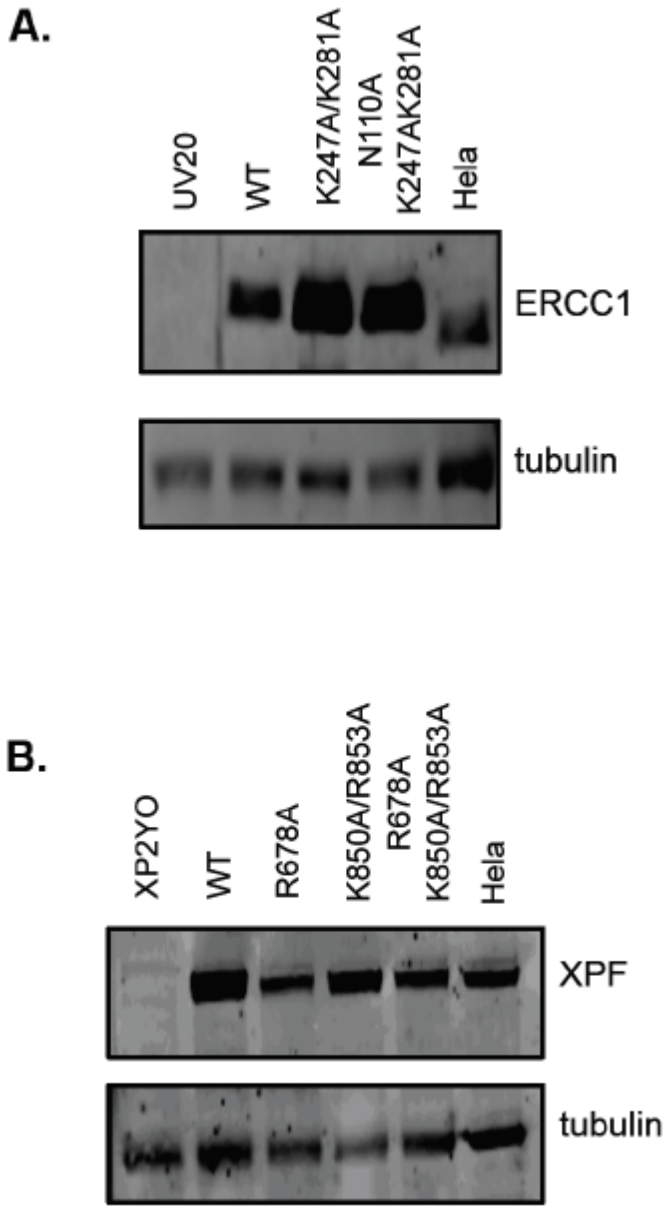

Figure 2-9 Expression level of ERCC1 and XPF protein in transduced UV20 and XP2YO cells

UV20 cells transduced with wild-type or mutant ERCC1 (A.) and XP2YO cells expressing wild-type or mutant XPF (B.) were lysed and 30 µg of protein from the extracts (60 µg for HeLa cell extracts) were separated on a 10% SDS gels and transferred to PVDF membrane. ERCC1 was detected using antibody FL-297 (A.), XPF using antibody 3F2/3 (B.). Tubulin was used as a loading control.

2.6 ACKNOWLEDGEMENTS

We thank Drs. Jill Fuss and John Tainer for help with the fluorescence anisotropy experiments, Dr. Jung-Eun Yeo for the gift of dG-AAF-containing plasmid, Dr. Arthur J. Campbell for help with Figure 1 and Drs. Tom Ellenberger and Oleg Tsodikov for a critical reading of the manuscript and helpful discussions.

In chapter 2, we examined the role of four C-terminal DNA binding domains in XPF-ERCC1. We have shown that there is a hierarchy of importance of these domains in interacting with DNA substrates. The effects of mutations in the DNA binding domains were also compared to the effect of mutations in the nuclease domain of XPF and the central domain of ERCC1. DNA binding residues located in the HhH domain of ERCC1 and the nuclease domain of XPF are more important to nuclease activity and NER activity than mutations in the DNA binding residues located in the HhH domain of XPF and mutations in the central domain of ERCC1.

Multiple protein:protein and protein:DNA interactions have been shown to drive NER. The results from chapter 2 highlight the importance of protein:DNA interactions for both NER and ICL repair. In addition, the interaction between ERCC1 and XPA through the central domain of ERCC1 has for long been shown to be absolutely essential for NER. The C-terminus of XPF-ERCC1, the central domain of ERCC1 and the nuclease domain of XPF have all been well characterized. However, very little is known about the N-terminus of XPF. To investigate whether the N-terminus of XPF is important to ICL repair, in chapter 3, described below, we engineered mutations in multiple conserved residues of the N-terminus and observed the sensitivities of the cell lines harboring the mutations to UV, MMC and IR

3.0 MUTATIONAL ANALYSIS OF *XPF*

Madireddy, A.[1], Derkunt, B.[2], Su, Y[2]., Bhagwat, N.R.[1], Scharer, O.D.[3], and L.J. Niedernhofer[4]

[1]Department of Human Genetics, University of Pittsburgh Graduate School of Public Health, 130 DeSoto Street, Pittsburgh, PA, 15261, USA

[2]Department of Chemistry, [3]Department of Pharmacological Sciences, Stony Brook University, Stony Brook, NY 11794-3400, 3current address: Herbert Irving Comprehensive Cancer Center, Columbia University, New York, NY 10032,

[4]Department of Microbiology and Molecular Genetics, University of Pittsburgh School of Medicine, Pittsburgh, Pennsylvania.

3.1 INTRODUCTION

The human genome is constantly exposed to extrinsic and intrinsic factors that cause chemical modification of DNA. Extrinsic factors include UV light, ionizing radiation, and chemotherapeutic drugs, while intrinsic include reactive oxygen species and by-products of lipid peroxidation (Friedberg, 1995). Organisms have evolved complex DNA repair mechanisms to resolve this damage (Weinert, 1998), which are critical for enabling basic cellular mechanisms such as replication and transcription. The cellular consequences of DNA damage are dependent

upon the type of lesion (e.g. strand break vs. adduct), when during the cell cycle the lesion is detected, and the abundance of damage. Misinterpretation of lesions by the replication machinery leads to mutations in the genome that may give rise to cancer (Hoeijmakers, 2009). However, extensive damage may result in programmed cell death (apoptosis) or cellular senescence both of which can contribute to aging (Schumacher et al., 2008). A mechanistic understanding of how DNA damage contributes to cancer and aging can be obtained by probing the robust DNA repair pathways that function in our cells to counter the damage induced.

XPF-ERCC1 is a structure-specific endonuclease (de Laat et al., 1998a; Sijbers et al., 1996a) that is essential for nucleotide excision repair (NER) (Biggerstaff et al., 1993; Petit and Sancar, 1999; Sijbers et al., 1996a), the repair of DNA interstrand crosslinks (ICL) (Bhagwat et al., 2009b; Kuraoka et al., 2000) and the repair of some DNA double strand breaks (Ahmad et al., 2008). They are obligate heterodimers in which XPF harbors the nuclease domain essential for its catalytic activity and ERCC1 is involved in DNA binding (Enzlin and Scharer, 2002). In NER, the two proteins aid in the removal of helix-distorting bulky lesions such as UV induced pyrimidine dimers (Biggerstaff et al., 1993). XPF-ERCC1 is recruited to the site of DNA damage by the interaction of XPA with ERCC1 (Orelli et al., 2010b; Tsodikov et al., 2007). In ICL repair, XPF-ERCC1 is involved in the second incision that unhooks the crosslink (Niedernhofer et al., 2004). It is well established that ICL repair is distinct from NER, requiring only XPF-ERCC1 and not other NER factors (McHugh et al., 2001; Niedernhofer et al., 2004). In addition, *in vitro* studies show that the amount of purified XPF-ERCC1 required for the incision of crosslinks requires a lot more enzyme than is physiologically relevant indicating that the in vitro reaction might be missing a recruiting factor that is contributing to this (Kuraoka et al., 2000).

Based on these observations, we hypothesize that similar to NER, XPF-ERCC1 is recruited to the DNA for ICL repair via a protein:protein interaction.

A novel component of ICL repair, FANCP, was identified recently. FANCP, also known as SLX4, is a structure-specific endonuclease that was first identified in a synthetic lethal screen for mutants that are lethal in the absence of Sgs1 (Mullen et al., 2001). In humans, SLX4 is thought to be a multi-domain scaffolding protein that regulates three structure-specific endonucleases, XPF-ERCC1, Mus81-EME1, and SLX1, by acting as a docking platform (Munoz et al., 2009a; Yildiz et al., 2002). Recently, individuals with Fanconi Anemia, caused by defective ICL repair, with mutations in the FANCP/SLX4 gene were identified (Kim et al., 2011; Stoepker et al., 2011a). Accordingly, SLX4-depleted cells are hypersensitive to crosslinking agents (Munoz et al., 2009a; Svendsen et al., 2009). Deletion analysis of the N-terminus of the FANCP protein disrupts its interaction with XPF (Fekairi et al., 2009). These point to an interaction between XPF and FANCP that is likely important for ICL repair. In this study, we test the hypothesis that disrupting the interaction between XPF and FANCP uncouples the functions of XPF-ERCC1 in NER and ICL repair.

To test this, several *XPF* mutants were designed and cloned, then expressed in XPF-deficient human fibroblast cells. The mutant cell lines include XPF^{HA}, which harbors an N-terminal HA tag, XPF^{G314E}, which harbors a point mutation affecting an amino acid essential for interaction with SLX4 in *Drosophila*, $XPF^{\Delta 5N}$, which harbors a 5 amino acid deletion in the N-terminus of XPF, and XPF^{D676A}, a catalytically dead mutant. Cells expressing these mutant proteins were tested for sensitivity to UV to measure NER, Mitomycin C to measure ICL repair and ionizing radiation (IR) to measure double-strand break repair (DSB repair). This study provides the first formal proof that the nuclease domain of XPF is absolutely essential for its

repair functions. The results also indicate that the G314E mutation renders the cells selectively sensitive to crosslinking agents, thus uncoupling repair. However, the inability of the wild-type *XPF* cDNA to correct sensitivity of XP-F cells to crosslinking agents led us to interrogate the sequence of the cDNA and endogenous protein. The published *XPF* sequence is 11 amino acids shorter than the endogenous protein (N-terminus) (Figure 3-10) and contains a G→D substitution at residue 703. Both of these are critical for rendering XPF fully functional in ICL repair.

3.2 RESULTS

3.2.1 Generation of mutations in conserved domains of XPF to uncouple DNA repair function

Based on structural studies (Andersen et al., 2009; Fekairi et al., 2009; Munoz et al., 2009a; Sgouros et al., 1999; Svendsen et al., 2009), modifications in multiple domains of XPF were identified as potentially important for ICL repair but not NER. Site-directed mutagenesis was used to generate the mutations in specific domains of *XPF* and lentiviral transduction used to generate stable mutant cell lines. To probe the functional importance of the nuclease domain, we generated a mutation in a highly conserved aspartic acid residue at position 676, changing it to an alanine (XPF^{D676A}). Based on preliminary data from our lab, we knew that a large tag such as the GFP tag in the N-terminus and not the C-terminus of XPF makes cells selectively hypersensitive to crosslinking agents (Figure 3-9). Consequently, to determine the importance of the N-terminus of XPF in protein folding, we generated a mutant that had only the N-terminal HA-tag, XPF^{HA}. In addition, a mutant *XPF* was also generated missing the first 5 amino acid

residues, XPF$^{\Delta 5N}$. Mutation of G306E in *mei-9*, the Drosophila homolog of XPF, disrupts its interaction with SLX4 (Yildiz et al., 2002). We mutated the corresponding residue in XPF to create XPF^{G314E}, and XPF$^{WLF\text{-}A}$ in which highly conserved residues W326, L327, F328 were mutated to alanines (Table 1).

Table 1-*XPF-ERCC1* Mutants

Gene	Mutation	Mutant name	Target domain	Anticipated Effect
XPF	Δ11 AA, G703D	XPF$^{\Delta 11NWT}$		ICL and DSB repair deficient
	G703D	XPF$^{WT+11aa}$		Full correction of XPF-ERCC1 deficient (XP2YO) cells
	Full length WT, D703G	XPF$^{WT+D703G}$		Full correction of XPF-ERCC1 deficient (XP2YO) cells
	D687A	XPF^{D687A}	Nuclease dead	ICL repair deficient
	G325E	XPF^{G325E}	SLX4 interaction	ICL repair deficient
	Deletion of Δ5N	XPF$^{\Delta 5N}$	Protein interaction	ICL and DSB repair deficient
	N-term HA tag	XPF^{HA}	Protein interaction	ICL and DSB repair deficient
	N-term GFP tag	XPF$^{N\text{-}GFP}$	Protein interaction	ICL and DSB repair deficient
	WLF to A	XPF$^{WLF\text{-}A}$	SLX4 interaction	ICL and DSB repair deficient
ERCC1	N110A/Y145A	ERCC1$^{N/Y}$	XPA-binding	NER deficient

Table listing all the *XPF* mutations generated the name of the mutant cell lines used, the target domain and the anticipated effect.

3.2.2 Expression of mutant XPF in the mutant cells by lentiviral transfection

The under expression of proteins can fail to correct sensitivity of the cell lines to genotoxic stress. To make sure that the expression levels of the exogenous XPF protein in each of the cell lines were comparable to the endogenous XPF levels in the wild-type cells, immunoblot analysis was carried out. Sixty micrograms of protein from whole cell extracts of each of the mutant cell lines was probed for XPF protein expression by immunoblot and compared to normal expression levels of the endogenous protein in wild-type cells. Wild-type cells showed a weak signal for ERCC1 and an even weaker one for XPF. XP2YO (XP-F) cells, which serve as a genetic negative control, showed a weak signal for ERCC1 but no signal for XPF. In XP2YO cells stably expressing mutant XPF, both XPF and ERCC1 expression was increased to greater than

endogenous levels (Figure 3-1). This indicates that the mutant constructs are over expressed. Since the constructs increased ERCC1 expression, it reveals that indeed ERCC1 is unstable the absence of XPF and that all of the mutant XPF proteins can bind and stabilize ERCC1. Overexpression of XPF-ERCC1 was approximately equal for all of the mutant cell lines. Therefore the differences in sensitivity of the mutant cells to genotoxic agents cannot be attributed to differences in nuclease expression.

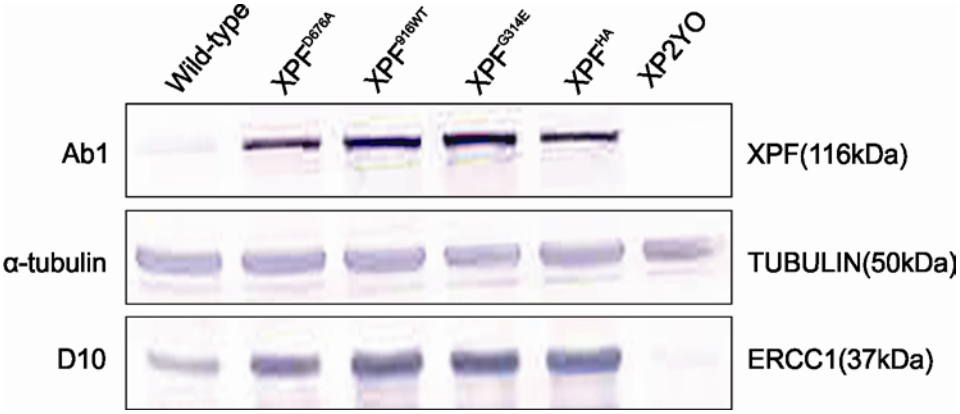

Figure 3-1 Comparing expression levels of XPF-ERCC1

Normal (wild-type) and XPF-ERCC1 deficient XPF mutant human fibroblasts (XP2YO), and XP2YO cells (transfected with the cDNA of wild-type XPF, XPF^{WT}, XPF^{D676A}, $XPF^{\Delta 5N}$, XPF^{HA}, XPF^{G314E} and $XPF^{WLF\text{-}A}$) were lysed and whole cell extracts were collected. The proteins were separated by SDS-PAGE (10% polyacrylamide gel), transferred onto nitrocellulose membranes and immunostained with antibodies (anti-XPF: Ab1, and anti-ERCC1: D-10). Tubulin was used as a loading control.

3.2.3 Clonogenic survival assay to measure NER, ICL repair and DSB repair

The data are reported as the percent of cells surviving (proliferating) at each dose of genotoxin compared to untreated cells. The three genotoxins employed were UV-C to measure NER, Mitomycin C to measure ICL repair, and IR to measure DSB repair. Reported are the average ± standard deviation from three independent experiments. In the figure, the survival curves of the wild-type cell line in response to all three forms of genotoxic stress is set to represent resistance

and the survival curve of the XP2YO cell line represents hypersensitivity. The survival curve of the wild-type corrected cell line is utilized as a second measure of resistance in exogenously expressed XPF to avoid bias that may be generated due to the mode of XPF expression. All three cell lines, for each genotoxin used, are utilized as controls so that the effect of the mutations on the protein function of XPF can be classified as resistant, sensitive or hypersensitive. The data reveals the survival curves of the XPF^{D676A} nuclease dead mutant, XPF^{G314E}, $XPF^{\Delta 5N}$ and the XPF^{HA} in response to UV, MMC and IR. In response to UV, the survival curves of the XPF^{G314E}, $XPF^{\Delta 5N}$ and the XPF^{HA} mutants indicated that they are resistant (Figure 3-2). The survival curve of the XPF^{D676A} mutant corresponds with, and in some cases is, more severe than the XP2YO cell line which lacks functional XPF (a).

In response to crosslinking agent Mitomycin C, all the mutants analyzed, XPF^{D676A}, XPF^{G314E}, $XPF^{\Delta 5N}$ and the XPF^{HA} were found to be hypersensitive (Figure 3-2b). The most perplexing observation however, was the hypersensitivity observed in the wild-type corrected cell line XPF^{WT} (Figure 3-2). This was highly unexpected and hinted at the possibility of alterations in the XPF gene that might be making the cells selectively sensitive to crosslinking agents.

The survival curves in response to ionizing radiation were used to probe proficiency of the DSB repair pathway. The results indicated again that XPF^{D676A}, XPF^{G314E}, $XPF^{\Delta 5N}$ were all hypersensitive to IR. However, the $XPF^{\Delta 11NWT}$ and XPF^{HA} were mildly sensitive if not resistant to the genotoxin (Figure 3-2c). These results established that alterations in the wild-type corrected cell line that was causing the hypersensitive phenotype in response to crosslinking agents did not have any effect on the NER or DSB repair ability of the cell line.

The hypersensitivity of the XPF^{D676A} mutant in response to UV, MMC and IR in comparison to the wild-type and the XP2YO cell line indisputably delineated the importance of the nuclease domain of XPF in all the repair pathways.

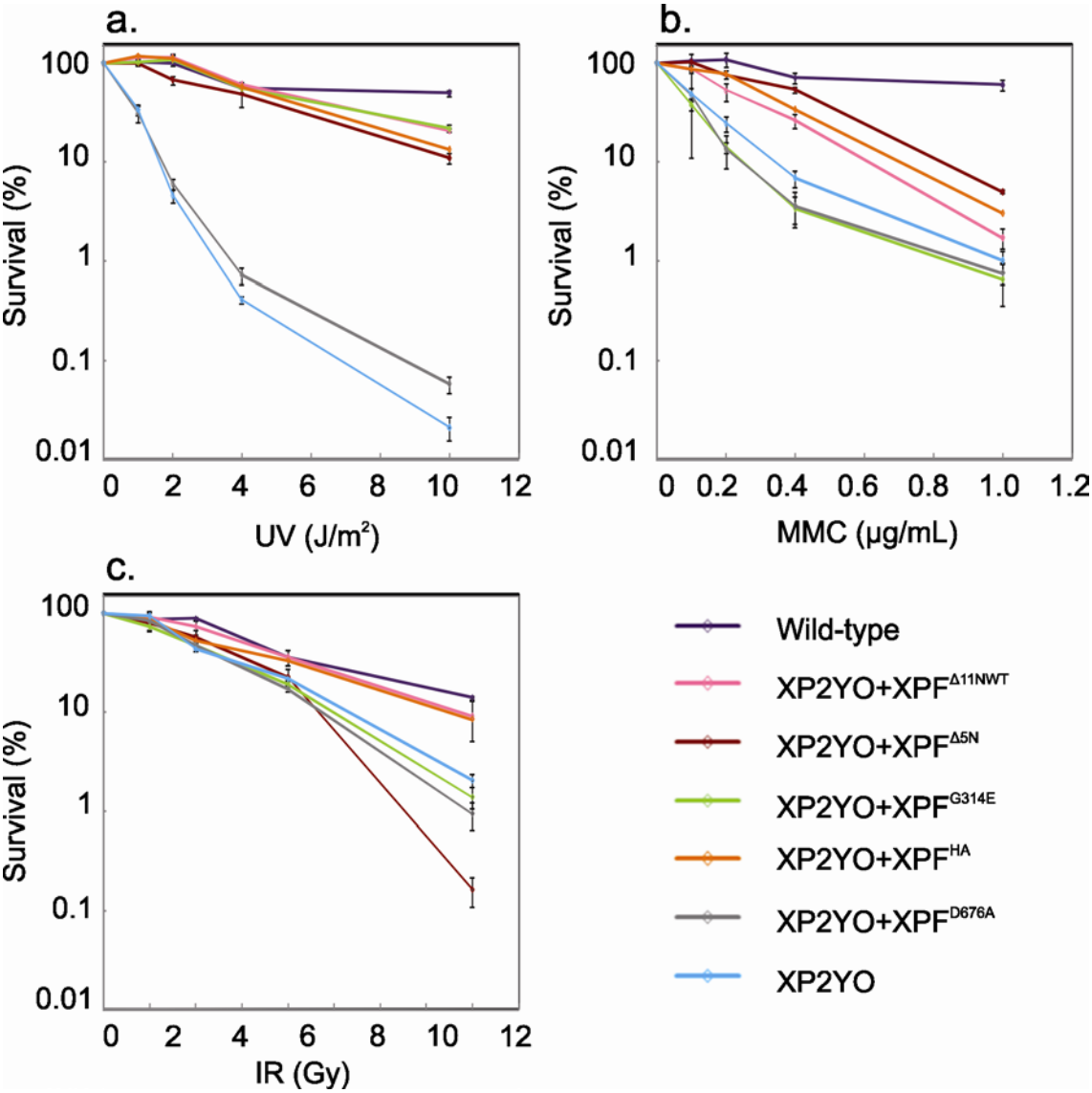

Figure 3-2 Clonogenic survival assay

Cells were challenged with UV (254nm) to determine the impact of the mutations on NER, with MMC to determine the impact on ICL repair, and IR to determine impact on DSB repair on WT (wild-type, SV40-transformed human fibroblasts), XPF-deficient (XP2YO) and complemented cell lines. The data were plotted as the percentage of colonies that were formed on the treated plates relative to the untreated plates ± S.E (error bars) for a minimum of 2 independent experiments each done in triplicate.

3.2.4 Immunodetection of UV lesions to interrogate NER

Since the survival assay is an indirect measure of repair, secondary endpoints that directly measure NER and ICL repair were employed. A local damage assay was used to determine the NER proficiency of each cell line. The experiment involved the treatment of cells with UV through filter meshes (Volker et al., 2001). The regions of the cell exposed to the UV treatment were expected to show both 6-4PP lesion formation and ERCC1 protein recruitment. The complete co-localization of the 6-4PP lesion with ERCC1 foci 30 m inutes after irradiation followed by the disappearance of both the lesion and the repair protein 24 hours after treatment denoted proficient repair. The first column of (Figure 3-3) represents the wild-type corrected cell line, XPF^{WT} that was used as the positive control for the experiment. The second column of the figure represents the cell line $ERCC1^{N110A/Y154A}$, which harbors a mutation in ERCC1 that disrupts interaction with XPA that is essential for the recruitment of XPF-ERCC1 to NER. This mutant has been previously been shown to be defective in NER (Orelli et al., 2010b) and was hence used as a negative control line. The recruitment of ERCC1 to the 6-4PP lesions was clearly visible 30 minutes post UV irradiation in all the cell lines with the exception of the negative control line $ERCC1^{N110A/Y154A}$ in which the recruitment of ERCC1 was not visible. 24h post irradiation, proficient NER, denoted by the disappearance of the lesions and ERCC1 foci, was observed in XPF^{G314E}, $XPF^{\Delta 5N}$ and the XPF^{HA} mutants in accordance with the wild-type control. The persistence of the damage foci in the nuclease dead cell line XPF^{D676A} supported the previous data obtained from the clonogenic survival assay and indicated that the nucleolytic activity of XPF was essential for its NER function and additionally implied that the activity was not required for the recruitment of XPF-ERCC1 to the NER pathway (Figure 3-3).

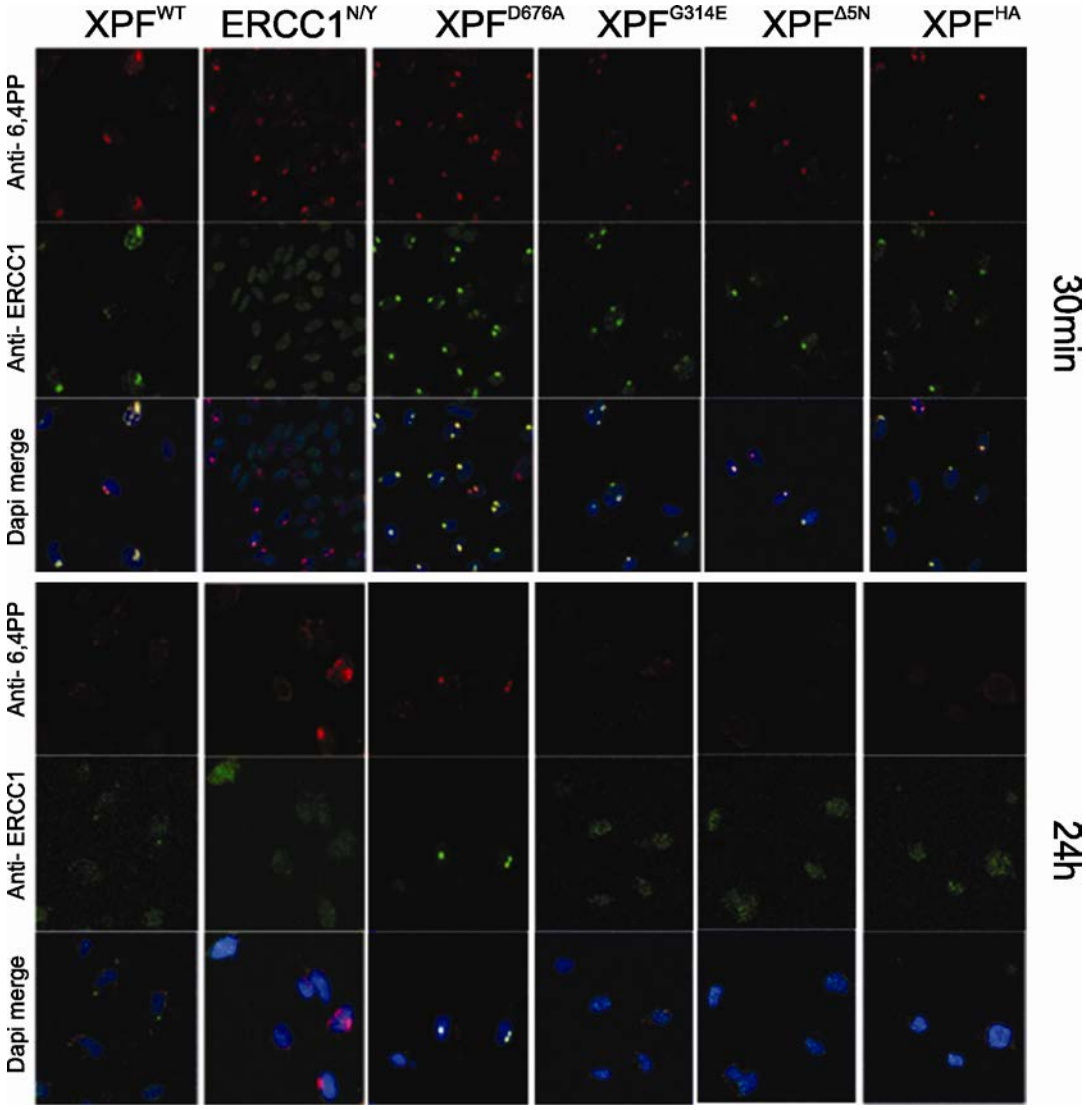

Figure 3-3 Local UV damage assay

Wild-type XPF complemented XPF-ERCC1 deficient (XP2YO) cell line (column 1; positive control), ERCC1-deficient UV20 cells complemented with NER deficient ERCC1$^{N110A/Y145A}$ (column 2; negative control) and XPF-deficient (XP2YO) complemented cell lines were challenged with UV light (254nm, 120 J/m2) through a polycarbonate filter with 5 μm pores and incubated at 37°C for 30 min or 24h. Cells were fixed and stained with antibodies against (6-4)PPs (red; row1), XPF-ERCC1 (green, using anti-ERCC1 antibody; row2). Nuclear DNA was visualized by DAPI staining. Merged images (row3).

3.2.5 Monoubiquitination of FANCD2 to interrogate ICL repair

Monoubiquitination of FANCD2 in response to Mitomycin C and the disappearance of the monoubiquitinated form are commonly used to interrogate the activation of ICL repair and success of that repair (Bhagwat et al., 2009b). Wild-type, XPF^{G314E}, XPF^{D676A}, and XP2YO cell lines were treated with 3μM MMC to induce DNA damage by the formation of ICLs. ICL repair proficiency, assessed as the function FANCD2 monoubiquitination, was determined by monitoring the increase and subsequent decrease in the ratio of FANCD2-L (monoubiquitinated) to FANCD2-S (non-ubiquitinated) band at 0, 12 and 4h respectively by immunoblot analysis. The wild-type cell line expressing endogenous XPF and the XP2YO cell line lacking XPF protein expression were utilized as positive and negative controls respectively. At the 0h time point representative of no treatment, the faint FANCD2-L band observed in all cell lines may be attributed to the repair that takes place in the cell due to endogenous DNA damage. At 24h, the activation of crosslink repair denoted by the formation of the FANCD2-L band was observed in all cell lines. By 48h, removal of the lesion characterized by the disappearance of FANCD2-L was observed in the wild-type cell line. The persistence of the FANCD2-L band in XPF^{G314E}, XPF^{D676A}, and XP2YO demonstrated the inability of the cell lines to complete ICL repair (Figure 3-4). This data was consistent with data from the clonogenic survival assay in which mutation at position 314 was rendering XPF^{G314E} cells selectively hypersensitive to crosslinking agents. In addition, this data revealed that FANCD2 is monoubiquitinated in response to cross-linking agents irrespective of the nucleolytic status of XPF implying that the nucleolytic ability of XPF-ERCC1 is not essential for FA pathway activation but is required for the subsequent completion of ICL repair.

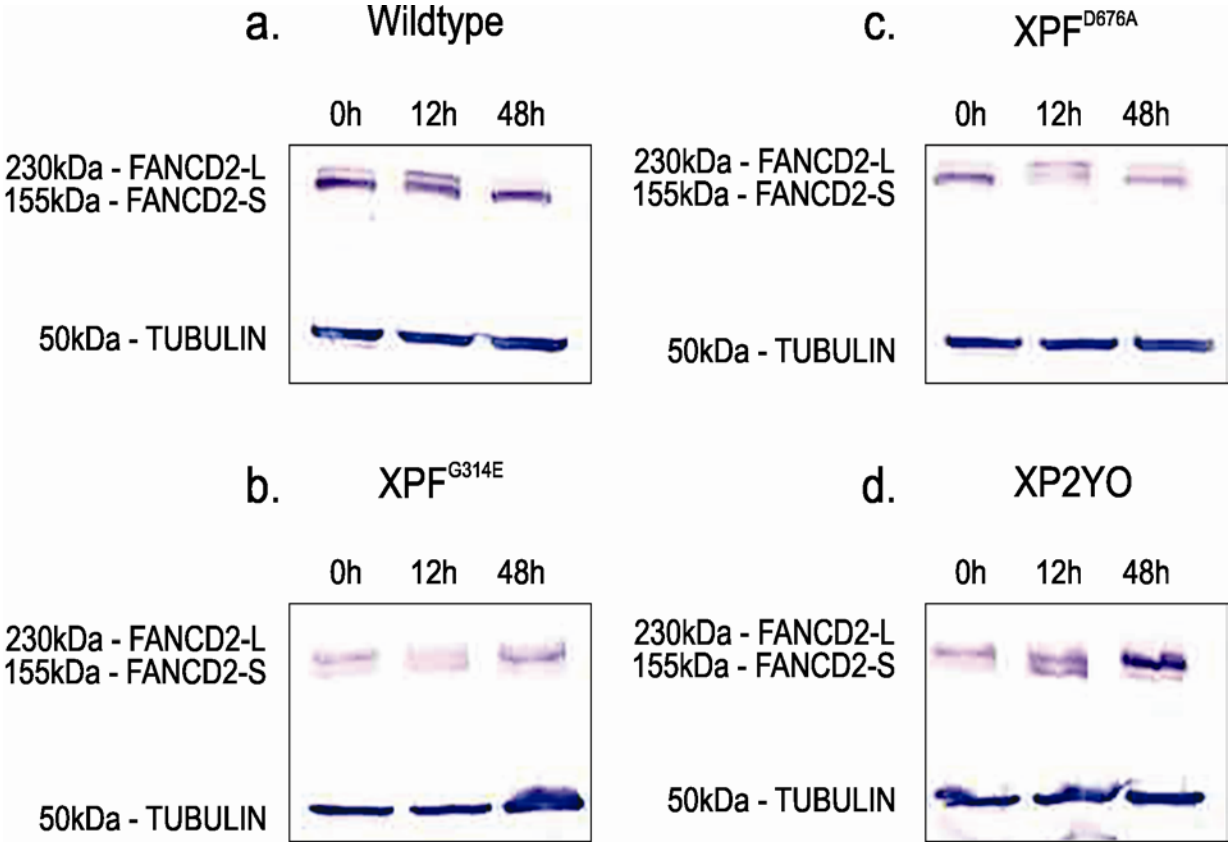

Figure 3-4 Monoubiquitination of FANCD2

Normal (wild type), XPF-ERCC1 deficient (XP2YO) cells and complemented cell lines were exposed to 0.3 μM MMC for 12 h and the WCEs were collected at 0, 12 and 48h following exposure for the immunodetection of FANCD2. Tubulin was used as the loading control.

3.2.6 Defects in the original *XPF* construct

Mass spectrometric analysis of the XPF protein and its degradation bands observed by silver staining (Figure 3-5) lead to the identification of the 11 amino acid deletion in the N-terminus of the *XPF* gene (Figure 3-10). This deletion was attributed to aberrant use of the methionine residue 11 amino acids downstream of the actual methionine start site of the gene. Since it was highly plausible that the ICL repair sensitivity observed in the mutant cell lines be caused by the 11 amino acid deletion, new constructs rectifying this deletion were made and the all the mutations were regenerated in the correct XPF construct.

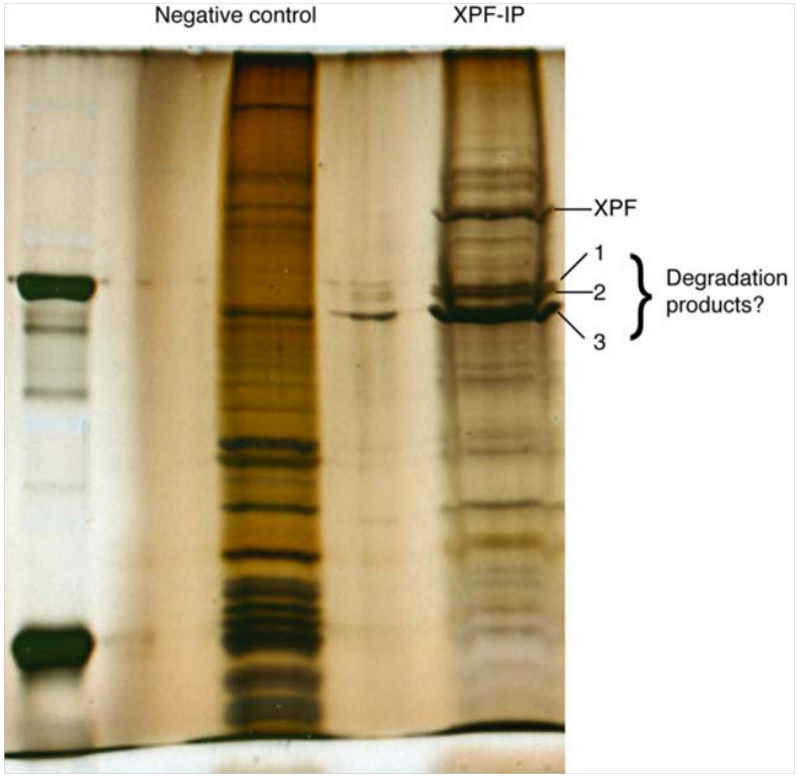

Figure 3-5 Silver staining of XPF-IP

The whole cell extract from HeLa cells was subject to immunoprecipitation to pull down XPF protein. The immunoprecipitated sample was resolved on a n 8% SDS-PAGE gel and silver stained. The XPF band along with the degradation products (1,2, and 3) were dissected from the gel for mass spectrometric analysis.

3.2.7 Addition of the 11 missing amino acids in the N-terminus of XPF does not correct ICL repair

The regenerated cell lines included, XPF^{916WT} the full length 916 amino acid wild-type corrected cell line, the XPF^{G325E} FANCP-XPF mutant and a third new mutant $XPF^{WLF\text{-}A}$ that had W326, L327, F328 mutated to alanines. These three bulky amino acids occur after the ICL sensitive glycine, and all of them have been known to be conserved in mice. In addition, the tryptophan and lysine residues are also conserved in the yeast protein. A ll the mutant cell lines and the $XPF^{WT+11aa}$ cell line were moderately sensitive to UV damage (Figure 3-6). The XPF^{G325E} and the

XPF^{WLF-A} mutants were hypersensitive to MMC confirming the importance of this region for the participation of XPF in ICL repair potentially through its interaction with FANCP (Figure 3-6). All the mutants were moderately sensitive to IR. The hypersensitivity of the wild-type corrected cell line XPF^{916WT} in response to MMC persisted. This raised questions of the possibility of additional imperfections in the original *XPF* construct. A sequence analysis identified a mutation at position 703 that had switched a glycine residue to aspartic acid.

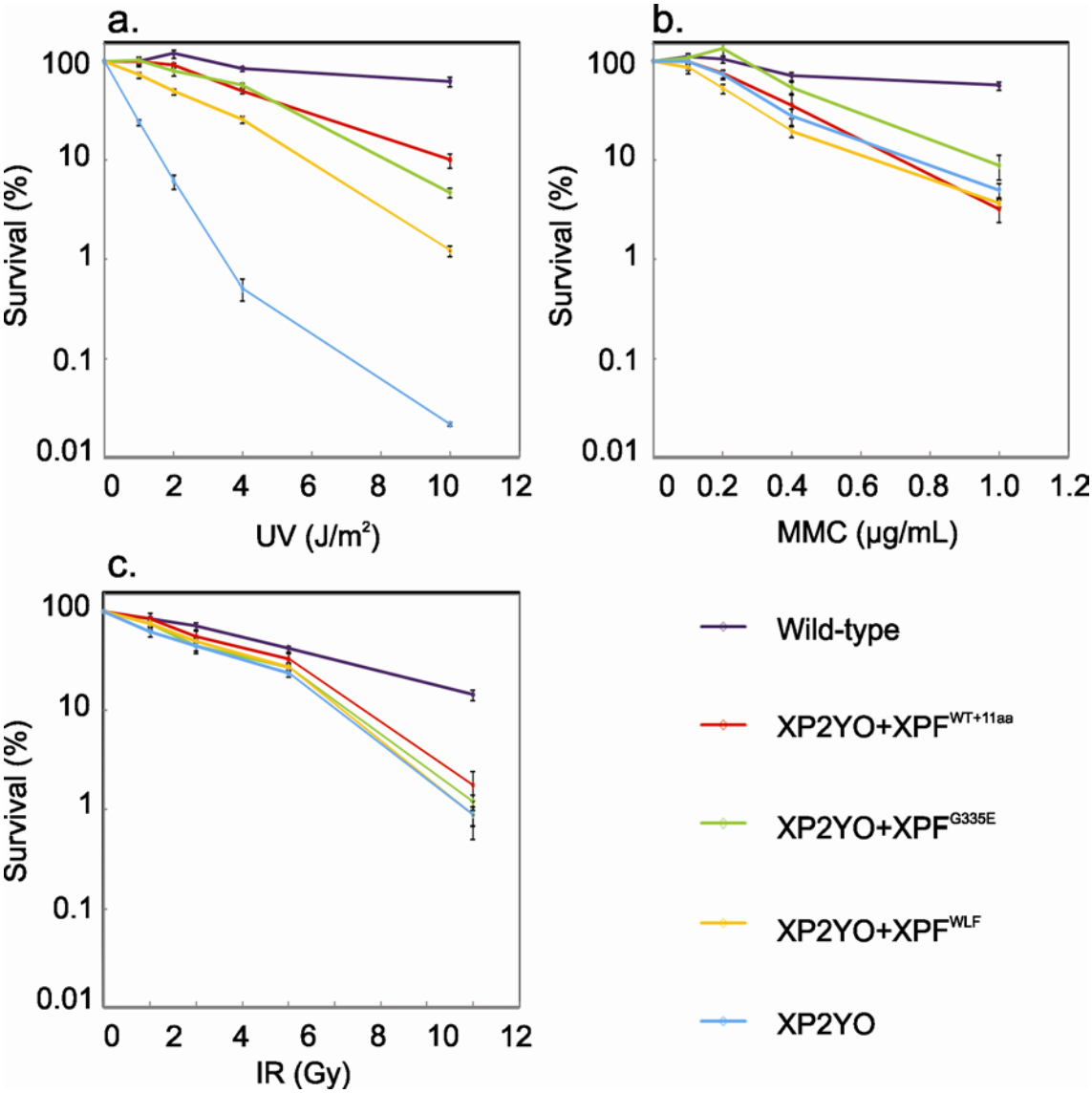

Figure 3-6 Analysis after addition of the first 11 a.a

Cells were challenged with UV (254nm) to determine the impact of the mutations on NER, with MMC to determine the impact on ICL repair, and IR to determine impact on DSB REPAIR on WT (wild-type, SV40-transformed human fibroblasts), XPF-deficient (XP2YO) and complemented cell lines. The data were plotted as the percentage of colonies that were formed on the treated plates relative to the untreated plates ± S.E (error bars) for a minimum of 2 independent experiments each done in triplicate.

3.2.8 Restoration of the glycine residue at position 703 fully corrects NER, and ICL repair sensitivity

To determine the effect of the D703G correction in XPF on the overall survival of the cell lines in response to genomic insult, the panel of wild-type corrected cell lines, $XPF^{11\Delta N}$, XPF^{916WT}, and $XPF^{WT+D703G}$ were compared with the wild-type and XP2YO controls. The results from Figure 5 showed that the $XPF^{WT+D703G}$ cell line is resistant to both UV and MMC thus indicating the complete correction of the XPF construct. Curiously, the $XPF^{WT+D703G}$ cell line was found to be moderately sensitive to IR (Figure 3-7). An immunoblot analysis was thus carried out to compare the XPF protein levels. The protein level in the newly generated $XPF^{WT+D703G}$ was much higher than the endogenous control and also the previous XPF^{916WT} cell line (Figure 3-8). This over expression could potentially explain the IR sensitivity observed in the new wild-type XPF cell line. These results showcase the importance of protein expression levels on cellular function. The effects of mutations in different residues in the N-terminus of *XPF* are summarized in Table 2 Table summarizing the observed effect of modification in different regions of *XPF* Table 2. Having corrected the XPF construct completely, new cell lines harboring our mutations of interest are being generated bearing in mind the importance of protein expression levels.

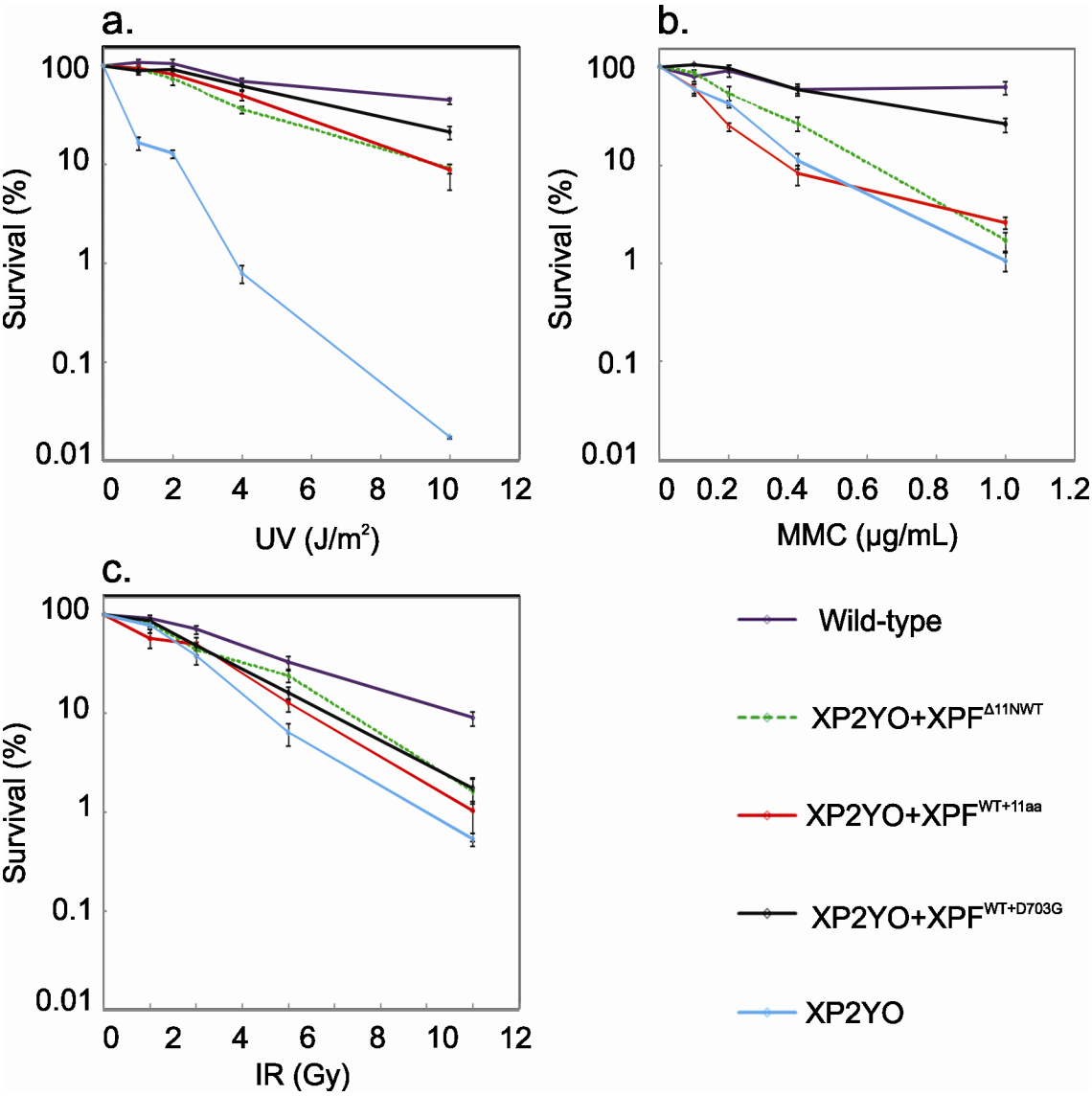

Figure 3-7 Comparison of wild-types after complete correction of XPF

Cells were challenged with UV (254nm) to determine the impact of the mutations on NER, with MMC to determine the impact on ICL repair, and IR to determine impact on DSB repair on WT (wild-type, SV40-transformed human fibroblasts), XPF-deficient (XP2YO) and complemented cell lines. The data were plotted as the percentage of colonies that were formed on the treated plates relative to the untreated plates ± S.E (error bars) for a minimum of 2 independent experiments each done in triplicate.

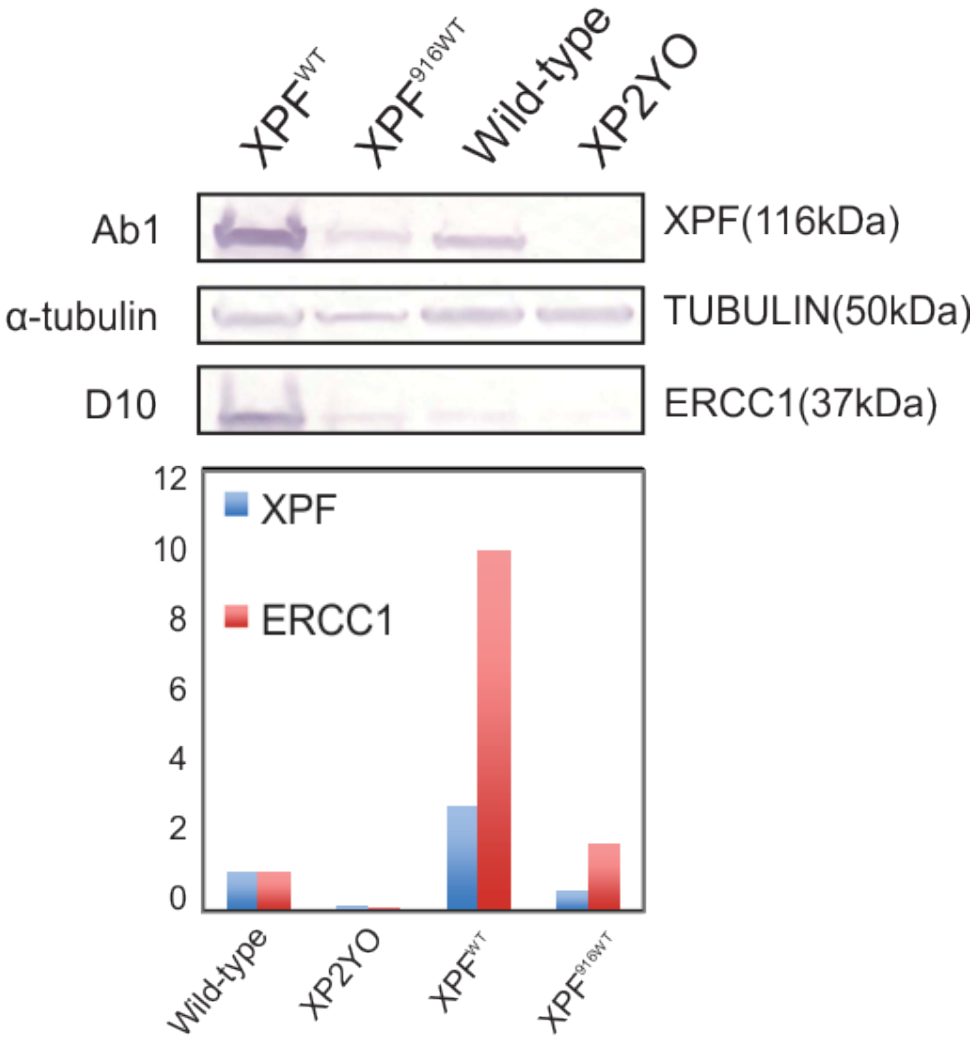

Figure 3-8 XPF-ERCC1 expression levels

Normal (wild-type) and XPF-ERCC1 deficient XPF mutant human fibroblasts (XP2YO), and XP2YO cells (transfected with the cDNA of $XPF^{WT+11aa}$, and $XPF^{WT+D703G}$) were lysed and whole cell extracts were collected. a. The proteins were separated by SDS-PAGE (10%

polyacrylamide gel), transferred onto nitrocellulose membranes and immunostained with antibodies (anti-XPF: Ab1, and anti-ERCC1: D-10). Tubulin was used as a loading control. b. Quantification of expression levels using Image J.

Table 2 Table summarizing the observed effect of modification in different regions of *XPF*

Mutant name	Target domain	Observed Effect
$XPF^{\Delta 11NWT}$		ICL and DSB repair deficient
$XPF^{WT+11aa}$		ICL and DSB repair deficient
$XPF^{WT+D703G}$		Full correction of XPF-ERCC1 deficient (XP2YO) cells
XPF^{D687A}	Nuclease dead	ICL repair deficient
XPF^{G325E}	SLX4 interaction	ICL repair deficient
$XPF^{\Delta 5N}$	Protein interaction	ICL and DSB repair deficient
XPF^{HA}	Protein interaction	Resistant
$XPF^{N\text{-}GFP}$	Protein interaction	ICL repair deficient
$XPF^{WLF\text{-}A}$	SLX4 interaction	ICL and DSB repair deficient
$ERCC1^{N/Y}$	XPA-binding	NER deficient

3.3 DISCUSSION

XPF-ERCC1 are heterodimeric structure specific endonucleases that have affinity for a wide range of substrates (de Laat et al., 1998a; Sijbers et al., 1996a). Both proteins originate from the XPF family of endonucleases. In eukaryotes, XPF has been known to have 3 major domains; the helicase like domain, the nuclease domain and the helix-hairpin-helix domain (Aravind et al., 1999; Sgouros et al., 1999). ERCC1, having lost the helicase like domain to gene divergence, has only two of the three conserved domains; the nuclease dead domain that serves as the DNA binding component (Tsodikov et al., 2005) and the helix-hairpin-helix domain. XPF and ERCC1 interact with each other through their HhH domains (Sijbers et al., 1996a). The nucleolytic activity of the complex is mediated by the nuclease domain of XPF (Enzlin and Scharer, 2002) and the DNA binding that is essential for the nucleolytic activity is carried out by ERCC1.

3.3.1 The nuclease domain of XPF

Even though we know a lot about the structure and the substrate specificity of XPF, the functional importance of the nuclease domain is still not well established. Our cellular studies show that the active nucleolytic activity of XPF is absolutely essential for NER, ICL repair and DSB repair. This is further established by the local damage assay that shows a persistence of the 6-4PP and ERCC1 foci even after 24h of UV treatment. Similarly, persistence of the monoubiquitinated form of FANCD2 provides additional proof that cells harboring the nuclease dead XPF are incapable of completing ICL repair (Figure 3-2Figure 3-4).

3.3.2 Uncoupling repair functions of XPF-ERCC1

Preliminary data from our lab has shown that the addition of a GFP tag to the N-terminus of the *XPF* gene makes cells hypersensitive to crosslinking agents. Our study has investigated the importance of the N-terminus of the *XPF* gene for ICL repair. A small HA-tag at the N-terminus of the protein does not seem to have an effect on the sensitivity of the cells to crosslinking agents however a deletion in the N-terminus of the *XPF* gene seems to have a profound effect on crosslink sensitivity (Figure3-2).

It is now well established that the recruitment of XPF-ERCC1 to the NER pathway is mediated by the interaction between XPA and ERCC1 (Orelli et al., 2010b; Tripsianes et al., 2007; Tsodikov et al., 2007). Our study investigates regions of the *XPF* gene involved in the recruitment of XPF-ERCC1 to the ICL repair pathway. The glycine residue in the 325 position of the *XPF* gene when mutated seems to make cells hypersensitive to crosslinking agents (Figure 3-6). Additionally, the conversion of bulky residues W, L and F in positions 326, 327 and 328 of

XPF to alanine residues, preferentially makes cells hypersensitive to crosslinking agents (Figure3-6). The unexpected mutation of G703D identified in the nuclease domain of the XPF mimics the hypersensitivity seen in the XPF^{G325E} and XPF^{WLF-A} cell lines (Figure 3-6). This result identifies a new region within the nuclease domain of XPF that seems to be important to its ICL repair function. The exact nature of the association remains unknown.

3.3.3 XPF-ERCC1 in aging

Mice deficient in Xpf-Ercc1 display an exaggerated accelerated aging phenotype characterized by numerous degenerative changes associated with aging including osteoporosis, neurodegeneration, bone marrow failure, thin skin and reduced kidney and liver function (Prasher et al., 2005). On the other hand, NER deficient *Xpa* null mice are almost identical to their wild type litter mates (van Steeg et al., 2001). Additionally, a new human progeroid syndrome, XFE, caused by a mutation in the *XPF* gene was identified in 2006 (Niedernhofer et al., 2006). XFE is characterized by death before sexual maturation, weight loss, epidermal atrophy, hypertension, liver dysfunction and renal insufficiency and an immunoblot analysis comparing the protein levels of XP patients with the XFE patient revealed highly reduced levels of XPF-ERCC1 in the XFE patient (Niedernhofer et al., 2006). This was an intriguing finding as mutations in the XP-family of genes usually result in Xeroderma pigmentosum, a disorder characterized by a deficiency in NER and patients with a deficiency in XPF usually show residual NER activity and only have mild XP (McWhir et al., 1993a; Sijbers et al., 1998). The phenotype of the XFE patient was found to be almost identical to the Ercc1 deficient mouse model and cells from the XFE patient were hypersensitive to crosslinking agents. All these observations collectively highlight the fact that dramatic depletion of XPF-ERCC1 results in an

exaggerated symptoms in both humans and mice that are characteristic of accelerated aging. This phenotype observed is due to functions of XPF-ERCC1 that are distinct from NER with a heavy implication towards ICL repair. Our study identifies mutations that uncouple the repair functions of the XPF-ERCC1 in NER and ICL repair (Figure 3-2) and provides us with a unique opportunity to test the hypothesis that the accumulation of unrepaired interstrand crosslinks in cells is accelerating the aging process. In the future, this contribution can be better understood by looking at the phenotype of a mouse model harboring these *XPF* mutations.

3.3.4 XPF-ERCC1 in chemoresistance

Numerous studies have implicated XPF-ERCC1 in platin-resistance (Reed, 2006). The initial assumption was that increased levels of NER mediated by XPF-ERCC1 was contributing to the resistance (Olaussen et al., 2007). This however was proved wrong by studies that have shown that the disruption of NER by knocking down proteins involved solely in the nucleotide excision repair pathway has no discernible effect on crosslink sensitivity of the cells. However, when ERCC1, involved in NER and ICL repair is knocked down by siRNA, the cells become hypersensitive to crosslinking agents (Cummings et al., 2006). This was further established by Orelli *et al*. in a study that showed that the disruption of the recruitment of XPF-ERCC1 by XPA to the NER pathway does not have an effect on crosslink sensitivity of the cells. Our study identifies regions of the XPF gene that are important for the function of XPF-ERCC1 in ICL repair but not NER (Figure 3-6). This work paves the way for the development of small molecule inhibitors to specific regions of the *XPF* gene that have the potential to overcome chemoresistance.

3.4 EXPERIMENTAL PROCEDURES

3.4.1 Cell Lines

SV40 transformed human fibroblast cell line wild type (normal), XP2YO (XP-F) were cultured in either Ham's F10 or RPMI supplemented with 10% fetal bovine serum albumin, antibiotics, and non-essential amino acids respectively. The cells were all grown at 37 ^{0}C in a 5% carbon dioxide (CO2) incubator.

3.4.2 Lentiviral Cell Transduction

The cDNA of wild-type XPF, XPF^{WT}, XPF^{D676A}, XPF$^{\Delta 5N}$, XPF^{HA}, XPF^{G314E} and XPF$^{WLF\text{-}A}$ were cloned into the lentiviral vector pWPXL by substituting the green fluorescent protein cDNA. 293T cells were co-transfected with the lentiviral vector containing the different constructs, the packaging plasmid psPAX2, and the envelope plasmid pMD2G. Details of the vectors, the production of high titer viruses, and lentiviral transduction can be found through LentiWeb (Salmon et al., 2000; Salmon and Trono, 2006). XPF deficient human XP2YO fibroblast cells at 50% confluency were infected with the viral particles containing the different XPF recombinant constructs with a multiplicity of infection of 10 a nd cultured as described above. The transduction efficiency was assessed by immunofluorescence.

3.4.3 Immunoblotting

Cells were trypnized, washed with PBS and were lysed with NETT buffer (100mM NaCl, 50mM Tris base, pH 7.5, 5mM EDTA, pH 8.0, 0.5% Triton X-100) containing Complete mini-protease inhibitor cocktail and phosphatase inhibitor cocktail (Roche). 60ug of total protein was boiled for 5 min in 4X protein loading buffer (0.25 M Tris-HCl, pH 8.5, 8% SDS, 1.6 mM EDTA, 0.1M DTT, 0.04% bromophenol blue and 40% glycerol), separated by SDS-PAGE (10% polyacrylamide gel), and transferred to a nitrocellulose membrane. The expression of XPF (anti-XPF: Ab1; Neomarkers; 1:1000) or ERCC1 (anti-ERCC1: D-10; Santa Cruz; 1:100) was estimated by immunodetection. Tubulin antibody (Promega) was used as the loading control.

3.4.4 Local UV Irradiation and Immunofluorescence

Cells were seeded and cultured on glass coverslips and processed as described (Volker et al., 2001). Briefly, cells were covered with a polycarbonate filter with 5-μm pores (Millipore) and irradiated with 120 J /m^2 using a UV-C lamp (EL series, UVP, model UVLS-28). After a recovery period, the cells were washed with PBS, permeabilized with 0.2% Triton X-100 in PBS for 30 s, and then fixed with 3% paraformaldehyde containing 0.2% Triton X-100 for 15 min at room temperature. Cells were washed with PBS containing 0.1% Triton five times. To detect (6-4)PP, cells were treated with 0.07 M NaOH in PBS for 5 min and washed. Cells were blocked with PBS+ (PBS containing 0.15% glycine and 0.5% bovine serum albumin) for 30 min and then incubated with the primary antibodies (murine monoclonal antibody 64M-2 against (6-4)PP (kindly provided by Stuart Clarkson, Geneva, Switzerland), 1:400; rabbit polyclonal antibody FL-297 against ERCC1 (Santa Cruz Biotechnology), 1:300, diluted in PBS+) for 2 h under dark

and humid conditions. The samples were embedded in VECTASHIELD mounting medium (Vector Laboratories) containing 4′-6′-diamino-2-phenylindole at a concentration of 0.1 mg/ml. Cells were analyzed using a confocal microscope (Zeiss LSM 510). For quantification, at least 100 cells were analyzed and counted each in three independent experiments.

3.4.5 Clonogenic Survival Assay

Exponentially growing cells were plated in 6 cm dishes in triplicate at a density of 1-20 x 10^3-cells/plate for human cells depending on the dose of genotoxin used and the predicted phenotype of the cells. For example for human cells, wild-type cells were plated as follows: 3 plates at 1000 cells/plate (untreated), 3 plates at 1000 cells/plate (dose 1), 3 plates at 1000 cells/plate (dose 2), 3 plates at 2000 cells/plate (dose 3), and 3 plates at 2000 cells/plate (dose 4). For human cells, knock-out cells were plated as follows: 3 plates at 1000 cells/plate (untreated) 3 plates at 1000 cells/plate (dose 1), 3 plates at 2000 cells/plate (dose 2), 3 plates at 4000 cells/plate (dose 3), and 3 plates at 20,000 cells/plate (dose 4). The next day, the cells were transiently exposed to genotoxins. For UV treatment, the media was aspirated from the plates, the cells were washed with PBS, irradiated with UV-C (254 nm, Spectroline X-15) and the cells were replenished with fresh medium. For Mitomycin C (MMC) treatment, the cells were treated with medium containing Mitomycin C (Fisher) dissolved in deionized water at 37 ^{0}C for 1 hr. The plates were then washed twice with PBS and replenished with fresh medium. Seven to ten days after exposure to genotoxins, when colonies are visible to the naked eye, the cells were fixed and stained with 50% methanol, 7% acetic acid and 0.1% Coomassie brilliant blue. The colonies (defined as containing >10 cells) were counted using an Olympus SZ61 stereomicroscope with a 10X eyepiece. The data was plotted as the number of colonies on treated plates divided by the

number of colonies on untreated plates ± S.E. for a minimum of 2 independent experiments, both done in triplicate.

3.4.6 Immunoprecipitation for silver staining

Protein A/G beads were incubated for 4 hours at 4˚C with 10µg of the anti-XPF antibody clone 219 (Neomarkers), then washed once with PBS and once with 0.2M Sodium Tetraborate Decahydrate ($Na_2B_4O_7.10H_2O$) (pH9.0) at room temperature. The beads were then incubated with crosslinking buffer containing 0.02M Dimethyl Pimelimidate (DMP) for 30 minutes at room temperature to crosslink the antibody to the beads and then in 0.2M Ethanolamine (pH8.0) for 30 minutes to stop the reaction. The beads were then thoroughly washed at 4˚C with two changes of PBS and two changes of RIPA buffer, and stored at 4˚C for further use.

HeLa cells were trypsinized, pelleted, washed twice with PBS and then lysed with RIPA buffer on ice for 30 minutes. The whole cell lysate (WCE) was clarified by centrifugation and then precleared with protein A/G beads. The precleared lysate was then mixed with the anti-XPF antibody crosslinked to protein A/G beads as described above, and incubated at 4˚C for 4 hours. The beads were spun down, washed thoroughly with RIPA buffer, and then incubated with 4xLaemmli buffer (0.25 M Tris-HCl, pH 8.5, 8% SDS, 1.6 mM EDTA, 0.1 M DTT, 0.04% bromophenol blue and 40% glycerol) for 10 minutes at 90˚C. The sample was resolved on an 8% SDS-PAGE gel and silver stained using the Bio-Rad silver stain plus kit according to the manufacturer's instructions. Bands corresponding to the expected mass of XPF were dissected and immediately frozen at -80˚C for mass spectrometric analysis.

3.4.7 LC-MS/MS and Data analysis

Gel bands of the protein of interest, obtained from silver staining, were subjected to in-gel digestion. The gel bands were destained in 50% acetonitrile in 50 mM NH_4HCO_3, pH 8.4 and vacuum dried. Trypsin (20 μg/ml in 25 mM NH_4HCO_3, pH 8.4) was added and samples were allowed to incubate on ice for 45 minutes. The supernatant was removed and the gel bands were covered with 25 mM NH_4HCO_3, pH 8.4, and incubated at 37 ^oC overnight. From the gel pieces, tryptic peptides were extracted using 70% acetonitrile, 5% formic acid, lyophilized to dryness and resuspended in 10 μl of 0.1% trifluoroacetic acid prior to mass spectrometry (MS) analysis.

3.4.8 Immunodetection of FANCD2 foci

Wild-type and XP2YO human fibroblasts were plated on glass coverslips at 50% confluence and then 16 h later were exposed to 3 μM MMC for 1 h or left untreated. At 6, 12, 24, and 48 h following exposure, cells were fixed as described previously (Wang et al., 2004) with some modifications. Briefly, cells were washed with PBS, permeabilized with ice-cold 0.5% Triton X-100 in PBS, and then fixed with 2% paraformaldehyde and blocked with 5% bovine serum albumin at room temperature. FANCD2 was detected by incubation with rabbit polyclonal anti-FANCD2 antibody (1:1,000; Novus Biologicals) for 90 min at room temperature and then with goat anti-rabbit antibody-Alexa-488 (1:1,000; Invitrogen). Images were taken of 20 fields of cells for each genotype. The total number of nuclei and the number of nuclei with foci were counted in each field. The sum from all fields was used to calculate the percent of nuclei with foci. The experiment was done in triplicate. Student's t test was used to probe significant differences between cell lines.

3.5 SUPPLEMENTARY DATA

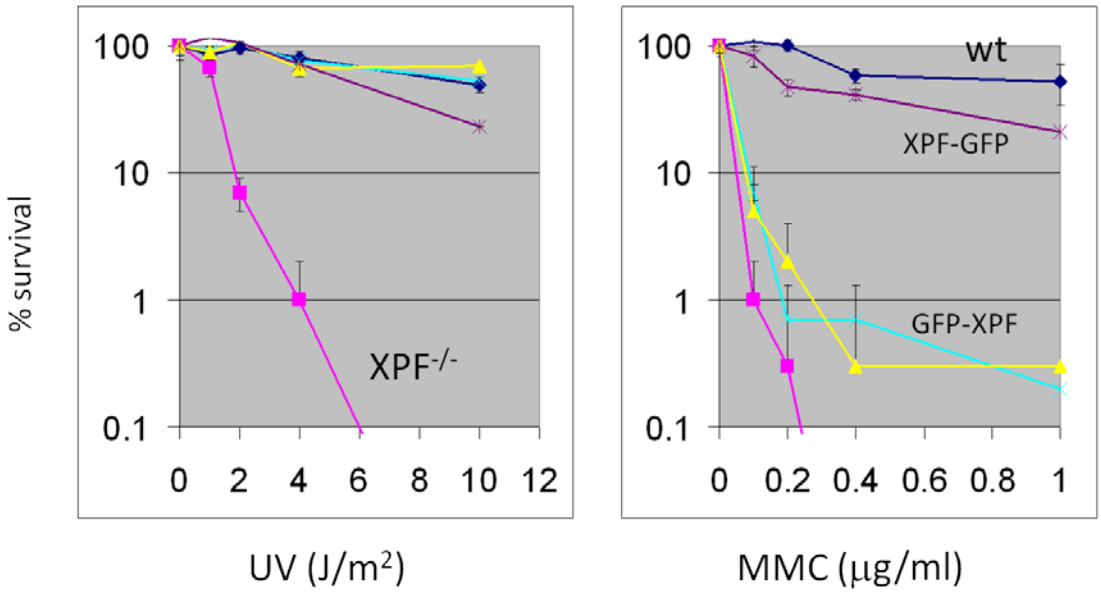

Figure 3-9 GFP tag in the N-terminus and not the C-terminus of XPF makes cells selectively hypersensitive

Cells were challenged with UV (254nm) to compare the impact of a GFP tag, in the N-terminus versus the C-terminus, on NER, and ICL repair. WT (wild-type, SV40-transformed human fibroblasts), XPF-deficient ($XPF^{-/-}$) and cell lines complemented with XPF harboring a N-terminal GFP tag (GFP-XPF), C-terminal GFP tag (XPF-GFP). The data were plotted as the percentage of colonies that were formed on the treated plates relative to the untreated plates ± S.E (error bars) for a minimum of two independent experiments each done in triplicate.

XPF

MESGQPARRIAMAPLLEYERQLVLELLDTDGLVVCARGLGADRLLYHFLQLHCHPACLVLVLNTQPAEEEYFINQLKIEG
VEHLPRRVTNEITSNSRYEVYTQGGVIFATSRILVVDFLTDRIPSDLITGILVYRAHRIIESCQEAFILRLFRQKNKRGFIKAFT
DNAVAFDTGFCHVERVMRNLFVRKLYLWPRFHVAVNSFLEQHKPEVVEIHVSMTPTMLAIQTAILDILNACLKELKCHN
PSLEVEDLSLENAIGKPFDKTIRHYLDPLWHQLGAKTKSLVQDLKILRTLLQYLSQYDCVTFLNLLESLRATEKAFGQNSG
WLFLDSSTSMFINARARVYHLPDAKMSKKEKISEKMEIKEGEETKKELVLESNPKWEALTEVLKEIEAENKESEALGGPG
QVLICASDDRTCSQLRDYITLGAEAFLLRLYRKTFEKDSKAEEVWMKFRKEDSSKRIRKSHKRPKDPQNKERASTKERTLK
KKKRKLTLTQMVGKPEELEEEGDVEEGYRREISSSPESCPEEIKHEEFDVNLSSDAAFGILKEPLTIIHPLLGCSDPYALTRVL
HEVEPRYVVLYDAELTFVRQLEIYRASRPGKPLRVYFLIYGGSTEEQRYLTALRKEKEAFEKLIREKASMVVPEEREGRDET
NLDLVRGTASADVSTDTRKAGGQEQNGTQQSIVVDMREFRSELPSLIHRRGIDIEPVTLEVGDYILTPEMCVERKSISDLI
GSLNNGRLYSQCISMSRYYKRPVLLIEFDPSKPFSLTSRGALFQEISSNDISSKLTLLTLHFPRLRILWCPSPHATAELFEELK
QSKPQPDAATALAITADSETLPESEKYNPGPQDFLLKMPGVNAKNCRSLMHHVKNIAELAALSQDELTSILGNAANAK
QLYDFIHTSFAEVVSKGKGKK

XPF degradation band 1

MESGQPARRIAMAPLLEYERQLVLELLDTDGLVVCARGLGADRLLYHFLQLHCHPACLVLVLNTQPAEEEYFINQLKIEG
VEHLPRRVTNEITSNS*RYEVYTQGGVIFATSRI*LVVDFLTDRIPSDLITGILVYRAHRIIESCQEAFILRLFRQKNKRGFIKAFT
DNAVAFDTGFCHVERVMRNLFVRKLYLWPRFHVAVNSFLEQHKPEVVEIHVSMTPTMLAIQTAILDILNACLKELKCHN
PSLEVEDLSLENAIGKPFDKTIRHYLDPLWHQLGAKTKSLVQDLKILRTLLQYLSQYDCVTFLNLLESLRATEKAFGQNSG
WLFLDSSTSMFINARARVYHLPDAKMSKKEKISEKMEIKEGEETKKELVLESNPKWEALTEVLKEIEAENKESEALGGPG
QVLICASDDRTCSQLRDYITLGAEAFLLRLYRKTFEKDSKAEEVWMKFRKEDSSKRIRKSHKRPKDPQNKERASTKERTLK
KKKRKLTLTQMVGKPEELEEEGDVEEGYRREISSSPESCPEEIKHEEFDVNLSSDAAFGILKEPLTIIHPLLGCSDPYALTRVL
HEVEPRYVVLYDAELTFVRQLEIYRASRPGKPLRVYFLIYGGSTEEQRYLTALRKEKEAFEKLIREKASMVVPEEREGRDET
NLDLVRGTASADVSTDTRKAGGQEQNGTQQSIVVDMREFRSELPSLIHRRGIDIEPVTLEVGDYILTPEMCVERKSISDLI
GSLNNGRLYSQCISMSRYYKRPVLLIEFDPSKPFSLTSRGALFQEISSNDISSKLTLLTLHFPRLRILWCPSPHATAELFEELK
QSKPQPDAATALAITADSETLPESEKYNPGPQDFLLKMPGVNAKNCRSLMHHVKNIAELAALSQDELTSILGNAANAK
QLYDFIHTSFAEVVSKGKGKK

XPF degradation band 2

MESGQPARRIAMAPLLEYERQLVLELLDTDGLVVCARGLGADRLLYHFLQLHCHPACLVLVLNTQPAEEEYFINQLKIEG
VEHLPRRVTNEITSNSRYEVYTQGGVIFATSRILVVDFLTDRIPSDLITGILVYRAHRIIESCQEAFILRLFRQKNKRGFIKAFT
DNAVAFDTGFCHVERVMRNLFVRKLYLWPRFHVAVNSFLEQHKPEVVEIHVSMTPTMLAIQTAILDILNACLKELKCHN
PSLEVEDLSLENAIGKPFDKTIRHYLDPLWHQLGAKTKSLVQDLKILRTLLQYLSQYDCVTFLNLLESLRATEKAFGQNSG
WLFLDSSTSMFINARARVYHLPDAKMSKKEKISEKMEIKEGEETKKELVLESNPKWEALTEVLKEIEAENKESEALGGPG
QVLICASDDRTCSQLRDYITLGAEAFLLRLYRKTFEKDSKAEEVWMKFRKEDSSKRIRKSHKRPKDPQNKERASTKERTLK
KKKRKLTLTQMVGKPEELEEEGDVEEGYRREISSSPESCPEEIKHEEFDVNLSSDAAFGILKEPLTIIHPLLGCSDPYALTRVL
HEVEPRYVVLYDAELTFVRQLEIYRASRPGKPLRVYFLIYGGSTEEQRYLTALRKEKEAFEKLIREKASMVVPEEREGRDET
NLDLVRGTASADVSTDTRKAGGQEQNGTQQSIVVDMREFRSELPSLIHRRGIDIEPVTLEVGDYILTPEMCVERKSISDLI
GSLNNGRLYSQCISMSRYYKRPVLLIEFDPSKPFSLTSRGALFQEISSNDISSKLTLLTLHFPRLRILWCPSPHATAELFEELK

Figure 3-10 Peptide coverage for different bands from silver stained XPF-IP

Each highlighted segment represents one fragment. Where fragments overlap, different emphasis (font color, underline or italics) was used. The bold letters are the first eleven amino acids in the new XPF sequence. The green highlight shows the peptide found by MS that confirms the new XPF sequence.

In Chapter 3, we investigated the importance of the N-terminus of XPF to NER, ICL repair and DSR repair by mutational analysis. The study included mutations in multiple conserved residues in the N-terminus, investigated for their importance in protein:protein interaction that recruit XPF-ERCC1 to the ICL repair pathway. We identified two mutations in the N-terminus of XPF that renders cells selectively sensitive to crosslinking agents thereby generating an ICL repair deficient mutant. This study was designed to identify regions of the *XPF* gene that could be exploited to answer two important questions. Is the accelerated aging phenotype observed in both mice and humans, deficient in XPF-ERCC1, due to the accumulation of unrepaired ICLs. This could be accomplished by making mouse models expressing the newly identified XPF proteins. Secondly, since XPF-ERCC1 have been implicated in conferring chemoresistance, designing small molecule inhibitors to the regions of the *XPF* gene identified in this study, will help overcome chemoresistance.

There are over thousand papers in the last few decades aimed at establishing a correlation between XPF-ERCC1 SNP data, mRNA levels and protein levels with chemoresistance. The perplexing fact is that there is yet no convincing evidence of such an association. Focusing on protein levels, the reason for the lack of a conclusive association between XPF-ERCC1 protein levels and sensitivity to chemotherapeutic regimes, is due to the unavailability of powerful antibodies. The kind of antibodies that have good specificity and sensitivity towards their antigen, and are compatible with immunohistochemical detection. Chapter four of this dissertation, described below, aims to develop and stringently characterize monoclonal antibodies raised against purified recombinant XPF-ERCC1 in complex.

4.0 CHARACTERIZATION OF MONOCLONAL ANTIBODIES FOR IMMUNODETECTION OF THE DNA REPAIR ENDONUCLEASE XPF-ERCC1 IN TUMOR SAMPLE

Madireddy, A.[1], Vaezi, A.[3], Kemp, C.[4], George, J.[5], Wood, R.D.[5], and L.J. Niedernhofer[2]

[1]Department of Human Genetics, University of Pittsburgh Graduate School of Public Health, 130 DeSoto Street, Pittsburgh, PA, 15261, USA

[2]Department of Microbiology and Molecular Genetics, University of Pittsburgh School of Medicine, Pittsburgh, PA.

[3]Departments of Otolaryngology and Head and Neck Surgery, Eye and Ear Institute, 200 Lothrop Street, Suite 500, University of Pittsburgh, Pittsburgh PA 15213.

[4]University of Pittsburgh Cancer Institute, Hillman Cancer Center, 5117 C enter Avenue, Pittsburgh, PA, 15213,

[5]Department of Carcinogenesis and The University of Texas Graduate School of Biomedical Sciences at Houston, The University of Texas M. D. Anderson Cancer Center, Science Park-Research Division, Smithville, Texas 78957, USA. rwood@mdanderson.org

4.1 INTRODUCTION

Many of the most effective cancer therapies involve genotoxic agents that induce DNA damage, including ionizing radiation, alkylating agents and platinum drugs. Cisplatin is a widely used chemotherapeutic agent that forms lesions that are thought to be selectively toxic to rapidly dividing cells (similar to tumor cells) by blocking DNA replication (McHugh et al., 2001; Rice et al., 1988). Cisplatin is used to treat a variety of solid tumors including ovarian, lung, and head and neck carcinoma (Lebwohl and Canetta, 1998; Lokich and Anderson, 1998) but 25-50% of tumors are resistant. Amongst the factors that are thought to contribute to chemoresistance is decreased tumor blood flow, defective binding of drug to ligand, reduced apoptosis, quiescent populations of cells in the tumor, multi-drug resistance pumps, and increased DNA repair (Rabik and Dolan, 2007; Stewart, 2007; Vasey, 2003).

Tumorigenesis occurs as cells acquire multiple mutations that contribute to a growth advantage. The accumulation of mutations is facilitated if cells have some aspect of DNA repair that is impaired. Hence, cancer cells are thought to be defective in at least one DNA repair mechanism in order to accumulate mutations at an accelerated rate. A novel approach to cancer therapy is to exploit this difference in DNA repair capacity between normal and tumoral cells to create synthetic lethality by treating with an inhibitor of a second DNA repair pathway. This will render tumor cells hypersensitive to genotoxic agents because they are missing two DNA repair mechanisms, compared to normal tissue in which only one pathway is inhibited. This is thought to give selective killing of the tumoral tissues over the host tissues. There is a huge body of literature that details attempts to analyze whether cancer cells preferentially up-regulate the expression of specific DNA repair proteins in order to tolerate the damage induced by genotoxic agents. But there is no conclusive evidence of this.

Most of the lesions formed by cisplatin are repaired by nucleotide excision repair. However, chemo effectiveness is majorly contributed by ICLs, which constitute less than 5% of the lesions, and are repaired by the ICL repair pathway (Bhagwat et al., 2009b; Dronkert and Kanaar, 2001; Lawley and Phillips, 1996). The endonuclease XPF-ERCC1 is essential for NER (Petit and Sancar, 1999; Sijbers et al., 1996a) and the repair of interstrand crosslinks (De Silva et al., 2000; Kuraoka et al., 2000). Being the only protein complex that is essential to both pathways has made XPF-ERCC1 a possible biomarker of tumor outcome. XPF harbors the catalytic domain that is required for nuclease activity (Enzlin and Scharer, 2002) and ERCC1 is required for DNA binding (Tsodikov et al., 2005). The proteins are known to bind and stabilize each other *in vivo* and this has been established by studies that show that the levels of XPF are reduced in ERCC1 deficient cells and vice versa (Niedernhofer et al., 2006). The obligate heterodimeric nature of the proteins suggests that either of the two could be used as a good biomarker to predict chemosensitivity.

Much effort has been put into determining if XPF-ERCC1 levels (mRNA or protein) could be predictive of chemotherapeutic outcome which determines whether or not a cancer patient will respond to genotoxic agents. A number of studies have suggested that ERCC1 levels correlate with chemotherapy effectiveness and that high ERCC1 expression correlates with a poor patient outcome (Lee et al., 2008; Zheng et al., 2007). Many of these studies use an antibody 8F1 that lacks specificity to ERCC1 (Niedernhofer et al., 2007), bringing into question their interpretation with respect to the mechanism of tumor resistance. Down-regulation of XPF-ERCC1 by RNAi in cells lines from NSCLC, breast and ovarian cancer patients leads to a significant increase in cisplatin cytotoxicity (Arora et al., 2010), suggesting that XPF-ERCC1 would be a good target to induce synthetic lethality or as a biomarker to tumor sensitivity to

genotoxins. The use of XPF as a biomarker to predict patient outcome has been largely unexplored with the exception of a recent study that reports a significant correlation between lower XPF protein expression and longer progression-free survival in HNSCC patients treated with DNA damaging agents (Vaezi et al., 2011).

In this study, we sought to identify and rigorously test a panel of novel murine monoclonal antibodies raised against recombinant XPF-ERCC1 complex. Our testing regime involves evaluating each hybridoma clone for its specificity for XPF-ERCC1 in several applications including immunohistochemistry, using XPF-ERCC1-deficient human cells as a negative control. Our ultimate aim is to identify an antibody that can reproducibly detect variations in expression levels of XFP-ERCC1 by immunohistochemical analysis. In addition, the novel approach of raising antibodies against the protein complex has the potential to yield antibodies that inhibit the complex or disrupt protein:protein interactions that are imperative for targeting the complex to specific repair pathways (Orelli et al., 2010a). This study has the promise to 1. identify an antibody that can be used to critically discern the utility of XPF-ERCC1 as a biomarker in cancer and 2. uncouple the functions of the XPF-ERCC1 in DNA repair and thereby be utilized for adjuvant antibody therapy. The combination has the potential to improve personalized cancer therapy and improve patient prognosis.

4.2 RESULTS

4.2.1 Antibodies

Murine antibodies were generated using full-length recombinant his-tagged XPF-ERCC1 as the antigen via hybridoma technology. XPF-ERCC1 is an obligate heterodimer (Biggerstaff et al., 1993) that is recruited to different DNA repair pathways via protein:protein interactions (Orelli et al., 2010a). Therefore, antibodies raised against the complex, as opposed to single subunits, could potentially be used to separate functions of the complex by disrupting some but not other protein:protein interactions. The ten best hybridoma cell lines were identified by Enzyme-linked immunosorbent assay using the antigen for solid-phase screening. Three milliliters of the crude supernatant from each of the ten clones were screened for specificity using a rigorous testing regime to determine the utility of each antibody in a multiple immune techniques. Validated negative controls, including cell lines from humans with inherited mutations in *XPF* or *ERCC1* affecting expression of the repair complex, were used at each step to demonstrate specificity of the antibodies, which has been a problem with commercially available antibodies (Niedernhofer et al., 2007).

4.2.2 Primary screening of the supernatants by immunoprecipitation

The crude antibody supernatants (30 μL) from the 10 hybridoma clones were tested for their ability to immunoprecipitate XPF-ERCC1 from whole cell extracts from normal human fibroblasts. The precipitates were probed for XPF via immunoblotting using antibody Ab1 (Neomarkers) and ERCC1 using antibody D10 (Santa Cruz), both of which we previously

validated for specificity (Bhagwat et al., 2009c). XPF-ERCC1 was immunoprecipitated by supernatants from all of the hybridoma clones with the exception of 2B-10 (Figure 4-1). The yield of XPF-ERCC1 by immunoprecipitation varied significantly between the different clones. To rank the utility of the various hybridoma clones for immunoprecipitation, they were classified as +, +/- or – based on the relative yield of XPF-ERCC1 immunoprecipitated with 10µl of the validated antibody D10.

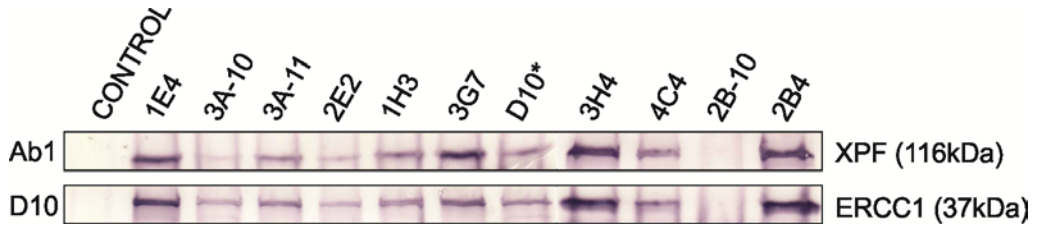

Figure 4-1 4-1 Immunoprecipitation of XPF-ERCC1 using crude antibody

WCEs from normal human fibroblasts were immunoprecipitated with test antibodies 1E4, 3A-11, 1H3, 3H4, 3G7, 2B4, 3A-10, 2B-10, 4C4, and 2E2. Anti-ERCC1 antibody D-10 was used as the control. Precipitates were separated by SDS-PAGE, blotted and immunostained with antibody Ab-1 to detect XPF protein and antibody D-10 to detect ERCC1.

4.2.3 Immunoblotting

Immunoprecipitation revealed if the antibodies recognized XPF-ERCC1, but cannot distinguish which subunit the antibody is recognizing. To determine this, the hybridoma supernatants were next screened for their ability to detect XPF and ERCC1 by immunoblotting. In addition, XPF-ERCC1-deficient cells were used to establish specificity of the antibodies. Whole cell extracts from normal and XP-F human fibroblasts were used. Ab1 (anti-XPF) and D10 (anti-ERCC1) were used as positive controls. Of the 10 antibodies screened, 1E4, 3H4, 3A-11, 3G7, and 1H3 detected XPF at varying intensities (Figure 4-2a). The 1E4 antibody appeared to be the most sensitive for detecting XPF. None of the supernatants detected exclusively ERCC1, suggesting

that XPF is more antigenic or occupies a significantly greater portion of the surface of the XPF-ERCC1 complex. Interestingly, 3G7 detected both XPF and ERCC1 with equivalent intensities. This was verified by probing recombinant His-tagged XPF-ERCC1 (Figure 4-2b).

Because of the utility of Chinese hamster ovary cells and murine models of XPF-ERCC1 deficiency for interrogating the function of the repair complex, the ability of the antibodies to detect hamster and mouse XPF-ERCC1 was determined by blotting whole cell extracts from wild-type hamster and mouse cells. *Xpf* mutant or *Ercc1* knock-out cells, respectively, were used as negative controls. 3H4 detected mouse XPF (Figure 4-2c). None of the other antibodies detected either XPF or ERCC1 in the mouse and hamster whole cell extracts (data not shown).

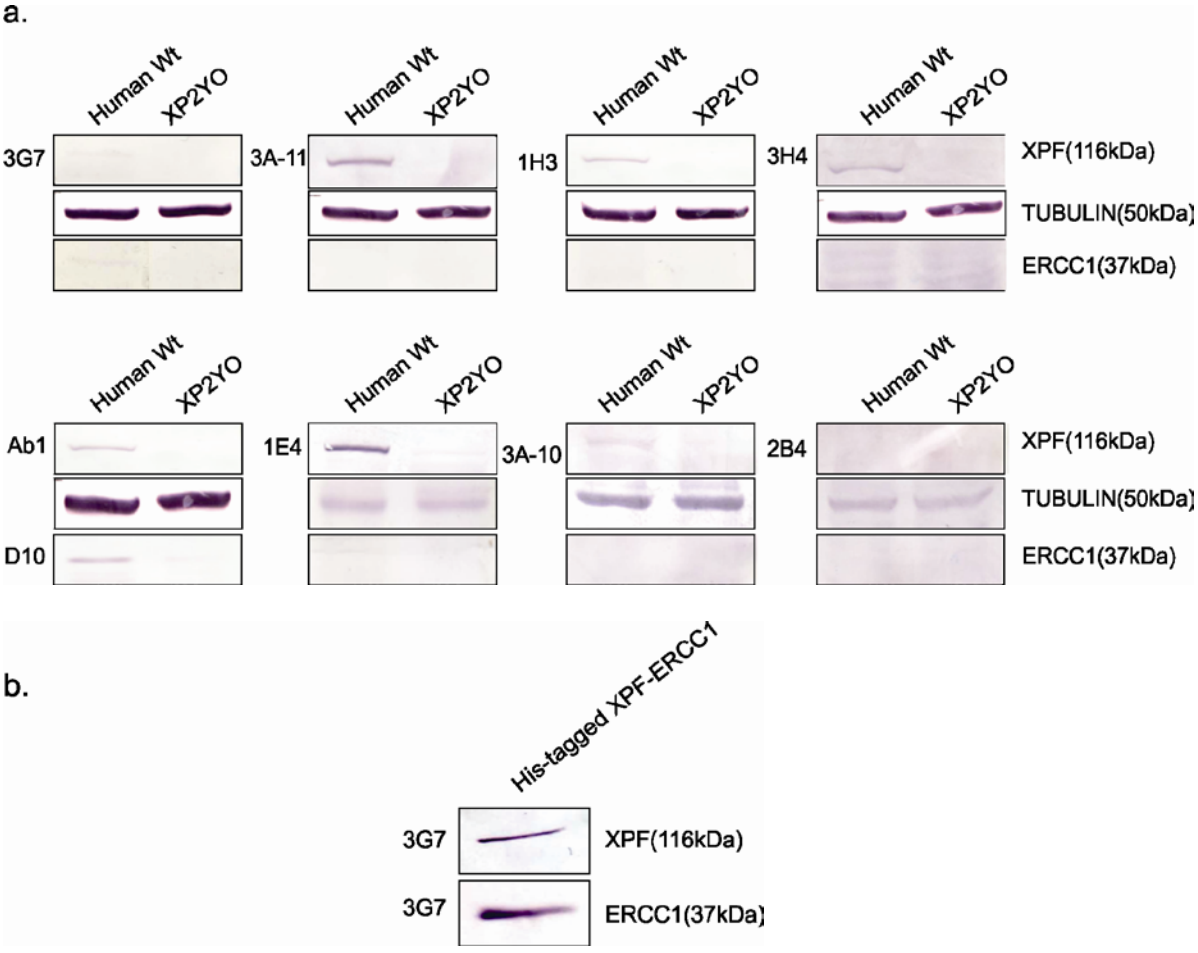

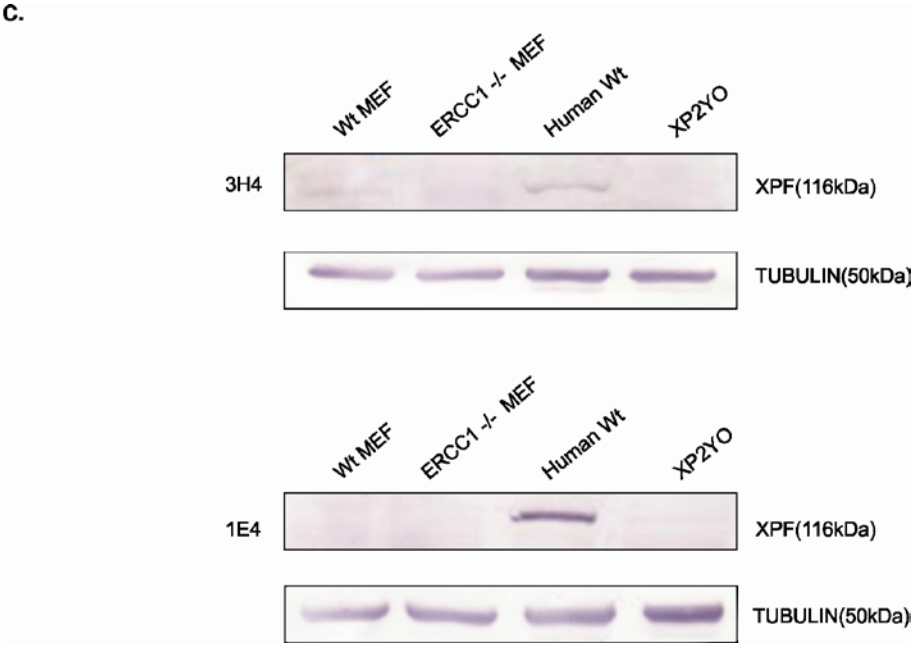

Figure 4-2 Immunodetection of XPF ERCC1 using crude antibody

a. Normal (wild-type) and XPF-ERCC1 deficient XPF mutant human fibroblasts (XP2YO) were lysed and whole cell extracts were collected. The proteins were separated SDS-PAGE (10% polyacrylamide gel), transferred onto nitrocellulose membranes and immunostained with each test antibody (1E4, 3A-11, 1H3, 3H4, 3G7, 2B4, 3A-10, 2B-10, 4C4, and 2E2). Previously characterized antibodies, anti-XPF: Ab1, and anti-ERCC1: D-10 were used as controls. Tubulin was used as a loading control. b. Recombinant His-tagged XPF-ERCC1 was separated by SDS-PAGE and was immunostained with 3G7 to confirm XPF and ERCC1 dual antigen specificity. c. Whole cell extracts from Normal (wild-type), XPF-ERCC1 deficient XPF mutant human fibroblasts (XP2YO), wild-type and ERCC1$^{-/-}$ mouse embryonic fibroblasts were SDS-PAGE separated and immunostained with antibodies, 1E4 and 3H4. Tubulin was used as a loading control.

4.2.4 Immunofluorescence

Immunofluorescence is an important method for determining the sub-cellular localization of proteins within a cell. The crude supernatants were screened for their ability to detect XPF-ERCC1 in cells fixed with paraformaldehyde. To establish specificity, differential immunofluorescence was used (Volker et al., 2001). Normal and XPF-ERCC1-deficient human fibroblasts (XP2YO) were labeled with 3µm and 0.6µm latex beads, respectively, and then

subsequently co-cultured on glass coverslips. The coverslips were immunostained with two antibodies: the test antibody and FL297 (anti-ERCC1; Santa Cruz), which was previously established to be specific (Bhagwat et al., 2009c). The expectation was that if the test antibodies were specific for XPF-ERCC1, then the signals from both antibodies would co-localize and only in the nuclei of cells with small beads (Figure 4-3). The test antibodies were detected by the FITC (green) channel and the control antibody FL297 was detected in the TRITC (red) channel. The nuclei of the cells were stained with DAPI. Bright-field microscopy was used to identify cells differentially labeled with beads. The test antibody was considered effective for immunofluorescence only if it preferentially stained the nuclei of cells labeled with the 3 μm beads and the FITC signal co-localized with that of the TRITC, similar to what was observed with the positive control (D10 anti-ERCC1). The antibodies 1E4, 1H3, and 3A-11 distinguished between cells with XPF-ERCC1 and those without (Figure 4-3). The remainder of the antibodies were unable to distinguish between normal and XP-F mutant cells or caused cytoplasmic staining under the conditions tested (Figure 4-8).

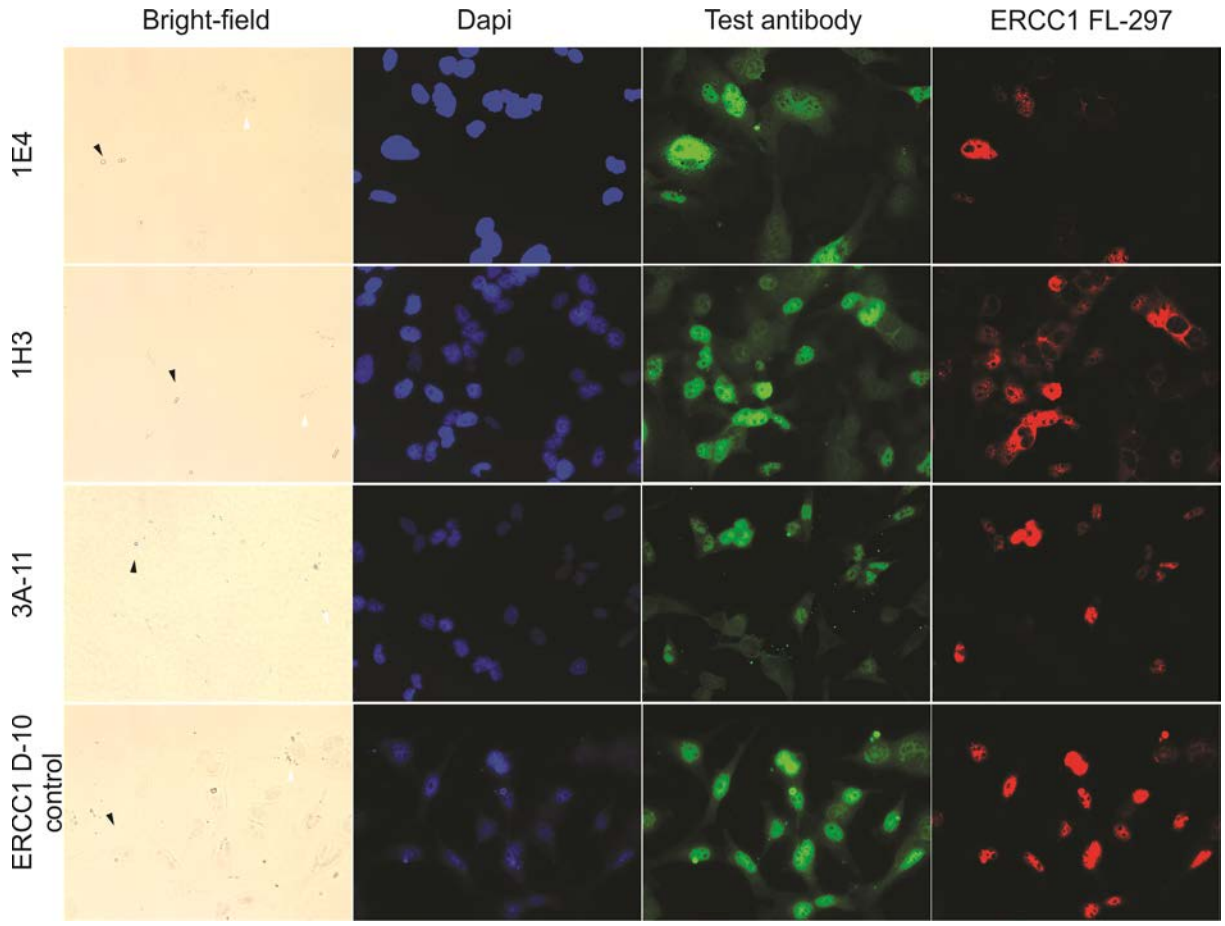

Figure 4-3 Immunofluorescence detection of XPF-ERCC1 using crude antibody

The cytoplasm of normal (wild-type) and XPF-ERCC1 deficient *XPF* mutant human fibroblasts (XP2YO) was labeled with large (black arrow) and small latex beads (white arrows), respectively. The cells were then co-cultured on glass coverslips, fixed and stained. (i) Brightfield images reveal differentially labelled cells in the same field. (ii) The nuclei are stained with DAPI. (iii) Immunostaining with test antibodies (1E4, 1H3, 3A-11, and D-10; secondary antibody Alexa 488, in green). (iv) Co-mmunostaining with antibody FL297 against ERCC1 to distinguish between the normal and XPF-ERCC1 deficient cells (Alexa 594, in red).

4.2.5 Immunohistochemistry

Immunohistochemistry is the most important application for antibodies that have potential to be used to detect tumor biomarkers due to the predominance of fixed tissues and tumor microarrays. However, the specificity of antibodies in immunohistochemical applications is rarely tested due to the lack of negative control tissues. To address this, we created paraffin blocks of normal

human fibroblasts (C5RO) and XP-F fibroblasts (XP51RO), deficient in XPF-ERCC1. These were sectioned and stained like tissue, using hematoxylin as a counterstain. An antibody was considered useful for immununohistochemistry if it gave a clear nuclear stain in the normal cells but not XP-F. The supernatants from clones 1E4 and 3A-11 were the only two that specifically stained cells containing XPF-ERCC1. The 1H3 antibody detected XPF-ERCC1 in both the positive and negative control slides reiterating the importance and the need for negative controls while screening antibodies for immunohistochemistry. The rest of the antibodies did not stain either sample brown indicating either their lack of sensitivity or their incompatibility with immunohistochemistry (Figure 4-4).

The results obtained from the preliminary screening of the crude antibody supertants is summarized in Table 3

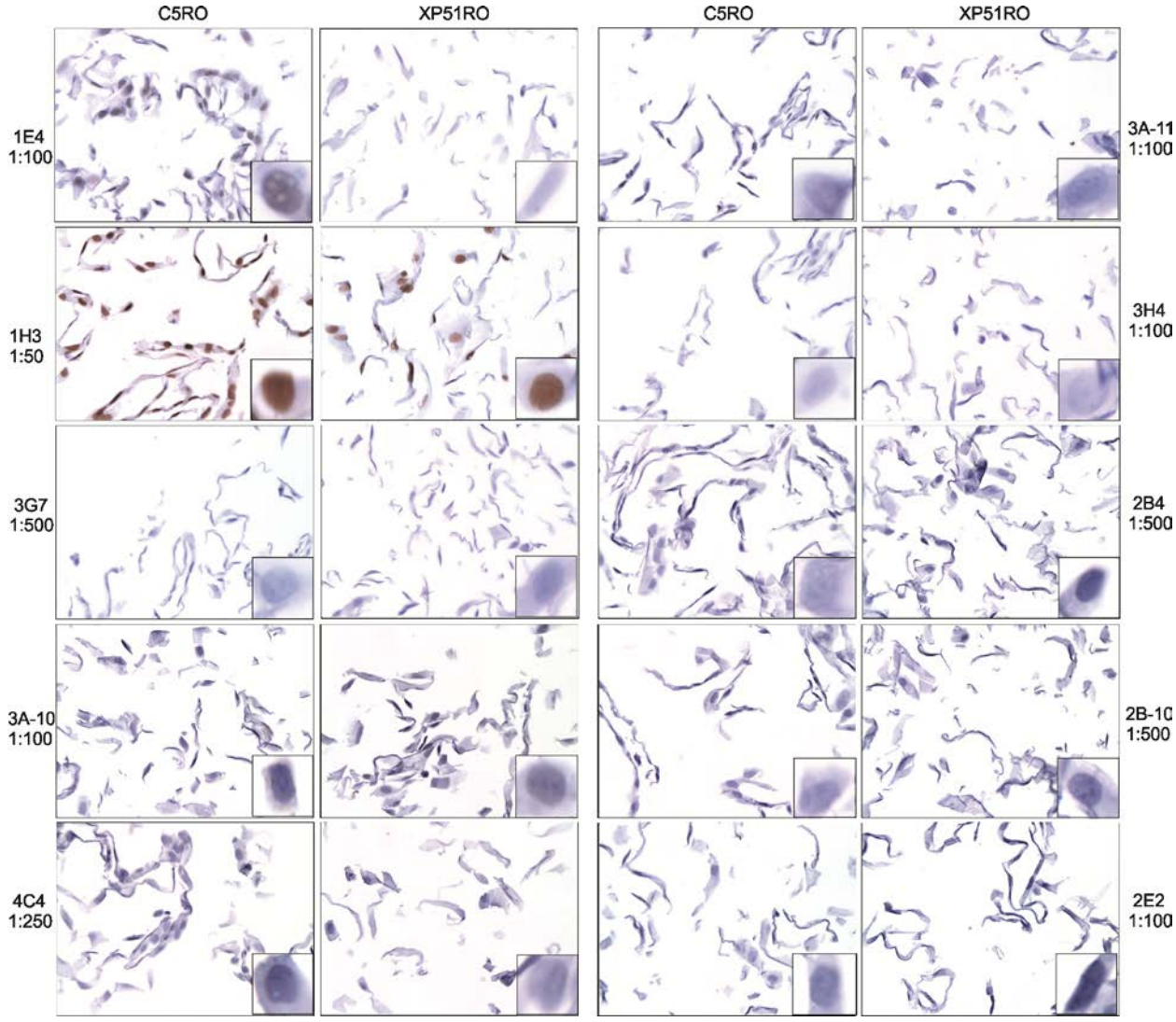

Figure 4-4 Immunohistochemical detection of XPF-ERCC1 using crude antibody

Immunohistochemical detection. Normal (C5RO) or XPF-ERCC1 deficient human fibroblasts (XP51RO) were fixed in paraformaldehyde, pelleted in agarose, paraffin embedded, sectioned and stained to serve as positive and negative controls, respectively. IHC was carried out with test antibodies against XPF (1E4, 3A-11, 1H3, 3H4, 3G7, 2B4, 3A-10, 2B-10, 4C4, and 2E2).

Table 3 Summary of results from preliminary screening of crude antibody supernatants

Antigen	Antibody	Source	Origin	Clonality	IP	WB			IF	IHC
					Human	Human	Hamster	Mouse	Human	
ERCC1-XPF	1E4	ABNOVA	Mouse	Mono	+	+	-	-	+	+
	1H3	ABNOVA	Mouse	Mono	+	+	-	-	-	-
	2B-10	ABNOVA	Mouse	Mono	+	-	-	-	-	-
	2B4	ABNOVA	Mouse	Mono	+	-	-	-	-	-
	2E2	ABNOVA	Mouse	Mono	+	-	-	-	-	-
	3A-10	ABNOVA	Mouse	Mono	+	-	-	-	-	-
	3A-11	ABNOVA	Mouse	Mono	+	+	-	-	+	+
	3G7	ABNOVA	Mouse	Mono	+	+	-	-	-	-
	3H4	ABNOVA	Mouse	Mono	+	+	-	+	-	-
	4C4	ABNOVA	Mouse	Mono	+	-	-	-	-	-

4.2.6 Purification and characterization of monoclonal antibodies

Based on the results obtained from the primary screening, two clones, 1E4 and 3H4, were amplified using roller bottle technique and the antibodies were protein A purified by Rockland Immunologicals. The yield was 23.0 mg for 1E4 and 83.7 mg for 3H4. These purified antibodies were tested for sensitivity and specificity by immunoblot, IF and IHC. For immunoblot, whole cell extracts from normal and XPF-ERCC1 deficient human fibroblasts and mouse embryonic fibroblasts were used in addition to recombinant His-tagged XPF-ERCC1 protein. 3H4 recognized both human and mouse XPF protein (Figure 4-5). The 1E4 antibody recognized only the human XPF protein (Figure 4-5). Neither of the antibodies detected ERCC1 in either human or mouse samples (data not shown). At a dilution of 1:500, the 1E4 antibody gave a more intense signal than the 3H4 antibody, indicating that it is more sensitive for detecting human XPF.

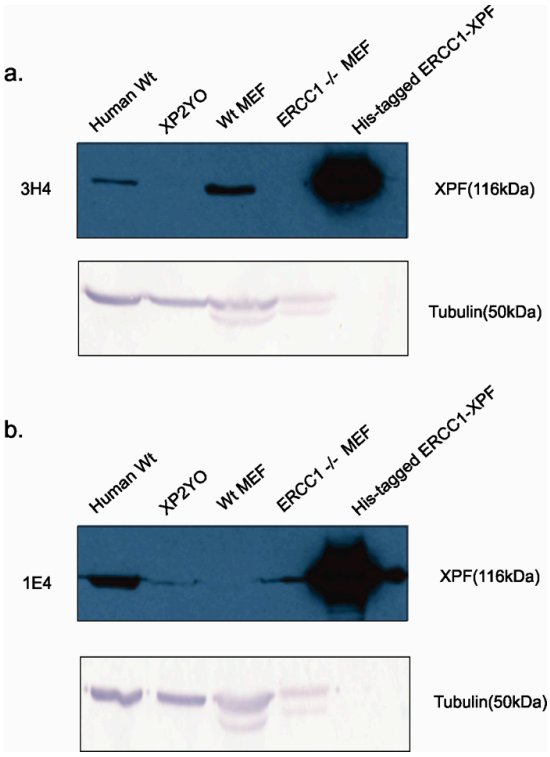

Figure 4-5 Immunodetection of XPF-ERCC1 using purified antibodies

Whole cell extracts were obtained from Normal (wild-type), XPF-ERCC1 deficient XPF mutant human fibroblasts (XP2YO), wild-type and ERCC1$^{-/-}$ mouse embryonic fibroblasts. Proteins were separated by SDS-PAGE and detected on the blot by loading recombinant His-tagged XPF-ERCC1. Blots were immunostained with test antibodies a. 3H4 and b. 1E4 and previously characterized antibodies, anti-XPF: Ab1, and anti-ERCC1: D-10 were used as controls. Tubulin was used as a loading control.

To test the utility of the antibodies for immunofluorescence, normal and XPF-ERCC1-deficient transformed human fibroblasts were fixed on coverslips and immunostained with the 1E4 and 3H4 antibodies. The samples were co-stained with FL297, a validated ERCC1 antibody. 1E4 stained normal but not XPF-ERCC1-deficient XP2YO cells, with a pattern identical to that of FL297 (Figure 4-6). The 3H4 antibody did not exclusively stain the nuclei of either cell type. When the same antibodies were tested on mouse cells, neither detected murine XPF by immunofluorescence (data not shown).

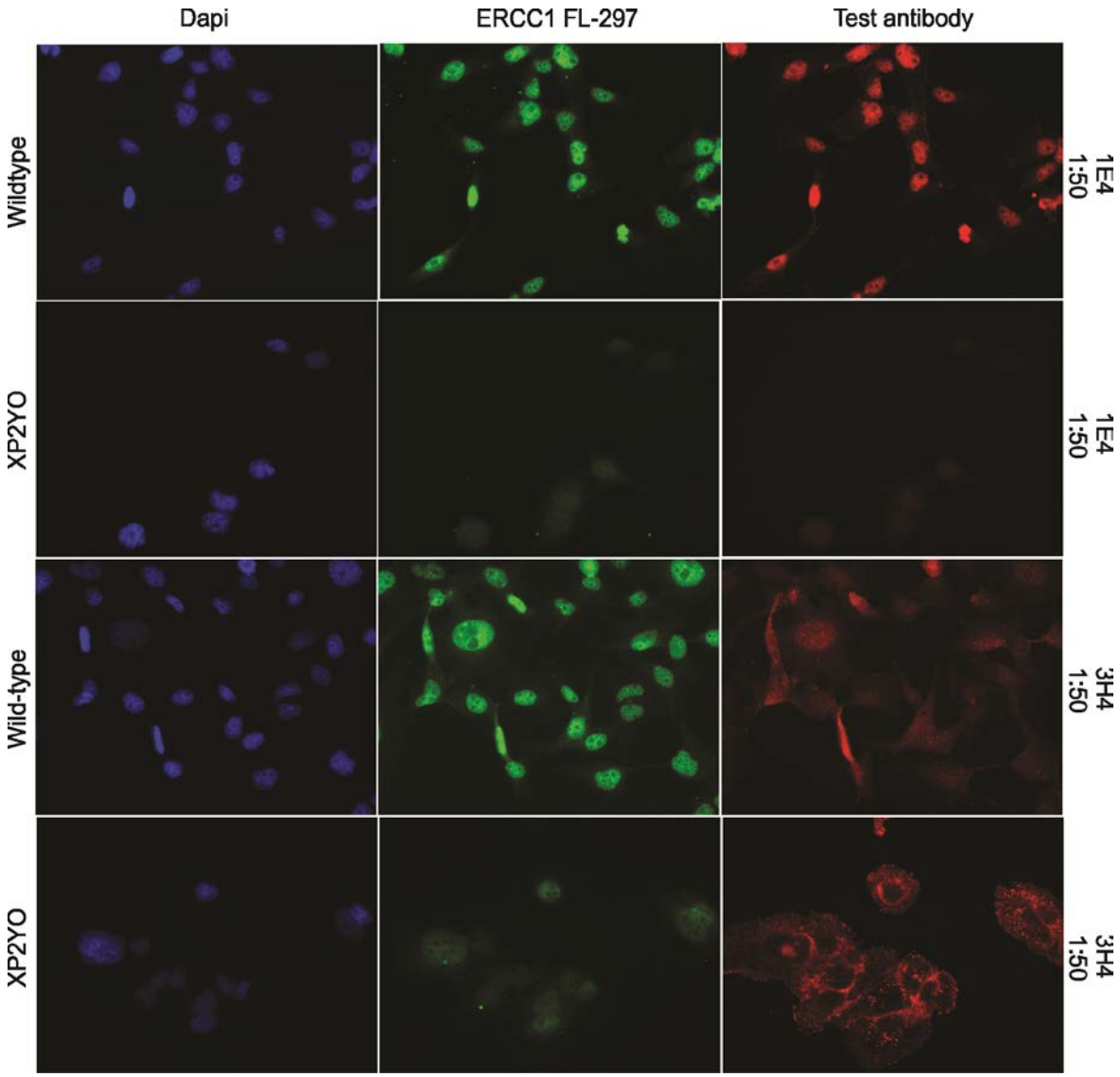

Figure 4-6 Immunofluorescence detection of XPF-ERCC1 using purified antibody

Normal (wild-type) and XPF-ERCC1 deficient *XPF* mutant human fibroblasts (XP2YO) was cultured on g lass coverslips, fixed and stained. (i) The nuclei are stained with DAPI. (ii) Immunostaining with antibody FL297 against ERCC1 to distinguish between the normal and XPF-ERCC1 deficient cells (Alexa 488, in green). (iii) Co-immunostaining with test antibodies (1E4, 1H3, 3A-11, and D-10; secondary antibody Alexa 594, in red).

The 1E4 antibody was next tested for immunohistochemical applications at dilutions ranging from 1:250, 1:350, 1:450 to 1:4000, 1: 7500 and 1:10,000. At a dilution of 1:4000, 1E4 gave a strong nuclear stain in paraffin sections of cells expressing XPF-ERCC1 (HeLa) but not in XP-F cells (XP51RO), indicating that the purified antibody does work for

immunohistochemistry (Figure 4-7a;i/ii). In addition, at a dilution of 1:250, 1E4 stained the nuclei of human tonsil sections, demonstrating the utility of the antibody in staining human tissues (Figure 4-7a;iii) The 1E4 and 3H4 antibodies were then tested for detecting XPF-ERCC1 in mouse tissues. Testis sections from wild-type and *Ercc1*$^{-/\Delta}$ mice, which express ~5% of the normal complement of XPF-ERCC1, were immunostained using an antibody dilution of 1:25 (Dolle et al., 2006), The 1E4 antibody stained the nuclei of both wild-type and the mutant tissue, whereas 3H4 stained the nuclei of wild-type testis only (Figure 4-7b). This indicates that 3H4 may be useful for immunohistochemistry of murine but not human tissues.

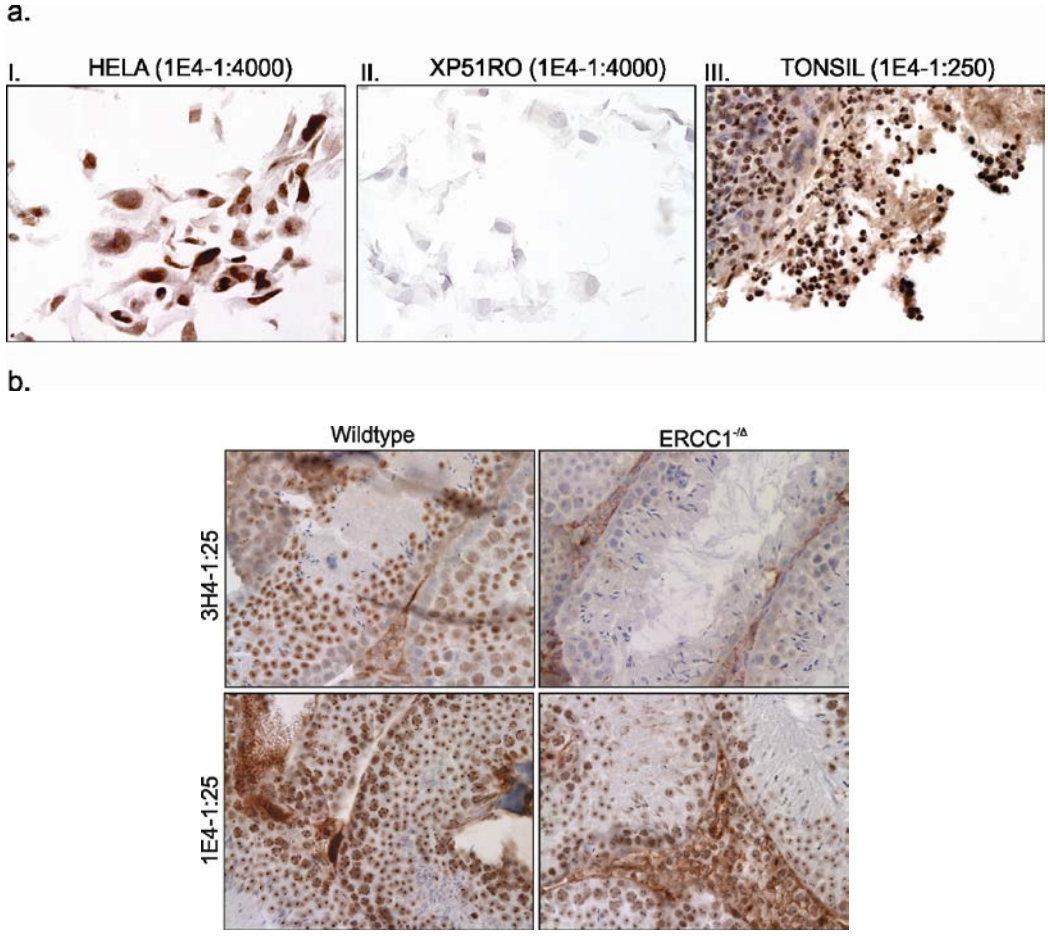

Figure 4-7 Immunohistochemical detection of XPF-ERCC1 using purified antibody

a. Mouse wild-type and ERCC1-/Δ testis was paraffin embedded, sectioned and stained by IHC using antibodies 1E4 and 3H4. (i) Normal (HeLa) or (ii) XPF-ERCC1 deficient human fibroblasts (XP51RO) were fixed in paraformaldehyde, pelleted in agarose, paraffin embedded,

sectioned and stained to serve as positive and negative controls, respectively. (iii) To standardize protocol to human tissue section, paraffin embedded human tonsil was sectioned and stained along with the cells by IHC with test antibodies against XPF (1E4, and 3H4).

4.3 DISCUSSION

Platin based drugs have been the mainstay for cancer chemotherapy ever since it was first approved by the FDA in 1978. The non responsiveness of more than 50-75% of the patients is a cause of major concern in the public health sector. Among the various tumors that develop resistance to cisplatin are head and neck squamous cell carcinoma, ovarian cancer, and NSCLC. There is an immediate need to devise a treatment plan which will improve patient prognosis and this calls for the identification of novel biomarkers that can help predict patient response so that therapy can be tailored to suite each individual.

In recent years, XPF and ERCC1 are two proteins that have gained a lot of importance as potential biomarkers to chemoresistance. XPF-ERCC1 is a structure specific endonuclease that is involved in multiple DNA repair pathways and telomere maintenance. They are obligate heterodimers that bind and stabilize each other. Fibroblasts isolated from human XPF patients show highly reduced levels of ERCC1 (Yagi et al., 1997). The same is true in the case of XPF where only a small level of the protein has been detected in ERCC1 deficient mammalian cells (Gaillard and Wood, 2001). XPF and ERCC1 can only function when they form a complex and so their individual functions are interdependent. Having observed that the levels of XPF and ERCC1 are closely correlated in normal human cells and mouse models, it would be safe to assume that the same would be true in the case of tumor samples. This has lead to the interchangeable usage of the two proteins as potential predictors of chemoresistance.

Immunohistochemical analysis is an invaluable tool that can be used to assess patient prognosis by measuring the expression levels of certain key proteins. The most important aspects of IHC analysis involve sample availability, sample fixation, antigen retrieval, the antibody utilized and the interpretation of results. Each of these steps is crucial and has to be fine tuned for every antibody developed. The selection of the best antibody for a specific antigen is complex, and it is essential to employ a highly selective and stringent screening strategy to characterize each antibody so that they can be confidently utilized for IHC analysis. One of the major drawbacks of IHC is that it is impossible to tell whether the antibody in question is detecting our proteins, XPF or ERCC1. The first reason for this is the lack of a molecular marker as in the case of an immunoblot analysis. This makes it essential to first confirm by immunoblotting that our antibody is highly specific to XPF-ERCC1 before using it for IHC analysis. Secondly, when we do an IHC analysis on tumor samples, it is very difficult if not impossible to procure a negative control and so to circumvent this problem, we have used paraffin embedded human cells from XPF-ERCC1 proficient and deficient cell lines. These measures ensure the specificity of the antibody being used.

The third issue that could confound our results is the sensitivity of the antibody to XPF-ERCC1. Most of the antibodies available commercially are polyclonal which means that they could be detecting more than one epitope on the antigen and this would lead to a lot of non specific background staining due to cross reactivity of the antibody with other proteins when applied to immunohistochemistry. In addition, the presence of multiple subtypes in a polyclonal antibody makes it tricky to choose a secondary antibody for accurate detection. To avoid any such issues, we have used only monoclonal antibodies in this study. They have very high

homogeneity and since they bind only one epitope, the results are reproducible and highly accurate.

Among the numerous XPF-ERCC1 antibodies that are available, only a small subset is applicable to immunohistochemical analysis. A critical evaluation of all the commercially available XPF and ERCC1 antibodies revealed that the ERCC1 antibodies FL297, 3F2 and 4H4 are the only ones compatible for IHC (Bhagwat et al., 2009c).

In this paper, with the help of Abnova, using the recombinant XPF-ERCC1 purified by Rick Wood as the antigen, we developed and tested a panel of ten monoclonal antibodies. Our testing regime involved using SV40 immortalized human fibroblasts or HeLa cells as the positive control and XPF-ERCC1 deficient patient cell line, XP2YO as the negative control. Using established methods and the above mentioned stringent controls, we discovered four antibodies that are applicable to a variety of immunodetection techniques. The antibodies 1E4, and 3A11 were successful in detecting human XPF in all the tested applications. The 3H4 antibody detected both human and mouse XPF by immunoblotting and immunohistochemistry (Figure 4-2Figure 4-5). Based on these results, the antibodies 1E4 and 3H4 were purified and were subsequently standardized for IHC analysis on tumor samples (Figure 4-7). In addition to these antibodies, a fourth monoclonal antibody, 3G7, that could detect both XPF and ERCC1 by immunoblotting was identified (Figure 4-2).

There are two major implications to this study; it has helped identify a very sensitive and specific monoclonal antibody, 1E4 that can be used for the immunodetection of XPF-ERCC1 in tumor samples to predict patient response to chemo radiotherapy. Secondly, the antibody 3G7 is of particular interest to us due to its dual antigen specificity. Mapping the epitope of this antibody will help elucidate the domain of XPF and ERCC1 that it is specific to. A monoclonal

antibody of this nature would be invaluable due to its potential application in adjuvant antibody therapy. We plan to explore the potential of this antibody in our future studies.

4.4 EXPERIMENTAL PROCEDURES

4.4.1 Cell Culture

SV40 transformed normal human fibroblast cell lines and XP2YO (XP-F) were cultured in either Ham's F10 or RPMI supplemented, respectively, each supplemented with 10% fetal bovine serum albumin, antibiotics and non-essential amino acids. Primary human fibroblasts immortalized by the stable expression of human telomerase, C5RO (normal) and XP51RO (XP-F) were cultured in Ham's F10 media supplemented with 10% fetal bovine serum albumin, antibiotics and non-essential amino acids. Wild-type and *Ercc1*$^{-/-}$ primary mouse embryonic fibroblasts were grown in a 1:1 mixture of Ham's F10 and DMEM supplemented with 10% fetal bovine serum albumin, antibiotics, and non-essential amino acids. The cells were all grown at 37ºC in a 5% CO_2 incubator.

4.4.2 Antibodies

Murine antibodies (1E4, 1H3, 2B-10, 2B4, 2E2, 3A-10, 3A-11, 3G7, 3H4, and 4C4) were generated using full-length recombinant his-tagged XPF-ERCC1 as the immunogen via hybridoma technology. The ten best hybridoma cell lines were identified by Enzyme-linked immunosorbent assay using the recombinant his-tagged XPF-ERCC1, his-tagged Protein A and

His-FLAG-tagged peptide B for solid-phase screening. Three milliliters of the crude supernatant from each of the ten clones were characterized for immunoblotting and immunostaining by immunofluorescence and immunohistochemistry.

4.4.3 Immunoprecipitation

Cells were trypsinized, washed with PBS and lysed with NETT buffer (100 mM NaCl, 50 mM Tris base, pH 7.5, 5 mM EDTA, pH 8.0 and 0.5% Triton X-100) containing Complete mini-protease inhibitor cocktail and phosphatase inhibitor cocktail (Roche). For immunoprecipitation, 80 µg of protein from WCEs of each cell line was pre-cleared by incubating them with protein A+G beads (Calbiochem) for 30 mins followed by incubation with 100 µl of each test antibody and 25 µl of protein A+G beads with continuous mixing overnight. The beads were then collected by centrifugation at 13,000 rpm for 15 mins, washed three times with the NETT buffer and PBS; boiled for 5 min in 4X protein loading buffer (0.25 M Tris-HCl, pH 8.5, 8% SDS, 1.6 mM EDTA, 0.1M DTT, 0.04% bromophenol blue and 40% glycerol), and the eluted proteins were separated by SDS-PAGE (10% polyacrylamide gel). Immunoprecipitated XPF was detected by anti-XPF antibody (Ab1; Neomarkers; 1:1000) and AP conjugated goat anti-mouse secondary antibody (Promega; 1:7500).

4.4.4 Immunoblotting

Cells were trypnized, washed with PBS and were lysed with NETT buffer (100mM NaCl, 50 mM Tris base, pH 7.5, 5 mM EDTA, pH 8.0, 0.5% Triton X-100) containing Complete mini-protease inhibitor cocktail and phosphatase inhibitor cocktail (Roche). 60 µg of total protein was

boiled for 5 min in 4X protein loading buffer (0.25 M Tris-HCl, pH 8.5, 8% SDS, 1.6 mM EDTA, 0.1M DTT, 0.04% bromophenol blue and 40% glycerol), separated by SDS-PAGE (10% polyacrylamide gel), and transferred to a nitrocellulose membrane. Antibodies were tested for their ability to specifically detect XPF or ERCC1.

4.4.5 Immunofluorescence

SV40 wild-type, XP2YO human fibroblast cells, and wild-type and ERCC1$^{-/-}$ primary mouse embryonic fibroblast cells were seeded and cultured on cover slips. After 24hr, the cells were fixed with 2% paraformaldehyde (ICN Biomedicals) at 37 ^{0}C for 15 min. The cells were then permeabilized with Triton X-100 (0.2% in PBS) by 2 10min washes, and blocked with 3% BSA in PBS for 20min. Antibodies were tested for their ability to specifically detect XPF or ERCC1 at a concentration of 1:100. Goat anti-mouse IgG (1:1000), chicken anti-rabbit IgG (1:1000) conjugated with Alexa fluor 488 or Alexa fluor 594 (Invitrogen) were used for visualization.

4.4.6 Immunohistochemistry

HeLa and XP2YO cells were grown to 75-80% confluence, fixed with 10% neutral-buffered formalin for 15min at room temperature, and collected by scraping. Cells were stored in neutral-buffered formalin at 4°C for at least 3 hr, then pelleted by centrifugation (1,200 rpm, 5 min) and washed twice with PBS. Cells were resuspended in 500 µl of 80% ethanol, transferred to Eppendorf tubes containing 300 µl of solidified 1% low melting point agarose in PBS, and re-pelleted. The ethanol was aspirated and the bottoms of the tubes cut off. The agarose plugs containing the cells were pushed and molded into the caps of Eppendorf tubes and snap frozen

on dry ice. The solidified pellets were extruded from the caps and paraffin embedded according to standard methods for tissue.

For immunohistochemical staining of the cell plug and paraffin embedded tissue sections, heat induced epitope retrieval was carried out with citrate buffer at pH 6 (Dako Target retrieval solution, Dako) at 95°C for 20 min. Endogenous peroxidase was quenched using 3% Hydrogen peroxide (Fisher Scientific) at room temperature (RT) for 15min. Cell lines were blocked with 5% goat serum and 3% BSA for 30 min followed by a avidin/biotin block at RT for 15min. Mouse testis sections were blocked using Biocare Rodent Block M for 10 minutes. The cell line sections and the mouse testis sections were then incubated with the primary antibodies (mouse monoclonal, 1:100, 1:250, 1:500 etc) for optimization for 60 min at room temperature. Primary antibody signal was then detected using biotinylated anti-rabbit or anti-mouse secondary antibody for 30 min and DAB+ for 10 min at room temperature (Vectastain ABC kit; Vector Laboratories). Haematoxylin was used for counterstaining.

For the purified antibodies, the same protocol was used to test paraffin embedded sections of HeLa cells, XP2YO cells and human tonsil section.

4.5 SUPPLEMENTARY DATA

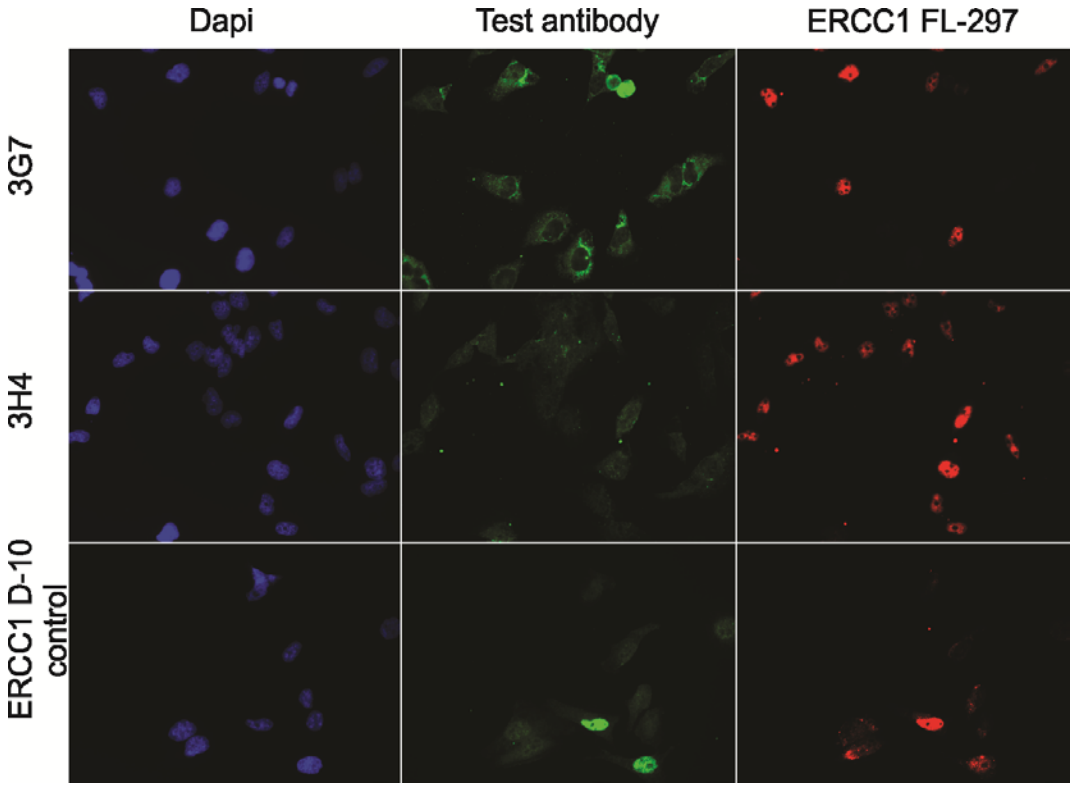

Figure 4-8 Immunofluorescence detection of XPF-ERCC1 using crude antibodies 3G7 and 3H4

Normal (wild-type) and XPF-ERCC1 deficient *XPF* mutant human fibroblasts (XP2YO) was cultured on g lass coverslips, fixed and stained. (i) The nuclei are stained with DAPI. (ii) Immunostaining with antibody FL297 against ERCC1 to distinguish between the normal and XPF-ERCC1 deficient cells (Alexa 488, in green). (iii) Co-immunostaining with test antibodies (1E4, 1H3, 3A-11, and D-10; secondary antibody Alexa 594, in red).

4.6 ACKNOWLEDGEMENTS

We would like to thank Marie B. Acquafondata for helping with the immunohistochemistry experiments. In addition, we would like to thank Trevigen, Inc. for funding this study.

Chapter four of the dissertation document describes the identification of a monoclonal antibody, IE4, against XPF that can be used for immunohistochemical detection of human tumor samples. In addition, three other antibodies were also identified. The antibody 3H4, sensitively detects human and mouse XPF protein by western blot analysis and is applicable to immunohistochemical detection of mouse tissues. Similar to the 1E4 antibody, the 3A-11 antibody detects human XPF. The most unique antibody identified however, was the 3G7 antibody that has specificity for both XPF and ERCC1. The dual antigen specificity is an invaluable tool that can be utilized, in the future, to destabilize the interaction between XPF-ERCC1. The 1E4 antibody identified can be used to measure different panels of tumors to establish a the presence of absence of a definitive correlation between protein levels and patient outcome as measured by immunohistochemical analysis.

Having established this, we designed our next study, described below in chapter five, to measure the nucleotide excision repair capacity of suspension cells. This project is designed to semi-automate the measurement of NER using flow cytometry and also to make the measurement applicable to blood cells so that the procedure can, in the future, be incorporated in diagnostic settings

5.0 A METHOD TO MEASURE NUCLEOTIDE EXCISION REPAIR IN SUSPENSION CELLS USING CLICK-IT CHEMISTRY AND FLOW CYTOMETRY

[1]Madireddy, A., [1]Kammerer, C.M. and L.J. Niedernhofer[2]

[1]Department of Human Genetics, University of Pittsburgh Graduate School of Public Health, 130 DeSoto Street, Pittsburgh, PA, 15261, USA

[2]Department of Microbiology and Molecular Genetics, University of Pittsburgh School of Medicine, Pittsburgh, PA.

5.1 INTRODUCTION

Our body is constantly exposed to endogenous and environmental agents that cause DNA damage. The magnitude of this damage is estimated to be >10,000 new DNA lesions per cell per day (Lindahl and Barnes, 2000). At the cellular level, this is combated by orchestrating one of five highly complex DNA repair pathways each specific for a particular type of lesion. This ensures that DNA can be accurately replicated and transcribed. The importance of each of these DNA repair pathways and their role in maintaining the integrity of the genome is clearly illustrated by the multitude of inherited diseases caused by defects in DNA repair. T hese diseases are predominantly characterized by early onset of malignant neoplasms and aging-

related degenerative changes, implicating DNA repair as critical for protecting against cancer and aging.

Nucleotide excision repair (NER) is an evolutionarily conserved DNA repair pathway that removes DNA lesions that are large or bulky enough to distort the DNA helix. These lesions arise as a consequence of exposure to aromatic hydrocarbons (e.g. cigarette smoke), chemotherapeutic drugs such as cisplatin, and the UV component of sunlight. UV light induces two major lesions: 6-4 photo products (6-4PP) (Mitchell and Nairn, 1989) and cyclobutane pyrimidine dimers (CPD) (Lippke et al., 1981), both of which are exclusively repaired by NER in placental mammals. There are two sub-pathways of NER. Global genome nucleotide excision repair (GG-NER) repairs lesions throughout the genome, while transcription-coupled nucleotide excision repair (TC-NER) repairs lesions only on the transcribed strand of actively transcribed genes (de Laat et al., 1999).

Inherited defects in NER lead to three diseases: xeroderma pigmentosum, Cockayne syndrome (Bertola et al., 2006) or Trichothiodystrophy (Tay, 1971). All three diseases are characterized by extreme sunlight sensitivity. Xeroderma pigmentosum is a can cer-prone syndrome in which patients have a >10,000-fold increased risk of skin cancer in sun-exposed areas of the skin (DiGiovanna and Kraemer, 2012). Cockayne syndrome and Trichothiodystrophy are characterized by developmental abnormalities and premature aging. This is attributed to defective TC-NER, which in turn leads to defects in transcription. The development of an approach to measure the DNA repair capacity of an individual to predict the predisposition of a person to such syndromes will help them make cautious choices so as to avoid exposure to agents that might make them vulnerable to faster disease progression and will thereby help ensure one's quality of life.

This can be better understood with the example of a child who has XP. The exposure of babies with XP to sunlight results in extreme sunlight sensitivity characterized by frequent sunburns. Only after multiple sunlight exposures do parents usually realize that there is something wrong with their child. The diagnosis of XP is carried out by functional tests that measure a patient cell's nucleotide excision repair capacity. But the tests that currently exist are restricted primarily by their applicability to adherent cells such as fibroblasts that can only be obtained by skin biopsies and secondarily by the extended time that it takes to establish the cell lines. Due to these reasons, molecular genetic testing is available only in a research setting and is not extended to clinical laboratories. An early diagnosis of the disease made using patient blood can help guide families to take necessary precaution to retard disease progression.

Taking a step back from disorders of NER, when we consider cancer, a large majority of the chemoradiotherapeutic regimes that exist exploit DNA damage as the key mediator of cytotoxicity. However, ~50% of the patients are resistant to treatment and DNA repair that counters the damage induced has been implicated as a major factor in conferring resistance. Consequently, measuring DNA repair in tumors has been a priority for over a decade and there are hundreds of studies that measure repair as a function of individual proteins (Koberle et al., 1999; Olaussen et al., 2006b). DNA repair is an important factor that determines the inter-individual differences that come into play in predicting a patient's response to a therapeutic regime. Much effort has been channeled into developing assays, such as the comet assay to measure strand breaks that can measure DNA repair. However, there is a lot of conflict over the validity of each of these assays in accurately measuring "DNA repair". The major cause for this concern stems from the fact that a large majority of the assays developed predict repair capacity based on the activity of one or more proteins. This is a problem because most repair pathways

such as NER, involve the coordinated activity of more than 30 different proteins (de Laat et al., 1999). Determining which of these proteins is rate limiting to repair is important to avoid misinterpretation of results obtained from these assays.

Unscheduled DNA synthesis (UDS) is a well-established assay that directly measures NER and is the mainstay of XP-diagnostic laboratories. It was first described by Rasmussen and Painter in 1964 and was used to discover that XP is caused by a defect in NER (Cleaver, 1968). UDS is also used to assign patients to different genetic complementation groups of XP (De Weerd-Kastelein et al., 1972). The attractive aspect of UDS is that the assay assesses the function of the entire NER pathway and not the activity of one protein. UDS is a measure DNA synthesis that takes place outside of the S-phase of the cell cycle. By definition this is DNA repair. Furthermore, in cells exposed to UV, UDS is by definition NER. Treatment of cells with UV results in the formation of bulky lesions in the DNA which are repaired by NER. When these cells are pulsed with ^{3}[H] –thymidine, this involves the incorporation of ^{3}[H] –thymidine into the DNA during the process of repair synthesis (Christmann et al., 2003; Kelly and Latimer, 2005). Repair is then measured as a function of thymidine uptake which is visualized as "repair foci" typically detected either using autoradiography or by liquid scintillation counting. The autoradiography based method of measuring UDS is extremely sensitive and accurate but the procedure is hazardous, time consuming (3 weeks) and laborious. In addition, the procedure requires adherent cells such as fibroblasts that are typically obtained from skin biopsies and main problem associated with this technique is that the procurement of skin biopsies is invasive and also the development of fibroblasts from the biopsies is time consuming (3 months). There is a driving need to automate the process in such a way that it can be applied to human peripheral

blood so that results can be obtained much faster and the technique can be efficiently used in a lab to measure DNA repair.

Here we report the development of a semi-automated UDS assay by flow cytometry. This assay has been adapted from a recent study where UDS is measured by a non-radioactive method by using an azide-conjugated thymidine analogue 5-ethynyl-2'-deoxyuridine (EdU) (Limsirichaikul et al., 2009). The degree of automation in the currently existing methods has been restricted to analysis using fluorescent imaging (Nakazawa et al., 2010). In our approach, repair synthesis is measured in UV-irradiated peripheral blood mononuclear cells using flow cytometry to detect non-replicating cells that have incorporated EdU into their genome. The chemistry permitting detection of genomic EdU was first described by Salic et al. in 2008. In this assay, live cells are labeled with a thymidine analogue EdU, which is incorporated into the nuclear DNA during replication in the S-phase of the cell cycle. The EdU is designed such that it has a terminal alkyne group that can be induced to react with a fluorescently-labeled azide moiety via "Click-iT" chemistry. The EdU is then detected by fluorescence emission, EdU incorporation is measured and the results are depicted as univariate histograms that depict EdU uptake across the x-axis or bivariate histograms that depict the EdU uptake of cells in different phases of the cell cycle. We attempted to adapt the existing protocol that measures UDS as a function of EdU uptake in lymphoblastoid cells using fluorescent imaging to make it compatible by flow cytometry.

5.2 RESULTS

We adapted an assay to measure the NER capacity of suspension cells by detecting the amount of EdU incorporated into the nuclear genome after UV radiation using "Click-iT" chemistry and flow cytometry. We used lymphoblastoid cells for standardization of the assay so that the assay can eventually be applied to peripheral blood cells, which are more readily obtained from patients than fibroblasts. The exact protocol for the assay is detailed in the methods but briefly, cells were treated with UV-C which was expected to induce DNA damage. The cells were then allowed to repair the damage induced by incubating them at 37 degrees and EdU was added at this step to trace the repair process. Following repair synthesis, the cells were collected, excess EdU was washed off, they were fixed and permeabilized, and the incorporated EdU was detected with a fluorescently labeled azide moiety by Click-iT chemistry. Cell cycle profiles of the cells were obtained by staining with a DNA dye and the samples were analyzed by flow cytometry (FCM). Repair synthesis can readily be distinguished from DNA replication by the fact that the EdU signal is significantly greater in replicating cells than cells undergoing DNA repair (Figure 5-1). A very strong, pan-nuclear fluorescent signal was observed in S-phase cells, whereas distinct foci were seen in cells carrying out DNA repair. This however, illustrates the biggest challenge of this assay and that is to detect a rather weak fluorescent signal representing DNA repair in a background of strong signal due to S-phase cells. Hence our first priority was to devise a means to arrest the cell cycle, in order to minimize the fraction of cells in S-phase.

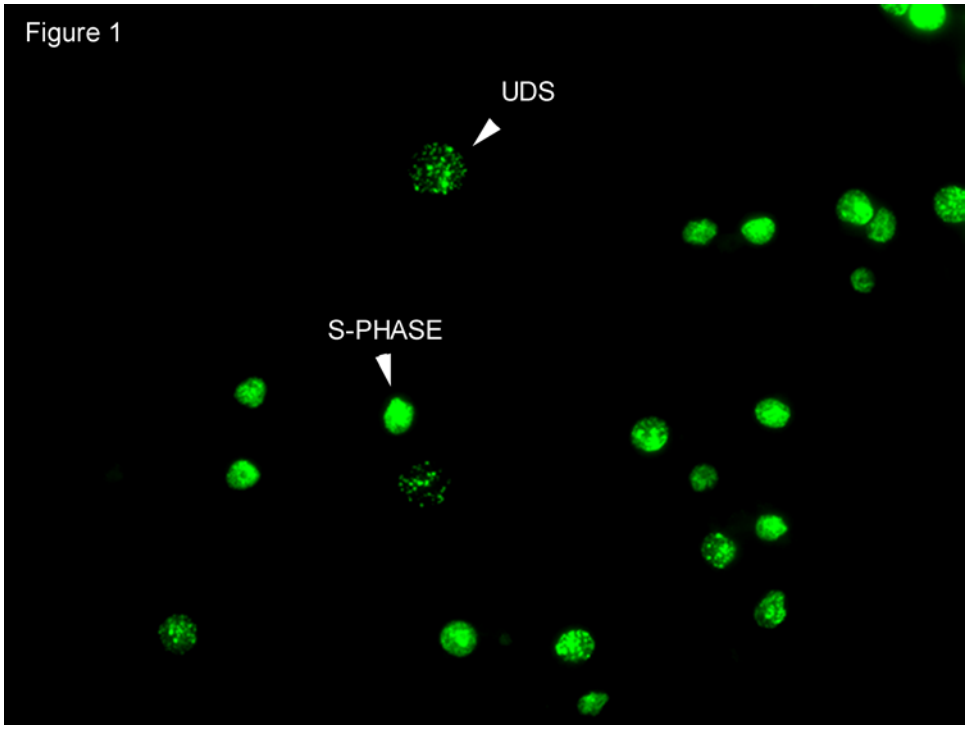

Figure 5-1 Fluorescent imaging of EdU labeled cells

EBV transformed wild-type human lymphoblastoid cells were irradiated with 60J/m2 of UV-C. The cells were allowed to repair the UV damage by incubation in media containing 10µM EdU for 1h at 37°C. Incorporated EdU was detected using Click-iT chemistry and the cells were cytospun onto glass slides and visualized by fluorescent imaging. The micrograph depicting the difference in the appearance of a cell undergoing unscheduled DNA synthesis (nuclei containing hotspots of fluorescence visible as foci) and cells in the S-phase of cell cycle are represented (completely fluorescent nuclei).

5.2.1 Synchronization: serum starvation

To synchronize cells by serum starvation, wild-type and XP-A lymphoblast cell lines were grow under standard conditions, but with different serum concentrations (0-2%) for 24 to 72 hrs and the impact on the cell cycle measured by flow cytometry using DAPI detect the DNA content of cells (Table 4). Upon serum starvation, this percentage appeared to increase two fold. The reason for this is unknown. The percentage of cells in each phase of the cell cycle is calculated but manually drawing gates in the software to calculate the percentages. This however is not the best

way due to the difficulty in properly representing the percentage of cells in each phase of the cell cycle considering they overlap with each other. Keeping this bias in mind, the percentage of cells in the different phases of the cell cycle was calculated after serum starvation. Under normal growth conditions (10% serum), the fraction of S-phase cells is 7%. This was not affected even by complete serum starvation for three days. This could be due to the fact that both cell lines are EBV transformed and the most prominent characteristics of a transformed cell are lower serum requirements, mitogen-stimulation independent division, loss of contact inhibition and anchorage independent growth (Hui-Yuen et al., 2011).

Table 4 Approaches to Minimize S-phase Cells: Serum Starvation

Sample Name	Time of starvation	Serum concentration	G0/G1 (%)	S (%)	G2/M (%)
Normal	24h	10.0%	74	16	12
Normal	24h	0.0%	82	14	2
Normal	24h	0.5%	77	17	4
Normal	24h	1.0%	80	15	3
Normal	24h	2.0%	80	15	3
Normal	72h	0.0%	73	20	6
Normal	72h	0.5%	74	20	4
Normal	72h	1.0%	73	21	4
Normal	72h	2.0%	74	20	4
XP-A	24h	0.0%	78	17	4
XP-A	24h	0.5%	73	20	5
XP-A	24h	1.0%	73	21	5
XP-A	24h	2.0%	73	20	5
XP-A	72h	0.0%	80	15	4
XP-A	72h	0.5%	79	15	4
XP-A	72h	1.0%	76	17	6
XP-A	72h	2.0%	77	17	5

5.2.2 Synchronization: Transiently using inhibitors of DNA replication such as hydroxyurea and mimosine

In an attempt to synchronize cells, cells were treated with two commonly used drugs Hydroxyurea and mimosine (Krek and DeCaprio, 1995; Lalande, 1990). A comparison of the cell cycle profiles of wild-type cells treated with mimosine and hydroxyurea individually did not show a decrease in the S-phase population of cells compared to untreated cells (Figure 5-2a). Hydroxyurea and mimosine can induce DNA damage (Darzynkiewicz et al., 2011; Mladenov and Anachkova, 2003; Sakano et al., 2001). To determine if this affected EdU incorporation, we compared the EdU uptake of cells treated with mimosine or hydroxyurea to untreated cells experiment in the absence of UV radiation. The results (Figure 5-2b) reveal that the treatment of cells with inhibitors of DNA replication does indeed increase the EdU incorporation by 20% as compared to the untreated cells.

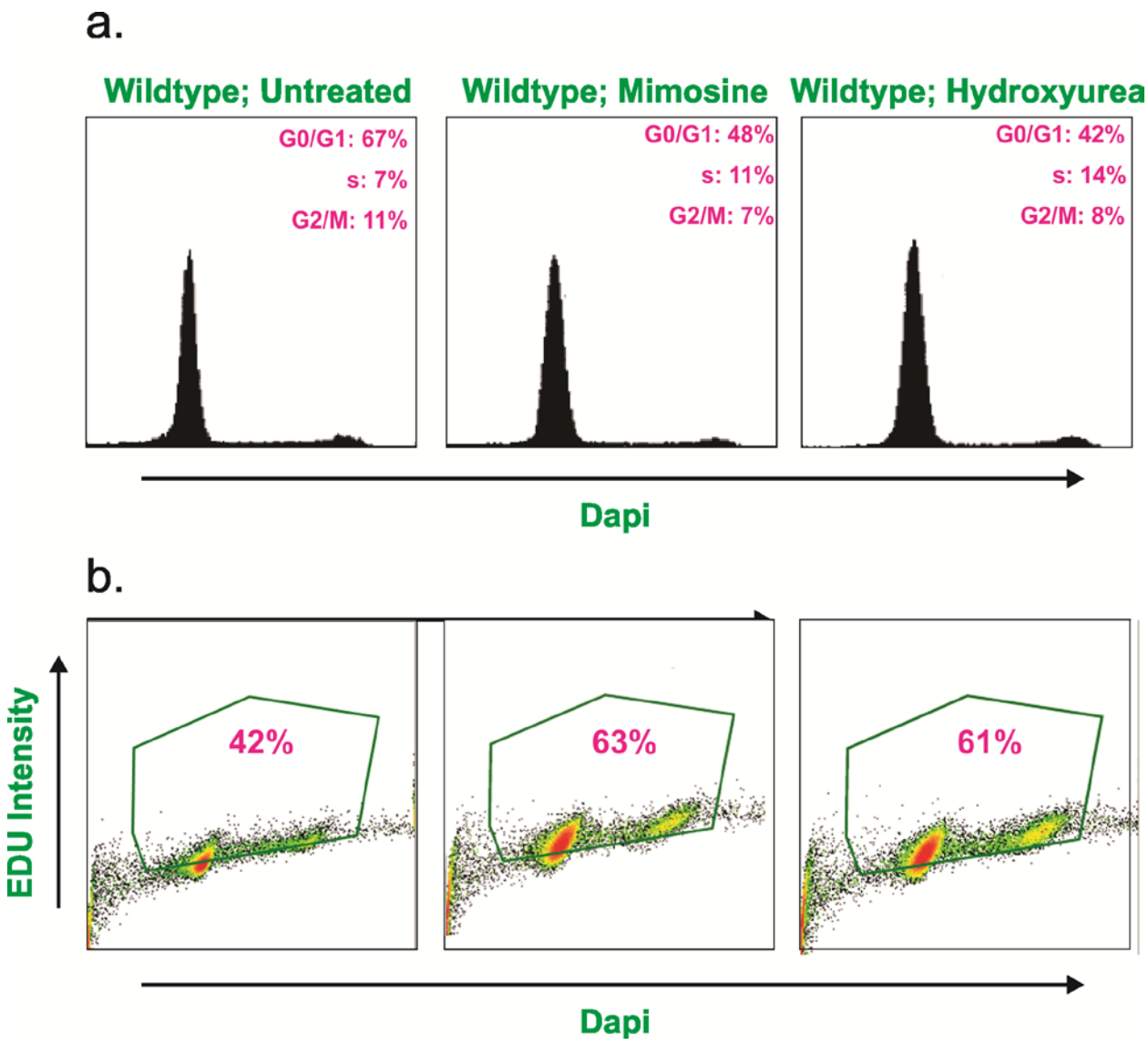

Figure 5-2 Approaches to minimize s-phase cells

Histograms showing the cell cycle profile and the EdU incorporation after treatment with mimosine or hydroxyurea. The cells were incubated in media containing either 0.4µM Mimosine or 10mM Hydroxyurea or were left untreated for 12h. Following incubation, the cells were washed with 1X PBS and incubated in media containing 10µM EdU for 1h at 37°C. After 1h, the cells were fixed and the incorporated EdU was fluorescently labeled by Click-iT chemistry. The DNA was stained (api, x-axis) and the fluorescence intensity (EDU-FITC, y-axis) of cells were analyzed using flow cytometry (FCM). **a.** Single parameter histogram representing the percentage of cells in different phases of the cell cycle upon treatment with inhibitors of DNA replication**. b.** Dual parameter histogram representing the cell cycle profile (DAPI, x-axis) and the corresponding EdU incorporation (EDU-FITC, y-axis) of cells in the different stages of the cell cycle.

5.2.3 Immunodetection of the S-phase antigen Ki67 to detect proliferating cells

Ki67 is a proliferation specific nuclear antigen (Gerdes et al., 1991). It is expressed in cells in all phases of the cell cycle with the exception of the G0 phase. PE-Ki67 (Invitrogen) was used to distinguish between resting cells that were only capable of repair synthesis from S-phase cells. Results from this experiment revealed that PE-Ki67 staining was successful only in cases where it was the only fluorophore used. When Ki67 staining was combined with EdU staining, the EdU staining turned out to be successful while no detectable signal was obtained from the PE channel that was used to measure Ki67 intensity (Figure 5-3). Switching to a different channel to detect the Ki67 turned out to be unsuccessful as well indicating perhaps that the Click-iT chemistry is incompatible with immunodetection.

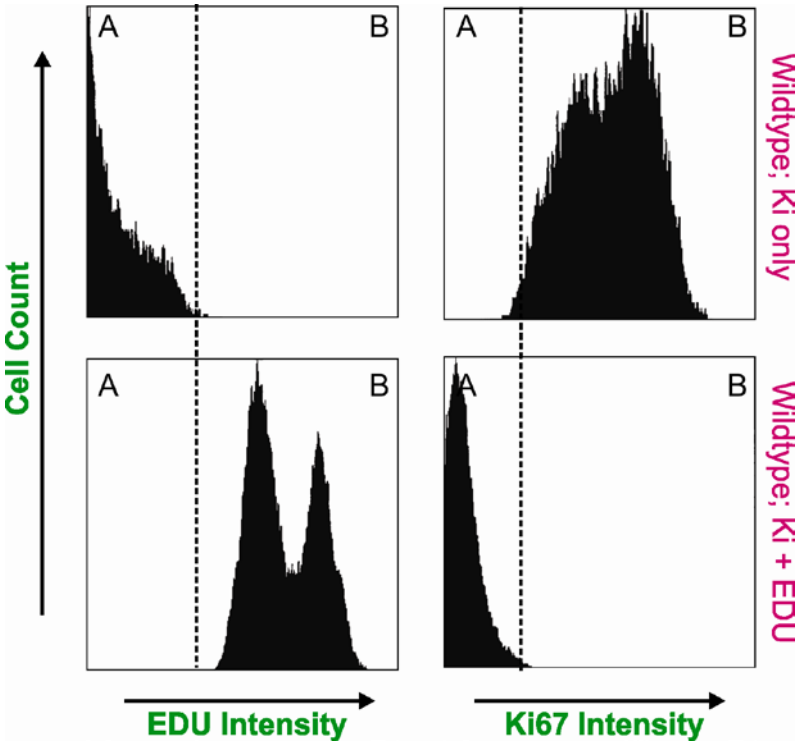

Figure 5-3 Immunostaining for Ki67 does not affect the number of S phase cells.

Single parameter histograms showing either EdU intensity or Ki67 intensity in samples labeled with Ki67 only and samples labeled with both Ki67 and EdU. Quadrant A represents the background fluorescence generated by autofluorescence. Quadrant B represents true signal.

5.2.4 Optimizing the UV dose

A second approach to increasing the signal to noise ratio is to increase the fraction of cells undergoing UDS in response to UV-induced DNA damage. To optimize this, various doses of UV-C were used to induce DNA damage. Wild-type and XP-A EBV-transformed lymphoblastoid cells were treated with 20, and 60 J/m^2 of UV-C. Following incubation, the cells were stained to detect UDS as described in the methods section. At 20 J/m^2 of UV, no increase in EdU incorporation was detected compared to unirradiated cells (Figure 5-4). Similar results were observed in the XP-A cells (data not shown). At 60 J /m^2 of UV-C, the level of EdU incorporation changed. There was a shift in the intensity of EdU signal in cells irradiated with 60 J/m2 compared to unirradiated cells (Figure 5-4). This would be consistent with a robust cell cycle arrest caused by high dose genotoxic stress leading to a loss of S-phase cells (high EdU signal), but an increase in DNA repair (UDS; low EdU signal). Treatment with 100 J/m^2 of UV produced the same results as 60J/m^2 UV-C but the percent of apoptotic cells was much higher (data not shown). Henceforth, 60 J/m^2 UV-C was used as the standard treatment dose for EBV-transformed lymphoblastoid cells in our assay.

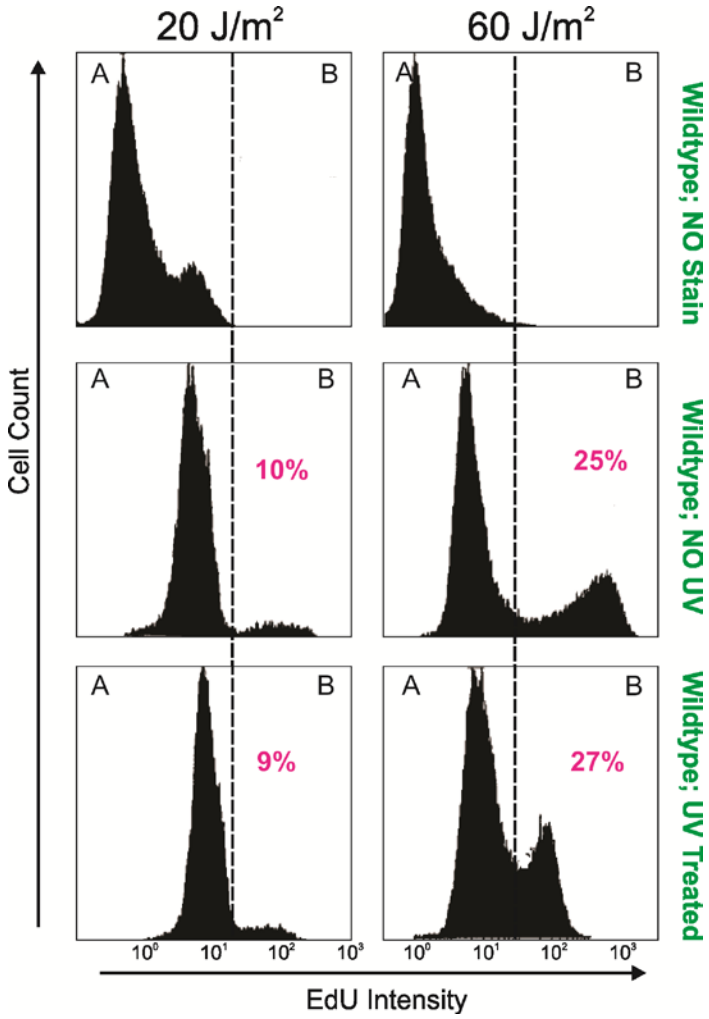

Figure 5-4 Optimization of the UV dosage for UDS measurement in EBV transformed lymphoblastoid cell

Wild-type cells were treated with **a.** 20J/m^2 or **b.** 60 J/m^2 of UV-C and incubated with media containing 10µM EdU for 1h at 37°C. Following incubation, the cells were collected, fixed, and EdU was fluorescently labeled with 25uM Alexa Fluor 488-azide using the Click-iT kit. cells were collected, filtered and analyzed by FCM for fluorescence intensity (EdU-FITC; x-axis) using single parameter histograms. Quadrant A represents the background fluorescence generated by autofluorescence. Quadrant B represents true signal.

5.2.5 Determination of time point for EdU addition and incorporation

UV has been known to induce cell cycle arrest (Gentile et al., 2003). Based on the robust cell cycle arrest that was observed in (Figure 5-4), we rationalized that exploiting this arrest to get

EdU incorporation only for UV-induced UDS and not replication will help eliminate some of the background. The next two experiments were planned to determine initially the time point at which synthesis-phase(s-phase) arrest was maximum and secondly, to determine the duration of EdU incubation to avoid s-phase restart. The duration of DNA repair synthesis however varies depending on the type of UV lesion being repaired. CPDs are repaired much slower by NER than 6,4PPs (Mitchell, 1988). Wild-type human fibroblasts take 6-8h to repair 50% of 6,4PPs where as XP-A cells take 24h to remove 15% of the 6-4 PP (Friedberg, 2006). Cells were treated with UV-C and were allowed to recover for varying periods of time. The cell cycle profile was measured at 15, 30, and 45 minutes post UV-C irradiation to identify the time-point when UV-induced cell cycle arrest was maximal (Figure 5-5a). The percent of cells in s-phase was found to be 9% 15 minutes after UV irradiation, 6% (lowest observed) at the 30 minutes time point, but this percent increased again and reached 13% by 45 minutes implying that maximal s-phase arrest took place at 30 minutes (Figure 5-5a). Hence, we concluded that the optimal time point to add EdU to the culture media was 30 minutes post-UV in order to minimize S-phase signal.

The determine incubation time for EdU incorporation that would be essential to avoid non specific EdU uptake upon replication restart, incorporating the 30 minutes time point from the previous experiment, we tried multiple time points to determine the time point at which non specific EdU uptake due to replication restart occurred. The data from the multiple time points was compared to the original 1h incubation time represented in quadrant 2. The first reaction involved treating cells with UV followed by incubation for 30 minutes at which point EdU was added. Upon EdU addition, the cells were allowed to recover for either 30 minutes (Quadrant 3) or 1hr (Quadrant 5). In one individual reaction, cells were exposed to two pulses of UV 15 minutes apart. EdU was added immediately after the second pulse and the cells were henceforth

given 30 minutes for repair synthesis (Quadrant 4). These experiments collectively helped determine that replicative arrest took place 30 minutes after UV irradiation (Figure 5-5a) and replication restart occurred 1h after UV irradiation (Figure 5-5b) implying that EdU must be added 30 minutes after irradiation and cells must be collected for analysis 30 minutes post EdU addition (Quadrant 3). However, the addition of EdU after 30 minutes followed by a 30 minute incubation resulted in very low EdU intensity peak (Quadrant 3) in comparison to the treated and untreated controls displayed in Quadrants 1 and 2 respectively. This raised the concern that the Flow cytometry approach might not be sensitive enough to detect signals of such low magnitude.

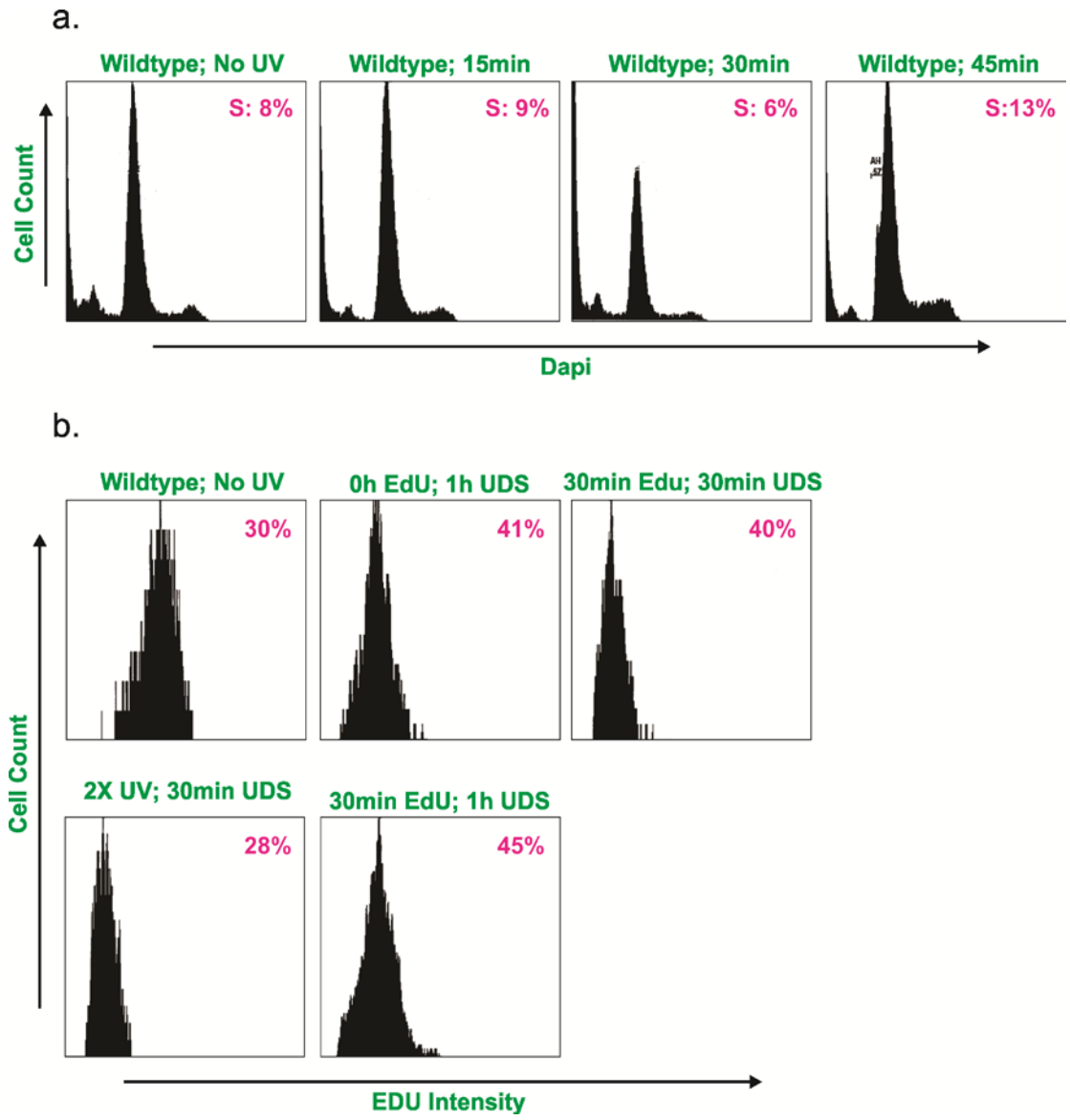

Figure 5-5 Analysis of time points for UV addition and incorporation

EBV transformed wild-type human lymphoblastoid cells were irradiated with 60 J/m^2 of UV-C. **a.** 15 minutes, 30 minutes and 45 minutes post irradiation, the cells were collected, DNA stained using DAPI and the cell cycle profiles were analyzed by FCM. **b.** 30 minutes post irradiation, the cells were incubated in media 10µM EdU for 1h at 37°C. The cells were then collected, fixed, and EdU was fluorescently labeled with 25uM Alexa Fluor 488-azide using the Click-iT kit. Analysis was conducted by FCM for fluorescence intensity (EdU-FITC; x-axis) using single parameter histograms. Quadrant 1 represents cells that were not irradiated. Quadrant 2 represents cells that received EdU immediately after irradiation (0h) with a 1h incubation. Quadrant 3 represents cells that received UV 30 minutes after irradiation with a 30 minutes incubation. Quadrant 4 represents cells that received 2 pulses of 60 J/m^2 of UV 15 minutes apart, EdU was added 15 minutes after the second UV pulse and the cells were then incubated for 30 minutes. Quadrant 5 represents cells that received EdU 30 minutes after irradiation with a 1h incubation.

5.2.6 Optimizing fixation and permeabilization

Cellular integrity can be detected during flow cytometry based on the populations of cells observed on a forwardscatter/sidescatter (FS/SS) histogram. When cells enter the flow cytometer, they scatter light that is represented as the forward and side scatter. Forward scatter measures size while the side scatter measures cellular density. Taken together, different cellular populations can be distinguished based on FS and SS. The initial method for the fixation of Epstein Barr virus (EBV) -transformed cells employed PBS containing 2% paraformaldehyde, 0.5% triton-X 100 and 300mM sucrose for 20 minutes on ice, as previously described (Nakazawa et al., 2010). However, this method compromised cell integrity as illustrated by the multiple cell populations on a FS/SS histogram (Figure 5-6). To troubleshoot this, cells were treated with different fixatives such as 70% ethanol, methanol, 100% ethanol and sequential treatment with 2% paraformaldehyde for fixation followed by treatment with 0.5% triton-X 100 (Figure 5-6) or 0.1 % triton-X for permeabilization. The forward scatter and side scatter plots generated by flow cytometry (FCM) analysis were used to determine cell size and integrity. The results revealed that treatment with 70% ethanol and 100% methanol for 30 minutes on ice helped retain cellular integrity while effectively fixing and permeabilizing cells (Figure 5-6). 70% ethanol was henceforth used in our analysis as the fixative due the reproducibility, optimal staining with Alexa fluor 488 and minimal background obtained.

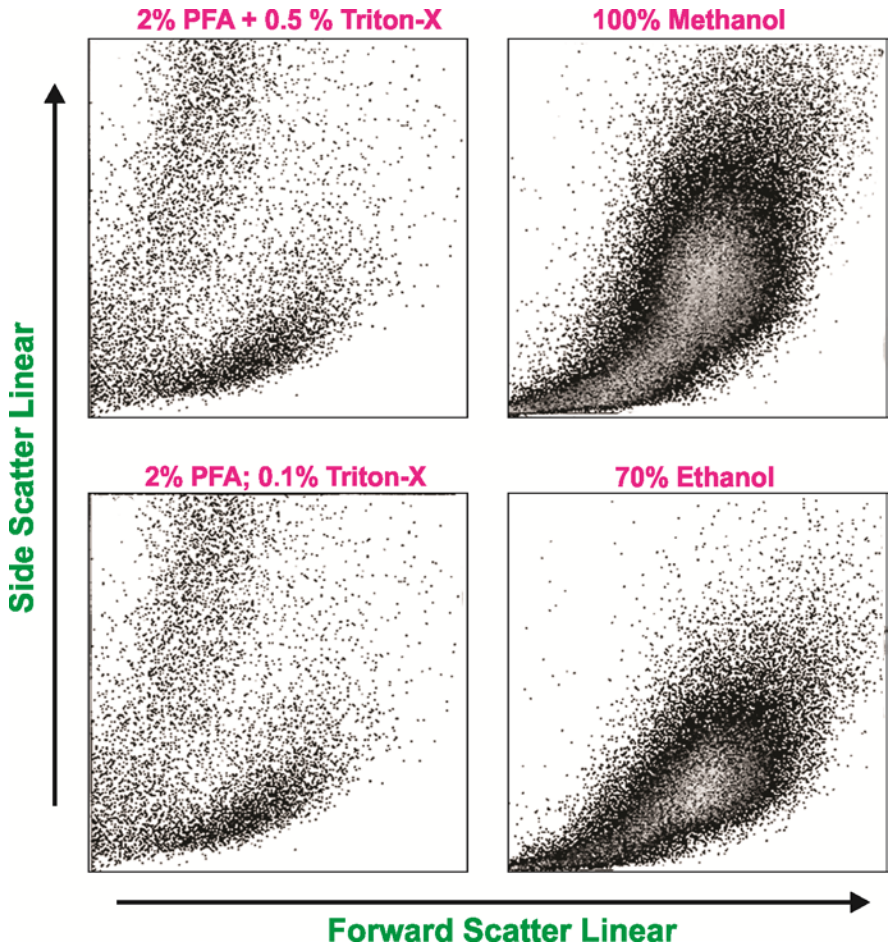

Figure 5-6 Optimization of the FIX/PERM method to protect cellular integrity

Exponentially growing EBV transformed wild-type human lymphoblastoid cells were fixed and permeabilized with 2% paraformaldehyde-0.5% Triton X-100, and 300mM sucrose for 15 minutes on ice, 2% paraformaldehyde for 15 minutes on ice followed by 0.1% Triton X-100 for 10 minutes at RT, Methanol for 30 minutes on ice, and 70% ethanol for 30 minutes on ice. Following incubation, the cells were washed twice with 1X PBS and were analyzed by FCM. Dual parameter histograms representing cellular size (forward scatter, x-axis) and cellular granularity (side scatter, y-axis) are shown.

5.2.7 Eliminating spectral overlap

Unscheduled DNA synthesis is carried out by cells outside the S-phase. To determine the proportion of cells that are non S-phase, a DNA staining step was incorporated after the EdU

staining. However, for efficient analysis, the DNA stain had to be chosen such that its spectra did not overlap, with the Alexa Fluor 488 that was used in our analysis, to minimize channel bleed through. Propidium iodide (PI) with an excitation (ex) wavelength of 488nm emission (em) wavelength of 619nm and DAPI ex 350nm em 461nm was checked for compatibility with Alexa Fluor-488 ex 495 nm em519 nm for our analysis. Ideally, these should not overlap with the excitation and emission wavelengths of the fluorophore used to detect EdU, which is Alex Fluor-488. When PI was used in combination with Alexa Fluor-488, the EdU signal (fluorescence at 488 nm) was completely quenched, likely due to spectral overlap between PI and Alexa-Fluor-488 (Figure 5-7a). In contrast, when DAPI was used there was no quenching of the EdU signal (b). The same results were obtained when EdU was detected with Alexa Fluor-647 in combination with PI (data not shown).

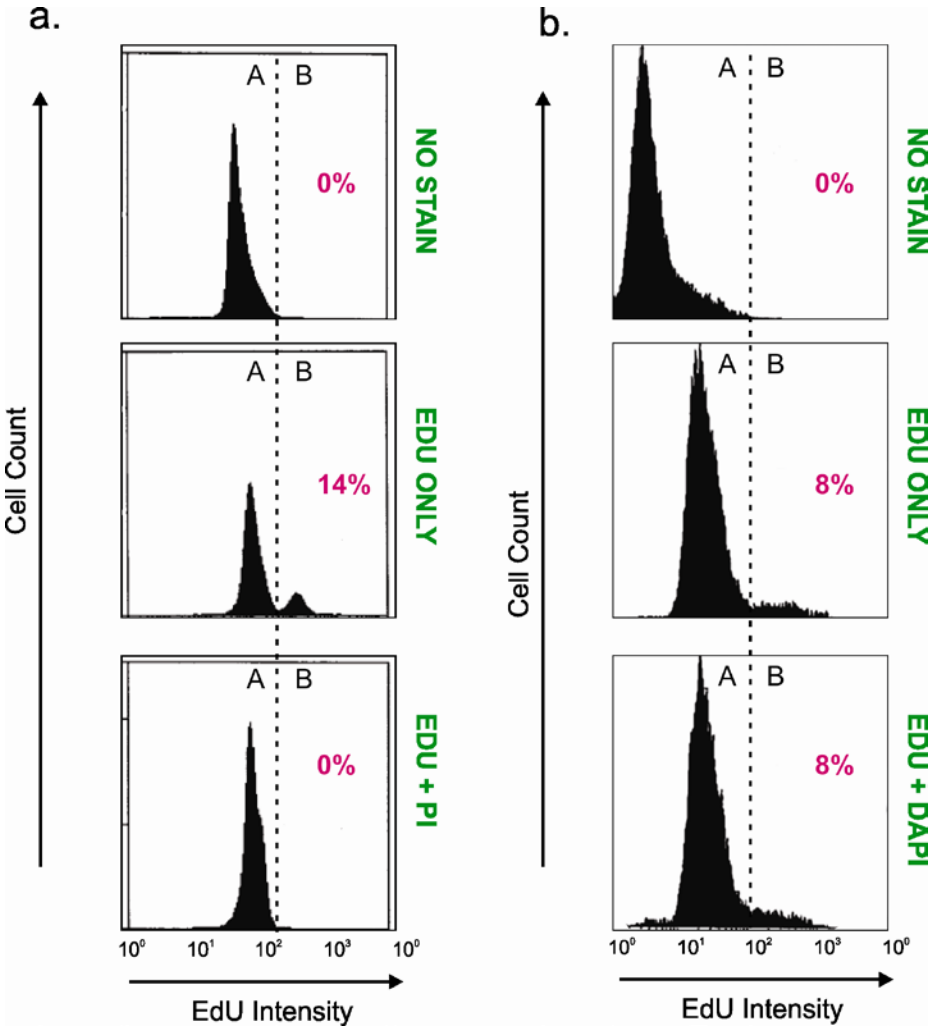

Figure 5-7 Optimizing the combination of fluorescent dyes

EBV transformed wild-type lymphoblastoid cells were irradiated with 60J/m2 of UV-C (or not). 10uM EdU was added to the samples. The cells were allowed to incubate at 37C for 1 hr to attempt repair of UV-induced DNA damage. Then the cells were fixed with 2% paraformaldehyde-0.5% Triton X-100, and 300mM sucrose and the click-it kit was used to fluorescently label EdU with 25uM Alexa Fluor 488-azide. The cells were collected, filtered and analyzed by FCM for DNA content and fluorescence intensity using a combination of **a.** EdU and PI; **b.** EdU and DAPI.

5.2.8 Click-iT reaction

The results from the standardized assay indicate that there was a 10 fold increase in the EdU incorporation between UV treated and untreated wild-type (Figure 5-8a) and that there is no

difference in the 13% incorporation observed in untreated XP-A cells when they were subjected to UV treatment (Figure 5-8b). Analysis of the results using a dual parameter histogram that measured the EdU intensity obtained from cells in distinct phases of the cell cycle revealed that there was a 30% increase in the EdU incorporation by wild-type cells in the G0/G1 phase of the cell cycle when they were treated with UV. Only 2% of untreated wild-type cells in G0/G1 showed EdU incorporation (Figure 5-8c). Furthermore, when XP-A cells were treated with UV, there was no increase in the percent of cells incorporating EdU between the UV treated (2%) and untreated samples (2%), as expected since the cells are NER-deficient and therefore should have no UDS (Figure 5-8c).

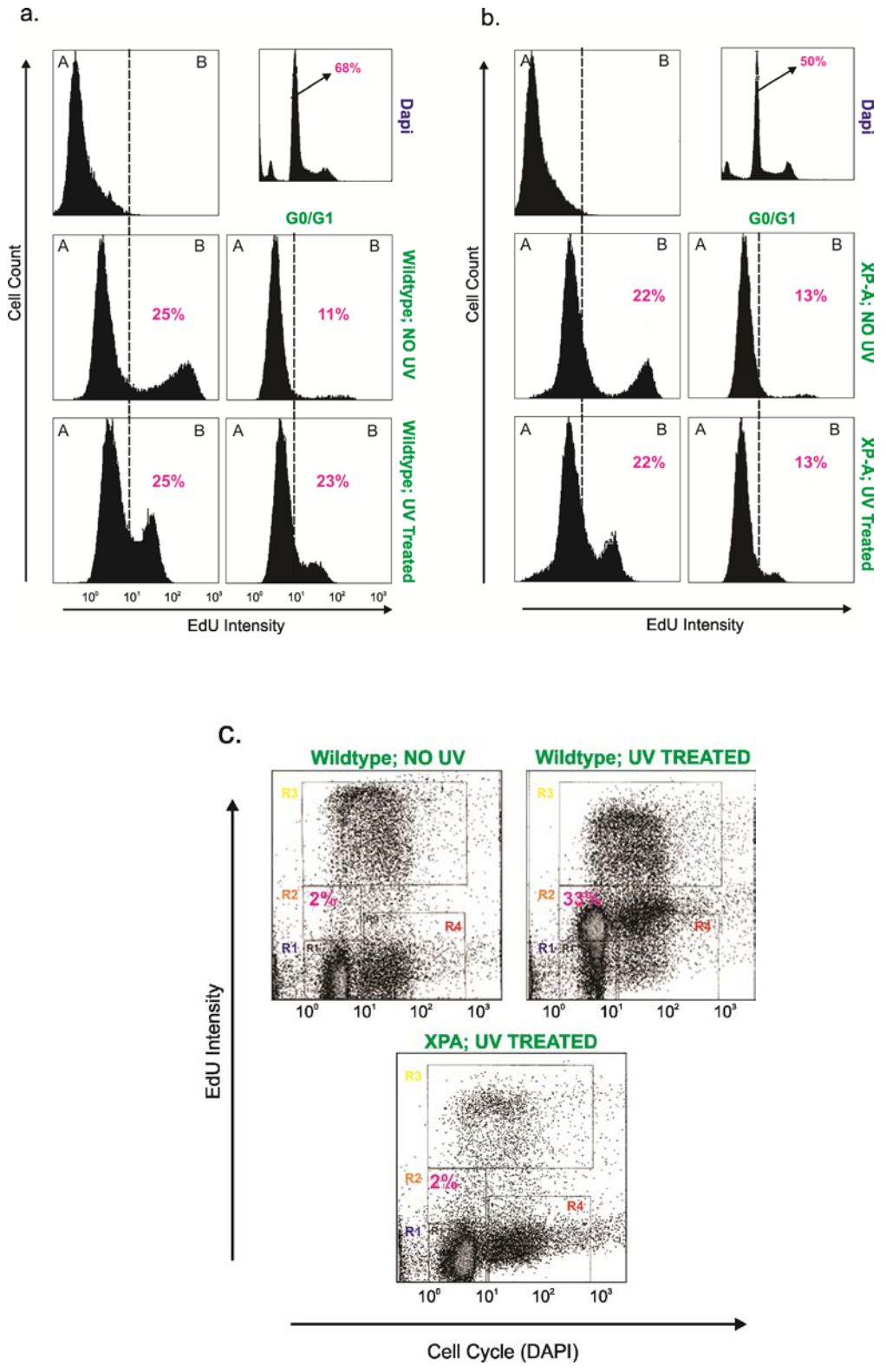

Figure 5-8 Flow cytometric detection of EdU labeled cells

DNA repair proficient (wild type) and DNA repair deficient (XP-A) cells were irradiated with 60J/m^2 of UV-C (or not). 10uM EdU was added to the samples. The cells were allowed to incubate at 37°C for 1 hr to attempt repair of UV-induced DNA damage. Then the cells were fixed with 70% ethanol and the Click-iT kit was used to fluorescently label EdU with 25uM Alexa Fluor 488-azide. The cells were collected, filtered and analyzed by flow for DNA content (DAPI, x-axis) and fluorescence intensity (EdU-FITC; y-axis). Single parameter histograms are shown for. **a.** Wild-type lymphoblastoid cells **b.** XP-A deficient lymphoblastoid cells where quadrant A represents autofluorescence and quadrant B represents true signal **c.** Dual parameter histograms where quadrant R1 (in blue; 2n DNA, low fluorescence) represents G0/G1 cells with no DNA synthesis; quadrant R2 (in orange; 2n DNA, intermediate fluorescence) represents NER of UV-induced DNA damage; quadrant R3 (in yellow; 2-4n DNA, high fluorescence) represents S phase cells; quadrant R4 (in red; 4n DNA, low fluorescence) represents G2/M cells.

5.3 DISCUSSION

Over the years, a plethora of assays have been developed in an attempt to measure DNA repair. The most common assays include those that measure repair synthesis such as the unscheduled DNA synthesis (UDS) assay, the comet assay which is used to measure strand breaks, the host cell reactivation assay that measures TC-NER, and the γH2AX assay that is usually used to measure double strand breaks. Since 1964 when the Unscheduled DNA synthesis assay was first developed to measure NER, it has been adapted in multiple ways to overcome the 3 major disadvantages of the initial technique: labor intensiveness, extensive duration of the assay and hazard issues due to the use of autoradiography.

Attempts made to accomplish this goal over the last decade involve immunodetection of the incorporated nucleoside analog bromodeoxyuridine (BrdU) using an anti-BrdU antibody. This approach has considerably shortened the time required for the assay from 3 months to 3 days but is still not automated and hence is very laborious. Flow cytometry (FCM) has been considered an attractive approach to semi automate measurement of repair synthesis. However, there is very minimal literature on the use of flow cytometry (FCM) to measure NER. In 1988,

Beisker and Hittelman described a flow cytometric approach to measure GG-NER by detecting the incorporation of BrdU into the DNA by cultured human fibroblasts after UV irradiation. Over the years, flow cytometry in combination with BrdU immunocytochemical staining has been employed in a number of studies that have measured repair by human fibroblasts, Chinese hamster ovary cells, cancerous cells and also primary rat hepatocytes (Affentranger and Burkart, 1992; Selden and Dolbeare, 1994; Selden et al., 1993; Srivastava et al., 1993). The major problem with the BrdU method is that for its detection, DNA is denatured with heat or HCl and such harsh treatments usually destroy the antigen recognition sites. In addition, it is not possible to combine cell cycle analysis dyes such as DAPI while using BrdU.

In this study, we have developed an assay to quantitatively measure NER in a semi-automated manner. The assay measures repair synthesis by the incorporation of EdU into the DNA of non S-phase cells after subjecting them to UV induced DNA damage using flow cytometry. In this version of the assay, ^{3}[H]-thymidine is replaced by the thymidine analogue EdU. This eliminates the need to use autoradiography as we can now use flow cytometry instead. In addition, this assay is standardized to measure the repair synthesis in suspension cells so as to eventually extend its application to human blood samples. During standardization, one of the most important things to ensure was the discrimination of signal obtained from cells in the S phase from cells in all other phases of the cell cycle and we accomplished this by (i) clearly segregating true signal from background generated through autofluorescence (ii) eliminating S-phase generated background (iii) accurately and sensitively measuring the "true signal" obtained from non S-phase cells. The first problem was efficiently resolved in 2 ways. Every experimental panel included stringent controls that were used to set the background generated by autofluorescence. This involved including unstained cells that did not receive either EdU or PI to

set the machine generated autofluorescence, single color controls such as cells stained with either the cell cycle dye or with EdU and each of these were used to determine the autofluorescence and also the color bleed from one channel to the other. This helped standardize the FCM machine prior to each analysis and using fresh controls with each experimental panel helped avoid variability introduced by the batch of reagents used, incubation temperature, and incubations times from one day to the other.

These modifications have reduced the total time taken for one reaction panel to 3 hours which is a tremendous change from the 3 months that the initial assay used to take. In addition to this assay being sensitive enough to distinguish between repair proficient and deficient cells (Figure 5-8), it is highly reproducible (data not shown) and by using an automated flow cytometer, 24 samples can be analyzed every 30 minutes. In conclusion, the flow cytometric measurement of NER by measuring EdU incorporation has the potential for being used as a future standard diagnostic measure in a clinical setting.

5.4 EXPERIMENTAL PROCEDURES

5.4.1 Cell Lines

GM02345 XP-A lymphoblastoid cell line and GM03798 normal wild-type lymphoblasts were obtained from Coriell. The cells were grown in RPMI Glutamax media (Invitrogen) supplemented with 10% FBS and Pen/Strep. The cells were all grown in a humidified 5% CO_2 incubator at 37ºC.

5.4.2 Serum Starvation

Exponentially growing cells were pelleted by centrifugation at 1000 rpm for 5 minutes at 37ºC. The supernatant was discarded and the cells were resuspended in media containing 0, 0.5, 1 and 2% serum and incubated for 0, 12, 24, 48 and 72h in a 5% CO_2 incubator at 37ºC.

5.4.3 Drug Treatments

Exponentially growing cells were pelleted by centrifugation at 1000 rpm for 5 minutes. The supernatant was discarded and the cells were resuspended in 20 ml of media containing either 10 µM hydroxyurea (Sigma) or 0.4 µM Mimosine (Sigma) and incubated for 12, 24 and 48 h in a 5% CO_2 incubator at 37ºC. Following incubation, the cells were pelleted and washed two times with PBS to remove the drug.

5.4.4 UV Irradiation

Exponentially growing cells were spun down in a 15 ml falcon tube at 1000 rpm for 5 minutes. The supernatant was discarded. The cell pellet was resuspended in 2 ml of PBS, and the cells were irradiated with 20, 60 or 100 J/m^2 of UV-C (Spectroline X-15 254nm) in an uncovered petri dish. The cells were then replenished with fresh medium containing 10 µM EdU (Invitrogen) and incubated at 37 ºC in a 5% CO_2 incubator.

5.4.5 Removing unincorporated EdU

After incubation, the cells were pelleted by centrifugation at 1000 rpm for 5 minutes. The supernatant was discarded and the cell pellet was resuspended in 5 ml PBS by pipeting gently up and down. The cells were then repelleted and the process was repeated one more time.

5.4.6 Fixing and Permeabilizing

The washed cell pellet was resuspended in 100 µl of PBS and the cell suspension was filtered through a 3µm filter (Falcon). The 2 ml of ice-cold 70% ethanol (Decon laboratories, Inc.) was added drop by drop to the cell suspension through the filter. Three more ml of 70% ethanol was added and the cells were incubated on ice for 30 minutes. After 30 minutes, the cells were pelleted by centrifugation at 1000 rpm for 5 minutes. The pellet was rehydrated and traces of 70% ethanol were removed by washing 2 times with PBS.

5.4.7 Blocking

The cells were then blocked by resuspending the pellet in 10% FBS or 3% BSA in PBS, and incubation at 37ºC for 20 minutes. After incubation, residual FBS/BSA was removed by centrifugation at 1000 rpm for 5 minutes and discarding the supernatant.

5.4.8 Ki67 Staining

The cell pellet was resuspended in 1 ml PBS containing 20 µl PE-Ki67 (Invitrogen) and incubated at RT for 30 minutes. Following incubation, the cells were pelleted by centrifugation at 1000 rpm for 5 minutes, the supernatant was discarded and the cells were washed two times with PBS as described previously.

5.4.9 Click-iT Reaction

For EdU staining, the Click-iT kit (Invitrogen) protocol was followed. Briefly, the cells were incubated in 500 µl of the reaction mixture which contained 25 µM Alexa Fluor647-azide, 50 mM TBS pH 7.3, 4mM copper and 10 mM sodium ascorbate. Each cell pellet was then gently resuspended in 500 µl of the reaction mixture and incubated at RT in the dark for 30 minutes.

5.4.10 Washing

After incubation, the cells were pelleted by centrifugation at 1000 rpm for 5 minutes. The supernatant was discarded and the cell pellet was resuspended in 5 ml PBS by pipeting up and down gently. The cells were then pelleted as described previously and the process was repeated one more time.

5.4.11 DNA Staining

The cell pellet was resuspended in 1ml PBS in a 5 ml poly propylene tube (Falcon). To this, 100 ug/ml RNase A and 40 ug/ml Propidium iodide was added and the cells were incubated at RT. After 30 minutes, the cells were directly analyzed by flow cytometry.

5.4.12 Flow Cytometry

Becton and Coulter Gallios, Becton, Coulter Cyan Blue and Accuri C6 flow cytometers were used to analyze the cells.

5.5 ACKNOWLEDGEMENTS

We would like to thank Ernest M. Meyer (Mike) for helping with the flow cytometry experiments. In addition, we would like to thank Center for Aging and Population Health (CAPH) for funding this study.

6.0 OVERALL DISCUSSION AND FUTURE DIRECTIONS

The overarching goal of my doctoral dissertation was to understand the contribution of DNA repair mediated by XPF-ERCC1 to cancer and aging. The basic foundation of this research arose from the fact that misinterpretation of lesions by the repair and replication machinery leads to mutations in the genome giving rise to cancer. However, extensive damage results in either programmed cell death (apoptosis) or cellular senescence both of which can contribute to aging. It is a well established that deficiency of NER proteins result in Xeroderma Pigmentosum, a disease characterized by extreme sensitivity to sunlight and a predisposition to cancer. However, a severe deficiency of the NER endonuclease XPF-ERCC1 leads to an accelerated aging phenotype in both mice and humans, implying that this exaggerated phenotype is due to the functions of XPF-ERCC1 outside of NER. Genetic dissection of the DNA repair mechanism or the type of DNA lesions that promote cancer and aging will help devise ways to delay degenerative changes that are associated with age and will also help improve cancer treatment. My dissertation lays the foundation to answering some of the key questions that remain unanswered in our field, such as (i) Do the accumulation of unrepaired crosslinks promote aging? (ii) Are XPF-ERCC1 good biomarkers of chemoresistance, and if so, what is the mechanism underlying this resistance? and finally, (iii) Can we efficiently and accurately measure the DNA repair capacity of an individual to use as a prognostic tool? The answers to these basic questions bring us one step closer to translating bench research to bedside treatment.

To accomplish this, we set out to uncouple the functions of XPF-ERCC1 in NER and ICL repair by engineering mutations in different regions of the XPF gene using site-directed mutagenesis. The evolutionary conservation of the proteins combined with the fact that XPF-ERCC1 has an essential role in multiple genome maintenance mechanisms highlight the biological importance of the complex.

In Chapter 2 of my dissertation, we have analyzed the importance of four DNA binding domains in the C-terminus of XPF-ERCC1 for NER. Based on data from structural and functional studies of XPF-ERCC1, two basic residues in the HhH domains, K247 and K281 in ERCC1 and K850 and R853 in XPF were chosen as they have previously been implicated in DNA binding (Figure 2-1). In addition, the R678 residue in the nuclease domain of XPF and the N110A mutant previously shown to have weakened interaction with XP-A were also included. Our results indicate that multiple protein and DNA binding domains of XPF-ERCC1 control its function in NER and that mutations in the HhH domain of ERCC1 affect DNA binding, nuclease and NER activity more severely than analogous mutations in XPF. The synergistic effect of mutations in multiple DNA binding domains is essential to affect NER activity.

In Chapter 3, we engineered mutations in specific domains of XPF to generate pathway specific defects. The regions selected for mutagenesis included the nuclease domain of XPF in the C-terminus, the FANCP interaction domain in the N-terminus, and a 5 amino acid deletion in the N-terminus of the protein. The data presented herein demonstrate that multiple domains of XPF are likely good candidates to uncouple the function of XPF-ERCC1 such that they are proficient in NER, but are deficient in ICL repair. This project also provides the first formal proof that the nuclease domain of XPF is essential for repair (Figure 3-2). The primary endpoint analyzed was the overall cellular survival in response to UV, crosslinking agent-mitomycin C

mitomycin C and ionizing radiation as measured by a clonogenic survival assay. The results from the initial survival curves identified the mutation in position 314 to make cells selectively hypersensitive to crosslinking agents (Figure 3-2b). To support and confirm the proficiency of each repair pathway in question, I examined secondary endpoints measuring either well known markers or key events in each repair pathway. The local damage assay used as a secondary endpoint for NER revealed that the D676A mutation in the nuclease domain of XPF that made it nucleolytically dead compromised the NER function of XPF-ERCC1 (Figure 3-3). In support of the primary data, the secondary endpoint for the ICL repair pathways, measured by the activation of the FA pathway denoted by FANCD2-L (monoubiquitinated form) and FANCD2-S (monoubiquitinated form) indicated that the potential disruption of the interaction betweeen XPF and FANCP compromises ICL repair ability (Figure 3-4). Much to our surprise, the hypersensitivity of the wild-type corrected cell line observed in response to MMC lead to the identification of defects in the XPF construct being used. The results shown in (Figure 3-7) confirm the complete rectification of the XPF construct. Based on the inferences drawn from this study, we in the future, plan to take this approach *in vivo* to determine the phenotype of a mouse carrying nucleolytically dead XPF, D687A and ICL repair deficient XPF, G325E and G703D independently. This study will aid in understanding the contribution of ICL repair to aging and also help identify regions of the XPF gene that when targeted with small molecule inhibitors, sensitizes cells specifically to crosslinking agents.

Chapter 4 of my dissertation details the development and stringent evaluation of a panel of new monoclonal antibodies that could be used to measure XPF-ERCC1 protein expression levels in tumors. The data herein demonstrates the applicability of three of the 10 monoclonal antibodies for immunoprecipitation, immunoblotting, immunofluorescence, and

immunohistochemistry (Table 3). The 1E4 antibody has excellent specificity and sensitivity toward human XPF protein (Figures 1 & 3). The 3H4 antibody identified has specificity toward both mouse and human XPF (Figure 4-2c). In addition, the identification of the 3G7 antibody that detects both XPF and ERCC1 (Figure 4-2b), is of special importance as it can help establish an accurate correlation of the expression levels of both proteins in tumor cells and an antibody of this nature has the potential to probe the functional domains of the complex. The two antibodies, 1E4 and 3H4, selectively purified were standardized for the IHC detection of XPF-ERCC1 in human and mouse tissue respectively. The initial standardization of the human 1E4 antibody for IHC was carried out using wild-type cell sections as positive control, XPF-deficient XP2YO cells as negative control and tonsil sections to estimate tissue applicability (Figure 4-7). I used cell lines for standardization to assess the specificity of the antibody to XPF as it is difficult if not impossible to procure tissue samples that can serve as negative controls. In addition, the use of negative controls that receive only the secondary antibody after treatment with serum in place of the primary antibody, helps ascertain that the signal obtained is purely due to accurate protein detection.

In the future, we plan to standardize the 3G7 antibody for IHC analysis so that a parallel measure of levels of both XPF and ERCC1 can be obtained. An antibody of this nature is invaluable as it eliminates issues of bias, sensitivity and specificity. In addition, we plan to map the epitope of the 3G7 antibody on X PF and ERCC1 to determine the region of binding. Depending on the region of binding, this antibody has the potential to disrupt interaction between XPF and ERCC1 and thereby disrupt DNA repair mediated by XPF-ERCC1 eliminating the need for mutagenesis.

Chapter 5 of my dissertation provides a detailed description of the development of an assay to measure the DNA repair capacity of cells. Even though there are multiple established ways to measure repair, the major disadvantage of most if not all of the protocols in that they measure the expression of one or more proteins in the repair pathways. In other cases, the assays employ complex transfection-based methods that are both laborious and time consuming with variations in applicability to specific cell types. To circumvent these problems, I took an approach that will measure repair as an event rather than as a measure of specific proteins. The most common repair pathways include base excision repair (BER), NER, ICL repair, and DSB repair. This study aimed to measure NER, ICL repair and DSB repair specifically as lesions repaired by BER are generated by endogenous sources of DNA damage where as the other repair pathways have a major environmental contribution. NER was first quantified by measuring Unscheduled DNA Synthesis using fluorescent nucleotides and flow cytometry. I used lymphoblastoid suspension cells for the standardization procedure so as to extend the potential of this approach in the future to clinical blood samples. Wild-type EBV-transformed cells were used as positive controls and NER deficient XP-A cells were used as negative controls to ascertain specificity of the assay. The repair capacity as measured by flow cytometry shows a 23% difference in UDS between UV exposed and UV non-exposed wild-type cells (Figure 5-7a). There was no difference in the UDS levels between the treated and untreated XP-A cells. The 13% difference in UDS between UV treated wild-type and UV treated XP-A cells is representative of the NER capacity between two individuals, one who is normal and one who has type A Xeroderma pigmentosum (Figure 5-8).

In the future, this study will be extended to measuring ICL repair capacity of the cells by treatment with mitomycin C following transfection of cells with the traffic light reporter (TLR)

plasmid. DSB will be measured by quantifying γH2AX foci generated in response to IR treatment by using the Amnis flow cytometer. These approaches have the potential to automate repair measure facilitating a quick and accurate estimate of the DNA repair capacity of an individual. The mean outcome of the measure of the three repair pathways can be the compared between long-lived individuals, their offspring and spouse controls to determine whether high DNA repair capacity contributes to longer survival of an individual and also to determine the heritability of DNA repair capacity. In addition, measuring the repair capacity of patients with cancer will help predict their response to chemoradiotherapeutic regimes and will help tailor therapy to each person.

These studies have made minor yet significant advances in understanding and tackling two major public health issues of the 21st century namely, aging and cancer.

7.0 PUBLIC HEALTH SIGNIFICANCE

DNA damage is one of the major contributing factors to cancer and a large number of age related degenerative changes. Somatic mutations that accumulate with age due to gradual functional decline, have the potential to disrupt controlled cellular proliferation giving rise to cancer. Aging is defined as the gradual but progressive functional decline in the physiological function of an organism. According to the World Health Organization (WHO), two billion people will be 65 years and above by 2050 and this is more than three times the number observed in the year 2000. Moving one step further, when we consider people over age 85, the population is projected to increase from 4.2 million in 2000 to 6.6 million in 2020. This poses a problem because the cost of providing health care for an older individual is nearly five times greater than someone younger (The State of Aging and health in America 2007 CDC Merck company). Based on this statistic, the nation's health care cost is projected to increase 25% by the year 2030. Therefore, it is crucial to understand the basic mechanisms behind aging. With advancing age comes the susceptibility to a wide range of age-associated disorders such as arthritis, cardiovascular disease, osteoporosis, and cancer. Cancer, the second most common cause of death in the United States of America, is a disorder of aging. Beyond the age of 60, the cancer incidence is known to double every 5 years and by 80 years, people have a 50% chance of developing cancer (Siegel et al., 2012). The year of 2012 has been estimated to have 1,638,910 new cancer cases with 577,190 representing the number of cancer deaths leading us to a staggering number of more

than 1,500 deaths per day. Looking at the contribution of cancer to overall mortality, this accounts for nearly 1 of every 4 deaths in the US. The four major cancer types include lung, colorectum, breast, and prostate. Current research has helped in the decline of lung cancer in men by almost 40% and decline of breast cancer accounting for 34% in women. The year 2012 has seen 1,024,400 fewer deaths due to cancer and this promising number is only predicted to increase by advocating and extending the current cancer control measures which include both public awareness and research generated therapeutic measures to all segments of society.

"The prolongation of life is the most noble of all medical pursuits, for if any such things be found out (it) would be the greatest of worldly donations" Francis Bacon

APPENDIX A

ABBREVIATIONS

BrdU –Bromodeoxyuridine

BSA- Bovine Serum Albumin

CPD- Cyclobutane Pyrimidine Dimers

DAB- 3,3'-Diaminobenzidine

DAPI - 4′-6′-diamino-2-phenylindole

DSB repair- Double strand Break Repair

EDTA- Ethylenediaminetetraacetic acid

EdU- 5-ethynyl-2'-deoxyuridine

em – emission

ERCC1-Excision Repair Cross Complementation group 1

FBS- Fetal Bovine Serum

FCM – Flow cytometry

GFP – Green Fluorescence Protein

GG-NER- Global Genome Nucleotide Excision Repair

HCl – Hydrochloric acid

ICL-R- Interstrand Crosslink Repair

IR –Ionizing Radiation

MMC-Mitomycin C

NER- Nucleotide exchange repair

P/S – Penicillin/streptomycin

PBS- Phosphate buffered saline

PBST- Phosphate buffered saline -Tween-20

PI – Propidium iodide

PP-Photo Products

RT- Room temperature

RT-Room Temperature

SDS-PAGE-Sodium dodecyl sulfate polyacrylamide gel electrophoresis

SDS-Sodium Dodecyl Sulfate

SS/FS- Side scatter/forward scatter

SSA- Single strand annealing

TBS- Tris buffered saline

UDS-Unscheduled DNA Synthesis

UV- Ultraviolet radiation

WCE- Whole Cell Extracts

XP- Xeroderma pigmentosum

XPF- Xeroderma pigmentosum group F

APPENDIX B

LIST OF CELL LINES

Table 5 List of Cell Lines

Cell line name	Organism	Primary/Immortalized	Tissue mutation
Wild-type	Human	SV40 transformed	Normal human fibroblast, no mutation
XP2YO	Human	SV40 transformed	Unidentified mutation that presents as XP
C5RO	Human	Immortalized by the stable expression of human telomerase	Normal human fibroblasts
XP51RO	Human	Immortalized by the stable expression of human telomerase	R153P mutation that presents as XFE
HeLa	Human	Have active telomerase	Cervical cancer cell line
Wild-type MEF	Mouse	Primary	$ERCC1^{+/+}$ mouse embryonic fibroblast
$ERCC1^{-/-}$ MEF	Mouse	Primary	$ERCC1^{-/-}$ mouse embryonic fibroblast
AA8	CHO	Immortalized	$ERCC1^{+/+}$ CHO cells
UV20	CHO	Immortalized	$ERCC1^{-/-}$ CHO cells
GM03798 wild-type	Human	Epstein-Barr Virus transformed	Normal lymphoblastoid cell line
GM02345 XP-A	Human	Epstein-Barr Virus transformed	XP-A lymphoblastoid cell line

BIBLIOGRAPHY

Abraham, J., Lemmers, B., Hande, M.P., Moynahan, M.E., Chahwan, C., Ciccia, A., Essers, J., Hanada, K., Chahwan, R., Khaw, A.K., et al. (2003). Eme1 is involved in DNA damage processing and maintenance of genomic stability in mammalian cells. The EMBO journal 22, 6137-6147.

Affentranger, M.I., and Burkart, W. (1992). Assessment of radiation-induced DNA strand breaks and their repair in unlabeled cells. Cytometry 13, 31-38.

Ahmad, A., Enzlin, J.H., Bhagwat, N.R., Wijgers, N., Raams, A., Appledoorn, E., Theil, A.F., JH, J.H., Vermeulen, W., NG, J.J., et al. (2010). Mislocalization of XPF-ERCC1 nuclease contributes to reduced DNA repair in XP-F patients. PLoS Genet 6, e1000871.

Ahmad, A., Robinson, A.R., Duensing, A., van Drunen, E., Beverloo, H.B., Weisberg, D.B., Hasty, P., Hoeijmakers, J.H., and Niedernhofer, L.J. (2008). ERCC1-XPF endonuclease facilitates DNA double-strand break repair. Mol Cell Biol 28, 5082-5092.

Al-Minawi, A.Z., Saleh-Gohari, N., and Helleday, T. (2008). The ERCC1/XPF endonuclease is required for efficient single-strand annealing and gene conversion in mammalian cells. Nucleic Acids Res 36, 1-9.

Altaha, R., Liang, X., Yu, J.J., and Reed, E. (2004). Excision repair cross complementing-group 1: gene expression and platinum resistance. International journal of molecular medicine 14, 959-970.

Andersen, S.L., Bergstralh, D.T., Kohl, K.P., LaRocque, J.R., Moore, C.B., and Sekelsky, J. (2009). Drosophila MUS312 and the vertebrate ortholog BTBD12 interact with DNA structure-specific endonucleases in DNA repair and recombination. Mol Cell 35, 128-135.

Andreassen, P.R., D'Andrea, A.D., and Taniguchi, T. (2004). ATR couples FANCD2 monoubiquitination to the DNA-damage response. Genes & development 18, 1958-1963.

Araki, M., Masutani, C., Takemura, M., Uchida, A., Sugasawa, K., Kondoh, J., Ohkuma, Y., and Hanaoka, F. (2001). Centrosome protein centrin 2/caltractin 1 is part of the xeroderma pigmentosum group C complex that initiates global genome nucleotide excision repair. J Biol Chem 276, 18665-18672.

Aravind, L., Walker, D.R., and Koonin, E.V. (1999). Conserved domains in DNA repair proteins and evolution of repair systems. Nucleic Acids Res 27, 1223-1242.

Arora, S., Kothandapani, A., Tillison, K., Kalman-Maltese, V., and Patrick, S.M. (2010). Downregulation of XPF-ERCC1 enhances cisplatin efficacy in cancer cells. DNA Repair (Amst) 9, 745-753.

Auerbach, A.D., and Wolman, S.R. (1976). Susceptibility of Fanconi's anaemia fibroblasts to chromosome damage by carcinogens. Nature 261, 494-496.

Bae, J.B., Mukhopadhyay, S.S., Liu, L., Zhang, N., Tan, J., Akhter, S., Liu, X., Shen, X., Li, L., and Legerski, R.J. (2008). Snm1B/Apollo mediates replication fork collapse and S Phase checkpoint activation in response to DNA interstrand cross-links. Oncogene 27, 5045-5056.

Bailly, V., Sommers, C.H., Sung, P., Prakash, L., and Prakash, S. (1992). Specific complex formation between proteins encoded by the yeast DNA repair and recombination genes RAD1 and RAD10. Proc Natl Acad Sci U S A 89, 8273-8277.

Baker, B.S., Carpenter, A.T., and Ripoll, P. (1978). The Utilization during Mitotic Cell Division of Loci Controlling Meiotic Recombination and Disjunction in DROSOPHILA MELANOGASTER. Genetics 90, 531-578.

Bardwell, A.J., Bardwell, L., Tomkinson, A.E., and Friedberg, E.C. (1994). Specific cleavage of model recombination and repair intermediates by the yeast Rad1-Rad10 DNA endonuclease. Science (New York, N.Y 265, 2082-2085.

Bardwell, L., Cooper, A.J., and Friedberg, E.C. (1992). Stable and specific association between the yeast recombination and DNA repair proteins RAD1 and RAD10 in vitro. Mol Cell Biol 12, 3041-3049.

Bertola, D.R., Cao, H., Albano, L.M., Oliveira, D.P., Kok, F., Marques-Dias, M.J., Kim, C.A., and Hegele, R.A. (2006). Cockayne syndrome type A: novel mutations in eight typical patients. Journal of human genetics 51, 701-705.

Bertrand, P., Tishkoff, D.X., Filosi, N., Dasgupta, R., and Kolodner, R.D. (1998). Physical interaction between components of DNA mismatch repair and nucleotide excision repair. Proc Natl Acad Sci U S A 95, 14278-14283.

Bhagwat, N., Olsen, A.L., Wang, A.T., Hanada, K., Stuckert, P., Kanaar, R., D'Andrea, A., Niedernhofer, L.J., and McHugh, P.J. (2009a). XPF-ERCC1 participates in the Fanconi anemia pathway of cross-link repair. Mol Cell Biol 29, 6427-6437.

Bhagwat, N., Olsen, A.L., Wang, A.T., Hanada, K., Stuckert, P., Kanaar, R., D'Andrea, A., Niedernhofer, L.J., and McHugh, P.J. (2009b). XPF-ERCC1 participates in the Fanconi anemia pathway of crosslink repair. Mol. Cell. Biol., MCB.00086-00009.

Bhagwat, N.R., Roginskaya, V.Y., Acquafondata, M.B., Dhir, R., Wood, R.D., and Niedernhofer, L.J. (2009c). Immunodetection of DNA repair endonuclease ERCC1-XPF in human tissue. Cancer research 69, 6831-6838.

Biggerstaff, M., Szymkowski, D.E., and Wood, R.D. (1993). Co-correction of the ERCC1, ERCC4 and xeroderma pigmentosum group F DNA repair defects in vitro. The EMBO journal 12, 3685-3692.

Biggerstaff, M., and Wood, R.D. (1999). Assay for nucleotide excision repair protein activity using fractionated cell extracts and UV-damaged plasmid DNA. Methods Mol Biol 113, 357-372.

Boddy, M.N., Gaillard, P.H., McDonald, W.H., Shanahan, P., Yates, J.R., 3rd, and Russell, P. (2001). Mus81-Eme1 are essential components of a Holliday junction resolvase. Cell 107, 537-548.

Boiteux, S., and Guillet, M. (2004). Abasic sites in DNA: repair and biological consequences in Saccharomyces cerevisiae. DNA Repair (Amst) 3, 1-12.

Brookman, K.W., Lamerdin, J.E., Thelen, M.P., Hwang, M., Reardon, J.T., Sancar, A., Zhou, Z.Q., Walter, C.A., Parris, C.N., and Thompson, L.H. (1996). ERCC4 (XPF) encodes a human nucleotide excision repair protein with eukaryotic recombination homologs. Mol Cell Biol 16, 6553-6562.

Brooks, P.J. (2008). The 8,5'-cyclopurine-2'-deoxynucleosides: candidate neurodegenerative DNA lesions in xeroderma pigmentosum, and unique probes of transcription and nucleotide excision repair. DNA Repair (Amst) 7, 1168-1179.

Carpenter, A.T., and Baker, B.S. (1982). On the Control of the Distribution of Meiotic Exchange in DROSOPHILA MELANOGASTER. Genetics 101, 81-89.

Carr, A.M., Schmidt, H., Kirchhoff, S., Muriel, W.J., Sheldrick, K.S., Griffiths, D.J., Basmacioglu, C.N., Subramani, S., Clegg, M., Nasim, A., et al. (1994). The rad16 gene of Schizosaccharomyces pombe: a h omolog of the RAD1 gene of Saccharomyces cerevisiae. Mol Cell Biol 14, 2029-2040.

Champoux, J.J. (2001). DNA topoisomerases: structure, function, and mechanism. Annu Rev Biochem 70, 369-413.

Chen, H., Shao, C., Shi, H., Mu, Y., Sai, K., and Chen, Z. (2007). Single nucleotide polymorphisms and expression of ERCC1 and ERCC2 vis-a-vis chemotherapy drug cytotoxicity in human glioma. Journal of neuro-oncology 82, 257-262.

Chen, X., Wu, J., Lu, H., Huang, O., and Shen, K. (2012). Measuring beta-tubulin III, Bcl-2, and ERCC1 improves pathological complete remission predictive accuracy in breast cancer. Cancer science 103, 262-268.

Christmann, M., Tomicic, M.T., Roos, W.P., and Kaina, B. (2003). Mechanisms of human DNA repair: an update. Toxicology 193, 3-34.

Chung, H.H., Kim, M.K., Kim, J.W., Park, N.H., Song, Y.S., Kang, S.B., and Lee, H.P. (2006). XRCC1 R399Q polymorphism is associated with response to platinum-based neoadjuvant chemotherapy in bulky cervical cancer. Gynecologic oncology 103, 1031-1037.

Ciccia, A., Ling, C., Coulthard, R., Yan, Z., Xue, Y., Meetei, A.R., Laghmani el, H., Joenje, H., McDonald, N., de Winter, J.P., et al. (2007). Identification of FAAP24, a Fanconi anemia core complex protein that interacts with FANCM. Mol Cell 25, 331-343.

Cleaver, J.E. (1968). Defective repair replication of DNA in xeroderma pigmentosum. Nature 218, 652-656.

Cobo, M., Isla, D., Massuti, B., Montes, A., Sanchez, J.M., Provencio, M., Vinolas, N., Paz-Ares, L., Lopez-Vivanco, G., Munoz, M.A., et al. (2007). Customizing cisplatin based on quantitative excision repair cross-complementing 1 mRNA expression: a phase III trial in non-small-cell lung cancer. J Clin Oncol 25, 2747-2754.

Coin, F., Auriol, J., Tapias, A., Clivio, P., Vermeulen, W., and Egly, J.M. (2004). Phosphorylation of XPB helicase regulates TFIIH nucleotide excision repair activity. The EMBO journal 23, 4835-4846.

Collins, A.R. (1993). Mutant rodent cell lines sensitive to ultraviolet light, ionizing radiation and cross-linking agents: a comprehensive survey of genetic and biochemical characteristics. Mutat Res 293, 99-118.

Collins, N.B., Wilson, J.B., Bush, T., Thomashevski, A., Roberts, K.J., Jones, N.J., and Kupfer, G.M. (2009). ATR-dependent phosphorylation of FANCA on s erine 1449 after DNA damage is important for FA pathway function. Blood 113, 2181-2190.

Crossan, G.P., and Patel, K.J. (2012). The Fanconi anaemia pathway orchestrates incisions at sites of crosslinked DNA. The Journal of pathology 226, 326-337.

Crossan, G.P., van der Weyden, L., Rosado, I.V., Langevin, F., Gaillard, P.-H.L., McIntyre, R.E., Project, S.M.G., Gallagher, F., Kettunen, M.I., Lewis, D.Y., et al. (2011a). Disruption of mouse Slx4, a regulator of structure-specific nucleases, phenocopies Fanconi anemia. Nature genetics 43, 147-152.

Crossan, G.P., van der Weyden, L., Rosado, I.V., Langevin, F., Gaillard, P.H., McIntyre, R.E., Gallagher, F., Kettunen, M.I., Lewis, D.Y., Brindle, K., et al. (2011b). Disruption of mouse Slx4, a regulator of structure-specific nucleases, phenocopies Fanconi anemia. Nature genetics 43, 147-152.

Cummings, M., Higginbottom, K., McGurk, C.J., Wong, O.G., Koberle, B., Oliver, R.T., and Masters, J.R. (2006). XPA versus ERCC1 as chemosensitising agents to cisplatin and

mitomycin C in prostate cancer cells: role of ERCC1 in homologous recombination repair. Biochemical pharmacology 72, 166-175.

Dabholkar, M., Bostick-Bruton, F., Weber, C., Bohr, V.A., Egwuagu, C., and Reed, E. (1992). ERCC1 and ERCC2 expression in malignant tissues from ovarian cancer patients. Journal of the National Cancer Institute 84, 1512-1517.

Dabholkar, M., Vionnet, J., Bostick-Bruton, F., Yu, J.J., and Reed, E. (1994). Messenger RNA levels of XPAC and ERCC1 in ovarian cancer tissue correlate with response to platinum-based chemotherapy. The Journal of clinical investigation 94, 703-708.

Darzynkiewicz, Z., Halicka, H.D., Zhao, H., and Podhorecka, M. (2011). Cell synchronization by inhibitors of DNA replication induces replication stress and DNA damage response: analysis by flow cytometry. Methods Mol Biol 761, 85-96.

Davies, A.A., Friedberg, E.C., Tomkinson, A.E., Wood, R.D., and West, S.C. (1995). Role of the Rad1 and Rad10 proteins in nucleotide excision repair and recombination. J Biol Chem 270, 24638-24641.

de Laat, W.L., Appeldoorn, E., Jaspers, N.G., and Hoeijmakers, J.H. (1998a). DNA structural elements required for ERCC1-XPF endonuclease activity. J Biol Chem 273, 7835-7842.

de Laat, W.L., Appeldoorn, E., Jaspers, N.G.J., and Hoeijmakers, J.H.J. (1998b). DNA structural elements required for ERCC1-XPF endonuclease activity. J Biol Chem 273, 7835-7842.

de Laat, W.L., Appeldoorn, E., Sugasawa, K., Weterings, E., Jaspers, N.G., and Hoeijmakers, J.H. (1998c). DNA-binding polarity of human replication protein A positions nucleases in nucleotide excision repair. Genes & development 12, 2598-2609.

de Laat, W.L., Jaspers, N.G., and Hoeijmakers, J.H. (1999). Molecular mechanism of nucleotide excision repair. Genes & development 13, 768-785.

de Laat, W.L., Sijbers, A.M., Odijk, H., Jaspers, N.G., and Hoeijmakers, J.H. (1998d). Mapping of interaction domains between human repair proteins ERCC1 and XPF. Nucleic Acids Res 26, 4146-4152.

De Silva, I.U., McHugh, P.J., Clingen, P.H., and Hartley, J.A. (2000). Defining the roles of nucleotide excision repair and recombination in the repair of DNA interstrand cross-links in mammalian cells. Mol Cell Biol 20, 7980-7990.

de Vries, A., van Oostrom, C.T., Hofhuis, F.M., Dortant, P.M., Berg, R.J., de Gruijl, F.R., Wester, P.W., van Kreijl, C.F., Capel, P.J., van Steeg, H., et al. (1995). Increased susceptibility to ultraviolet-B and carcinogens of mice lacking the DNA excision repair gene XPA. Nature 377, 169-173.

De Weerd-Kastelein, E.A., Keijzer, W., and Bootsma, D. (1972). Genetic heterogeneity of xeroderma pigmentosum demonstrated by somatic cell hybridization. Nature: New biology 238, 80-83.

de Weerd-Kastelein, E.A., Keijzer, W., and Bootsma, D. (1974). A third complementation group in xeroderma pigmentosum. Mutat Res 22, 87-91.

Decottignies, A. (2007). Microhomology-mediated end joining in fission yeast is repressed by pku70 and relies on genes involved in homologous recombination. Genetics 176, 1403-1415.

Deloia, J.A., Bhagwat, N.R., Darcy, K.M., Strange, M., Tian, C., Nuttall, K., Krivak, T.C., and Niedernhofer, L.J. (2012). Comparison of ERCC1/XPF genetic variation, mRNA and protein levels in women with advanced stage ovarian cancer treated with intraperitoneal platinum. Gynecologic oncology.

DiGiovanna, J.J., and Kraemer, K.H. (2012). Shining a light on xeroderma pigmentosum. The Journal of investigative dermatology 132, 785-796.

Doecke, J., Zhao, Z.Z., Pandeya, N., Sadeghi, S., Stark, M., Green, A.C., Hayward, N.K., Webb, P.M., and Whiteman, D.C. (2008). Polymorphisms in MGMT and DNA repair genes and the risk of esophageal adenocarcinoma. Int J Cancer 123, 174-180.

Doherty, A.J., Serpell, L.C., and Ponting, C.P. (1996). The helix-hairpin-helix DNA-binding motif: a structural basis for non- sequence-specific recognition of DNA. Nucleic Acids Res 24, 2488-2497.

Doig, J., Anderson, C., Lawrence, N.J., Selfridge, J., Brownstein, D.G., and Melton, D.W. (2006). Mice with skin-specific DNA repair gene (Ercc1) inactivation are hypersensitive to ultraviolet irradiation-induced skin cancer and show more rapid actinic progression. Oncogene 25, 6229-6238.

Dolle, M.E., Busuttil, R.A., Garcia, A.M., Wijnhoven, S., van Drunen, E., Niedernhofer, L.J., van der Horst, G., Hoeijmakers, J.H., van Steeg, H., and Vijg, J. (2006). Increased genomic instability is not a prerequisite for shortened lifespan in DNA repair deficient mice. Mutat Res 596, 22-35.

Dronkert, M.L., de Wit, J., Boeve, M., Vasconcelos, M.L., van Steeg, H., Tan, T.L., Hoeijmakers, J.H., and Kanaar, R. (2000). Disruption of mouse SNM1 causes increased sensitivity to the DNA interstrand cross-linking agent mitomycin C. Mol Cell Biol 20, 4553-4561.

Dronkert, M.L., and Kanaar, R. (2001). Repair of DNA interstrand cross-links. Mutat Res 486, 217-247.

Dunand-Sauthier, I., Hohl, M., Thorel, F., Jaquier-Gubler, P., Clarkson, S.G., and Scharer, O.D. (2005). The spacer region of XPG mediates recruitment to nucleotide excision repair complexes and determines substrate specificity. J Biol Chem 280, 7030-7037.

Duncan, J., Hamilton, L., and Friedberg, E.C. (1976). Enzymatic degradation of uracil-containing DNA. II. Evidence for N-glycosidase and nuclease activities in unfractionated extracts of Bacillus subtilis. J Virol 19, 338-345.

Durant, S.T., Morris, M.M., Illand, M., McKay, H.J., McCormick, C., Hirst, G.L., Borts, R.H., and Brown, R. (1999). Dependence on RAD52 and RAD1 for anticancer drug resistance mediated by inactivation of mismatch repair genes. Curr Biol 9, 51-54.

Enzlin, J.H., and Scharer, O.D. (2002). The active site of the DNA repair endonuclease XPF-ERCC1 forms a highly conserved nuclease motif. The EMBO journal 21, 2045-2053.

Enzlin, J.H., and Schärer, O.D. (2002). The active site of XPF-ERCC1 forms a highly conserved nuclease motif. The EMBO journal 21, 2045-2053.

Fagbemi, A.F., Orelli, B., and Scharer, O.D. (2011). Regulation of endonuclease activity in human nucleotide excision repair. DNA Repair (Amst) 10, 722-729.

Fekairi, S., Scaglione, S., Chahwan, C., Taylor, E.R., Tissier, A., Coulon, S., Dong, M.Q., Ruse, C., Yates, J.R., 3rd, Russell, P., et al. (2009). Human SLX4 is a Holliday junction resolvase subunit that binds multiple DNA repair/recombination endonucleases. Cell 138, 78-89.

Feldmann, E., Schmiemann, V., Goedecke, W., Reichenberger, S., and Pfeiffer, P. (2000). DNA double-strand break repair in cell-free extracts from Ku80-deficient cells: implications for Ku serving as an alignment factor in non-homologous DNA end joining. Nucleic Acids Res 28, 2585-2596.

Fishman-Lobell, J., and Haber, J.E. (1992). Removal of nonhomologous DNA ends in double-strand break recombination: the role of the yeast ultraviolet repair gene RAD1. Science (New York, N.Y 258, 480-484.

Fousteri, M., Vermeulen, W., van Zeeland, A.A., and Mullenders, L.H. (2006). Cockayne syndrome A and B proteins differentially regulate recruitment of chromatin remodeling and repair factors to stalled RNA polymerase II in vivo. Mol Cell 23, 471-482.

Friedberg, E.C. (1995). Out of the shadows and into the light: the emergence of DNA repair. Trends in biochemical sciences 20, 381.

Friedberg, E.C. (2006). Retraction notice to "The yeast RAD2, but not RAD1, gene is involved in the transcription-coupled repair of thymine glycols" [Mutat. Res. 337 (1995) 169-178]. DNA Repair (Amst) 5, 1507.

Fujiwara, Y., and Tatsumi, M. (1977). Cross-link repair in human cells and its possible defect in Fanconi's anemia cells. Journal of molecular biology 113, 635-649.

Gaillard, P.H., and Wood, R.D. (2001). Activity of individual ERCC1 and XPF subunits in DNA nucleotide excision repair. Nucleic Acids Res 29, 872-879.

Gao, Y., Chaudhuri, J., Zhu, C., Davidson, L., Weaver, D.T., and Alt, F.W. (1998). A targeted DNA-PKcs-null mutation reveals DNA-PK-independent functions for KU in V(D)J recombination. Immunity 9, 367-376.

Garcia-Closas, M., Malats, N., Real, F.X., Welch, R., Kogevinas, M., Chatterjee, N., Pfeiffer, R., Silverman, D., Dosemeci, M., Tardon, A., et al. (2006). Genetic variation in the nucleotide excision repair pathway and bladder cancer risk. Cancer Epidemiol Biomarkers Prev 15, 536-542.

Gentile, M., Latonen, L., and Laiho, M. (2003). Cell cycle arrest and apoptosis provoked by UV radiation-induced DNA damage are transcriptionally highly divergent responses. Nucleic Acids Res 31, 4779-4790.

Gerdes, J., Li, L., Schlueter, C., Duchrow, M., Wohlenberg, C., Gerlach, C., Stahmer, I., Kloth, S., Brandt, E., and Flad, H.D. (1991). Immunobiochemical and molecular biologic characterization of the cell proliferation-associated nuclear antigen that is defined by monoclonal antibody Ki-67. The American journal of pathology 138, 867-873.

Gillet, L.C., Alzeer, J., and Schärer, O.D. (2005). Site-specific incorporation of N-(deoxyguanosin-8-yl)-2-acetylaminofluorene (dG-AAF) into oligonucleotides using modified 'ultra-mild' DNA synthesis. Nucleic Acids Res 33, 1961-1969.

Gillet, L.C., and Scharer, O.D. (2006). Molecular mechanisms of mammalian global genome nucleotide excision repair. Chem Rev 106, 253-276.

Gillet, L.C., and Schärer, O.D. (2006). Molecular mechanisms of Mammalian global genome nucleotide excision repair. Chem Rev 106, 253-276.

Graham, J.M., Jr., Anyane-Yeboa, K., Raams, A., Appeldoorn, E., Kleijer, W.J., Garritsen, V.H., Busch, D., Edersheim, T.G., and Jaspers, N.G. (2001). Cerebro-oculo-facio-skeletal syndrome with a nucleotide excision-repair defect and a mutated XPD gene, with prenatal diagnosis in a triplet pregnancy. American journal of human genetics 69, 291-300.

Gregg, S.Q., Robinson, A.R., and Niedernhofer, L.J. (2011). Physiological consequences of defects in ERCC1-XPF DNA repair endonuclease. DNA Repair (Amst) 10, 781-791.

Guillet, M., and Boiteux, S. (2002). Endogenous DNA abasic sites cause cell death in the absence of Apn1, Apn2 and Rad1/Rad10 in Saccharomyces cerevisiae. The EMBO journal 21, 2833-2841.

Guillet, M., and Boiteux, S. (2003). Origin of endogenous DNA abasic sites in Saccharomyces cerevisiae. Mol Cell Biol 23, 8386-8394.

Guirouilh-Barbat, J., Huck, S., Bertrand, P., Pirzio, L., Desmaze, C., Sabatier, L., and Lopez, B.S. (2004). Impact of the KU80 pathway on NHEJ-induced genome rearrangements in mammalian cells. Mol Cell 14, 611-623.

Haber, J.E. (2006). Transpositions and translocations induced by site-specific double-strand breaks in budding yeast. DNA Repair (Amst) 5, 998-1009.

Hanada, K., Budzowska, M., Davies, S.L., van Drunen, E., Onizawa, H., Beverloo, H.B., Maas, A., Essers, J., Hickson, I.D., and Kanaar, R. (2007). The structure-specific endonuclease Mus81 contributes to replication restart by generating double-strand DNA breaks. Nat Struct Mol Biol 14, 1096-1104.

Hanada, K., Budzowska, M., Modesti, M., Maas, A., Wyman, C., Essers, J., and Kanaar, R. (2006). The structure-specific endonuclease Mus81-Eme1 promotes conversion of interstrand DNA crosslinks into double-strands breaks. The EMBO journal 25, 4921-4932.

Hanawalt, P.C., and Spivak, G. (2008). Transcription-coupled DNA repair: two decades of progress and surprises. Nature reviews. Molecular cell biology 9, 958-970.

Hansen, R.D., Sorensen, M., Tjonneland, A., Overvad, K., Wallin, H., Raaschou-Nielsen, O., and Vogel, U. (2008). A haplotype of polymorphisms in ASE-1, RAI and ERCC1 and the effects of tobacco smoking and alcohol consumption on r isk of colorectal cancer: a Danish prospective case-cohort study. BMC Cancer 8, 54.

Hazrati, A., Ramis-Castelltort, M., Sarkar, S., Barber, L.J., Schofield, C.J., Hartley, J.A., and McHugh, P.J. (2008). Human SNM1A suppresses the DNA repair defects of yeast pso2 mutants. DNA Repair (Amst) 7, 230-238.

Hefner, E., Preuss, S.B., and Britt, A.B. (2003). Arabidopsis mutants sensitive to gamma radiation include the homologue of the human repair gene ERCC1. J Exp Bot 54, 669-680.

Henning, K.A., Li, L., Iyer, N., McDaniel, L.D., Reagan, M.S., Legerski, R., Schultz, R.A., Stefanini, M., Lehmann, A.R., Mayne, L.V., et al. (1995). The Cockayne syndrome group A gene encodes a WD repeat protein that interacts with CSB protein and a subunit of RNA polymerase II TFIIH. Cell 82, 555-564.

Henriques, J.A., and Moustacchi, E. (1980). Isolation and characterization of pso mutants sensitive to photo-addition of psoralen derivatives in Saccharomyces cerevisiae. Genetics 95, 273-288.

Henriques, J.A., Vicente, E.J., Leandro da Silva, K.V., and Schenberg, A.C. (1989). PSO4: a novel gene involved in error-prone repair in Saccharomyces cerevisiae. Mutat Res 218, 111-124.

Hirata, H., Hinoda, Y., Matsuyama, H., Tanaka, Y., Okayama, N., Suehiro, Y., Zhao, H., Urakami, S., Kawamoto, K., Kawakami, T., et al. (2006). Polymorphisms of DNA repair genes are associated with renal cell carcinoma. Biochemical and biophysical research communications 342, 1058-1062.

Hoeijmakers, J.H. (2009). DNA damage, aging, and cancer. The New England journal of medicine 361, 1475-1485.

Hooker, S., Bonilla, C., Akereyeni, F., Ahaghotu, C., and Kittles, R.A. (2008). NAT2 and NER genetic variants and sporadic prostate cancer susceptibility in African Americans. Prostate Cancer Prostatic Dis 11, 349-356.

Houtsmuller, A.B., Rademakers, S., Nigg, A.L., Hoogstraten, D., Hoeijmakers, J.H., and Vermeulen, W. (1999). Action of DNA repair endonuclease ERCC1/XPF in living cells. Science (New York, N.Y 284, 958-961.

Hoy, C.A., Thompson, L.H., Mooney, C.L., and Salazar, E.P. (1985). Defective DNA cross-link removal in Chinese hamster cell mutants hypersensitive to bifunctional alkylating agents. Cancer research 45, 1737-1743.

Hsia, K.T., Millar, M.R., King, S., Selfridge, J., Redhead, N.J., Melton, D.W., and Saunders, P.T. (2003). DNA repair gene Ercc1 is essential for normal spermatogenesis and oogenesis and for functional integrity of germ cell DNA in the mouse. Development (Cambridge, England) 130, 369-378.

Hsiang, Y.H., Lihou, M.G., and Liu, L.F. (1989). Arrest of replication forks by drug-stabilized topoisomerase I-DNA cleavable complexes as a m echanism of cell killing by camptothecin. Cancer research 49, 5077-5082.

Hui-Yuen, J., McAllister, S., Koganti, S., Hill, E., and Bhaduri-McIntosh, S. (2011). Establishment of Epstein-Barr virus growth-transformed lymphoblastoid cell lines. Journal of visualized experiments : JoVE.

Hwang, I.G., Ahn, M.J., Park, B.B., Ahn, Y.C., Han, J., Lee, S., Kim, J., Shim, Y.M., Ahn, J.S., and Park, K. (2008). ERCC1 expression as a prognostic marker in N2(+) nonsmall-cell lung cancer patients treated with platinum-based neoadjuvant concurrent chemoradiotherapy. Cancer.

Ishiai, M., Kimura, M., Namikoshi, K., Yamazoe, M., Yamamoto, K., Arakawa, H., Agematsu, K., Matsushita, N., Takeda, S., Buerstedde, J.M., et al. (2004). DNA cross-link repair protein SNM1A interacts with PIAS1 in nuclear focus formation. Mol Cell Biol 24, 10733-10741.

Isla, D., Sarries, C., Rosell, R., Alonso, G., Domine, M., Taron, M., Lopez-Vivanco, G., Camps, C., Botia, M., Nunez, L., et al. (2004). Single nucleotide polymorphisms and outcome in docetaxel-cisplatin-treated advanced non-small-cell lung cancer. Ann Oncol 15, 1194-1203.

Ivanov, E.L., and Haber, J.E. (1995). RAD1 and RAD10, but not other excision repair genes, are required for double-strand break-induced recombination in Saccharomyces cerevisiae. Mol Cell Biol 15, 2245-2251.

Jachymczyk, W.J., von Borstel, R.C., Mowat, M.R., and Hastings, P.J. (1981). Repair of interstrand cross-links in DNA of Saccharomyces cerevisiae requires two systems for DNA repair: the RAD3 system and the RAD51 system. Mol Gen Genet 182, 196-205.

Jaspers, N.G., Raams, A., Silengo, M.C., Wijgers, N., Niedernhofer, L.J., Robinson, A.R., Giglia-Mari, G., Hoogstraten, D., Kleijer, W.J., Hoeijmakers, J.H., et al. (2007). First reported patient with human ERCC1 deficiency has cerebro-oculo-facio-skeletal syndrome with a mild defect in nucleotide excision repair and severe developmental failure. American journal of human genetics 80, 457-466.

Joshi, M.B., Shirota, Y., Danenberg, K.D., Conlon, D.H., Salonga, D.S., Herndon, J.E., 2nd, Danenberg, P.V., and Harpole, D.H., Jr. (2005). High gene expression of TS1, GSTP1, and ERCC1 are risk factors for survival in patients treated with trimodality therapy for esophageal cancer. Clin Cancer Res 11, 2215-2221.

Joyce, E.F., Tanneti, S.N., and McKim, K.S. (2009). Drosophila hold'em is required for a subset of meiotic crossovers and interacts with the dna repair endonuclease complex subunits MEI-9 and ERCC1. Genetics 181, 335-340.

Jun, H.J., Ahn, M.J., Kim, H.S., Yi, S.Y., Han, J., Lee, S.K., Ahn, Y.C., Jeong, H.S., Son, Y.I., Baek, J.H., et al. (2008). ERCC1 expression as a predictive marker of squamous cell carcinoma of the head and neck treated with cisplatin-based concurrent chemoradiation. British journal of cancer 99, 167-172.

Kabotyanski, E.B., Gomelsky, L., Han, J.O., Stamato, T.D., and Roth, D.B. (1998). Double-strand break repair in Ku86- and XRCC4-deficient cells. Nucleic Acids Res 26, 5333-5342.

Kalikaki, A., Kanaki, M., Vassalou, H., Souglakos, J., Voutsina, A., Georgoulias, V., and Mavroudis, D. (2009). DNA repair gene polymorphisms predict favorable clinical outcome in advanced non-small-cell lung cancer. Clin Lung Cancer 10, 118-123.

Keijzer, W., Jaspers, N.G., Abrahams, P.J., Taylor, A.M., Arlett, C.F., Zelle, B., Takebe, H., Kinmont, P.D., and Bootsma, D. (1979). A seventh complementation group in excision-deficient xeroderma pigmentosum. Mutat Res 62, 183-190.

Kelly, C.M., and Latimer, J.J. (2005). Unscheduled DNA synthesis: a functional assay for global genomic nucleotide excision repair. Methods Mol Biol 291, 303-320.

Khanna, K.K., and Jackson, S.P. (2001). DNA double-strand breaks: signaling, repair and the cancer connection. Nature genetics 27, 247-254.

Kim, J.M., Kee, Y., Gurtan, A., and D'Andrea, A.D. (2008a). Cell cycle dependent chromatin loading of the fanconi anemia core complex by FANCM/FAAP24. Blood.

Kim, M.K., Cho, K.J., Kwon, G.Y., Park, S.I., Kim, Y.H., Kim, J.H., Song, H.Y., Shin, J.H., Jung, H.Y., Lee, G.H., et al. (2008b). Patients with ERCC1-negative locally advanced esophageal cancers may benefit from preoperative chemoradiotherapy. Clin Cancer Res 14, 4225-4231.

Kim, Y., Lach, F.P., Desetty, R., Hanenberg, H., Auerbach, A.D., and Smogorzewska, A. (2011). Mutations of the SLX4 gene in Fanconi anemia. Nature genetics 43, 142-146.

Kiyohara, C., and Yoshimasu, K. (2007). Genetic polymorphisms in the nucleotide excision repair pathway and lung cancer risk: a meta-analysis. International journal of medical sciences 4, 59-71.

Koberle, B., Brenner, W., Albers, A., Usanova, S., Thuroff, J.W., and Kaina, B. (2010). ERCC1 and XPF expression in human testicular germ cell tumors. Oncology reports 23, 223-227.

Koberle, B., Masters, J.R., Hartley, J.A., and Wood, R.D. (1999). Defective repair of cisplatin-induced DNA damage caused by reduced XPA protein in testicular germ cell tumours. Curr Biol 9, 273-276.

Kohn, K.W., Steigbigel, N.H., and Spears, C.L. (1965). Cross-linking and repair of DNA in sensitive and resistant strains of E. coli treated with nitrogen mustard. Proc Natl Acad Sci U S A 53, 1154-1161.

Komori, K., Fujikane, R., Shinagawa, H., and Ishino, Y. (2002). Novel endonuclease in Archaea cleaving DNA with various branched structure. Genes Genet Syst 77, 227-241.

Kraemer, K.H., De Weerd-Kastelein, E.A., Robbins, J.H., Keijzer, W., Barrett, S.F., Petinga, R.A., and Bootsma, D. (1975). Five complementation groups in xeroderma pigmentosum. Mutat Res 33, 327-340.

Kraemer, K.H., Lee, M.M., and Scotto, J. (1987). Xeroderma pigmentosum. Cutaneous, ocular, and neurologic abnormalities in 830 published cases. Arch Dermatol 123, 241-250.

Krek, W., and DeCaprio, J.A. (1995). Cell synchronization. Methods in enzymology 254, 114-124.

Kuraoka, I., Kobertz, W.R., Ariza, R.R., Biggerstaff, M., Essigmann, J.M., and Wood, R.D. (2000). Repair of an interstrand DNA cross-link initiated by ERCC1-XPF repair/recombination nuclease. J Biol Chem 275, 26632-26636.

Lalande, M. (1990). A reversible arrest point in the late G1 phase of the mammalian cell cycle. Experimental cell research 186, 332-339.

Langer, R., Specht, K., Becker, K., Ewald, P., Bekesch, M., Sarbia, M., Busch, R., Feith, M., Stein, H.J., Siewert, J.R., et al. (2005). Association of pretherapeutic expression of chemotherapy-related genes with response to neoadjuvant chemotherapy in Barrett carcinoma. Clin Cancer Res 11, 7462-7469.

Lawley, P.D., and Brookes, P. (1965). Molecular mechanism of the cytotoxic action of difunctional alkylating agents and of resistance to this action. Nature 206, 480-483.

Lawley, P.D., and Brookes, P. (1968). Cytotoxicity of alkylating agents towards sensitive and resistant strains of Escherichia coli in relation to extent and mode of alkylation of cellular macromolecules and repair of alkylation lesions in deoxyribonucleic acids. The Biochemical journal 109, 433-447.

Lawley, P.D., and Phillips, D.H. (1996). DNA adducts from chemotherapeutic agents. Mutat Res 355, 13-40.

Lawrence, N.J., Sacco, J.J., Brownstein, D.G., Gillingwater, T.H., and Melton, D.W. (2008). A neurological phenotype in mice with DNA repair gene Ercc1 deficiency. DNA Repair (Amst) 7, 281-291.

Leadon, S.A., and Lawrence, D.A. (1991). Preferential repair of DNA damage on the transcribed strand of the human metallothionein genes requires RNA polymerase II. Mutat Res 255, 67-78.

Lebwohl, D., and Canetta, R. (1998). Clinical development of platinum complexes in cancer therapy: an historical perspective and an update. European journal of cancer (Oxford, England : 1990) 34, 1522-1534.

Lee, K., and Lee, S.E. (2007). Saccharomyces cerevisiae Sae2- and Tel1-dependent single-strand DNA formation at DNA break promotes microhomology-mediated end joining. Genetics 176, 2003-2014.

Lee, K.H., Min, H.S., Han, S.W., Oh, D.Y., Lee, S.H., Kim, D.W., Im, S.A., Chung, D.H., Kim, Y.T., Kim, T.Y., et al. (2008). ERCC1 expression by immunohistochemistry and EGFR mutations in resected non-small cell lung cancer. Lung Cancer 60, 401-407.

Lehmann, A.R. (2003). DNA repair-deficient diseases, xeroderma pigmentosum, Cockayne syndrome and trichothiodystrophy. Biochimie 85, 1101-1111.

Lehmann, A.R., Kirk-Bell, S., Arlett, C.F., Paterson, M.C., Lohman, P.H., de Weerd-Kastelein, E.A., and Bootsma, D. (1975). Xeroderma pigmentosum cells with normal levels of excision repair have a defect in DNA synthesis after UV-irradiation. Proc Natl Acad Sci U S A 72, 219-223.

Li, L., Elledge, S.J., Peterson, C.A., Bales, E.S., and Legerski, R.J. (1994). Specific association between the human DNA repair proteins XPA and ERCC1. Proc Natl Acad Sci U S A 91, 5012-5016.

Li, L., Peterson, C.A., Lu, X., and Legerski, R.J. (1995). Mutations in XPA that prevent association with ERCC1 are defective in nucleotide excision repair. Mol Cell Biol 15, 1993-1998.

Li, L., Peterson, C.A., Zhang, X., and Legerski, R.J. (2000). Requirement for PCNA and RPA in interstrand crosslink-induced DNA synthesis. Nucleic Acids Res 28, 1424-1427.

Li, W., and Melton, D.W. (2012). Cisplatin regulates the MAPK kinase pathway to induce increased expression of DNA repair gene ERCC1 and increase melanoma chemoresistance. Oncogene 31, 2412-2422.

Limsirichaikul, S., Niimi, A., Fawcett, H., Lehmann, A., Yamashita, S., and Ogi, T. (2009). A rapid non-radioactive technique for measurement of repair synthesis in primary human fibroblasts by incorporation of ethynyl deoxyuridine (EdU). Nucleic Acids Res 37, e31.

Lindahl, T. (1976). New class of enzymes acting on damaged DNA. Nature 259, 64-66.

Lindahl, T. (1979). DNA glycosylases, endonucleases for apurinic/apyrimidinic sites, and base excision-repair. Prog Nucleic Acid Res Mol Biol 22, 135-192.

Lindahl, T., and Barnes, D.E. (2000). Repair of endogenous DNA damage. Cold Spring Harbor symposia on quantitative biology 65, 127-133.

Lindahl, T., and Karlstrom, O. (1973). Heat-induced depyrimidination of deoxyribonucleic acid in neutral solution. Biochemistry 12, 5151-5154.

Lippke, J.A., Gordon, L.K., Brash, D.E., and Haseltine, W.A. (1981). Distribution of UV light-induced damage in a defined sequence of human DNA: detection of alkaline-sensitive lesions at pyrimidine nucleoside-cytidine sequences. Proc Natl Acad Sci U S A 78, 3388-3392.

Liu, C., Pouliot, J.J., and Nash, H.A. (2002). Repair of topoisomerase I covalent complexes in the absence of the tyrosyl-DNA phosphodiesterase Tdp1. Proc Natl Acad Sci U S A 99, 14970-14975.

Liu, N., Lamerdin, J.E., Tebbs, R.S., Schild, D., Tucker, J.D., Shen, M.R., Brookman, K.W., Siciliano, M.J., Walter, C.A., Fan, W., et al. (1998). XRCC2 and XRCC3, new human Rad51-family members, promote chromosome stability and protect against DNA cross-links and other damages. Mol Cell 1, 783-793.

Lokich, J., and Anderson, N. (1998). Carboplatin versus cisplatin in solid tumors: an analysis of the literature. Ann Oncol 9, 13-21.

Lord, R.V., Brabender, J., Gandara, D., Alberola, V., Camps, C., Domine, M., Cardenal, F., Sanchez, J.M., Gumerlock, P.H., Taron, M., et al. (2002). Low ERCC1 expression correlates with prolonged survival after cisplatin plus gemcitabine chemotherapy in non-small cell lung cancer. Clin Cancer Res 8, 2286-2291.

Ma, J.L., Kim, E.M., Haber, J.E., and Lee, S.E. (2003). Yeast Mre11 and Rad1 proteins define a Ku-independent mechanism to repair double-strand breaks lacking overlapping end sequences. Mol Cell Biol 23, 8820-8828.

Matsumura, Y., Nishigori, C., Yagi, T., Imamura, S., and Takebe, H. (1998). Characterization of molecular defects in xeroderma pigmentosum group F in relation to its clinically mild symptoms. Hum Mol Genet 7, 969-974.

Matsuoka, S., Ballif, B.A., Smogorzewska, A., McDonald, E.R., 3rd, Hurov, K.E., Luo, J., Bakalarski, C.E., Zhao, Z., Solimini, N., Lerenthal, Y., et al. (2007). ATM and ATR

substrate analysis reveals extensive protein networks responsive to DNA damage. Science (New York, N.Y 316, 1160-1166.

McCabe, K.M., Hemphill, A., Akkari, Y., Jakobs, P.M., Pauw, D., Olson, S.B., Moses, R.E., and Grompe, M. (2008). ERCC1 is required for FANCD2 focus formation. Mol Genet Metab 95, 66-73.

McHugh, P.J., Gill, R.D., Waters, R., and Hartley, J.A. (1999). Excision repair of nitrogen mustard-DNA adducts in Saccharomyces cerevisiae. Nucleic Acids Res 27, 3259-3266.

McHugh, P.J., Spanswick, V.J., and Hartley, J.A. (2001). Repair of DNA interstrand crosslinks: molecular mechanisms and clinical relevance. The lancet oncology 2, 483-490.

McPherson, J.P., Lemmers, B., Chahwan, R., Pamidi, A., Migon, E., Matysiak-Zablocki, E., Moynahan, M.E., Essers, J., Hanada, K., Poonepalli, A., et al. (2004). Involvement of mammalian Mus81 in genome integrity and tumor suppression. Science (New York, N.Y 304, 1822-1826.

McWhir, J., Selfridge, J., Harrison, D.J., Squires, S., and Melton, D.W. (1993a). Mice with DNA repair gene (ERCC-1) deficiency have elevated levels of p53, liver nuclear abnormalities and die before weaning. Nature genetics 5, 217-224.

McWhir, J., Selfridge, J., Harrison, D.J., Squires, S., and Melton, D.W. (1993b). Mice with DNA repair gene (ERCC-1) deficiency have elevated levels of p53, liver nuclear abnormalities and die before weaning [see comments]. Nature genetics 5, 217-224.

McWilliams, R.R., Bamlet, W.R., Cunningham, J.M., Goode, E.L., de Andrade, M., Boardman, L.A., and Petersen, G.M. (2008). Polymorphisms in DNA repair genes, smoking, and pancreatic adenocarcinoma risk. Cancer research 68, 4928-4935.

Meetei, A.R., de Winter, J.P., Medhurst, A.L., Wallisch, M., Waisfisz, Q., van de Vrugt, H.J., Oostra, A.B., Yan, Z., Ling, C., Bishop, C.E., et al. (2003). A novel ubiquitin ligase is deficient in Fanconi anemia. Nature genetics 35, 165-170.

Meetei, A.R., Medhurst, A.L., Ling, C., Xue, Y., Singh, T.R., Bier, P., Steltenpool, J., Stone, S., Dokal, I., Mathew, C.G., et al. (2005). A human ortholog of archaeal DNA repair protein Hef is defective in Fanconi anemia complementation group M. Nature genetics 37, 958-963.

Meira, L.B., Graham, J.M., Jr., Greenberg, C.R., Busch, D.B., Doughty, A.T., Ziffer, D.W., Coleman, D.M., Savre-Train, I., and Friedberg, E.C. (2000). Manitoba aboriginal kindred with original cerebro-oculo- facio-skeletal syndrome has a mutation in the Cockayne syndrome group B (CSB) gene. American journal of human genetics 66, 1221-1228.

Metzger, R., Leichman, C.G., Danenberg, K.D., Danenberg, P.V., Lenz, H.J., Hayashi, K., Groshen, S., Salonga, D., Cohen, H., Laine, L., et al. (1998). ERCC1 mRNA levels complement thymidylate synthase mRNA levels in predicting response and survival for

gastric cancer patients receiving combination cisplatin and fluorouracil chemotherapy. J Clin Oncol 16, 309-316.

Min, J.H., and Pavletich, N.P. (2007). Recognition of DNA damage by the Rad4 nucleotide excision repair protein. Nature 449, 570-575.

Mitchell, D.L. (1988). The induction and repair of lesions produced by the photolysis of (6-4) photoproducts in normal and UV-hypersensitive human cells. Mutat Res 194, 227-237.

Mitchell, D.L., and Nairn, R.S. (1989). The biology of the (6-4) photoproduct. Photochemistry and photobiology 49, 805-819.

Mladenov, E., and Anachkova, B. (2003). DNA breaks induction by mimosine. Zeitschrift fur Naturforschung. C, Journal of biosciences 58, 732-735.

Monzo, M., Moreno, I., Navarro, A., Ibeas, R., Artells, R., Gel, B., Martinez, F., Moreno, J., Hernandez, R., and Navarro-Vigo, M. (2007). Single nucleotide polymorphisms in nucleotide excision repair genes XPA, XPD, XPG and ERCC1 in advanced colorectal cancer patients treated with first-line oxaliplatin/fluoropyrimidine. Oncology 72, 364-370.

Mortensen, U.H., Bendixen, C., Sunjevaric, I., and Rothstein, R. (1996). DNA strand annealing is promoted by the yeast Rad52 protein. Proc Natl Acad Sci U S A 93, 10729-10734.

Moser, J., Kool, H., Giakzidis, I., Caldecott, K., Mullenders, L.H., and Fousteri, M.I. (2007). Sealing of chromosomal DNA nicks during nucleotide excision repair requires XRCC1 and DNA ligase III alpha in a cell-cycle-specific manner. Mol Cell 27, 311-323.

Motycka, T.A., Bessho, T., Post, S.M., Sung, P., and Tomkinson, A.E. (2004). Physical and functional interaction between the XPF/ERCC1 endonuclease and hRad52. J Biol Chem 279, 13634-13639.

Mu, D., Wakasugi, M., Hsu, D.S., and Sancar, A. (1997). Characterization of reaction intermediates of human excision repair nuclease. J Biol Chem 272, 28971-28979.

Mullen, J.R., Kaliraman, V., Ibrahim, S.S., and Brill, S.J. (2001). Requirement for three novel protein complexes in the absence of the Sgs1 DNA helicase in Saccharomyces cerevisiae. Genetics 157, 103-118.

Munoz, I.M., Hain, K., Declais, A.C., Gardiner, M., Toh, G.W., Sanchez-Pulido, L., Heuckmann, J.M., Toth, R., Macartney, T., Eppink, B., et al. (2009a). Coordination of structure-specific nucleases by human SLX4/BTBD12 is required for DNA repair. Mol Cell 35, 116-127.

Munoz, P., Blanco, R., de Carcer, G., Schoeftner, S., Benetti, R., Flores, J.M., Malumbres, M., and Blasco, M.A. (2009b). TRF1 controls telomere length and mitotic fidelity in epithelial homeostasis. Mol Cell Biol 29, 1608-1625.

Munoz, P., Blanco, R., Flores, J.M., and Blasco, M.A. (2005). XPF nuclease-dependent telomere loss and increased DNA damage in mice overexpressing TRF2 result in premature aging and cancer. Nature genetics 37, 1063-1071.

Murray, D., Macann, A., Hanson, J., and Rosenberg, E. (1996). ERCC1/ERCC4 5'-endonuclease activity as a determinant of hypoxic cell radiosensitivity. International journal of radiation biology 69, 319-327.

Murray, D., and Rosenberg, E. (1996). The importance of the ERCC1/ERCC4[XPF] complex for hypoxic-cell radioresistance does not appear to derive from its participation in the nucleotide excision repair pathway. Mutat Res 364, 217-226.

Nakatsu, Y., Asahina, H., Citterio, E., Rademakers, S., Vermeulen, W., Kamiuchi, S., Yeo, J.P., Khaw, M.C., Saijo, M., Kodo, N., et al. (2000). XAB2, a novel tetratricopeptide repeat protein involved in transcription-coupled DNA repair and transcription. J Biol Chem 275, 34931-34937.

Nakazawa, Y., Yamashita, S., Lehmann, A.R., and Ogi, T. (2010). A semi-automated non-radioactive system for measuring recovery of RNA synthesis and unscheduled DNA synthesis using ethynyluracil derivatives. DNA Repair (Amst) 9, 506-516.

Newman, M., Murray-Rust, J., Lally, J., Rudolf, J., Fadden, A., Knowles, P.P., White, M.F., and McDonald, N.Q. (2005). Structure of an XPF endonuclease with and without DNA suggests a model for substrate recognition. The EMBO journal 24, 895-905.

Niedernhofer, L.J., Bhagwat, N., and Wood, R.D. (2007). ERCC1 and non-small-cell lung cancer. The New England journal of medicine 356, 2538-2540; author reply 2540-2531.

Niedernhofer, L.J., Essers, J., Weeda, G., Beverloo, B., de Wit, J., Muijtjens, M., Odijk, H., Hoeijmakers, J.H., and Kanaar, R. (2001). The structure-specific endonuclease Ercc1-Xpf is required for targeted gene replacement in embryonic stem cells. The EMBO journal 20, 6540-6549.

Niedernhofer, L.J., Garinis, G.A., Raams, A., Lalai, A.S., Robinson, A.R., Appeldoorn, E., Odijk, H., Oostendorp, R., Ahmad, A., van Leeuwen, W., et al. (2006). A new progeroid syndrome reveals that genotoxic stress suppresses the somatotroph axis. Nature 444, 1038-1043.

Niedernhofer, L.J., Odijk, H., Budzowska, M., van Drunen, E., Maas, A., Theil, A.F., de Wit, J., Jaspers, N.G., Beverloo, H.B., Hoeijmakers, J.H., et al. (2004). The structure-specific endonuclease Ercc1-Xpf is required to resolve DNA interstrand cross-link-induced double-strand breaks. Mol Cell Biol 24, 5776-5787.

Nishino, T., Komori, K., Ishino, Y., and Morikawa, K. (2003). X-ray and biochemical anatomy of an archaeal XPF/Rad1/Mus81 family nuclease: similarity between its endonuclease domain and restriction enzymes. Structure 11, 445-457.

Nishino, T., Komori, K., Ishino, Y., and Morikawa, K. (2005a). Structural and functional analyses of an archaeal XPF/Rad1/Mus81 nuclease: Asymmetric DNA binding and cleavage mechanisms. Structure 13, 1183-1192.

Nishino, T., Komori, K., Tsuchiya, D., Ishino, Y., and Morikawa, K. (2005b). Crystal structure and functional implications of Pyrococcus furiosus hef helicase domain involved in branched DNA processing. Structure 13, 143-153.

Nunez, F., Chipchase, M.D., Clarke, A.R., and Melton, D.W. (2000). Nucleotide excision repair gene (ERCC1) deficiency causes G(2) arrest in hepatocytes and a reduction in liver binucleation: the role of p53 and p21. Faseb J 14, 1073-1082.

O'Donnell, L., and Durocher, D. (2010). DNA repair has a new FAN1 club. Mol Cell 39, 167-169.

Ogi, T., Limsirichaikul, S., Overmeer, R.M., Volker, M., Takenaka, K., Cloney, R., Nakazawa, Y., Niimi, A., Miki, Y., Jaspers, N.G., et al. (2010). Three DNA polymerases, recruited by different mechanisms, carry out NER repair synthesis in human cells. Mol Cell 37, 714-727.

Olaussen, K.A., Dunant, A., Fouret, P., Brambilla, E., Andre, F., Haddad, V., Taranchon, E., Filipits, M., Pirker, R., Popper, H.H., et al. (2006a). DNA repair by ERCC1 in non-small-cell lung cancer and cisplatin-based adjuvant chemotherapy. The New England journal of medicine 355, 983-991.

Olaussen, K.A., Dunant, A., Fouret, P., Brambilla, E., Andre, F., Haddad, V., Taranchon, E., Filipits, M., Pirker, R., Popper, H.H., et al. (2006b). DNA repair by ERCC1 in non-small-cell lung cancer and cisplatin-based adjuvant chemotherapy. The New England journal of medicine 355, 983-991.

Olaussen, K.A., Fouret, P., and Kroemer, G. (2007). ERCC1-specific immunostaining in non-small-cell lung cancer. The New England journal of medicine 357, 1559-1561.

Orans, J., McSweeney, E.A., Iyer, R.R., Hast, M.A., Hellinga, H.W., Modrich, P., and Beese, L.S. (2011). Structures of human exonuclease 1 DNA complexes suggest a unified mechanism for nuclease family. Cell 145, 212-223.

Orelli, B., McClendon, T.B., Tsodikov, O.V., Ellenberger, T., Niedernhofer, L.J., and Scharer, O.D. (2010a). The XPA-binding domain of ERCC1 is required for nucleotide excision repair but not other DNA repair pathways. J Biol Chem 285, 3705-3712.

Orelli, B., McClendon, T.B., Tsodikov, O.V., Ellenberger, T., Niedernhofer, L.J., and Schärer, O.D. (2010b). The XPA-binding domain of ERCC1 is required for nucleotide excision repair but not other DNA repair pathways. J Biol Chem 285, 3705-3712.

Pan, J., Lin, J., Izzo, J., Liu, Y., Xing, J., Huang, M., Ajani, J., and Wu, X. (2009). Genetic Susceptibility to Esophageal Cancer: The Role of the Nucleotide Excision Repair Pathway. Carcinogenesis.

Paques, F., and Haber, J.E. (1997). Two pathways for removal of nonhomologous DNA ends during double-strand break repair in Saccharomyces cerevisiae. Mol Cell Biol 17, 6765-6771.

Paques, F., and Haber, J.E. (1999). Multiple pathways of recombination induced by double-strand breaks in Saccharomyces cerevisiae. Microbiol Mol Biol Rev 63, 349-404.

Park, C.H., and Sancar, A. (1994). Formation of a ternary complex by human XPA, ERCC1, and ERCC4(XPF) excision repair proteins. Proc Natl Acad Sci U S A 91, 5017-5021.

Park, S.Y., Hong, Y.C., Kim, J.H., Kwak, S.M., Cho, J.H., Lee, H.L., and Ryu, J.S. (2006). Effect of ERCC1 polymorphisms and the modification by smoking on the survival of non-small cell lung cancer patients. Medical oncology (Northwood, London, England) 23, 489-498.

Parmar, K., D'Andrea, A., and Niedernhofer, L.J. (2009). Mouse models of Fanconi anemia. Mutat Res 668, 133-140.

Pena, S.D., and Shokeir, M.H. (1974). Autosomal recessive cerebro-oculo-facio-skeletal (COFS) syndrome. Clin Genet 5, 285-293.

Petit, C., and Sancar, A. (1999). Nucleotide excision repair: from E. coli to man. Biochimie 81, 15-25.

Pichierri, P., and Rosselli, F. (2004). The DNA crosslink-induced S-phase checkpoint depends on ATR-CHK1 and ATR-NBS1-FANCD2 pathways. The EMBO journal 23, 1178-1187.

Pouliot, J.J., Yao, K.C., Robertson, C.A., and Nash, H.A. (1999). Yeast gene for a Tyr-DNA phosphodiesterase that repairs topoisomerase I complexes. Science (New York, N.Y 286, 552-555.

Prasher, J.M., Lalai, A.S., Heijmans-Antonissen, C., Ploemacher, R.E., Hoeijmakers, J.H., Touw, I.P., and Niedernhofer, L.J. (2005). Reduced hematopoietic reserves in DNA interstrand crosslink repair-deficient Ercc1-/- mice. The EMBO journal 24, 861-871.

Qiao, F., Mi, J., Wilson, J.B., Zhi, G., Bucheimer, N.R., Jones, N.J., and Kupfer, G.M. (2004). Phosphorylation of fanconi anemia (FA) complementation group G protein, FANCG, at serine 7 is important for function of the FA pathway. J Biol Chem 279, 46035-46045.

Quintela-Fandino, M., Hitt, R., Medina, P.P., Gamarra, S., Manso, L., Cortes-Funes, H., and Sanchez-Cespedes, M. (2006). DNA-repair gene polymorphisms predict favorable clinical outcome among patients with advanced squamous cell carcinoma of the head and neck treated with cisplatin-based induction chemotherapy. J Clin Oncol 24, 4333-4339.

Rabik, C.A., and Dolan, M.E. (2007). Molecular mechanisms of resistance and toxicity associated with platinating agents. Cancer treatment reviews 33, 9-23.

Raschle, M., Knipscheer, P., Enoiu, M., Angelov, T., Sun, J., Griffith, J.D., Ellenberger, T.E., Scharer, O.D., and Walter, J.C. (2008). Mechanism of replication-coupled DNA interstrand crosslink repair. Cell 134, 969-980.

Reed, E. (2006). ERCC1 measurements in clinical oncology. The New England journal of medicine 355, 1054-1055.

Reed, E., Dabholkar, M., Thornton, K., Thompson, C., Yu, J.J., and Bostick-Bruton, F. (2000). Evidence for in the appearance of mRNAs of nucleotide excision repair genes, in human ovarian cancer tissues. Oncology reports 7, 1123-1128.

Reynolds, R.J., Love, J.D., and Friedberg, E.C. (1981). Molecular mechanisms of pyrimidine dimer excision in Saccharomyces cerevisiae: excision of dimers in cell extracts. J Bacteriol 147, 705-708.

Rice, J.A., Crothers, D.M., Pinto, A.L., and Lippard, S.J. (1988). The major adduct of the antitumor drug cis-diamminedichloroplatinum(II) with DNA bends the duplex by approximately equal to 40 degrees toward the major groove. Proc Natl Acad Sci U S A 85, 4158-4161.

Riedl, T., Hanaoka, F., and Egly, J.M. (2003). The comings and goings of nucleotide excision repair factors on damaged DNA. The EMBO journal 22, 5293-5303.

Rosell, R., Lord, R.V., Taron, M., and Reguart, N. (2002). DNA repair and cisplatin resistance in non-small-cell lung cancer. Lung Cancer 38, 217-227.

Roth, D.B., and Wilson, J.H. (1986). Nonhomologous recombination in mammalian cells: role for short sequence homologies in the joining reaction. Mol Cell Biol 6, 4295-4304.

Rouillon, C., and White, M.F. (2011). The evolution and mechanisms of nucleotide excision repair proteins. Res Microbiol 162, 19-26.

Ruhland, A., Kircher, M., Wilborn, F., and Brendel, M. (1981). A yeast mutant specifically sensitive to bifunctional alkylation. Mutat Res 91, 457-462.

Saijo, M., Kuraoka, I., Masutani, C., Hanaoka, F., and Tanaka, K. (1996). Sequential binding of DNA repair proteins RPA and ERCC1 to XPA in vitro. Nucleic Acids Res 24, 4719-4724.

Sakano, K., Oikawa, S., Hasegawa, K., and Kawanishi, S. (2001). Hydroxyurea induces site-specific DNA damage via formation of hydrogen peroxide and nitric oxide. Japanese journal of cancer research : Gann 92, 1166-1174.

Salmon, P., Kindler, V., Ducrey, O., Chapuis, B., Zubler, R.H., and Trono, D. (2000). High-level transgene expression in human hematopoietic progenitors and differentiated blood lineages after transduction with improved lentiviral vectors. Blood 96, 3392-3398.

Salmon, P., and Trono, D. (2006). Production and titration of lentiviral vectors. Current protocols in neuroscience / editorial board, Jacqueline N. Crawley ... [et al.] Chapter 4, Unit 4 21.

Sargent, R.G., Meservy, J.L., Perkins, B.D., Kilburn, A.E., Intody, Z., Adair, G.M., Nairn, R.S., and Wilson, J.H. (2000). Role of the nucleotide excision repair gene ERCC1 in formation of recombination-dependent rearrangements in mammalian cells. Nucleic Acids Res 28, 3771-3778.

Sargent, R.G., Rolig, R.L., Kilburn, A.E., Adair, G.M., Wilson, J.H., and Nairn, R.S. (1997). Recombination-dependent deletion formation in mammalian cells deficient in the nucleotide excision repair gene ERCC1. Proc Natl Acad Sci U S A 94, 13122-13127.

Sarkar, S., Davies, A.A., Ulrich, H.D., and McHugh, P.J. (2006). DNA interstrand crosslink repair during G1 involves nucleotide excision repair and DNA polymerase zeta. The EMBO journal 25, 1285-1294.

Sasaki, M.S., and Tonomura, A. (1973). A high susceptibility of Fanconi's anemia to chromosome breakage by DNA cross-linking agents. Cancer research 33, 1829-1836.

Schaeffer, L., Moncollin, V., Roy, R., Staub, A., Mezzina, M., Sarasin, A., Weeda, G., Hoeijmakers, J.H., and Egly, J.M. (1994). The ERCC2/DNA repair protein is associated with the class II BTF2/TFIIH transcription factor. The EMBO journal 13, 2388-2392.

Schaeffer, L., Roy, R., Humbert, S., Moncollin, V., Vermeulen, W., Hoeijmakers, J.H., Chambon, P., and Egly, J.M. (1993). DNA repair helicase: a component of BTF2 (TFIIH) basic transcription factor. Science (New York, N.Y 260, 58-63.

Schmidt, H., Kapitza-Fecke, P., Stephen, E.R., and Gutz, H. (1989). Some of the swi genes of Schizosaccharomyces pombe also have a function in the repair of radiation damage. Curr Genet 16, 89-94.

Schrader, C.E., Vardo, J., Linehan, E., Twarog, M.Z., Niedernhofer, L.J., Hoeijmakers, J.H., and Stavnezer, J. (2004). Deletion of the nucleotide excision repair gene Ercc1 reduces immunoglobulin class switching and alters mutations near switch recombination junctions. The Journal of experimental medicine 200, 321-330.

Schumacher, B., Garinis, G.A., and Hoeijmakers, J.H. (2008). Age to survive: DNA damage and aging. Trends in genetics : TIG 24, 77-85.

Scrima, A., Konickova, R., Czyzewski, B.K., Kawasaki, Y., Jeffrey, P.D., Groisman, R., Nakatani, Y., Iwai, S., Pavletich, N.P., and Thoma, N.H. (2008). Structural basis of UV DNA-damage recognition by the DDB1-DDB2 complex. Cell 135, 1213-1223.

Selden, J.R., and Dolbeare, F. (1994). A flow cytometric technique for detection of DNA repair in mammalian cells. Methods in cell biology 42 Pt B, 1-19.

Selden, J.R., Dolbeare, F., Clair, J.H., Nichols, W.W., Miller, J.E., Kleemeyer, K.M., Hyland, R.J., and DeLuca, J.G. (1993). Statistical confirmation that immunofluorescent detection

of DNA repair in human fibroblasts by measurement of bromodeoxyuridine incorporation is stoichiometric and sensitive. Cytometry 14, 154-167.

Selfridge, J., Hsia, K.T., Redhead, N.J., and Melton, D.W. (2001). Correction of liver dysfunction in DNA repair-deficient mice with an ERCC1 transgene. Nucleic Acids Res 29, 4541-4550.

Selfridge, J., Pow, A.M., McWhir, J., Magin, T.M., and Melton, D.W. (1992). Gene targeting using a mouse HPRT minigene/HPRT-deficient embryonic stem cell system: inactivation of the mouse ERCC-1 gene. Somatic cell and molecular genetics 18, 325-336.

Sengerova, B., Wang, A.T., and McHugh, P.J. (2011). Orchestrating the nucleases involved in DNA interstrand cross-link (ICL) repair. Cell cycle 10, 3999-4008.

Sgouros, J., Gaillard, P.H., and Wood, R.D. (1999). A relationship betweena DNA-repair/recombination nuclease family and archaeal helicases. Trends in biochemical sciences 24, 95-97.

Shannon, M., Lamerdin, J.E., Richardson, L., McCutchen-Maloney, S.L., Hwang, M.H., Handel, M.A., Stubbs, L., and Thelen, M.P. (1999). Characterization of the mouse Xpf DNA repair gene and differential expression during spermatogenesis. Genomics 62, 427-435.

Shen, M.R., Jones, I.M., and Mohrenweiser, H. (1998). Nonconservative amino acid substitution variants exist at polymorphic frequency in DNA repair genes in healthy humans. Cancer research 58, 604-608.

Shirota, Y., Stoehlmacher, J., Brabender, J., Xiong, Y.P., Uetake, H., Danenberg, K.D., Groshen, S., Tsao-Wei, D.D., Danenberg, P.V., and Lenz, H.J. (2001). ERCC1 and thymidylate synthase mRNA levels predict survival for colorectal cancer patients receiving combination oxaliplatin and fluorouracil chemotherapy. J Clin Oncol 19, 4298-4304.

Shivji, M.K., Moggs, J.G., Kuraoka, I., and Wood, R.D. (1999). Dual-incision assays for nucleotide excision repair using DNA with a lesion at a specific site. Methods Mol Biol 113, 373-392.

Shivji, M.K., Podust, V.N., Hubscher, U., and Wood, R.D. (1995). Nucleotide excision repair DNA synthesis by DNA polymerase epsilon in the presence of PCNA, RFC, and RPA. Biochemistry 34, 5011-5017.

Siegel, R., Naishadham, D., and Jemal, A. (2012). Cancer statistics, 2012. CA: a cancer journal for clinicians 62, 10-29.

Sijbers, A.M., de Laat, W.L., Ariza, R.R., Biggerstaff, M., Wei, Y.F., Moggs, J.G., Carter, K.C., Shell, B.K., Evans, E., de Jong, M.C., et al. (1996a). Xeroderma pigmentosum group F caused by a defect in a structure-specific DNA repair endonuclease. Cell 86, 811-822.

Sijbers, A.M., van der Spek, P.J., Odijk, H., van den Berg, J., van Duin, M., Westerveld, A., Jaspers, N.G., Bootsma, D., and Hoeijmakers, J.H. (1996b). Mutational analysis of the human nucleotide excision repair gene ERCC1. Nucleic Acids Res 24, 3370-3380.

Sijbers, A.M., van Voorst Vader, P.C., Snoek, J.W., Raams, A., Jaspers, N.G., and Kleijer, W.J. (1998). Homozygous R788W point mutation in the XPF gene of a patient with xeroderma pigmentosum and late-onset neurologic disease. The Journal of investigative dermatology 110, 832-836.

Smogorzewska, A., Desetty, R., Saito, T.T., Schlabach, M., Lach, F.P., Sowa, M.E., Clark, A.B., Kunkel, T.A., Harper, J.W., Colaiacovo, M.P., et al. (2010). A genetic screen identifies FAN1, a Fanconi anemia-associated nuclease necessary for DNA interstrand crosslink repair. Mol Cell 39, 36-47.

Smogorzewska, A., Matsuoka, S., Vinciguerra, P., McDonald, E.R., 3rd, Hurov, K.E., Luo, J., Ballif, B.A., Gygi, S.P., Hofmann, K., D'Andrea, A.D., et al. (2007). Identification of the FANCI Protein, a Monoubiquitinated FANCD2 Paralog Required for DNA Repair. Cell.

Srivastava, V., Miller, S., and Busbee, D. (1993). Immunofluorescent evaluation of DNA repair synthesis using interactive laser cytometry. Cytometry 14, 144-153.

Staresincic, L., Fagbemi, A.F., Enzlin, J.H., Gourdin, A.M., Wijgers, N., Dunand-Sauthier, I., Giglia-Mari, G., Clarkson, S.G., Vermeulen, W., and Scharer, O.D. (2009a). Coordination of dual incision and repair synthesis in human nucleotide excision repair. The EMBO journal.

Staresincic, L., Fagbemi, A.F., Enzlin, J.H., Gourdin, A.M., Wijgers, N., Dunand-Sauthier, I., Giglia-Mari, G., Clarkson, S.G., Vermeulen, W., and Schärer, O.D. (2009b). Coordination of dual incision and repair synthesis in human nucleotide excision repair. The EMBO journal 28, 1111-1120.

Stauffer, M.E., and Chazin, W.J. (2004). Structural mechanisms of DNA replication, repair, and recombination. J Biol Chem 279, 30915-30918.

Steffensen, K.D., Waldstrom, M., Jeppesen, U., Brandslund, I., and Jakobsen, A. (2008). Prediction of response to chemotherapy by ERCC1 immunohistochemistry and ERCC1 polymorphism in ovarian cancer. Int J Gynecol Cancer 18, 702-710.

Stewart, D.J. (2007). Mechanisms of resistance to cisplatin and carboplatin. Critical reviews in oncology/hematology 63, 12-31.

Stiff, T., Walker, S.A., Cerosaletti, K., Goodarzi, A.A., Petermann, E., Concannon, P., O'Driscoll, M., and Jeggo, P.A. (2006). ATR-dependent phosphorylation and activation of ATM in response to UV treatment or replication fork stalling. The EMBO journal 25, 5775-5782.

Stoepker, C., Hain, K., Schuster, B., Hilhorst-Hofstee, Y., Rooimans, M.A., Steltenpool, J., Oostra, A.B., Eirich, K., Korthof, E.T., Nieuwint, A.W., et al. (2011a). SLX4, a

coordinator of structure-specific endonucleases, is mutated in a n ew Fanconi anemia subtype. Nature genetics 43, 138-141.

Stoepker, C., Hain, K., Schuster, B., Hilhorst-Hofstee, Y., Rooimans, M.A., Steltenpool, J., Oostra, A.B., Eirich, K., Korthof, E.T., Nieuwint, A.W.M., et al. (2011b). SLX4, a coordinator of structure-specific endonucleases, is mutated in a n ew Fanconi anemia subtype. Nature genetics 43, 138-141.

Su, D., Ma, S., Liu, P., Jiang, Z., Lv, W., Zhang, Y., Deng, Q., Smith, S., and Yu, H. (2007). Genetic polymorphisms and treatment response in advanced non-small cell lung cancer. Lung Cancer 56, 281-288.

Sugasawa, K., Akagi, J., Nishi, R., Iwai, S., and Hanaoka, F. (2009). Two-step recognition of DNA damage for mammalian nucleotide excision repair: Directional binding of the XPC complex and DNA strand scanning. Mol Cell 36, 642-653.

Sugasawa, K., Ng, J.M., Masutani, C., Iwai, S., van der Spek, P.J., Eker, A.P., Hanaoka, F., Bootsma, D., and Hoeijmakers, J.H. (1998). Xeroderma pigmentosum group C protein complex is the initiator of global genome nucleotide excision repair. Mol Cell 2, 223-232.

Sugasawa, K., Okuda, Y., Saijo, M., Nishi, R., Matsuda, N., Chu, G., Mori, T., Iwai, S., Tanaka, K., Tanaka, K., et al. (2005). UV-induced ubiquitylation of XPC protein mediated by UV-DDB-ubiquitin ligase complex. Cell 121, 387-400.

Sugawara, N., and Haber, J.E. (1992). Characterization of double-strand break-induced recombination: homology requirements and single-stranded DNA formation. Mol Cell Biol 12, 563-575.

Sugawara, N., Ira, G., and Haber, J.E. (2000). DNA length dependence of the single-strand annealing pathway and the role of Saccharomyces cerevisiae RAD59 in double-strand break repair. Mol Cell Biol 20, 5300-5309.

Sugawara, N., Paques, F., Colaiacovo, M., and Haber, J.E. (1997). Role of Saccharomyces cerevisiae Msh2 and Msh3 repair proteins in double-strand break-induced recombination. Proc Natl Acad Sci U S A 94, 9214-9219.

Sun, H., Treco, D., and Szostak, J.W. (1991). Extensive 3'-overhanging, single-stranded DNA associated with the meiosis-specific double-strand breaks at the ARG4 recombination initiation site. Cell 64, 1155-1161.

Svendsen, J.M., Smogorzewska, A., Sowa, M.E., O'Connell, B.C., Gygi, S.P., Elledge, S.J., and Harper, J.W. (2009). Mammalian BTBD12/SLX4 assembles a Holliday junction resolvase and is required for DNA repair. Cell 138, 63-77.

Swanson, R.L., Morey, N.J., Doetsch, P.W., and Jinks-Robertson, S. (1999). Overlapping specificities of base excision repair, nucleotide excision repair, recombination, and translesion synthesis pathways for DNA base damage in Saccharomyces cerevisiae. Mol Cell Biol 19, 2929-2935.

Takenaka, T., Yano, T., Kiyohara, C., Miura, N., Kouso, H., Ohba, T., Kometani, T., Shoji, F., Yoshino, I., and Maehara, Y. (2009). Effects of excision repair cross-complementation group 1 (ERCC1) single nucleotide polymorphisms on the prognosis of non-small cell lung cancer patients. Lung Cancer.

Tan, L.J., Saijo, M., Kuraoka, I., Narita, T., Takahata, C., Iwai, S., and Tanaka, K. (2012). Xeroderma pigmentosum group F protein binds to Eg5 and is required for proper mitosis: implications for XP-F and XFE. Genes to cells : devoted to molecular & cellular mechanisms 17, 173-185.

Tapias, A., Auriol, J., Forget, D., Enzlin, J.H., Scharer, O.D., Coin, F., Coulombe, B., and Egly, J.M. (2004). Ordered conformational changes in damaged DNA induced by nucleotide excision repair factors. J Biol Chem 279, 19074-19083.

Tay, C.H. (1971). Ichthyosiform erythroderma, hair shaft abnormalities, and mental and growth retardation. A new recessive disorder. Arch Dermatol 104, 4-13.

Thompson, L.H., and Hinz, J.M. (2009). Cellular and molecular consequences of defective Fanconi anemia proteins in replication-coupled DNA repair: Mechanistic insights. Mutat Res 668, 54-72.

Tian, M., Shinkura, R., Shinkura, N., and Alt, F.W. (2004). Growth retardation, early death, and DNA repair defects in mice deficient for the nucleotide excision repair enzyme XPF. Mol Cell Biol 24, 1200-1205.

Torres-Ramos, C.A., Johnson, R.E., Prakash, L., and Prakash, S. (2000). Evidence for the involvement of nucleotide excision repair in the removal of abasic sites in yeast. Mol Cell Biol 20, 3522-3528.

Tripsianes, K., Folkers, G., Ab, E., Das, D., Odijk, H., Jaspers, N.G.J., Hoeijmakers, J.H.J., Kaptein, R., and Boelens, R. (2005). The structure of the human ERCC1/XPF interaction domains reveals a complementary role for the two proteins in nucleotide excision repair. Structure 13, 1849-1858.

Tripsianes, K., Folkers, G.E., Zheng, C., Das, D., Grinstead, J.S., Kaptein, R., and Boelens, R. (2007). Analysis of the XPA and ssDNA-binding surfaces on the central domain of human ERCC1 reveals evidence for subfunctionalization. Nucleic Acids Res 35, 5789-5798.

Troelstra, C., van Gool, A., de Wit, J., Vermeulen, W., Bootsma, D., and Hoeijmakers, J.H. (1992). ERCC6, a member of a subfamily of putative helicases, is involved in Cockayne's syndrome and preferential repair of active genes. Cell 71, 939-953.

Tsodikov, O.V., Enzlin, J.H., Scharer, O.D., and Ellenberger, T. (2005). Crystal structure and DNA binding functions of ERCC1, a subunit of the DNA structure-specific endonuclease XPF-ERCC1. Proc Natl Acad Sci U S A 102, 11236-11241.

Tsodikov, O.V., Ivanov, D., Orelli, B., Staresincic, L., Shoshani, I., Oberman, R., Scharer, O.D., Wagner, G., and Ellenberger, T. (2007). Structural basis for the recruitment of ERCC1-XPF to nucleotide excision repair complexes by XPA. The EMBO journal 26, 4768-4776.

Tsutakawa, S.E., Classen, S., Chapados, B.R., Arvai, A.S., Finger, L.D., Guenther, G., Tomlinson, C.G., Thompson, P., Sarker, A.H., Shen, B., et al. (2011). Human flap endonuclease structures, DNA double-base flipping, and a unified understanding of the FEN1 superfamily. Cell 145, 198-211.

Vaezi, A., Wang, X., Buch, S., Gooding, W., Wang, L., Seethala, R.R., Weaver, D.T., D'Andrea, A.D., Argiris, A., Romkes, M., et al. (2011). XPF expression correlates with clinical outcome in squamous cell carcinoma of the head and neck. Clin Cancer Res 17, 5513-5522.

van Duin, M., de Wit, J., Odijk, H., Westerveld, A., Yasui, A., Koken, H.M., Hoeijmakers, J.H., and Bootsma, D. (1986). Molecular characterization of the human excision repair gene ERCC-1: cDNA cloning and amino acid homology with the yeast DNA repair gene RAD10. Cell 44, 913-923.

van Steeg, H., de Vries, A., van Oostrom, C., van Benthem, J., Beems, R.B., and van Kreijl, C.F. (2001). DNA repair-deficient Xpa and Xpa/p53+/- knock-out mice: nature of the models. Toxicologic pathology 29 Suppl, 109-116.

Vance, J.R., and Wilson, T.E. (2001). Repair of DNA strand breaks by the overlapping functions of lesion-specific and non-lesion-specific DNA 3' phosphatases. Mol Cell Biol 21, 7191-7198.

Vance, J.R., and Wilson, T.E. (2002). Yeast Tdp1 and Rad1-Rad10 function as redundant pathways for repairing Top1 replicative damage. Proc Natl Acad Sci U S A 99, 13669-13674.

Vannier, J.B., Depeiges, A., White, C., and Gallego, M.E. (2009). ERCC1/XPF protects short telomeres from homologous recombination in Arabidopsis thaliana. PLoS Genet 5, e1000380.

Vasey, P.A. (2003). Resistance to chemotherapy in advanced ovarian cancer: mechanisms and current strategies. British journal of cancer 89 Suppl 3, S23-28.

Venema, J., Bartosova, Z., Natarajan, A.T., van Zeeland, A.A., and Mullenders, L.H. (1992). Transcription affects the rate but not the extent of repair of cyclobutane pyrimidine dimers in the human adenosine deaminase gene. J Biol Chem 267, 8852-8856.

Volker, M., Mone, M.J., Karmakar, P., van Hoffen, A., Schul, W., Vermeulen, W., Hoeijmakers, J.H., van Driel, R., van Zeeland, A.A., and Mullenders, L.H. (2001). Sequential assembly of the nucleotide excision repair factors in vivo. Mol Cell 8, 213-224.

Wakasugi, M., Reardon, J.T., and Sancar, A. (1997). The non-catalytic function of XPG protein during dual incision in human nucleotide excision repair. J Biol Chem 272, 16030-16034.

Wakasugi, M., and Sancar, A. (1998). Assembly, subunit composition, and footprint of human DNA repair excision nuclease. Proc Natl Acad Sci U S A 95, 6669-6674.

Wang, A.T., Sengerova, B., Cattell, E., Inagawa, T., Hartley, J.M., Kiakos, K., Burgess-Brown, N.A., Swift, L.P., Enzlin, J.H., Schofield, C.J., et al. (2011). Human SNM1A and XPF-ERCC1 collaborate to initiate DNA interstrand cross-link repair. Genes & development 25, 1859-1870.

Wang, X., Andreassen, P.R., and D'Andrea, A.D. (2004). Functional interaction of monoubiquitinated FANCD2 and BRCA2/FANCD1 in chromatin. Mol Cell Biol 24, 5850-5862.

Wang, X., Kennedy, R., Ray, K., Stuckert, P., Ellenberger, T., and D'Andrea, A.D. (2007). Chk1-mediated Phosphorylation of FANCE is Required for the Fanconi Anemia/BRCA Pathway. Mol Cell Biol.

Ward, I.M., and Chen, J. (2001). Histone H2AX is phosphorylated in an ATR-dependent manner in response to replicational stress. J Biol Chem 276, 47759-47762.

Warnecke-Eberz, U., Metzger, R., Miyazono, F., Baldus, S.E., Neiss, S., Brabender, J., Schaefer, H., Doerfler, W., Bollschweiler, E., Dienes, H.P., et al. (2004). High specificity of quantitative excision repair cross-complementing 1 m essenger RNA expression for prediction of minor histopathological response to neoadjuvant radiochemotherapy in esophageal cancer. Clin Cancer Res 10, 3794-3799.

Weeda, G., Donker, I., de Wit, J., Morreau, H., Janssens, R., Vissers, C.J., Nigg, A., van Steeg, H., Bootsma, D., and Hoeijmakers, J.H. (1997a). Disruption of mouse ERCC1 results in a novel repair syndrome with growth failure, nuclear abnormalities and senescence. Current biology : CB 7, 427-439.

Weeda, G., Donker, I., de Wit, J., Morreau, H., Janssens, R., Vissers, C.J., Nigg, A., van Steeg, H., Bootsma, D., and Hoeijmakers, J.H.J. (1997b). Disruption of mouse ERCC1 results in a novel repair syndrome with growth failure, nuclear abnormalities and senescence. Curr Biol 7, 427-439.

Wei, Q., Wang, L.E., Sturgis, E.M., and Mao, L. (2005). Expression of nucleotide excision repair proteins in lymphocytes as a marker of susceptibility to squamous cell carcinomas of the head and neck. Cancer Epidemiol Biomarkers Prev 14, 1961-1966.

Weinert, T. (1998). DNA damage and checkpoint pathways: molecular anatomy and interactions with repair. Cell 94, 555-558.

Welsh, C., Day, R., McGurk, C., Masters, J.R., Wood, R.D., and Koberle, B. (2004). Reduced levels of XPA, ERCC1 and XPF DNA repair proteins in testis tumor cell lines. Int J Cancer 110, 352-361.

Wilcox, D.R., and Prakash, L. (1981). Incision and postincision steps of pyrimidine dimer removal in excision-defective mutants of Saccharomyces cerevisiae. J Bacteriol 148, 618-623.

Wu, Y., Mitchell, T.R., and Zhu, X.D. (2008). Human XPF controls TRF2 and telomere length maintenance through distinctive mechanisms. Mech Ageing Dev 129, 602-610.

Wu, Y., Zacal, N.J., Rainbow, A.J., and Zhu, X.D. (2007). XPF with mutations in its conserved nuclease domain is defective in DNA repair but functions in TRF2-mediated telomere shortening. DNA Repair (Amst) 6, 157-166.

Yagi, T., Matsumura, Y., Sato, M., Nishigori, C., Mori, T., Sijbers, A.M., and Takebe, H. (1998). Complete restoration of normal DNA repair characteristics in group F xeroderma pigmentosum cells by over-expression of transfected XPF cDNA. Carcinogenesis 19, 55-60.

Yagi, T., Wood, R.D., and Takebe, H. (1997). A low content of ERCC1 and a 120 kDa protein is a frequent feature of group F xeroderma pigmentosum fibroblast cells. Mutagenesis 12, 41-44.

Yamashita, T., Kupfer, G.M., Naf, D., Suliman, A., Joenje, H., Asano, S., and D'Andrea, A.D. (1998). The fanconi anemia pathway requires FAA phosphorylation and FAA/FAC nuclear accumulation. Proc Natl Acad Sci U S A 95, 13085-13090.

Yildiz, O., Kearney, H., Kramer, B.C., and Sekelsky, J.J. (2004). Mutational analysis of the Drosophila DNA repair and recombination gene mei-9. Genetics 167, 263-273.

Yildiz, O., Majumder, S., Kramer, B., and Sekelsky, J.J. (2002). Drosophila MUS312 interacts with the nucleotide excision repair endonuclease MEI-9 to generate meiotic crossovers. Mol Cell 10, 1503-1509.

Yin, J., Vogel, U., Gerdes, L.U., Dybdahl, M., Bolund, L., and Nexo, B.A. (2003). Twelve single nucleotide polymorphisms on c hromosome 19q13.2-13.3: linkage disequilibria and associations with basal cell carcinoma in Danish psoriatic patients. Biochemical genetics 41, 27-37.

Yu, J.J., Mu, C., Lee, K.B., Okamoto, A., Reed, E.L., Bostick-Bruton, F., Mitchell, K.C., and Reed, E. (1997). A nucleotide polymorphism in ERCC1 in human ovarian cancer cell lines and tumor tissues. Mutat Res 382, 13-20.

Yu, V.P., Koehler, M., Steinlein, C., Schmid, M., Hanakahi, L.A., van Gool, A.J., West, S.C., and Venkitaraman, A.R. (2000). Gross chromosomal rearrangements and genetic exchange between nonhomologous chromosomes following BRCA2 inactivation. Genes & development 14, 1400-1406.

Yu, X., and Gabriel, A. (2003). Ku-dependent and Ku-independent end-joining pathways lead to chromosomal rearrangements during double-strand break repair in Saccharomyces cerevisiae. Genetics 163, 843-856.

Zhang, N., Kaur, R., Lu, X., Shen, X., Li, L., and Legerski, R.J. (2005). The Pso4 mRNA splicing and DNA repair complex interacts with WRN for processing of DNA interstrand cross-links. J Biol Chem 280, 40559-40567.

Zhang, N., Lu, X., and Legerski, R.J. (2003). Partial reconstitution of human interstrand cross-link repair in vitro: characterization of the roles of RPA and PCNA. Biochemical and biophysical research communications 309, 71-78.

Zhang, N., Lu, X., Zhang, X., Peterson, C.A., and Legerski, R.J. (2002). hMutSbeta is required for the recognition and uncoupling of psoralen interstrand cross-links in vitro. Mol Cell Biol 22, 2388-2397.

Zheng, Z., Chen, T., Li, X., Haura, E., Sharma, A., and Bepler, G. (2007). DNA synthesis and repair genes RRM1 and ERCC1 in lung cancer. The New England journal of medicine 356, 800-808.

Zhu, X.D., Niedernhofer, L., Kuster, B., Mann, M., Hoeijmakers, J.H., and de Lange, T. (2003). ERCC1/XPF removes the 3' overhang from uncapped telomeres and represses formation of telomeric DNA-containing double minute chromosomes. Mol Cell 12, 1489-1498.

Zienolddiny, S., Campa, D., Lind, H., Ryberg, D., Skaug, V., Stangeland, L., Phillips, D.H., Canzian, F., and Haugen, A. (2006). Polymorphisms of DNA repair genes and risk of non-small cell lung cancer. Carcinogenesis 27, 560-567.